

University of Alberta

**DEVELOPMENT OF STAT-3 TARGETING siRNA NANO-CARRIERS
FOR CANCER THERAPY**

by

AWS ALSHAMSAN

A thesis submitted to the Faculty of Graduate Studies and Research
in partial fulfillment of the requirements for the degree of

DOCTOR OF PHILOSOPHY
in
PHARMACEUTICAL SCIENCES

Faculty of Pharmacy and Pharmaceutical Sciences

©Aws Alshamsan
Fall 2010
Edmonton, Alberta

Permission is hereby granted to the University of Alberta Libraries to reproduce single copies of this thesis and to lend or sell such copies for private, scholarly or scientific research purposes only. Where the thesis is converted to, or otherwise made available in digital form, the University of Alberta will advise potential users of the thesis of these terms.

The author reserves all other publication and other rights in association with the copyright in the thesis and, except as herein before provided, neither the thesis nor any substantial portion thereof may be printed or otherwise reproduced in any material form whatsoever without the author's prior written permission.

Examining Committee

Dr. Ayman El-Kadi, Faculty of Pharmacy and Pharmaceutical Sciences

Dr. Afsaneh Lavasanifar, Faculty of Pharmacy and Pharmaceutical Sciences

Dr. Mavanur R. Suresh, Faculty of Pharmacy and Pharmaceutical Sciences

Dr. Hasan Uludağ, Chemical and Materials Engineering

Dr. Larry D. Unsworth, Department of Chemical and Materials Engineering

Dr. Adil Nazarali, Division of Pharmacy, University of Saskatchewan

“Our Lord! Punish us not if we forget or fall into error”

-The Holy Quran-

Dedication

I dedicate this thesis to my parents, Ibrahim Alshamsan and Wasmyah Almansour, my first and most precious tutors for their love and endless support; to my small family: my wife Raghad for her unconditional love, support, encouragement, and patience, and my lovely daughter, Maise, who interrupted me several times during my thesis writing to remind me how to sing the alphabet; and to my brother Badr and my sisters Deemah and Budoor, who are always proud of their older brother. I also dedicate this thesis to my mentor and supervisor the late Prof. John Samuel, who planted the seeds of this work and taught me how to take care of it. Then, before he left, he gave me his last advice, "Aws, be systematic."

ABSTRACT

In many tumors, persistently-active signal transducer and activator of transcription 3 (STAT3) imparts several oncogenic features such as survival, proliferation, angiogenesis, and immune escape. Therefore, STAT3 targeting in cancer and cancer-exposed dendritic cells (DCs) is important for cancer therapy. Our objective is developing delivery modalities of STAT3-targeting small interfering RNA (siRNA) using lipid-modified polyethylenimine (PEI) polyplexes and poly(D,L lactic-*co*-glycolic) acid (PLGA) nanoparticles (NPs), and evaluating the therapeutic outcomes *in vitro* and *in vivo*. Significant increase in siRNA condensation, protection, and cellular uptake by B16.F10 melanoma was seen by stearic-acid-modified PEI (PEI-StA) compared to unmodified PEI. Moreover, PEI-StA increased the STAT3 silencing potency of siRNA compared to PEI. STAT3 knockdown was accompanied with significant induction of interleukin-6 (IL-6) secretion and reduction of vascular endothelial growth factor (VEGF) production and cytotoxicity evidenced by increased Caspase 3 activity *in vitro* and *in vivo*, and significant inhibition in tumor growth. Analysis of tumor microenvironment showed CD3⁺ cells infiltration corresponding to STAT3 knockdown. The levels of CD4⁺ helper cells, CD8⁺ cytotoxic cells, and NKT cells significantly increased. DC infiltration and activation significantly increased in tumor mass following STAT3 knockdown as evidenced by high expression of CD86 and CD40. Moreover, IFN- γ , IL-12, and TNF- α significantly increased following STAT3 knockdown by PEI-StA compared to PEI, suggesting Th1-type immunity. Allogenic capacity of DCs isolated from siRNA-treated mice was evidenced by the high T cell proliferation and IL-2 production in mixed lymphocytes reaction (MLR). Then, we explored STAT3 knockdown in DCs exposed to

tumor derived factors (TDFs). We investigated encapsulation of siRNA complexes (PEI or PEI-StA) into PLGA NPs (PLGA-P and PLGA-PS). PLGA-P and PLGA-PS had an average diameter of ~ 370 nm and zeta potential of ~ -16 mV. Uptake and endosomal localization was confirmed. After TDFs exposure, DCs showed high STAT3 and low CD86 expression. STAT3 silencing by PLGA-P and PLGA-PS restored DC functionality as evidenced by upregulation of CD86, IL-12, and TNF- α and MLR activity. PLGA significantly reduced PEI-associated toxicity. Therefore, STAT3 targeting in B16 cells by siRNA polyplexes of PEI and PEI-StA, or in DCs by PLGA-P and PLGA-PS provide potential strategies for cancer therapy.

ACKNOWLEDGEMENTS

I would like to express my gratitude to the following people:

- My supervisor, the late Dr. John Samuel, whose expertise and knowledge added considerably to my graduate experience. I doubt that I will ever be able to convey my appreciation fully, but I dedicate to him all the success I had or will have in my future career life.
- My supervisor Dr. Ayman El-Kadi who took my responsibility after Dr. Samuel's tragic death. I cannot thank him enough for his kindness, guidance, advice, and endless support.
- My co-supervisor Dr. Afsaneh Lavasanifar who guided our research team after the sad loss of Dr. John Samuel. I am greatly indebted to her assistance and guidance at all stages of my work.
- Dr. Hasan Uludağ who welcomed me in his lab with open arms and provided me with the materials and expertise to develop the initial formulation.
- My supervisory committee members and examination committee for their advice and constructive feedback.
- Dr. Samar Hamdy and Dr. Azita Haddadi who were the unknown soldiers in my experimental work. I would have never made it without them. Beside Samar's invaluable help in most of my experiments, and especially during animal work, her continuous encouragement was a source of confidence that I cannot deny. Also, Azita's dedication and productivity had set an example for me. I had always felt confident when she is next to me at the bench.
- My friends and lab mates for the fruitful discussions, the endless help and support they have given me throughout the whole program.
- My dear wife, Raghad and my lovely daughter Maise who joined me during the whole process and helped me in every way with their love, support and patience.
- My dear parents and my dear brother and sisters for their love, encouragement and support throughout my whole life

Finally, I would like to thank the following institutes:

- King Saud University, Riyadh, Saudi Arabia, for providing me with my scholarship.
- The Saudi Cultural Bureau in Canada, for managing my tuition fees and academic expenses.
- The Faculty of Pharmacy and Pharmaceutical Sciences, University of Alberta, Edmonton, Canada, for accepting me in the graduate studies program and providing me with the facilities, training, and qualification.

TABLE OF CONTENTS

Chapter 1- Introduction	1
1.1 Cancer: A Historical Précis	2
1.1.1 Elimination Phase	6
1.1.2 Equilibrium Phase	6
1.1.3 Escape Phase	7
1.2 Physiological and Pathological Roles of Stat3	11
1.2.1 Physiological Importance of Stat3	12
1.2.2 Stat3 as an Oncogene	13
1.3 Stat3 Protein and Signaling Pathway	18
1.3.1 Stat3 Structure Activity Relationship	20
1.3.2 Jak/Stat3 Signaling Pathway	22
1.4 Stat3 Disruption Modalities	27
1.5 Strategies for siRNA Delivery	38
1.5.1 Polyethylenimine	39
1.5.2 Poly(D,L lactic- <i>co</i> -glycolic) acid	40
1.6 Rationale and Hypotheses	42
1.7 Objectives	44
1.8 References	45
Chapter 2 - Preparation and Characterization of siRNA Polyplexes of Lipid-Modified PEIs	63
2.1 Introduction	64

2.2 Materials and Methods	67
2.2.1 Materials	67
2.2.2 Cell Culture	68
2.2.3 Synthesis and Characterization of Lipid-Modified Polymers	68
2.2.4 Determination of siRNA Condensation by Gel Retardation Assay	69
2.2.5 Polyanion Competition Assay	69
2.2.6 Zeta Potential Measurement	70
2.2.7 Serum Stability Studies	70
2.2.8 Uptake of siRNA by B16 Melanoma Cells	71
2.2.9 siRNA-Mediated Inhibition of Integrin $\alpha(v)$	72
2.2.10 Cytotoxicity Study	72
2.2.11 Statistical Analysis	73
2.3 Results	73
2.3.1 siRNA Condensation by Oleic- and Stearic-acid Modified PEI	73
2.3.2 Zeta Potential of siRNA-Complexes	77
2.3.3 Protection of siRNA in Complexes from Degradation in Serum	79
2.3.4 Uptake of siRNA Complexes by B16 Melanoma Cells	81
2.3.5 Effect of Polymer Ratio in Complexes on siRNA Delivery	86
2.3.6 Knockdown of Integrin $\alpha(v)$ by siRNA Using Modified PEIs	88
2.3.7 Cytotoxicity Studies	90
2.4 Discussion	92
2.5 References	99

Chapter 3 - siRNA Silencing of Stat3 in Murine Melanoma Model	103
3.1 Introduction	104
3.2 Materials and Methods	108
3.3 Materials	108
3.2.2 Cells and Animals	109
3.2.3 Preparation and Characterization of siRNA Complexes	109
3.2.4 STAT3 Knockdown by siRNA Complexes	109
3.2.5 Western Blot	110
3.2.6 MTT Assay	111
3.2.7 Caspase 3 Activity Study	112
3.2.8 STAT3 silencing <i>in vivo</i>	113
3.2.9 Data Analysis	113
3.3. Results	114
3.3.1 Characterization of siRNA Complexes	114
3.3.2 STAT3 Knockdown by siRNA Complexes	116
3.3.3 Effect of STAT3 Knockdown on B16 Survival <i>in vitro</i>	118
3.3.4 <i>In vitro</i> Cytokine Secretion by B16 Cells	121
3.3.5 Effect of STAT3 Knockdown on B16 Tumor <i>in vivo</i>	123
3.4 Discussion	128
3.5 References	136
Chapter 4 - Bystander Immune Response in Stat3-Silenced Melanoma	141
4.1 Introduction	142

4.2 Materials and Methods	145
4.3 Materials	145
4.2.2 Preparation of siRNA Complexes	146
4.2.3 Assessing the Effect of Media from Untreated and siRNA Treated B16 Cells on <i>in vitro</i> DC Maturation and Function	146
4.2.3.1 Cell Culture	146
4.2.3.2 Treatments	148
4.2.3.2.1 B16.F10 Treatment	148
4.2.3.2.2 DCs Treatment	148
4.2.3.3 Western Blot	149
4.2.3.4 MTT Assay	150
4.2.3.5 Caspase 3 Activity Assay	150
4.2.3.6 FACS Analysis	151
4.2.3.7 Mixed Lymphocyte Reaction	151
4.2.4 Assessing the Effect of Anti-STAT3 siRNA Complex Treatment of B16 Tumors on Immune Response <i>in vivo</i>	152
4.2.4.1 Tumor Establishment and Treatment	152
4.2.4.2 Assessing tumor growth and STAT3 expression	152
4.2.4.3 Evaluating the Immunological Profile in Tumor Milieu	153
4.2.4.4 Evaluation of DC Functionality following siRNA Treatment <i>in vivo</i> ...	153
4.2.5 Data Analysis	154
4.3 Results	155
4.3.1 Comparison between Primary DCs and DC Cell Line (DC2.4)	155

4.3.2 STAT3 Knockdown in B16 by siRNA Induces DC Maturation and Activation <i>in vitro</i>	157
4.3.3 Tumor Regression following STAT3 Knockdown <i>in vivo</i>	162
4.3.4 Induction of DC Activation <i>in vivo</i> following STAT3 Knockdown in B16 Tumor	164
4.3.5 Alloreactivity of DCs from Tumor-Bearing Mice	166
4.3.6 Tumor Infiltration of T Cells following STAT3 Knockdown	168
4.4 Discussion	170
4.5 References	178
Chapter 5 - Stat3 Silencing in DCs by PLGA NPs of siRNA Polyplexes	181
5.1 Introduction	182
5.2 Materials and Methods	186
5.2.1 Materials	186
5.2.2 Preparation of Primary DC Culture	187
5.2.3 Preparation of PLGA NPs of siRNA Complexes	187
5.2.4 Characterization of PLGA-P and PLGA-PS NPs	188
5.2.4.1 Surface Morphology, Particle Size, and Surface Charge Analysis	188
5.2.4.2 Determination of siRNA Content	188
5.2.4.3 <i>In vitro</i> Release Study	190
5.2.5 Cytotoxicity Studies	190
5.2.6 Uptake of PLGA-P and PLGA-PS by DCs	191
5.2.7 Treatment of Malfunctioned DCs	191

5.2.7.1 Western Blot	192
5.2.7.2 FACS Analysis	193
5.2.7.3 ELISA Assay.....	193
5.2.7.4 Mixed Lymphocytes Reaction	194
5.2.8 Data Analysis	194
5.3 Results	195
5.3.1 Characterization of PLGA-P and PLGA-PS	195
5.3.2 <i>In vitro</i> Release Profile of siRNA from PLGA-P and PLGA-PS	199
5.3.3. Assessment of PLGA-P and PLGA-PS Cytotoxicity	201
5.3.4 Cellular Uptake of PLGA-P and PLGA-PS by DCs	203
5.3.5 Restoration of DC Functionality Following STAT3 Knockdown	205
5.4 Discussion	210
5.5 References	217
Chapter 6 - General Discussion, Conclusions, and Future Directions	221
6.1 GENERAL DISCUSSION	222
6.2 CONCLUSIONS	237
6.3 FUTURE DIRECTIONS	238
6.3.1 Development of i.v. siRNA delivery system	238
6.3.2 Co-delivery of STAT3 siRNA and cancer vaccines	243
6.4 References	244

LIST OF FIGURES

Figure 1.1 Cancer Immunoediting	5
Figure 1.2 Role of STAT3 in Tumor Immune Escape	9
Figure 1.3 Tumor-Induced STAT3 Activation in Immune Cells	17
Figure 1.4 STAT3 Signaling Pathway	19
Figure 1.5 Molecular Topology of STAT Proteins	21
Figure 1.6 IL-6R α and gp130 Structures	24
Figure 1.7 Chemical Structures of PEI and PLGA	38
Figure 1.8 Research Hypotheses	43
Figure 2.1 Assessment of siRNA complexation by gel migration assay	76
Figure 2.2 Determination of net surface charge by zeta potential analysis	78
Figure 2.3 Determination of siRNA stability in presence of serum	80
Figure 2.4 Cellular uptake of siRNA complexes by B16 cells	84
Figure 2.5 Effect of polymer:siRNA ratio on siRNA delivery	87
Figure 2.6 Inhibition of integrin $\alpha(v)$ expression by siRNA in B16 cells	89
Figure 2.7 Cytotoxicity study	91
Figure 3.1 Fatty-acid attachment on PEI backbone	115
Figure 3.2 STAT3 knockdown by siRNA complexes <i>in vitro</i>	117
Figure 3.3 Effect of multiple administrations of 50 nM siRNA complexes	120
Figure 3.4 Analysis of cytokine profile after STAT3 knockdown <i>in vitro</i>	122
Figure 3.5 Effect of siRNA complexes on tumor growth <i>in vivo</i>	124
Figure 3.6 Molecular analysis following siRNA administration <i>in vivo</i>	127
Figure 4.1 Effects of B16-CM on STAT3 activation and DC maturation	156

Figure 4.2 B16.F10 cell death following STAT3 knockdown <i>in vitro</i>	159
Figure 4.3 Restoration of DC phenotypic maturation <i>in vitro</i>	160
Figure 4.4 Allogenic MLR following STAT3 silencing <i>in vitro</i>	161
Figure 4.5 Tumor regression following STAT3 knockdown by siRNA	163
Figure 4.6 DC infiltration, activation, and cytokine production <i>in vivo</i>	165
Figure 4.7 Allogenic MLR following STAT3 silencing <i>in vivo</i>	167
Figure 4.8 Evaluation of tumor-infiltrating lymphocytes <i>in vivo</i>	169
Figure 5.1 PLGA-P or PLGA-PS NPs with relative sizes polyplexes	185
Figure 5.2 Characterization of PLGA-P or PLGA-PS NPs	196
Figure 5.3 Gel retardation assay of extracted siRNA PLGA-P and -PS	198
Figure 5.4 <i>In vitro</i> release of siRNA and NPs surface analysis	200
Figure 5.5 Cytotoxicity assessment of PEI NPs and PEI-StA NPs	202
Figure 5.6 Cellular uptake of PEI NPs and PEI-StA NPs	204
Figure 5.7 Evaluation of immunostimulatory potential	208
Figure 6.1 Physiological barriers to the systemic delivery of siRNA NPs	225
Figure 6.2 Possible roles of fatty chains in enhancing siRNA properties	231
Figure 6.3 Illustration of barriers for intravenous gene delivery	242

LIST OF TABLES

Table 1.1 Various modalities of disrupting STAT3 signaling	36
Table 1.2 Fundamental differences between antisense ODN and siRNA	37
Table 2.1 PEI substitution with fatty acid chains	74
Table 5.1 siRNA E.E. and Loading in PLGA-based NPs	197

LIST OF ABBREVIATIONS

Ab	antibody
ANOVA	analysis of variance
APCs	antigen presenting cells
APRF	acute phase response factor
ATCC	American Type Culture Collection
BCA	bicinchoninic acid
Bcl	B cell lymphoma
BMDC	bone marrow derived dendritic cells
C	celsius
CA	caprylic acid
CD	cluster of differentiation
CDCl ₃	deuterated chloroform
CD40L	CD40 ligand
cDNA	complementary DNA
CLSM	confocal laser scanning microscopy
CM	conditioned medium
CNTF	ciliary neurotrophic factor
CpG	cytosine-phosphate-guanine
cpm	counts per minute
CRM	chromosome recognition maintenance
CT-1	cardiotrophin 1
CTL	cytotoxic T lymphocyte

Da	Dalton
DAPI	4',6-diamidino-2-phenylindole
DCs	dendritic cells
DCM	dichloromethane
DMEM	Dulbecco's modified Eagle's medium
DMSO	dimethyl sulfoxide
E.E.	encapsulation efficiency
EGTA	ethylene glycol tetraacetic acid
ELISA	enzyme-linked immunosorbent assay
EPR	enhanced permeability and retention
ERK	extracellular signal-regulated kinase
FACS	fluorescence activated cell sorting
FAM	carboxyfluorescein
FBS	fetal bovine serum
FCM	flow cytometry
FCS	fetal calf serum
FDA	food and drug administration
FITC	fluorescein isothiocyanate
FOXP3	forkhead box P3
<i>g</i>	gravitation force
GM-CSF	granulocyte-macrophage colony stimulating factor
h	hour
HDAC	histone deacetylase

HLA	human leukocyte antigen
HNSSC	head and neck squamous cell carcinoma
HRCC	human renal carcinoma cells
ICAM	intercellular adhesion molecule
I κ B	inhibitory binding protein κ B
IKK	I κ B kinase
IFN	interferon
IL	interleukin
i.p.	intraperitoneal
IP-10	IFN-inducible protein-10
i.t.	intratumoral
JAK	Janus kinase
kDa	kiloDalton
L	liter
LA	linoleic acid
LIF	leukemia inhibitory factor
LPS	lipopolysaccharide
M	molar
mAb	monoclonal antibody
MAPK	mitogen-activated protein kinase
Mcl	myeloid cell leukemia
mg	milligram
MFI	mean florescence intensity

MHC	major histocompatibility complex
min	minute
MIP	macrophage inflammatory protein
mL	milliliter
MLR	mixed lymphocytes reaction
MM	multiple myeloma
MPLA	monophosphoryl lipid A
MTT	3-(4,5-Dimethylthiazol-2-yl)-2,5-diphenyltetrazolium bromide
MUC1	mucin-1
NaF	sodium fluoride
Na ₃ VO ₄	sodium orthovanadate
NES	nuclear export signal
NFκB	nuclear factor κB
ng	nanogram
NK	natural killer cells
NKT	NK T cells
nm	nanometer
NO	nitric oxide
N/P	protonable nitrogens/nucleic-acid phosphates
NPs	nanoparticles
NPC	nuclear pore complexes
NLS	nuclear-localization signal
NSCLC	non-small cell lung cancer

OA	oleic acid
OD	optical density
ONOO ⁻	peroxynitrite
OSM	oncostatin M
o/w	oil-in-water
PAGE	polyacrylamide gel electrophoresis
PBS	phosphate buffer saline
PE	phycoerythrin
PEG	polyethylene glycol
PEI	polyethylenimine
PEI-CA	polyethylenimine-caprylic acid
PEI-LA	polyethylenimine-linoleic acid
PEI-OA	polyethylenimine-oleic acid
PEI-StA	polyethylenimine-stearic acid
pg	picogram
PGA	poly glycolic acid
p-gp	p-glycoprotein
PIAS	protein inhibitor of activated STAT
PKC	protein kinase C
PLA	poly lactic acid
PLGA	poly(D,L-lactic-co-glycolic acid)
PTPase	proteins and protein tyrosine phosphatase
PVA	polyvinyl alcohol

PVDF	polyvinylidene fluoride
r^2	correlation coefficient
RANTES	regulated on activation normal T-cell expressed and secreted
RES	reticular endothelial system
RISC	RNA-induced silencing complex
RNAi	RNA interference
s.c.	subcutaneous
SCCHN	squamous cell carcinoma of the head and neck
SCID	severe combined immunodeficiency
SD	standard deviation
SDS	sodium dodecyl sulfate
SE	standard error
sec	second
SEM	scanning electron microscopy
siRNA	small interfering RNA
SOCS	suppressor of cytokine signaling
StA	stearic acid
STAT	signal transducer and activator of transcription
TAM	tumor-associated macrophages
TDFs	tumor-derived factors
TEA	triethylamine
TF	transferrin protein
TGF- β	transformation growth factor beta

Th	T helper
TK	tyrosine kinase
TLR	toll-like receptor
TNF	tumor necrosis factor alpha
TRAIL	TRIF-related apoptosis-inducing ligand
T _{Reg}	regulatory T cells
TRP2	tyrosinase related protein-2
TYK2	tyrosine kinase 2
UV	ultraviolet
V	volt
VEGF	vascular endothelial growth factor
VEGFR	VEGF receptor
Vis	visible
vol	volume
VPF	vascular permeability factor
w/o/w	water-in-oil-in-water
WT	wild-type
ζ	Zeta Potential

AMINO ACIDS

A	alanine
C	cysteine
D	aspartic acid
E	glutamic acid
F	phenylalanine
G	glycine
H	histidine
I	isoleucine
K	lysine
L	leucine
N	asparagine
P	proline
Q	glutamine
R	arginine
S	serine
T	threonine
V	valine
W	tryptophan
Y	tyrosine

CHAPTER ONE

INTRODUCTION

1.1 CANCER: A HISTORICAL PRÉCIS

Cancer is an ancient disease. The morphological evidence provided by anthropologists indicate the occurrence of malignant tumors in the remains of Egyptian mummies (1). Like ancient Egyptians, other ancient civilizations recognized malignant tumors, as described in their writings and pictures, where they attributed the causes of cancer to various gods (2). Later on, the Greek physician Hippocrates provided the first theory that attributed cancer to natural causes where he used the term “*karkinoma*” (carcinoma), the Greek word for crab, to describe tumors (2, 3). Although our understanding of cancer biology today is incomparably wider and deeper than ancient Egyptians and Greeks, the cancer rate is prominently increasing. According to the Canadian Cancer Statistics, 171,000 new cases of cancer and 75,300 deaths from cancer in Canada were estimated in 2009. This represents an increase of 4,600 newly-diagnosed cases and 1,500 deaths compared to 2008 (4). Therefore, effort has been directed toward intensive research for better understanding of cancer and the discovery of more effective approaches for therapy.

Modern scientific consensus on cancer development had been swinging between two sides: intracellular and extracellular factors for cancer development. In the 1800s, Rudolf Virchow proposed two notions that immensely contributed to these two concepts of cancer progression today. The first was in 1858 when Virchow declared that cells arise from pre-existing cells (5). This notion shaped the paradigm of carcinogenesis in the next century as a disease of normal cellular genes, especially after the emergence of cancer genetics (6). Shortly after,

Virchow proposed another notion in 1863 based on his discovery of the presence of leukocytes in neoplastic tissues. He suggested that these “infiltrates” at sites with chronic inflammation reflect the origin of cancer (7). Since then, immunologists struggled to understand the relationship between inflammation, immunity, and cancer. Only recently, owing to modern methods of gene targeting, transgenic animal systems, and monoclonal antibodies (mAb), the understanding of tumor progression was moved in research beyond the “cell-centric” concept and toward a wider concept of tumors sculpting by stromal microenvironment, inflammation, and immunity (8).

As a concept, the role of immunity in cancer recognition and elimination has existed since 1909, when Paul Ehrlich proposed that cellular immunity is directed against malignancy (9). About fifty years later, Sir Macfarlane Burnet and Lewis Thomas formalized this concept in a hypothesis known as “cancer immunosurveillance” (10, 11). They speculated that lymphocytes are able to recognize and eliminate newly transformed cells (12, 13). However, this hypothesis was quickly abandoned due to the lack of conclusive evidence, despite further experimental development with the immunology field (14). In addition, the findings of Osias Stutman stood against the immunosurveillance hypothesis, where he demonstrate a similarity in the incidence of tumor formation between nude mice and immunocompetent mice (15). These findings, corroborated by other groups, were convincing enough to lead to the general rejection of the hypothesis of cancer immunosurveillance; especially with the limited understanding of nude-mouse immunological defects at that time (14). However,

by the turn of the 21st century, two important findings revived the interest in cancer immunosurveillance: first, the discovery of the protective effects of endogenously-produced interferon- γ (IFN- γ) against transplanted, chemically-induced, and spontaneous tumors (16-19); and second, mice lacking perforin (pfp^{-/-}), a protein produced by cytotoxic T lymphocytes (CTL) and Natural Killer (NK) cells (20), are more susceptible to tumor formation than their wild-type counterparts (18, 19, 21-23). Ever since, evidence has accumulated to support cancer immunosurveillance in mice and in humans (14, 24).

However, that early understanding of cancer immunosurveillance as a host-protective mechanism of the adaptive immune system against newly transformed cells is refined today. Recently, Robert Schreiber and colleagues eloquently described how both innate and adaptive immunity have “dual roles in promoting host protection against cancer and facilitating tumor escape from immune destruction” (14). In other words, the host immune response against cancer could edit the immunogenicity of developing tumors (25). With this novel vision that cancer is not only a disease of malignant cells but also a disease of immunity and microenvironment, they proposed the hypothesis of “cancer immunoediting” (14, 24, 25). This hypothesis consists of three consecutive phases: elimination, equilibrium, and escape (Figure 1.1) (25).

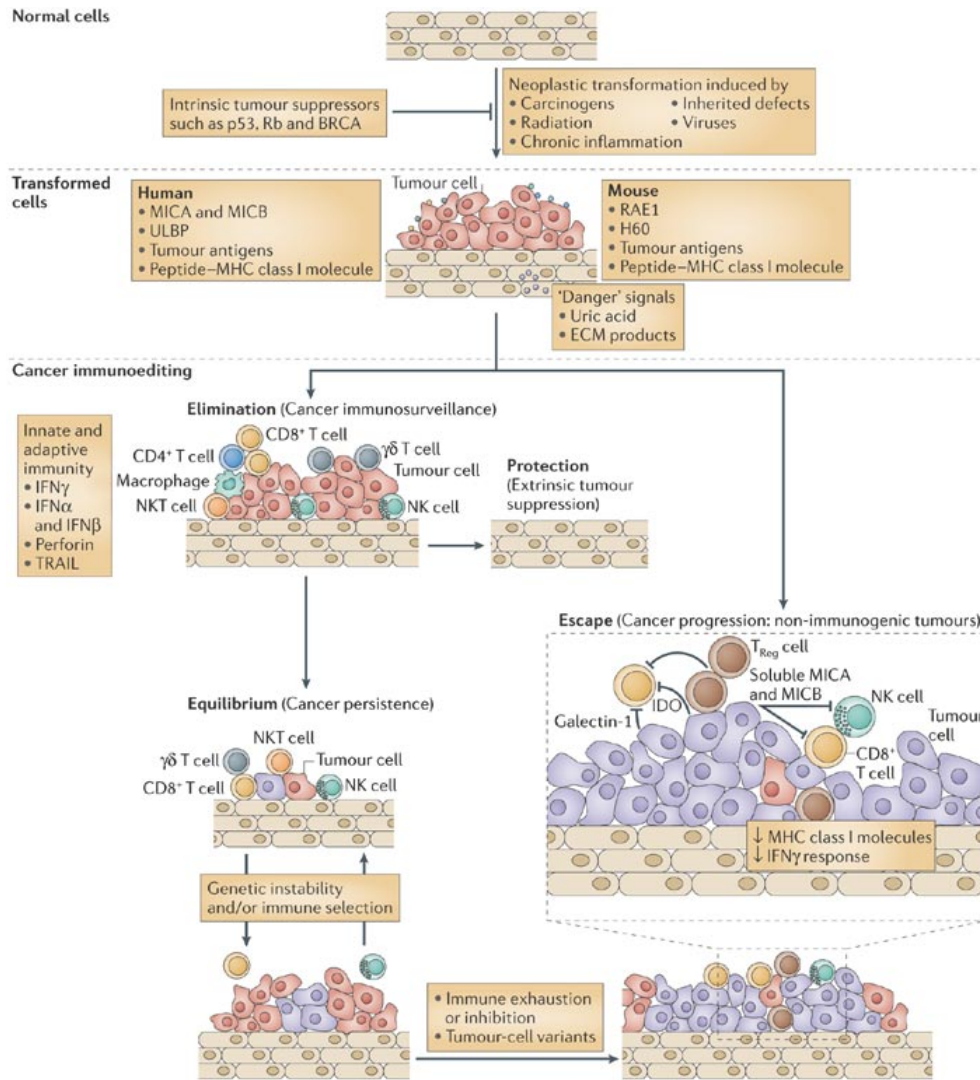


Figure 1.1 Cancer immunoediting. [adopted from (25)]: The elimination phase consists of the recognition of transformed cells by the innate and the adaptive immune system, leading to the killing of these cells as well as production of chemokines and other cytokines that facilitate killing of tumor cells. If some tumor cells are not killed in the elimination phase, the process progresses to the equilibrium phase, in which the tumor persists but is prevented from expanding by immune pressure. The escape phase begins when the balance between the immune response and the tumor tilts towards tumor growth as a result of immune exhaustion or inhibition or as a result of the emergence of tumor-cell variants that enable the tumor to evade immune pressure. Clinically detectable and progressively growing tumors appear in this phase.

1.1.1 Elimination Phase

The first phase represents cancer immunosurveillance where innate and adaptive immune components work to eradicate tumor cells. Initially, tumor-mediated angiogenesis and tissue invasiveness produce proinflammatory mediators and chemokines that recruit components of the innate immune system such as NK cells, NKT cells, and γ/δ T cells. Upon the recognition of transformed cells, these components initiate the anti-tumor process leading to IFN- γ production (24, 26-28). As a result of the innate response, tumor antigens from dead tumor cells become available for the adaptive immune systems. Here, dendritic cells (DCs) are recruited to the scene where they acquire tumor antigens and then migrate to the draining lymph node to activate naïve helper T cells ($CD4^+$) and naïve cytotoxic T cells ($CD8^+$), which become CTL upon activation (29-31). In a perfect scenario, tumor cells are completely eradicated as a result of IFN- γ production and $CD8^+$ T cells activation (14, 24). However, if any tumor cells survived the elimination phase, they will enter a longer phase where cancer cells and the host immune system will be in dynamic equilibrium.

1.1.2 Equilibrium Phase

This is probably the longest phase in the process of cancer immunoediting reaching as long as 20 years in human (24, 32). The unstable nature of cancer genes is thought to be the reason for tumor survival from immune attack during this phase (33). Moreover, clinical evidence has supported this hypothesis. It has been reported that two allograft recipients developed metastatic melanoma 1-2 years after each of them received a kidney from the same donor. This donor was

diagnosed with melanoma but was surgically treated and considered melanoma free for 16 years before the donation (34). This scenario suggests that the immunosuppressive treatment received by the recipients facilitated the growth of tumors that had been otherwise controlled in the equilibrium phase by the donor's immune system (24). The equilibrium shifts at this stage toward tumor progression, where tumor cells enter the escape phase.

1.1.3 Escape Phase

In this phase, tumor cells grow to a clinically detectable level in the presence of an intact immunological environment (14, 24). Owing to their genetic instability, the selected variants of cancer cells in this stage develop the means to circumvent innate and adaptive immune responses (35). Identifying those means is currently a major focus of research, and they could be subcategorized today into: extrinsic factors that are the influence of non-cancerous cells but present in tumor milieu such as immunosuppressive cells (e.g regulatory T cells (T_{Reg}) and tumor-associated macrophages (TAM)) and immunosuppressive cytokines (e.g. interleukin 10 (IL-10), IL-4, and transforming growth factor β (TGF- β)) (36); and intrinsic factors that cancer cells produce or modify, such as loss of antigen expression and/or components of the major histocompatibility complex (MHC) (37), developing IFN- γ insensitivity (17), overexpression of proteins such as integrins (38), cytokines (e.g. IL-6 (39) and IL-10 (40),) growth factors (e.g. TGF- β (41), vascular endothelial growth factor (VEGF) (42), epidermal growth factor (EGF) (43) and their receptors (44),) enzymes (e.g. indoleamine 2,3-dioxygenase

(IDO) (45),) and transcription factors (e.g. signal transducer and activator of transcription 3 (STAT3)) (46).

Among these factors, STAT3 has gained special interest as it has been shown to be involved in different scenarios of cancer immune escape, mediated by both intrinsic and extrinsic factors, as well as sustaining tumor survival and proliferation. On one hand, STAT3 mediates the production of some tumor derived factors (TDFs) responsible for cancer progression and immunosuppression such as cytokines (e.g. IL-6 and IL-10 (47)) and growth factors (e.g. VEGF (48)). On the other hand, these TDFs induce STAT3 activation in multiple components of the immune systems (Figure 1.2) (49). This induction of STAT3 activity in innate and adaptive immune cells drives these cells to participate further as extrinsic factors for cancer immune escape. Therefore, targeting hyperactive STAT3 in tumor cells as well as in immune cells is considered a key strategy for cancer therapy (46).

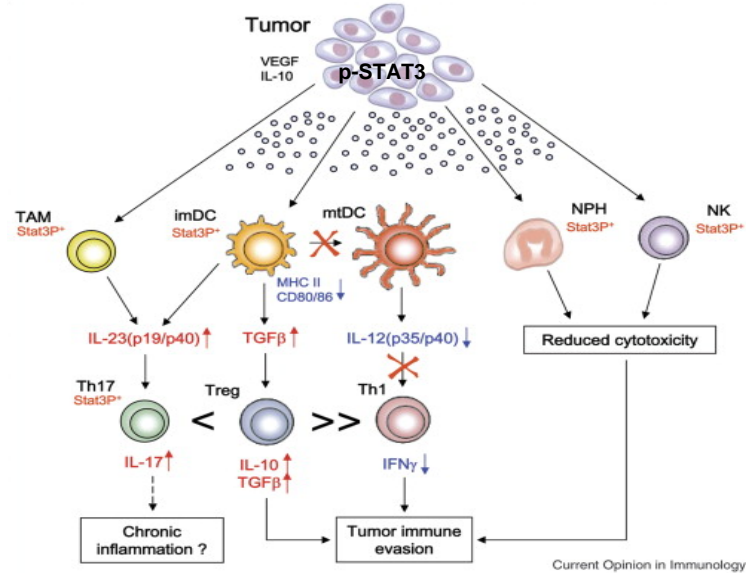


Figure 1.2 Role of STAT3 in Tumor Immune Escape. [adopted from (49)]: STAT3 is constitutively activated in tumor cells of diverse origin. Activated STAT3 (p-STAT3) in tumor cells promotes production of TDFs that activate STAT3 in various immune subsets, such as tumor-associated macrophages (TAM), immature DC (imDC), neutrophils and natural killer (NK) cells leading to reduction in their ability inhibit tumor growth.

This chapter will discuss the disruption of STAT3 activity as a promising mean to treat cancer. Three main elements are taken into account in designing the targeting strategy: (i) the mechanism of inhibition (i.e. the step(s) of STAT3 signaling pathway that will be targeted,) (ii) the agent (inhibitor) used to disrupt STAT3 function, and (iii) the delivery system that optimally delivers the agent to the site of action. First, in order to rationalize STAT3 targeting as a mean for cancer therapy, this chapter will highlight the physiological and oncological roles of STAT3. Special attention will be given to the role of tumor-induced STAT3 activation in DCs as they are the link between both innate and adaptive arms of the immune system. Thereafter, we will analyze STAT3 signaling pathway to expose possible targeting spots and will provide an up-to-date review of STAT3 targeting. Additionally, we will compare different modalities of targeting along with an evaluation of their clinical significance. In this regard, emphasis will be on small interfering RNA (siRNA) as a novel strategy for STAT3 disruption in tumor cells as well as in DCs. The advantages and problems of siRNA will be discussed in this context. Lastly, the delivery strategies of siRNA to both cell types (tumor and DCs) will be described and compared. Among the delivery systems discussed, polyethylenimine (PEI) complexes and poly-(D,L-lactic-co-glycolic acid) (PLGA) nanoparticles (NPs) will be highlighted. The model used in this thesis is B16.F10 murine melanoma cells which constitutively activate STAT3, and bone-marrow derived DCs. Since recent discussion have emphasized on the importance of immunotherapy for melanoma patients, we find enough

clinical relevance in our experimental melanoma model and intervention strategy for cancer therapy (50).

1.2 PHYSIOLOGICAL AND PATHOLOGICAL ROLES OF STAT3

STATs are latent cytoplasmic proteins that are responsive to cytokine and growth factor receptor stimulation (51). The acronym STAT was coined by James Darnell Jr. after he isolated a 91 kDa protein that gets phosphorylated upon IFN treatment (52). Darnell stated (53):

“In the Spring of 1991 Chris Schindler and X.Y. Fu in our lab had succeeded in purifying sufficiently ISGF3 [interferon-stimulated gene factor 3] ... so that we had some hope of identifying the constituent protein(s). The sizes of the proteins were identified in an experiment that Dan Kessler and I cooked up.... revealing the presence of 91, 84, 113 and 48 [kDa] molecules [that] were collected, fragmented and peptide sequenced by Ruedi Aebersold allowing by the early Fall the cloning of what came to be called STATs 1 α and 1 β as well as STAT2.”

After Darnell's discovery of STAT1 and STAT2, five additional members were subsequently discovered, STAT3 (54, 55), STAT4 (55, 56), STAT5a and STAT5b (57), and STAT6 (58) forming a total of seven members in the STAT family. STATs transduce several signals from cytokines and growth factors and activate the transcription of multiple genes, leading to different, and sometimes opposing, cellular outcomes based on target genes (59). STAT3 was first described in 1994 as a DNA-binding activity in IL-6-stimulated hepatocytes that selectively interacts with an enhancer element in the promoter of acute-phase genes, known as the acute-phase response element; hence, STAT3 was known as

acute phase response factor (APRF) (54, 60-62). However, it has been revealed that STAT3 is also activated by numerous other cytokines and growth factors, which indicates a wider capacity of STAT3 to mediate several functions in physiological and pathological contexts (63).

1.2.1 Physiological Importance of STAT3

One of the first noted roles of STAT3 was its importance for early embryonic development, as the embryos of STAT3-disrupted mice showed rapid degeneration before embryogenesis was completed (64). In the liver, STAT3 disruption lead to the impairment of the acute phase response, as well as the impairment of liver regeneration (65, 66). Furthermore, it was recently shown that serine-phosphorylated STAT3 is located in liver mitochondria where it modulates mitochondrial respiration as a general mechanism in metabolism (67). Moreover, it is involved in neuronal development and survival after injury (68, 69). Also, STAT3 is important for epithelium remodeling as it has been shown to be indispensable for wound healing (70), mammary involution (71, 72), and protection of gut epithelium from uncontrolled inflammation (73, 74). Furthermore, the role of STAT3 in hematopoietic cells has been established. Specific deletion of STAT3 in T cells suppresses their proliferation and survival since it mediates CD25 expression; an important component of the high-affinity IL-2 receptor (73, 75). In myeloid cell lineage, STAT3 disruption leads to inflammatory manifestations indicating a regulatory function of STAT3 in inflammatory responses. STAT3-mutant mice showed higher mortality from over sensitivity to lipopolysaccharide (LPS)-induced cytotoxic shock, as well as

exaggerated levels in serum proinflammatory cytokines (76). In physiological conditions, STAT3 functions are under tight control. However, uncontrolled STAT3 activity has been shown to facilitate cellular transformation. Therefore, STAT3 is considered as an oncogene.

1.2.2 STAT3 as an Oncogene

Unlike the previous scenario in normal cells, STAT3 is persistently active in a variety of primary tumors and cancer cell lines (77). The first direct evidence suggesting a critical role of STAT3 in cancer growth in human emerged with the finding that inhibition of STAT3 in cell lines derived from patients with squamous cell carcinoma of the head and neck (SCCHN) reduces the proliferation of SCCHN cells (78). Further molecular investigation on multiple-myeloma cells, separated from patients' bone-marrow aspirates, and on U266 myeloma cell line provided evidence for STAT3 contribution in survival and malignant progression of multiple myeloma (79). Furthermore, in a study involving prostate cancer patients, 82% of tumor specimens obtained by radical prostatectomy showed elevated levels of STAT3 compared with matched non-tumor prostate tissues (80). STAT3 was also found to be essential for leptin-induced survivin expression in breast cancer cells (81). Recently, studies on melanoma patients also suggested that tyrosine-phosphorylated STAT3 (p-STAT3) is a biomarker for atypical nevi progression and a potential target for chemoprevention of melanoma (82). Subsequent studies revealed that STAT3 is also persistently activated in other solid tumors including colon cancer, pancreatic cancer, brain tumors, lung

carcinomas, ovarian, and cervical tumors, as well as hematological malignancies (i.e. leukemias and lymphomas (reviewed in (77, 83-88))).

Evidence has demonstrated the ability of STAT3 to transform normal cells into cancerous, indicating an intrinsic oncogenic quality in STAT3. For instance, cellular transformation using viruses (89, 90), protein tyrosine kinases (91, 92), and several other oncogenes are accompanied by persistence in STAT3 activity (93-95). additional evidence confirming the intrinsic oncogenic potential of STAT3 emerged from a chemically-modified form of STAT3, designated STAT3C, which is constitutively activated without tyrosine phosphorylation (93). In STAT3C, an introduced cysteine group in STAT3 monomer forms a disulfide bond with a corresponding cysteine in another STAT3 molecule, allowing for STAT3/STAT3 dimerization and DNA binding without phosphotyrosine/SH2 interaction. This protein was sufficient to mediate malignant transformation in immortalized fibroblasts, which were capable of forming tumors in nude mice (77, 93).

It has been concluded that persistently activated STAT3 mediates four critical properties in tumorigenesis (77, 96) namely: tumor cells survival (79), proliferation (97), angiogenesis and metastasis (98), and immune escape (49, 99). Nevertheless, these oncogenic properties can be considered as an exaggerated or unregulated form of the physiological functions of STAT3. Therefore, they could be explained by studying STAT3 target genes. Numerous studies have shown that STAT3 activates gene expression of various proteins that are involved in cell survival and prevention of apoptosis such as survivin (81), Bcl-2 (100), Bcl-xL,

and Mcl-1 (101). Similarly, cancer cell proliferation mediated by STAT3 has been attributed to the expression of growth-promoting proteins such as cyclin D1 and c-myc (102-105). Moreover, STAT3 is known to activate the expression of VEGF, which is a critical growth factor for tumoral angiogenesis (48). Therefore, STAT3 is critical for meeting the nutritional demand in tumors as well as mediating metastasis and tissue invasion. Moreover, recent studies have demonstrated that STAT3 mediates cancer tissue invasion by regulating matrix metalloproteinase (MMP) expression (106-108). The fourth oncogenic property of STAT3 is immune escape. This hallmark involves two aspects. The first aspect is cancer-cell modifications e.g. STAT3-mediated downregulation of the tumor-cell-surface expression of Fas receptor (CD95), which is a proapoptotic protein involved in CTL-dependant cytotoxicity (109); or suppression of T-cell chemotactic agents (RANTES and IP-10) production of by tumor cells (86). The second aspect is the ability of STAT3 to mediate a cross talk between cancer and immune cells (49, 99, 110). As mentioned earlier, in order to escape immune eradication, TDFs produced by STAT3-activated tumors induce STAT3 activation in multiple subsets of innate and adaptive immune cells (49, 111). Upon STAT3 activation, innate immune cells such as NK cells, TAM, NKT, and neutrophils lose their ability of tumor inhibition or effective production of immunostimulatory molecules (49). Additionally, STAT3 contributes to procarcinogenic T_{Reg} cells expansion through upregulation of forkhead box P3 (FOXP3) expression (112, 113). Moreover, a newly discovered IL-17-producing

T helper cell subtype (Th17) was found to depend on STAT3 for their proliferation, and promote tumor growth through IL-6-STAT3 signal (113, 114).

Nevertheless, DCs are the most important subsets in this equation, as they link innate and adaptive immune responses. Therefore, in the presence of cancer, DC malfunction causes an immunological paralysis if not potentiation of cancer progression. Typically, immature DCs (imDCs) serve as sentinels in most peripheral tissues where they encounter, internalize, and process antigens (115). As a result, imDCs get activated and upregulate the expression of MHC-I/II, co-stimulatory molecules (CD40 and CD86), as well as proinflammatory cytokines in order to activate naïve CD4⁺ and CD8⁺ T cells in the draining lymph node (116, 117). However, in tumor microenvironment, STAT3 activity influences DCs to remain immature i.e. expressing low levels of MHC-I/II, CD86, CD40, and IL-12. As a result those DCs are not able to polarize immune response toward T helper type 1 (Th1) and CTL response (99, 118-121). In that context, DCs become, not only functionless, but also tolerogenic owing to their induction of T_{Reg} cells accumulation (122) and secretion of immunosuppressive cytokines such as IL-10 and TGF- β (123, 124), which inhibit DC maturation even further (99, 125, 126) (Figure 1.3). The work of (Wang et. al, 2004), on melanoma provided the first molecular evidence showing that STAT3 activity inhibits Th1-type immune response and induces the production of immunosuppressive TDFs that inhibit DC maturation (86). TDFs such as IL-6, IL-10, and VEGF, were shown to suppress IL-12 production by DCs (127, 128).

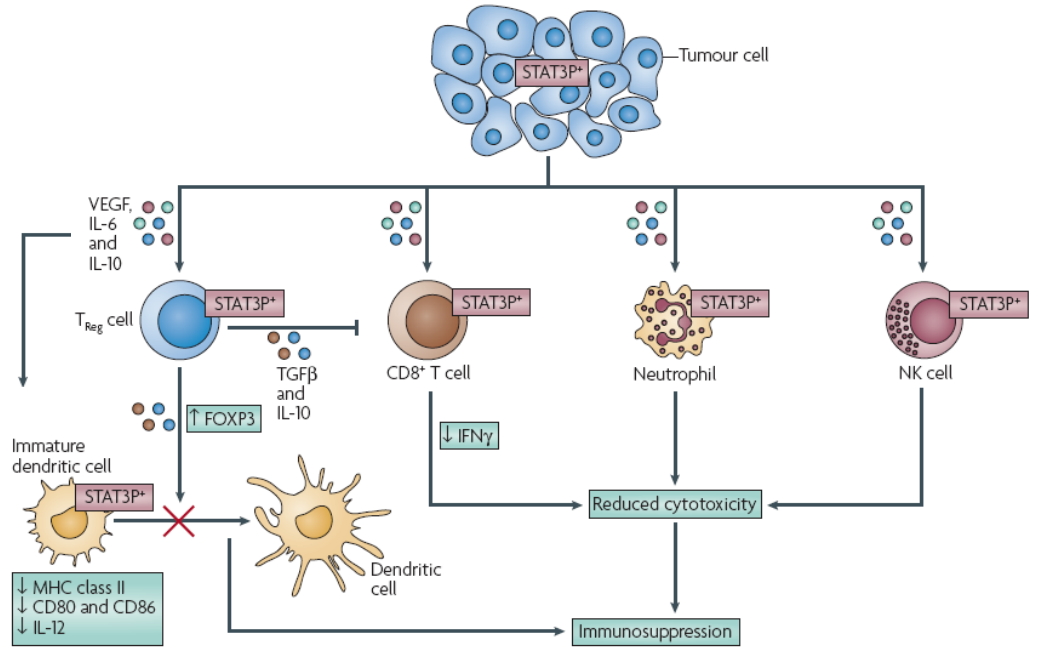
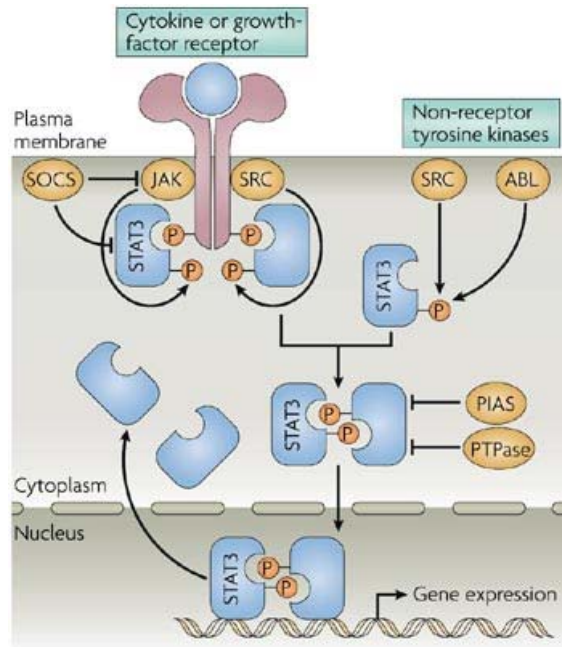


Figure 1.3 Tumor-Induced STAT3 Activation in Immune Cells. [adopted from (99)]: STAT3 activity is increased in tumor-associated T_{Reg} cells. STAT3 signaling in T_{Reg} cells can upregulate the expression of FOXP3, TGFβ and IL-10, which, in turn, restrain CD8⁺ T cells, as well as dendritic-cell maturation. NK cells and neutrophils in the tumor stroma also have persistently activated STAT3, which inhibits the tumor-killing activity of both types of effector cell.

With all these oncogenic properties mediated by constitutively activated STAT3, it is not surprising to find out that STAT3-active tumors are chemo- and radioresistant (129-131). Therefore, targeting STAT3 is currently considered a key element for cancer treatment (46, 110, 132). In order to achieve this goal, we have to study the STAT3 protein and its associated signaling pathway in order to highlight potential spots for therapeutic intervention.

1.3 STAT3 PROTEIN AND SIGNALING PATHWAY

STAT3 signaling is summarized in Figure 1.4 (99). Like all other STATs, STAT3 signal follows the general paradigm which is based on receptor engagement, followed by activation of different tyrosine kinases (TKs) e.g. Janus kinase (JAK) family members: JAK1, JAK2, JAK3 and tyrosine kinase 2 (TYK2) (133, 134). These TKs mediate the phosphorylation of receptor tyrosine motifs to which subsequent recruitment of the desired STAT proteins takes place (134, 135). Then, they mediate the phosphorylation of a critical tyrosine on the STAT molecule leading to the dimerization of two STAT monomers into an active transcription factor that transport to the nucleus and activate the transcription of target genes (134, 136). The details of STAT3 signaling will be discussed further in this chapter.



Nature Reviews | Immunology

Figure 1.4 STAT3 Signaling Pathway. [adopted from (99)]: Activation of intrinsic growth-factor-receptor TKs, and cytokine-receptor-associated JAK and SRC TKs, which, in turn, phosphorylate STAT3. In transformed cells, STAT3 can also be activated by constitutively active non-receptor TKs. Then, p-STAT3 molecules dimerize and translocate to the nucleus, where they directly regulate gene expression. Regulatory proteins are shown: suppressor of cytokine signaling (SOCS) proteins, and protein inhibitor of activated STAT (PIAS) proteins and protein tyrosine phosphatases (PTPases).

1.3.1 STAT3 Structure Activity Relationship

STAT3 is a 92 kDa protein consisting of 770 amino acids that is naturally expressed in two isoforms, STAT3- α and STAT3- β (137). The resolved X-ray crystal of STAT3 revealed six common STAT structural features (Figure 1.5) (77):

- ***NH₂-Terminal Portion:*** provides protein-protein interaction sites required for dimer-dimer interaction. The formed tetramer contributes to stabilize STAT/DNA-binding on weak promoters. Nevertheless, this interaction is not essential for the transactivation (138, 139).
- ***Coiled-Coil Domain:*** another protein-protein interaction site that provides potential contacts with regulatory proteins (140). It also has a role in nuclear transportation of STAT3 (141, 142).
- ***DNA-Binding Domain:*** in the centre of the molecule and it determines DNA sequence specificity. It makes direct contact with STAT-binding sites in gene promoters, which have the consensus core sequence TT(N₄₋₆)AA (137).
- ***Linker Region:*** participates in DNA binding leads to the C-terminal SH2 domain, which is required for the recruitment of STAT3 to phosphorylated receptors and for reciprocal SH2-phosphotyrosine interaction between monomers (143).
- ***Critical Tyrosine Residue (Y⁷⁰⁵):*** required for reciprocal SH2-phosphotyrosine interaction to form a dimer. This dimerization is essential for STAT3-DNA interaction.

• **Transactivation Domain (TAD):** at the C-terminal end of the molecule is involved in communication with transcription complexes and contains a serine phosphorylation site (S^{727}) that enhances transcriptional activation of target genes (144).

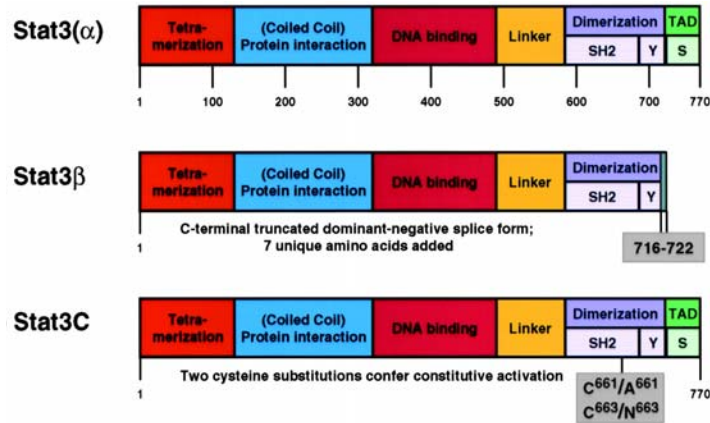


Figure 1.5 Molecular Topology of STAT Proteins. [adopted from (77)]: top diagram represents the domain structure of full-length STAT3 protein (STAT3- α), while the middle one represents the STAT3- β splice variant that has C-terminal deletion, resulting in an altered open reading frame with the addition of seven new amino acids downstream of the deletion, and loss of the TAD domain. This naturally occurring truncated isoform still dimerizes and binds to DNA but fails to activate gene expression. The bottom diagram represents chemically modified STAT3C, which is spontaneously active without tyrosine phosphorylation. Y, critical phosphotyrosine in STAT3 (amino acid 705); S, critical phosphoserine in some STATs (amino acid 727).

1.3.2 JAK/STAT3 Signaling Pathway

Like other STAT proteins, STAT3 signal has seven major consecutive events (63, 145) (Figure 1.6). For STAT3 activity, IL-6 play a major role (146):

- ***Ligand/Receptor Interaction:*** IL-6 interacts with its receptor complex that consists of two IL-6R α (gp 80) (the non-signaling subunit) and two gp130 (the signal transducer subunit) (147, 148). IL-6R α is a type I membrane protein consisting of an extracellular domain of 339 amino acids, transmembrane domain of 28 amino acids, and intracellular domain of 82 amino acids (149), while gp130 consists of an extracellular domain of 597 amino acids, transmembrane domain of 22 amino acids, and intracellular domain of 277 amino acids (63).

- ***Receptor Complexation and Orientation:*** evidence have shown that the binding of IL-6 to IL-6R α induces the dimerization of two gp130 chains (145). This dimerization permits the activation of members of Janus kinases (JAK) by an auto/trans-phosphorylation mechanisms (150). Moreover, the dimerization of two extracellular segments of gp130 leads to receptor re-orientation that reduces the distance between the two C-termini of gp130 homodimer, which makes all cytoplasmic components close enough to be activated by JAK (151).

- ***JAK/Receptor Interaction:*** IL-6 induces the activation of three members of JAK family: JAK1, JAK2, and TYK2 (61, 152). Upon gp130 dimerization, JAK binds to specific motifs in the membrane-proximal region of gp130 called box 1, which is critical for JAK binding to gp130, and box 2 which increases binding affinity (153, 154). Although IL-6 antagonism could prevent STAT3 activation, such upstream inhibition carries a huge potential for non-specificity.

• ***STAT3 Recruitment and Activation:*** gp130-associated JAK proteins phosphorylate specific tyrosine residues within the cytoplasmic domain of gp130. The human gp130 contains six tyrosine residues in its cytoplasmic domain: Y⁶⁸³ located within the box 1/2 region (145); Y⁷⁵⁹ which forms a docking sites for SH2-Containing Phosphotyrosine Phosphatase 2 (SHP2) and Suppressor of Cytokine Signaling 3 (SOCS3) proteins, which negatively regulate signal transduction mediated by gp130 (155, 156); and four tyrosine residues of YXXQ motifs (Y⁷⁶⁷RHQ, Y⁸¹⁴FKQ, Y⁹⁰⁵LPQ and Y⁹¹⁵MPQ) that are recognized by the SH2 domain of STAT3, while SH2 of STAT1 only recognizes the distal two tyrosine residues (Y⁹⁰⁵ and Y⁹¹⁵) (157). Upon STAT3 recruitment to the phosphorylated YXXQ motifs in gp130, it becomes in close proximity to JAK, which phosphorylate the recruited STAT3 on a single tyrosine residue (Y⁷⁰⁵) (158, 159). This tyrosine phosphorylation is critical for STAT3 dimerization step, by which an active transcription factor is conformed (143). In addition to Y⁷⁰⁵ phosphorylation, serine (S⁷²⁷) phosphorylation has also been documented to activate STAT3 signaling (160). Although not essential for STAT3 activity, S⁷²⁷ phosphorylation enhances the transcriptional activities of STAT3 since mutations of S⁷²⁷ compromise STAT3 activity and downstream effects (161). In other words, full activation of STAT3 requires both tyrosine and serine phosphorylation (162). Therefore, inhibition of STAT3 phosphorylation in cancer cells is a rational modality for STAT3 targeting.

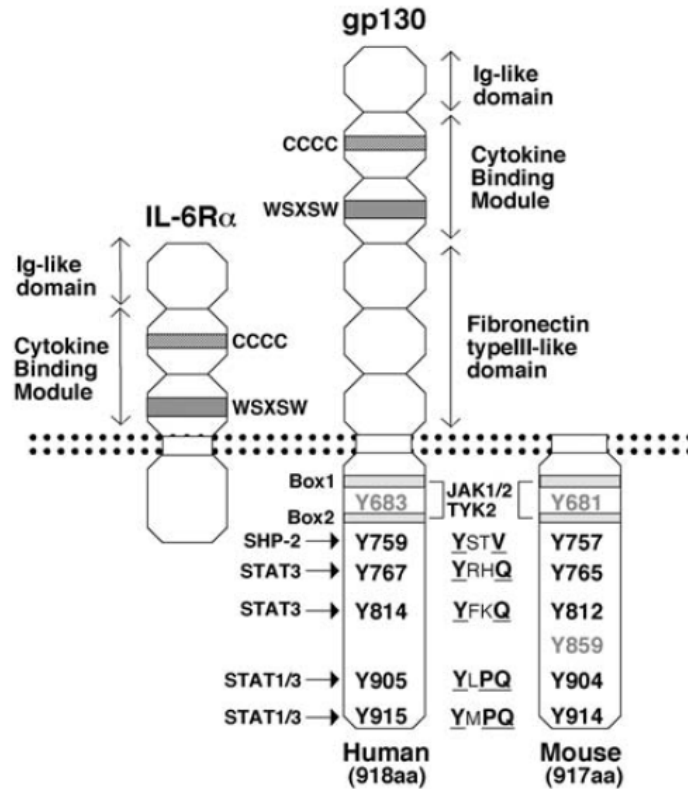


Figure 1.6 IL-6R α and gp130 Structures. [adopted from (146)]. Amino acid residues are denoted with the single-letter code, followed by their position in the human and mouse gp130 amino acid sequences. JAK kinases are constitutively associated with gp130 through the Box domains. In response to IL-6 stimulation, SHP-2 and STAT1/3 molecules are recruited to respective tyrosine residues in gp130, indicated with arrows. CCCC four-cysteine motif, WSXWS tryptophan-serine-any-tryptophan-serine motif.

• ***STAT3 Dimerization:*** After STAT3 phosphorylation, (Y705) phosphotyrosine of one STAT3 monomer will be recognized by SH2 domain from another STAT3 monomer leading to STAT3/STAT3 dimerization by reciprocal phosphotyrosine-SH2 recognition (137, 143). In this complex, the two SH2 domains form a tunnel that is passed by the two phosphotyrosine-containing tail segments (137). Generally, STAT3 forms STAT3/STAT3 homodimers. However, STAT1/STAT3 heterodimers have been found as well upon gp130-mediated signaling. This is because of the three-dimensional structural similarity in SH2 domains of STAT1 and STAT3 in spite of the low sequence homology (163). Also, it is worth noting that STAT3 dimerization is stabilized by acetylation on a single lysine residue (K685) by histone acetyltransferase, which is reversed by type I histone deacetylase (HDAC) (164). Stable dimers are transported to the nucleus in order to bind to the responsive elements in DNA and mediate gene expression. Prevention of STAT3 dimerization is another strategy of disrupting STAT3 signaling in cancer.

• ***STAT3 Nuclear Transportation:*** this step is controlled by specialized portals known as nuclear pore complexes (NPCs) (165). These complexes consist of proteins of karyopherin- β family that are two categories: either importins, which recognize nuclear-localization signal (NLS) and function in nuclear import, or exportins, which recognize nuclear export signal (NES) and function in nuclear export (166). The event of protein transportation in and out the nucleus is either constitutive or inducible based on modification, such as phosphorylation, of the protein to be transported (134). Some studies reported that importin- $\alpha 5$ is a major

mediator for nuclear accumulation of p-STAT3 where specific sequence in STAT3 coiled-coil domain strongly interact with importin- α 5 (141, 142). Moreover, phosphorylated and unphosphorylated STAT3 constantly shuttle between nuclear and cytoplasmic compartments (167). While STAT3 interaction with importin- α 5 was found to be only after cytokine stimulation, a different mechanism was identified to accommodate for nuclear translocation of unphosphorylated STAT3 (134, 141, 168). Importin- α 3, which associates with specific NLS (amino acids 152-163) in the coiled-coil domain STAT3, was found to import STAT3 to the nucleus as silencing of importin- α 3 by RNA interference (RNAi) inhibited nuclear accumulation of STAT3 (134, 168). Therefore, importin- α 3 was proposed to mediate the nuclear translocation of both STAT3 and p-STAT3 (134). On the other hand, STAT3 export from the nucleus back to the cytoplasm was found to be mediated by an exportin known as Chromosome Region Maintenance 1 (CRM1) (169). The export mechanism completes a reactivation cycle of STAT3, which is extremely important for signal activation from cell surface. Breaking this cycle by blocking STAT3 nuclear export, reduces STAT3 phosphorylation and induction of STAT3-responsive genes (170).

• ***DNA Binding and Gene Expression:*** transcriptional activity of STAT3 is maximized by S⁷²⁷ phosphorylation by various serine kinases including protein kinase C (PKC) and mitogen-activated protein kinases (MAPK) (171, 172). Inhibiting DNA-binding activity of STAT3 is another therapeutic strategy (111).

1.4 STAT3 DISRUPTION MODALITIES

Numerous modalities have been employed to achieve effective STAT3 inhibition in cancer (reviewed in (132, 173)). These modalities could be categorized according to the mode of action to: receptor antagonists, phosphorylation inhibitors, dimerization inhibitors, nuclear translocation inhibitors, DNA-binding inhibitors, and STAT3 synthesis inhibitors (Table 1.1).

- **Receptor Antagonists:** Although approaches of blocking upstream STAT3 signal, e.g. by antagonizing IL-6 receptor complex, might be effective for STAT3-signal shutdown, it is a non-specific approach that may possibly lead to several side effects. Moreover, since the activation of STAT3 in cancer is promoted by collateral pathways i.e. growth factor receptor and non-receptor TKs, blocking one upstream factor might not be sufficient for optimum tumor-cell killing. Inhibition of IL-6/gp130/STAT3 in multiple myeloma (MM), both primary cells isolated from patients' bone marrows and MM cell line, using IL-6 super-antagonist (Sant7) or anti-gp130 mAb showed significant inhibition of p-STAT3 and suppression of tumor cells proliferation. However, this was quickly reversed by stromal factors rendering the upstream strategy of inhibition rather insufficient for cancer therapy (174). Another study indicated that Sant7 treatment of IL-6-dependent B cell lymphoma efficiently inhibited STAT3 activation but was associated with only marginal induction of apoptosis and minor reduction in cell proliferation (175). In the same study, Sant7 was compared with a STAT3-phosphorylation inhibitor (AG490), which showed a significant reduction in both p-STAT3 expression and B lymphoma cells proliferation (175).

• **Phosphorylation Inhibitors:** Owing to the availability of an arsenal of natural and synthetic phosphorylation inhibitors, inhibition of STAT3 phosphorylation is probably the mostly carried out strategy in research (95, 173). Small molecules with TKs inhibitory activity such as tyrphostins (79) (AG490 (176, 177), WP1066 (178, 179), and TG101209 (180)), resveratrol (181, 182), and indirubin (183) have been reported to inhibit p-STAT3 in a variety of tumor cell lines (184). However, mechanistic understanding of these molecules remains to be fully elucidated. Moreover, the apparently-general manner by which these inhibitors perform suggests the possibility of various toxicities (173). JSI-124 (cucurbitacin I) is another small-molecular-weight inhibitor of STAT3 phosphorylation, which was not clearly shown to inhibit the catalytic activity of JAK, but has induced cell death and inhibited cell growth of transformed murine fibroblasts and human breast cancer at 10 μ M (185). However, due to the incomplete understanding of its mechanism of inhibition, as well as associated non-specific toxicities, the clinical application of JSI-124 was not possible. At effective JAK2/STAT3 inhibitory concentration, JSI-124 was shown to profoundly affect actin cytoskeleton *via* STAT3-independent mechanism in both cancerous and non-cancerous cells (186). More tolerable natural agents, such as curcumin, were reported to exert STAT3 inhibitory action in cancer (187). It was shown that curcumin inhibition of STAT3 phosphorylation is time dependent, where complete suppression of p-STAT3 was achieved after 4 h (188). However, the relatively high curcumin concentration used in these studies (40-50 μ M) raised a concern for its potential non-specific effects. Moreover, a phase II clinical trial

investigating the anti-cancer potential of curcumin in prostate cancer patients indicated the low bioavailability of curcumin when administered orally (189). Resveratrol is another inhibitor of p-STAT3 that carries a high potential for an anticancer therapeutic (181, 190). Originally, resveratrol was a naturally occurring phytoalexin with antioxidant and anti-inflammatory properties, and recently was shown to possess anti-STAT3 activity in several human cancer cell lines (129, 181, 191), where it induced apoptosis and inhibited proliferation and invasion in tumor cells (191, 192). However, the rather general effects of resveratrol on multiple proteins regulating cell cycle indicate the need for further mechanistic studies before clinical applications. Additionally, a more clinically-relevant agent was tested for p-STAT3 disruption. In a phase I/II clinical trial, tipifarnib (a farnesyl transferase inhibitor) was administered to patients with breast cancer in combination with doxorubicin and cyclophosphamide (193). The authors found that p-STAT3 was inhibited in tipifarnib-treated group of patients, which produced higher pathologic complete response rate than chemotherapy alone. Overall, since the inhibitory effect of STAT3 phosphorylation is suggested to be indirect through disrupting upstream components in STAT3 signaling pathway (173), potential side effects and toxicities at levels required for STAT3 inhibition limit clinical application of these compounds along with solubility, bioavailability and biological stability problems.

- ***Dimerization Inhibitors:*** Peptides and peptidomimetics were introduced as inhibitors of STAT3 dimerization (194). These compounds consist of a short sequence of aminoacids designed to contain a phosphotyrosine that interacted

with the SH2 domain of STAT molecules to prevent their dimerization (195). They are designed to perform high selectivity toward STAT3 over the structurally related STAT5 and STAT1 (194). *In vitro* studies demonstrated the ability of peptidomimetics to block STAT3 dimerization and consecutive DNA binding (194, 196). However, the effectiveness of these molecules was limited by the poor cellular permeability and insufficient stability profile, which explains the need for the high-concentration needed (μM - mM) (173, 194, 196). An inverse approach to interact with STAT3 phosphotyrosyl residue, rather than SH2 domain, is exploited by peptide aptamers (197, 198). However, a lot of investigations are still needed regarding the effectiveness of these molecules as therapeutics. Non-peptidic small molecules have also been identified for STAT3-dimerization inhibition such as STA-1 (199, 200), S3I-201 (201), Stattic (202), and catechol (1,2-dihydroxybenzene) compounds (203). Although these dimerization inhibitors have better physicochemical properties than their peptidic counterparts, they are still potent in the μM range indicating the need for more pharmaco-chemical improvement. Moreover, a unique form of non-antisense G-rich DNA sequences called G-quartet-forming oligodeoxynucleotides (GQ-ODN) have been designed to disrupts STAT3 in cancer (204, 205). These molecules form four-stranded structures via inter- and intra-molecular bonding and stabilized by guanine residues (206). With the aid of computational modeling, GQ-ODN were designed to insert between two SH2 domains in STAT3 molecules to disrupt dimer formation (204-206). This modality was effective in inhibiting the growth of p-STAT3⁺ human cell lines such as prostate, breast, head and neck squamous cell

carcinoma (HNSCC), and non-small cell lung cancer (NSCLC) (204, 205, 207, 208). However, in spite of the promising efficacy, the specificity of GQ-ODN interaction with STAT3 but not other STATs still requires further investigation. Moreover, improvement of physicochemical properties of these nucleic acids is needed for pharmaceutical applications.

- **Nuclear translocation Inhibitors:** Since STAT3 dimer binds to a specific sequence in the promoter region of the target gene, a modality called Decoy-ODN exploiting this mechanism was developed to present similar sequence of double-stranded oligonucleotide to STAT3 dimers in the cytoplasm (209). As a result, STAT3 dimers will bind to this decoy and then be precluded from nuclear translocation leading to STAT3 signaling disruption (209). The efficacy of this strategy was proven in human SCCHN cells *in vitro* and *in vivo* as inhibition of cancer cells proliferation and induction of apoptosis (209, 210), along with other human cancer cell lines such as lung (211) and hepatocellular carcinoma (HCC) (212). A decoy ODN is currently in phase III clinical trials for the prevention of vein graft failure in lower extremity after bypass surgery (213). This is a good indication for the transition of this approach from bench to bedside. Although encouraging, further evaluation of this strategy for cancer therapy is needed especially that the mechanism of action suggests a temporary nature of intervention.

- **DNA Binding Inhibitors:** Platinum (IV) compounds were investigated as they are shown to interfere with the interaction of STAT3 dimers with the corresponding *cis*-element in the target gene leading to inhibition of cyclin D1

and Bcl-xL production, cell proliferation, and malignant transformation in NIH/v-Src mouse fibroblasts and human breast cancer cells (173, 214). The presence of a clinically-approved platinum compound for cancer treatment, cisplatin, increased the potential of other platinum compounds that shows anti-cancer effect such as CPA-1 and CPA-7 to be clinically evaluated (215). However, cisplatin differs from CPA-1 and CPA-7 in two major aspects. First, it is platinum (II) not platinum (IV) compound. Second, cisplatin has no activity against STAT3 (173, 214, 215). Therefore, it is quite difficult to extrapolate the clinical relevance of platinum (IV) compounds from cisplatin efficacy or safety records. In fact, platinum (IV) compounds require concentrations in μM range to exert their inhibitory action (214). This might be a cause for potential side effects especially when molecular evidence showed that they are only 2.4 times selective for STAT3 over the structurally related protein STAT1 (215). Nevertheless, the effectiveness of platinum (IV) compounds in preventing STAT3/DNA interaction in several *in vivo* tumor models such as CT-26 mouse colon carcinoma and makes its further investigation for therapeutic application worthwhile. Especially that the mass production of such molecules is easier, more reproducible, and probably less than a biological counterpart from a pharmaceutical point of view. Other agents have shown inhibitory effects on STAT3/DNA binding. The natural product galiellalactone showed efficacy on many human tumor cell lines including HepG2 hepatoma cells (216) and DU145 human prostate xenograft (217). Similarly, peptide aptamers were shown to inhibit STAT3/DNA binding in human U266 multiple myeloma cells and B16 murine melanoma cells (198, 218). However,

turning these agents into therapeutics require more optimization of physicochemical properties and biological efficacy.

- ***STAT3 Synthesis Inhibitors:*** Probably, the most specific approach to tackle diseases emerged with the concept of targeting disease-causing proteins at the mRNA level (219). The mostly investigated modalities for this purpose are antisense ODN and siRNA. Both share the basis of complementary interaction of a short nucleic acid segment with a target mRNA leading to its destruction and eventually inhibition of protein synthesis. Therefore, they provide a rational strategy to overcome oncogenic proteins that are overexpressed in cancer cells. Nevertheless, antisense ODN and siRNA carry fundamental differences that may reflect on their therapeutic potential (summarized in Table 1.2).

Antisense ODN is a short single-stranded nucleic acid segment (17-22 bp) designed to bind with its complementary region in the target mRNA via Watson-Crick base pairing system. The formed hetero-duplex recognized as foreign gets destroyed by the triggered nuclease RNase H (220). On the other hand, siRNA which is a short double-stranded RNA segment (19-21 bp) incorporates first into an endogenous cytoplasmic protein machinery to form a complex known as RNA-induced silencing complex (RISC). This complex mediates the unwinding of siRNA keeping only the antisense strand, which binds to its complementary region on mRNA. Thereafter, a catalytic protein within RISC cleaves the mRNA exactly in the middle of the recognition region leaving the siRNA intact (220). This mechanistic difference gives an advantage to RNA interference (RNAi) by siRNA over antisense ODN approach because unlike antisense ODN which gets

digested with the target mRNA upon RNase H degradation, siRNA incorporated in RISC complex is reused to destroy many copies of the target mRNA.

For STAT3 downregulation, antisense ODN introduced into cells caused selective degradation of STAT3 mRNA accompanied by tumor growth inhibition of prostate carcinoma (80) and LGL leukemia (221). Consistently, in a mouse xenograft model, SSCHN treated with STAT3 antisense plasmid resulted in decreased constitutive Stat3 activity, decreased Bcl-xL levels and increased apoptosis, compared to tumors treated with vehicle control (222). Although antisense ODNs preceded siRNA in approval for clinical practice or in clinical trials (reviewed in (223, 224)), no anti-STAT3 ODNs are in clinical trials yet. It is just recently a recent phase I trial was published that indirectly exploit STAT3 mechanism by targeting EGFR with antisense ODNs for head and neck cancer treatment (225). Similarly, STAT3 silencing by siRNA was shown to induce apoptosis in astrocytoma cells (226) and was shown to induce apoptosis and limit invasiveness and motility of human prostate cancer cells (227). It also significantly suppressed human breast cancer cell growth in xenograft model (228). Although RNAi is a newly introduced technology, siRNA rapidly advanced from research to clinical trials for genetic and viral disease (reviewed in (229)). This transition is encouraging to explore the clinical applicability of anti-STAT3 siRNA for cancer treatment. The fact that a single siRNA could be reused by cellular machinery to attack more than one copy of mRNA might contribute to the significantly lower concentrations needed for siRNA to mediate the silencing process compared to antisense ODN. In turn, by reducing the amount

administered for therapy, patients are less exposed to possible off-target effects of the nucleic acids and potential toxicities of the used vehicle. However, siRNA suffer from significant drawbacks that prevent its direct application in a biological system (reviewed in (220)). These drawbacks include: instability in presence of serum nucleases (230), poor pharmacokinetic and biodistribution profile (231), and low cellular internalization (232). Therefore, in order to be considered for therapeutic applications, siRNA needs optimal delivery strategy.

Table 1.1 Various modalities of disrupting STAT3 signaling pathway used in cancer cells. Advantages and disadvantages are listed from a therapeutic prospective [adopted from (173)].

Target Step	Inhibitor(s)	Advantages	Disadvantages
Receptor	Sant7 gp130 mAb	Complete blocking activity	None specificity
Phosphorylation	Tyrphostins JSI-124 Curcumin G-quartet ODN	High effectiveness Ease of production Direct application	Low oral bioavailability Unknown mechanisms Cytotoxicity None specificity
Dimerization	Peptide derivatives Non-peptidic compounds	Moderate specificity	Low effectiveness Impermeability Instability
Translocation	Decoy ODN	High specificity	High dose requirement Temporary intervention Impermeability Instability
DNA Binding	Platinum (IV) Compounds Gaiellactone Peptide aptamers	Clinical relevance Ease of production Direct application	Unknown mechanisms Cytotoxicity None specificity
STAT3 Synthesis	Antisense ODN siRNA	Very high specificity Low concentration (nM) Low chance for off-target effects	Temporary intervention Impermeability Instability

Table 1.2 Fundamental differences between antisense ODN and siRNA

	Antisense ODN	siRNA
Nucleotide sugar	Deoxyribose	Ribose
Structure	Single stranded	Double stranded
Length	16-30 bp	19-21 bp
Molecular weight	~ 6-9 kDa	~ 13-14 kDa
Precursor availability	No	Yes
Site of action	Cytoplasm and nucleus	Cytoplasm
mRNA cleavage	RNase H	RISC
Degradation upon activity	Yes	No
Effective concentration	50-400 nM	5-100 nM

1.5 STRATEGIES FOR siRNA DELIVERY

Vectors used for nucleic acid delivery are either of viral or non-viral origins. For clinical use, viral vectors are not preferred because they are associated with numerous drawbacks. They have been shown to cause inflammation of the transduced tissue (233), elicit an immune reaction to viral particles (234), and possibly lead to uncontrolled cell proliferation of transduced cells (235). On the other hand, non-viral vectors are considered more favorable in therapy because of their improved safety profiles and their relatively more convenient preparation techniques (236-239).

Numerous non-viral carriers were investigated for siRNA delivery including: cationic liposomes (240), polyelectrolyte-complex micelles (241), water soluble lipopolymers (242), polycationic dendrimers (243), polyethylenimines (PEIs) polyplexes (239), and polymeric NPs (244). In this chapter the focus will be given to two systems for anti-STAT3 siRNA delivery (Figure 1.7): (i) complexes of PEI and its derivatives for cancer cell targeting, and (ii) PLGA NPs for DCs targeting.

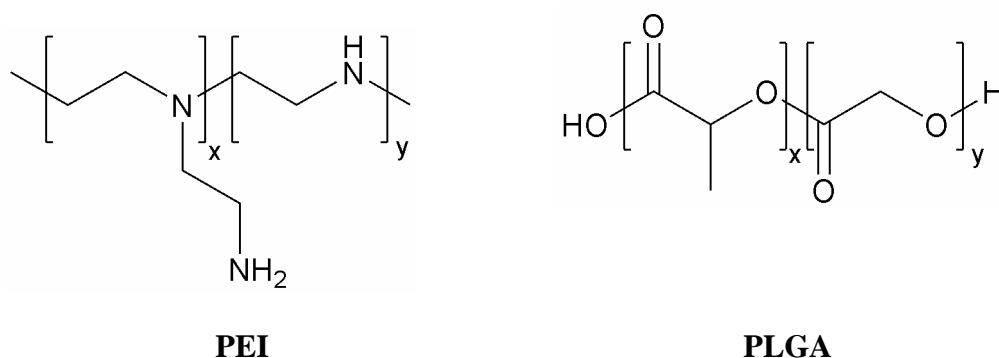


Figure 1.7 Chemical Structures of PEI and PLGA. PEI (left) showing 1°, 2°, and 3° amines, x represents number of branching units. PLGA (right), x and y represent number of lactic and glycolic acid, respectively.

1.5.1 Polyethylenimine

PEI is a linear or branched cationic poly-amine that has been used for paper production, shampoo manufacturing, and water purification, and it is considered the gold standard for gene delivery in cancer (245). It is an attractive carrier for intracellular gene delivery because of its well-established ability to condense nucleic acids *via* electrostatic interaction between the anionic phosphate in the nucleic acid backbone and the cationic primary, secondary, and tertiary amines of the polymer (246, 247). PEI was shown to be effective in condensing and delivering siRNA to target mRNA *in vitro* and *in vivo* (248, 249). Moreover, it was able to transfer functionally active siRNA to a variety of cancer cells (250). For instance, PEI-complexed siRNAs were shown to promote antitumoral effect in U87 orthotopic mouse glioblastoma model growing intracranially (251). A significant reduction in tumor growth was also observed after intraperitoneal (i.p.) administration of PEI-siRNA complexes in mouse model targeting the c-erbB2/neu (HER-2) receptor (249). Additionally, PEI complexes of polyethylene glycol (PEG)-siRNA conjugates targeting VEGF showed over 95% effective silencing of VEGF expression in human prostate cell line PC-3 (252). However, the efficacy of PEI-mediated siRNA delivery was shown to be dependent on the structure and molecular weight of the PEI used in the formulation (239). Overall, branched PEI (25 kDa) is a more effective system for nucleic acid delivery than its linear counterpart owing to higher complexation ability, smaller size of its particles, and better interaction with target cells (253).

One of PEI's advantages is the relative simplicity in modifying its backbone to generate delivery systems that are target specific and possibly less toxic than native PEI. In one study, grafting PEG-folate residues to PEI was shown to efficiently deliver functionally-active siRNA into the high-folate-receptor-expressing KB cells (254). In addition, targeting cancer neovasculature *in vivo* lead to efficient silencing of VEGFR-2 by PEI complexes that were decorated with Arg-Gly-Asp (RGD) peptides (255). Hydrophobic modification of PEI to improve cell membrane interactions is an alternative approach for siRNA delivery, as compared to receptor-specific modifications. One study has demonstrated that attaching cholesterol to PEI backbone promoted siRNA stability in water-soluble lipopolyplexes and inhibited VEGF expression in PC-3 cells *in vitro*, and ultimately induced tumor regression *in vivo* (242). PEI-cholesterol conjugates were also shown to enhance intracellular uptake of DNA and improve transfection efficiency (256). This system was effective for intratumoral (i.t.) delivery *in vivo* as well (257, 258). Such results highlight the importance of lipid components in cationic polymers for efficient siRNA delivery in cancer.

1.5.2 Poly(D,L lactic-co-glycolic) acid

PLGA is an FDA approved biodegradable polymer that has been widely used in the manufacturing of surgical sutures and controlled release drug products (259, 260). This co-polymer is an aliphatic polyester that is composed of varying proportions of lactic and glycolic acids. Upon encountering aqueous media, PLGA gets hydrolyzed into its monomeric components lactic and glycolic acid,

which in turn enter Krebs cycle (259). PLGA has been widely used to formulate NPs that can encapsulate a wide range of biologically active compounds of various physicochemical properties (e.g low molecular weight drugs, peptides and proteins, lipids, and nucleic acids), which explains the broad spectrum of PLGA NPs application (261).

PLGA NPs were extensively employed for cancer vaccine delivery to DCs because of the controlled release profile, preferential uptake by DCs, and possibility of co-delivering immunomodulatory molecules with cancer antigens to activate DCs (reviewed in (262, 263)). Therefore, it is rational to include anti-STAT3 siRNA in this regimen to counter tumor-induced STAT3 activation in DCs. This concept was proven by the work of Hua Yu's group who found out that targeting DCs by combining the immunostimulatory molecule CpG with siRNA against STAT3 leads to the activation of tumor-associated immune cells and potentiating of antitumor immune response (264). Although PLGA has been used to as a vehicle for siRNA delivery targeting a variety of molecular targets in multiple cancer cell types (265-267), no attempt was taken to deliver anti-STAT3 siRNA to DCs as a part of tumor management application. Only recently, a strategy to target DCs with PEI-decorated PLGA NPs encapsulating anti-IL-10 siRNA and DNA vaccine has lead to significant switch toward Th1 response, which is the favorable response for cancer immunotherapy (268). This is an indirect indication of the validity of STAT3 knockdown by siRNA in DCs using PLGA NPs because IL-10 and STAT3 perform an autocrine loop in DC (269).

1.6 RATIONALE and HYPOTHESES

In the previous sections, we have provided evidence from literature on the potential of constitutively active STAT3 as a target for cancer therapy. Owing to its role as a cross-talk mediator between cancer and immune cells, targeting STAT3 in cancer cells as well as DCs would be beneficial for a better therapeutic outcome. The rationale of our work was based on targeting STAT3, in both cell types, at the mRNA level, i.e. preventing STAT3 synthesis, rather than upstream inhibition of STAT3 signaling pathway. Moreover, we propose using siRNA for mRNA targeting owing to the higher specificity and potency compared to anti-sense ODNs. In this context, nano-carriers to deliver siRNA silencing STAT3 to cancer cells and DCs were designed. We chose fatty-acid modified PEI polyplexes for cancer targeting, while, for DC targeting, we further formulated those polyplexes in PLGA NPs. Our hypotheses (summarized in Figure 1.8) state that:

- 1) STAT3 knockdown by siRNA in B16 cells using fatty-acid modified PEI polyplexes nano-carriers leads to apoptosis *in vitro* and tumor regression *in vivo*.
- 2) Down-modulation of STAT3 by siRNA nano-carriers of fatty-acid modified PEI polyplexes in tumor cells induces bystander immune response *in vitro* and *in vivo*.
- 3) In tumor-exposed DCs, direct knockdown of STAT3 by siRNA using PLGA nanoparticles loaded with fatty-acid modified polyplexes restores DC phenotypic maturation and functional activation in an otherwise inhibitory microenvironment.

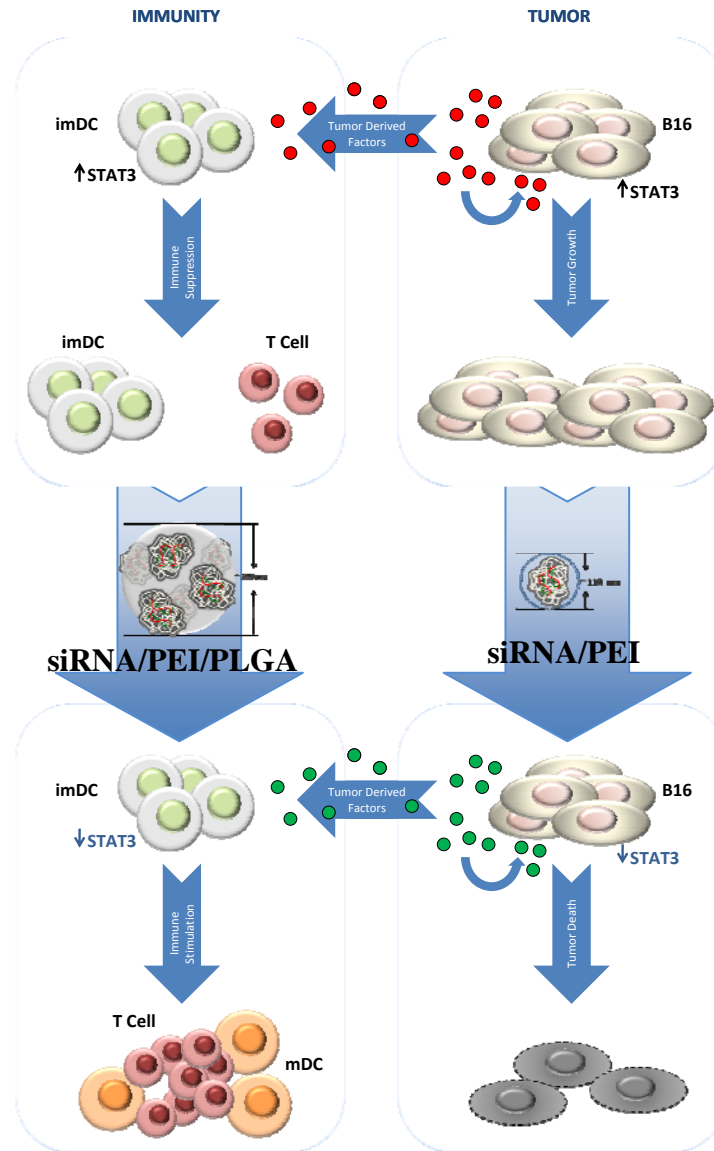


Figure 1.8 Research Hypotheses. The knockdown of STAT3 in B16 melanoma cells by siRNA/PEI polyplexes leads to tumor cell death and changes the cytokine profile in tumor milieu toward pro-apoptotic immunostimulatory microenvironment. Moreover, the direct inhibition of STAT3 by siRNA in tumor-exposed DCs using PLGA NPs leads to DC maturation, activation, and ability to stimulate T cell proliferation.

1.7 OBJECTIVES

- 1) Formulation and characterization of siRNA/PEI complexes using novel lipid-modified PEI derivatives for B16 cells targeting.
- 2) Studying the inhibitory effect of siRNA complexes on STAT3 by targeting B16 melanoma *in vitro* and *in vivo*.
- 3) Developing a model for tumor-mediated immune suppression *via* STAT3 hyperactivation in DCs using B16 melanoma and evaluation of bystander immune response upon STAT3 knockdown in cancer cells *in vitro* and *in vivo*.
- 4) Developing a PLGA-based NP formulation for anti-STAT3 siRNA in tumor-exposed DCs and determining DC re-activation upon STAT3 knockdown.

1.8 REFERENCES

1. Strouhal E. Tumors in the remains of ancient Egyptians. *Am J Phys Anthropol.* 1976 Nov;45(3 pt. 2):613-20.
2. Harrington L, Bristow RG, Hill RP, Tannock IF. Introduction to Cancer Biology. In: Harrington L, Bristow RG, Hill RP, Tannock IF, editors. *The Basic Science of Oncology.* 4 ed: McGraw-Hill Professional; 2005. p. 1-3.
3. Antman KH, Eilber FR, Shiu MH. Soft tissue sarcomas: current trends in diagnosis and management. *Curr Probl Cancer.* 1989 Nov-Dec;13(6):337-67.
4. Canadian Cancer Society's Steering Committee: *Canadian Cancer Statistics 2009.* Toronto. Canadian Cancer Society; 2009. p. 1-127.
5. Baluska F, Volkmann D, Barlow PW. Eukaryotic cells and their cell bodies: Cell Theory revised. *Ann Bot (Lond).* 2004 Jul;94(1):9-32.
6. Bishop JM, Weinberg RA. *Molecular oncology.* New York: Scientific American Inc; 1996.
7. Balkwill F, Mantovani A. Inflammation and cancer: back to Virchow? *Lancet.* 2001 Feb 17;357(9255):539-45.
8. Prendergast GC, Jaffee EM. Introduction-Cancer Immunotherapy. In: C. PG, Jaffee EM, editors. *Cancer Immunotherapy.* 1 ed: Academic Press; 2007. p. 3-8.
9. Ehrlich P. Ueber den jetzigen stand der karzinomforschung. *Ned Tijdschr Geneesk.* 1909;53:273-90.
10. Burnet M. Cancer: a biological approach. III. Viruses associated with neoplastic conditions. IV. Practical applications. *Br Med J.* 1957 Apr 13;1(5023):841-7.
11. Thomas L. In: Lawrence HS, editor. *Cellular and Humoral Aspects of the Hypersensitive State.* New York: Hoeber-Harper; 1959. p. 529-32.
12. Burnet FM. The concept of immunological surveillance. *Prog Exp Tumor Res.* 1970;13:1-27.
13. Wilson DB. Immunological surveillance. *Cell Immunol.* 1970 Jul;1(2):245-9.
14. Dunn GP, Bruce AT, Ikeda H, Old LJ, Schreiber RD. Cancer immunoediting: from immunosurveillance to tumor escape. *Nat Immunol.* 2002 Nov;3(11):991-8.
15. Stutman O. Tumor development after 3-methylcholanthrene in immunologically deficient athymic-nude mice. *Science.* 1974 Feb 8;183(124):534-6.
16. Dighe AS, Richards E, Old LJ, Schreiber RD. Enhanced in vivo growth and resistance to rejection of tumor cells expressing dominant negative IFN gamma receptors. *Immunity.* 1994 Sep;1(6):447-56.
17. Kaplan DH, Shankaran V, Dighe AS, Stockert E, Aguet M, Old LJ, et al. Demonstration of an interferon gamma-dependent tumor surveillance system in immunocompetent mice. *Proc Natl Acad Sci U S A.* 1998 Jun 23;95(13):7556-61.
18. Street SE, Cretney E, Smyth MJ. Perforin and interferon-gamma activities independently control tumor initiation, growth, and metastasis. *Blood.* 2001 Jan 1;97(1):192-7.

19. Street SE, Trapani JA, MacGregor D, Smyth MJ. Suppression of lymphoma and epithelial malignancies effected by interferon gamma. *J Exp Med.* 2002 Jul 1;196(1):129-34.
20. Russell JH, Ley TJ. Lymphocyte-mediated cytotoxicity. *Annu Rev Immunol.* 2002;20:323-70.
21. van den Broek ME, Kagi D, Ossendorp F, Toes R, Vamvakas S, Lutz WK, et al. Decreased tumor surveillance in perforin-deficient mice. *J Exp Med.* 1996 Nov 1;184(5):1781-90.
22. Smyth MJ, Thia KY, Street SE, Cretney E, Trapani JA, Taniguchi M, et al. Differential tumor surveillance by natural killer (NK) and NKT cells. *J Exp Med.* 2000 Feb 21;191(4):661-8.
23. Smyth MJ, Thia KY, Street SE, MacGregor D, Godfrey DI, Trapani JA. Perforin-mediated cytotoxicity is critical for surveillance of spontaneous lymphoma. *J Exp Med.* 2000 Sep 4;192(5):755-60.
24. Dunn GP, Old LJ, Schreiber RD. The three Es of cancer immunoediting. *Annu Rev Immunol.* 2004;22:329-60.
25. Dunn GP, Koebel CM, Schreiber RD. Interferons, immunity and cancer immunoediting. *Nat Rev Immunol.* 2006 Nov;6(11):836-48.
26. Carmeliet P, Jain RK. Angiogenesis in cancer and other diseases. *Nature.* 2000 Sep 14;407(6801):249-57.
27. Sternlicht MD, Werb Z. How matrix metalloproteinases regulate cell behavior. *Annu Rev Cell Dev Biol.* 2001;17:463-516.
28. Krieg C, Boyman O. The role of chemokines in cancer immune surveillance by the adaptive immune system. *Semin Cancer Biol.* 2009 Apr;19(2):76-83.
29. Albert ML, Sauter B, Bhardwaj N. Dendritic cells acquire antigen from apoptotic cells and induce class I-restricted CTLs. *Nature.* 1998 Mar 5;392(6671):86-9.
30. Sallusto F, Mackay CR, Lanzavecchia A. The role of chemokine receptors in primary, effector, and memory immune responses. *Annu Rev Immunol.* 2000;18:593-620.
31. Srivastava RM, Khar A. Dendritic cells and their receptors in antitumor immune response. *Curr Mol Med.* 2009 Aug;9(6):708-24.
32. Loeb LA, Loeb KR, Anderson JP. Multiple mutations and cancer. *Proc Natl Acad Sci U S A.* 2003 Feb 4;100(3):776-81.
33. Loeb LA, Bielas JH, Beckman RA. Cancers exhibit a mutator phenotype: clinical implications. *Cancer Res.* 2008 May 15;68(10):3551-7; discussion 7.
34. MacKie RM, Reid R, Junor B. Fatal melanoma transferred in a donated kidney 16 years after melanoma surgery. *N Engl J Med.* 2003 Feb 6;348(6):567-8.
35. Liu JQ, Bai XF. Overcoming immune evasion in T cell therapy of cancer: lessons from animal models. *Curr Mol Med.* 2008 Feb;8(1):68-75.
36. Seruga B, Zhang H, Bernstein LJ, Tannock IF. Cytokines and their relationship to the symptoms and outcome of cancer. *Nat Rev Cancer.* 2008 Nov;8(11):887-99.

37. Marincola FM, Jaffee EM, Hicklin DJ, Ferrone S. Escape of human solid tumors from T-cell recognition: molecular mechanisms and functional significance. *Adv Immunol.* 2000;74:181-273.
38. Eble JA, Haier J. Integrins in cancer treatment. *Curr Cancer Drug Targets.* 2006 Mar;6(2):89-105.
39. Heikkila K, Ebrahim S, Lawlor DA. Systematic review of the association between circulating interleukin-6 (IL-6) and cancer. *Eur J Cancer.* 2008 May;44(7):937-45.
40. Urosevic M, Dummer R. HLA-G and IL-10 expression in human cancer--different stories with the same message. *Semin Cancer Biol.* 2003 Oct;13(5):337-42.
41. Jones E, Pu H, Kyprianou N. Targeting TGF-beta in prostate cancer: therapeutic possibilities during tumor progression. *Expert Opin Ther Targets.* 2009 Feb;13(2):227-34.
42. Grothey A, Galanis E. Targeting angiogenesis: progress with anti-VEGF treatment with large molecules. *Nat Rev Clin Oncol.* 2009 Sep;6(9):507-18.
43. Wilson KJ, Gilmore JL, Foley J, Lemmon MA, Riese DJ, 2nd. Functional selectivity of EGF family peptide growth factors: implications for cancer. *Pharmacol Ther.* 2009 Apr;122(1):1-8.
44. Hatake K, Tokudome N, Ito Y. Next generation molecular targeted agents for breast cancer: focus on EGFR and VEGFR pathways. *Breast Cancer.* 2007;14(2):132-49.
45. Prendergast GC. Immune escape as a fundamental trait of cancer: focus on IDO. *Oncogene.* 2008 Jun 26;27(28):3889-900.
46. Yu H, Jove R. The STATs of cancer--new molecular targets come of age. *Nat Rev Cancer.* 2004 Feb;4(2):97-105.
47. Liu X, Li J, Zhang J. STAT3-decoy ODN inhibits cytokine autocrine of murine tumor cells. *Cell Mol Immunol.* 2007 Aug;4(4):309-13.
48. Chen Z, Han ZC. STAT3: a critical transcription activator in angiogenesis. *Med Res Rev.* 2008 Mar;28(2):185-200.
49. Kortylewski M, Yu H. Role of Stat3 in suppressing anti-tumor immunity. *Curr Opin Immunol.* 2008 Apr;20(2):228-33.
50. Riker AI, Jove R, Daud AI. Immunotherapy as part of a multidisciplinary approach to melanoma treatment. *Front Biosci.* 2006;11:1-14.
51. Darnell JE, Jr., Kerr IM, Stark GR. Jak-STAT pathways and transcriptional activation in response to IFNs and other extracellular signaling proteins. *Science.* 1994 Jun 3;264(5164):1415-21.
52. Schindler C, Fu XY, Improtta T, Aebersold R, Darnell JE, Jr. Proteins of transcription factor ISGF-3: one gene encodes the 91-and 84-kDa ISGF-3 proteins that are activated by interferon alpha. *Proc Natl Acad Sci U S A.* 1992 Aug 15;89(16):7836-9.
53. Darnell JE, Jr. Introduction: a brief history of the STATs and a glance at the future. In: Sehgal PB, Levy DE, Hirano T, editors. *Signal Transducers and Activators of Transcription (STATs) Activation and Biology.* 1 ed: Springer; 2003. p. 1-8.

54. Zhong Z, Wen Z, Darnell JE, Jr. Stat3: a STAT family member activated by tyrosine phosphorylation in response to epidermal growth factor and interleukin-6. *Science*. 1994 Apr 1;264(5155):95-8.
55. Zhong Z, Wen Z, Darnell JE, Jr. Stat3 and Stat4: members of the family of signal transducers and activators of transcription. *Proc Natl Acad Sci U S A*. 1994 May 24;91(11):4806-10.
56. Yamamoto K, Quelle FW, Thierfelder WE, Kreider BL, Gilbert DJ, Jenkins NA, et al. Stat4, a novel gamma interferon activation site-binding protein expressed in early myeloid differentiation. *Mol Cell Biol*. 1994 Jul;14(7):4342-9.
57. Wakao H, Gouilleux F, Groner B. Mammary gland factor (MGF) is a novel member of the cytokine regulated transcription factor gene family and confers the prolactin response. *Embo J*. 1995 Feb 15;14(4):854-5.
58. Hou J, Schindler U, Henzel WJ, Ho TC, Brasseur M, McKnight SL. An interleukin-4-induced transcription factor: IL-4 Stat. *Science*. 1994 Sep 16;265(5179):1701-6.
59. Shuai K. The STAT family of proteins in cytokine signaling. *Prog Biophys Mol Biol*. 1999;71(3-4):405-22.
60. Akira S, Nishio Y, Inoue M, Wang XJ, Wei S, Matsusaka T, et al. Molecular cloning of APRF, a novel IFN-stimulated gene factor 3 p91-related transcription factor involved in the gp130-mediated signaling pathway. *Cell*. 1994 Apr 8;77(1):63-71.
61. Luticken C, Wegenka UM, Yuan J, Buschmann J, Schindler C, Ziemiecki A, et al. Association of transcription factor APRF and protein kinase Jak1 with the interleukin-6 signal transducer gp130. *Science*. 1994 Jan 7;263(5143):89-92.
62. Raz R, Durbin JE, Levy DE. Acute phase response factor and additional members of the interferon-stimulated gene factor 3 family integrate diverse signals from cytokines, interferons, and growth factors. *J Biol Chem*. 1994 Sep 30;269(39):24391-5.
63. Heinrich PC, Behrmann I, Muller-Newen G, Schaper F, Graeve L. Interleukin-6-type cytokine signalling through the gp130/Jak/STAT pathway. *Biochem J*. 1998 Sep 1;334 (Pt 2):297-314.
64. Takeda K, Noguchi K, Shi W, Tanaka T, Matsumoto M, Yoshida N, et al. Targeted disruption of the mouse Stat3 gene leads to early embryonic lethality. *Proc Natl Acad Sci U S A*. 1997 Apr 15;94(8):3801-4.
65. Alonzi T, Maritano D, Gorgoni B, Rizzuto G, Libert C, Poli V. Essential role of STAT3 in the control of the acute-phase response as revealed by inducible gene inactivation [correction of activation] in the liver. *Mol Cell Biol*. 2001 Mar;21(5):1621-32.
66. Li W, Liang X, Kellendonk C, Poli V, Taub R. STAT3 contributes to the mitogenic response of hepatocytes during liver regeneration. *J Biol Chem*. 2002 Aug 9;277(32):28411-7.
67. Wegrzyn J, Potla R, Chwae YJ, Sepuri NB, Zhang Q, Koeck T, et al. Function of mitochondrial Stat3 in cellular respiration. *Science*. 2009 Feb 6;323(5915):793-7.

68. Alonzi T, Middleton G, Wyatt S, Buchman V, Betz UA, Muller W, et al. Role of STAT3 and PI 3-kinase/Akt in mediating the survival actions of cytokines on sensory neurons. *Mol Cell Neurosci*. 2001 Sep;18(3):270-82.
69. Schweizer U, Gunnarsen J, Karch C, Wiese S, Holtmann B, Takeda K, et al. Conditional gene ablation of Stat3 reveals differential signaling requirements for survival of motoneurons during development and after nerve injury in the adult. *J Cell Biol*. 2002 Jan 21;156(2):287-97.
70. Sano S, Itami S, Takeda K, Tarutani M, Yamaguchi Y, Miura H, et al. Keratinocyte-specific ablation of Stat3 exhibits impaired skin remodeling, but does not affect skin morphogenesis. *Embo J*. 1999 Sep 1;18(17):4657-68.
71. Chapman RS, Lourenco PC, Tonner E, Flint DJ, Selbert S, Takeda K, et al. Suppression of epithelial apoptosis and delayed mammary gland involution in mice with a conditional knockout of Stat3. *Genes Dev*. 1999 Oct 1;13(19):2604-16.
72. Humphreys RC, Bierie B, Zhao L, Raz R, Levy D, Hennighausen L. Deletion of Stat3 blocks mammary gland involution and extends functional competence of the secretory epithelium in the absence of lactogenic stimuli. *Endocrinology*. 2002 Sep;143(9):3641-50.
73. Akaishi H, Takeda K, Kaisho T, Shineha R, Satomi S, Takeda J, et al. Defective IL-2-mediated IL-2 receptor alpha chain expression in Stat3-deficient T lymphocytes. *Int Immunol*. 1998 Nov;10(11):1747-51.
74. Takeda K, Clausen BE, Kaisho T, Tsujimura T, Terada N, Forster I, et al. Enhanced Th1 activity and development of chronic enterocolitis in mice devoid of Stat3 in macrophages and neutrophils. *Immunity*. 1999 Jan;10(1):39-49.
75. Takeda K, Kaisho T, Yoshida N, Takeda J, Kishimoto T, Akira S. Stat3 activation is responsible for IL-6-dependent T cell proliferation through preventing apoptosis: generation and characterization of T cell-specific Stat3-deficient mice. *J Immunol*. 1998 Nov 1;161(9):4652-60.
76. Kano A, Wolfgang MJ, Gao Q, Jacoby J, Chai GX, Hansen W, et al. Endothelial cells require STAT3 for protection against endotoxin-induced inflammation. *J Exp Med*. 2003 Nov 17;198(10):1517-25.
77. Buettner R, Mora LB, Jove R. Activated STAT Signaling in Human Tumors Provides Novel Molecular Targets for Therapeutic Intervention. *Clin Cancer Res*. 2002;8:945-54.
78. Grandis JR, Drenning SD, Chakraborty A, Zhou MY, Zeng Q, Pitt AS, et al. Requirement of Stat3 but not Stat1 activation for epidermal growth factor receptor-mediated cell growth *In vitro*. *J Clin Invest*. 1998 Oct 1;102(7):1385-92.
79. Catlett-Falcone R, Landowski TH, Oshiro MM, Turkson J, Levitzki A, Savino R, et al. Constitutive Activation of Stat3 Signaling Confers Resistance to Apoptosis in Human U266 Myeloma Cells. *Immunity*. 1999;10:105-15.
80. Mora LB, Buettner R, Seigne J, Diaz J, Ahmad N, Garcia R, et al. Constitutive activation of Stat3 in human prostate tumors and cell lines: direct inhibition of Stat3 signaling induces apoptosis of prostate cancer cells. *Cancer Res*. 2002 Nov 15;62(22):6659-66.

81. Jiang H, Yu J, Guo H, Song H, Chen S. Upregulation of survivin by leptin/STAT3 signaling in MCF-7 cells. *Biochem Biophys Res Commun*. 2008 Mar 28;368(1):1-5.
82. Wang W, Edington HD, Rao UN, Jukic DM, Wang H, Shipe-Spotloe JM, et al. STAT3 as a biomarker of progression in atypical nevi of patients with melanoma: dose-response effects of systemic IFNalpha therapy. *J Invest Dermatol*. 2008 Aug;128(8):1997-2002.
83. Bowman T, Garcia R, Turkson J, Jove R. STATs in oncogenesis. *Oncogene*. 2000 May 15;19(21):2474-88.
84. Darnell JE, Jr. Transcription factors as targets for cancer therapy. *Nat Rev Cancer*. 2002 Oct;2(10):740-9.
85. Turkson J. STAT proteins as novel targets for cancer drug discovery. *Expert Opin Ther Targets*. 2004 Oct;8(5):409-22.
86. Wang T, Niu G, Kortylewski M, Burdelya L, Shain K, Zhang S, et al. Regulation of the innate and adaptive immune responses by Stat-3 signaling in tumor cells. *Nat Med*. 2004 Jan;10(1):48-54.
87. Darnell JE. Validating Stat3 in cancer therapy. *Nat Med*. 2005 Jun;11(6):595-6.
88. Haura EB, Turkson J, Jove R. Mechanisms of disease: Insights into the emerging role of signal transducers and activators of transcription in cancer. *Nat Clin Pract Oncol*. 2005 Jun;2(6):315-24.
89. Migone TS, Lin JX, Cereseto A, Mulloy JC, O'Shea JJ, Franchini G, et al. Constitutively activated Jak-STAT pathway in T cells transformed with HTLV-I. *Science*. 1995 Jul 7;269(5220):79-81.
90. Yoshida T, Hanada T, Tokuhisa T, Kosai K, Sata M, Kohara M, et al. Activation of STAT3 by the hepatitis C virus core protein leads to cellular transformation. *J Exp Med*. 2002 Sep 2;196(5):641-53.
91. Yu CL, Meyer DJ, Campbell GS, Larner AC, Carter-Su C, Schwartz J, et al. Enhanced DNA-binding activity of a Stat3-related protein in cells transformed by the Src oncoprotein. *Science*. 1995 Jul 7;269(5220):81-3.
92. Bromberg JF, Horvath CM, Besser D, Lathem WW, Darnell JE, Jr. Stat3 activation is required for cellular transformation by v-src. *Mol Cell Biol*. 1998 May;18(5):2553-8.
93. Bromberg JF, Wrzeszczynska MH, Devgan G, Zhao Y, Pestell RG, Albanese C, et al. Stat3 as an Oncogene. *Cell*. 1999;98:295-303.
94. Zhang YW, Wang LM, Jove R, Vande Woude GF. Requirement of Stat3 signaling for HGF/SF-Met mediated tumorigenesis. *Oncogene*. 2002 Jan 10;21(2):217-26.
95. Aggarwal BB, Kunnumakkara AB, Harikumar KB, Gupta SR, Tharakan ST, Koca C, et al. Signal transducer and activator of transcription-3, inflammation, and cancer: how intimate is the relationship? *Ann N Y Acad Sci*. 2009 Aug;1171:59-76.
96. Hirano T, Ishihara K, Hibi M. Roles of STAT3 in mediating the cell growth, differentiation and survival signals relayed through the IL-6 family of cytokine receptors. *Oncogene*. 2000 May 15;19(21):2548-56.

97. Horiguchi A, Oya M, Marumo K, Murai M. STAT3, but not ERKs, mediates the IL-6-induced proliferation of renal cancer cells, ACHN and 769P. *Kidney Int.* 2002 Mar;61(3):926-38.
98. Wei D, Le X, Zheng L, Wang L, Frey JA, Gao AC, et al. Stat3 activation regulates the expression of vascular endothelial growth factor and human pancreatic cancer angiogenesis and metastasis. *Oncogene.* 2003 Jan 23;22(3):319-29.
99. Yu H, Kortylewski M, Pardoll D. Crosstalk between cancer and immune cells: role of STAT3 in the tumour microenvironment. *Nat Rev Immunol.* 2007 Jan;7(1):41-51.
100. Bhattacharya S, Ray RM, Johnson LR. STAT3-mediated transcription of Bcl-2, Mcl-1 and c-IAP2 prevents apoptosis in polyamine-depleted cells. *Biochem J.* 2005 Dec 1;392(Pt 2):335-44.
101. Zhuang L, Lee CS, Scolyer RA, McCarthy SW, Zhang XD, Thompson JF, et al. Mcl-1, Bcl-XL and Stat3 expression are associated with progression of melanoma whereas Bcl-2, AP-2 and MITF levels decrease during progression of melanoma. *Mod Pathol.* 2007 Apr;20(4):416-26.
102. Masuda M, Suzui M, Yasumatu R, Nakashima T, Kuratomi Y, Azuma K, et al. Constitutive activation of signal transducers and activators of transcription 3 correlates with cyclin D1 overexpression and may provide a novel prognostic marker in head and neck squamous cell carcinoma. *Cancer Res.* 2002 Jun 15;62(12):3351-5.
103. Ishii Y, Waxman S, Germain D. Tamoxifen stimulates the growth of cyclin D1-overexpressing breast cancer cells by promoting the activation of signal transducer and activator of transcription 3. *Cancer Res.* 2008 Feb 1;68(3):852-60.
104. Kiuchi N, Nakajima K, Ichiba M, Fukada T, Narimatsu M, Mizuno K, et al. STAT3 is required for the gp130-mediated full activation of the c-myc gene. *J Exp Med.* 1999 Jan 4;189(1):63-73.
105. Hong J, Zhao Y, Huang W. Blocking c-myc and stat3 by E. coli expressed and enzyme digested siRNA in mouse melanoma. *Biochem Biophys Res Commun.* 2006 Sep 22;348(2):600-5.
106. Xie TX, Wei D, Liu M, Gao AC, Ali-Osman F, Sawaya R, et al. Stat3 activation regulates the expression of matrix metalloproteinase-2 and tumor invasion and metastasis. *Oncogene.* 2004 Apr 29;23(20):3550-60.
107. Itoh M, Murata T, Suzuki T, Shindoh M, Nakajima K, Imai K, et al. Requirement of STAT3 activation for maximal collagenase-1 (MMP-1) induction by epidermal growth factor and malignant characteristics in T24 bladder cancer cells. *Oncogene.* 2006 Feb 23;25(8):1195-204.
108. Xiong H, Zhang ZG, Tian XQ, Sun DF, Liang QC, Zhang YJ, et al. Inhibition of JAK1, 2/STAT3 signaling induces apoptosis, cell cycle arrest, and reduces tumor cell invasion in colorectal cancer cells. *Neoplasia.* 2008 Mar;10(3):287-97.
109. Ivanov VN, Bhoumik A, Krasilnikov M, Raz R, Owen-Schaub LB, Levy D, et al. Cooperation between STAT3 and c-jun suppresses Fas transcription. *Mol Cell.* 2001 Mar;7(3):517-28.

110. Kortylewski M, Yu H. Stat3 as a potential target for cancer immunotherapy. *J Immunother.* 2007 Feb-Mar;30(2):131-9.
111. Xu Q, Briggs J, Park S, Niu G, Kortylewski M, Zhang S, et al. Targeting Stat3 blocks both HIF-1 and VEGF expression induced by multiple oncogenic growth signaling pathways. *Oncogene.* 2005 Aug 25;24(36):5552-60.
112. Kasprzycka M, Marzec M, Liu X, Zhang Q, Wasik MA. Nucleophosmin/anaplastic lymphoma kinase (NPM/ALK) oncoprotein induces the T regulatory cell phenotype by activating STAT3. *Proc Natl Acad Sci U S A.* 2006 Jun 27;103(26):9964-9.
113. Kortylewski M, Kujawski M, Herrmann A, Yang C, Wang L, Liu Y, et al. Toll-like receptor 9 activation of signal transducer and activator of transcription 3 constrains its agonist-based immunotherapy. *Cancer Res.* 2009 Mar 15;69(6):2497-505.
114. Wu S, Rhee KJ, Albesiano E, Rabizadeh S, Wu X, Yen HR, et al. A human colonic commensal promotes colon tumorigenesis via activation of T helper type 17 T cell responses. *Nat Med.* 2009 Sep;15(9):1016-22.
115. Shortman K, Liu YJ. Mouse and human dendritic cell subtypes. *Nat Rev Immunol.* 2002 Mar;2(3):151-61.
116. Kalinski P, Hilkens CM, Wierenga EA, Kapsenberg ML. T-cell priming by type-1 and type-2 polarized dendritic cells: the concept of a third signal. *Immunol Today.* 1999 Dec;20(12):561-7.
117. Trombetta ES, Mellman I. Cell biology of antigen processing in vitro and in vivo. *Annu Rev Immunol.* 2005;23:975-1028.
118. Vicari AP, Caux C, Trinchieri G. Tumour escape from immune surveillance through dendritic cell inactivation. *Semin Cancer Biol.* 2002 Feb;12(1):33-42.
119. Gabrilovich D. Mechanisms and functional significance of tumour-induced dendritic-cell defects. *Nat Rev Immunol.* 2004 Dec;4(12):941-52.
120. Zou W. Immunosuppressive networks in the tumour environment and their therapeutic relevance. *Nat Rev Cancer.* 2005 Apr;5(4):263-74.
121. Yanagawa Y, Iwabuchi K, Onoe K. Co-operative action of interleukin-10 and interferon-gamma to regulate dendritic cell functions. *Immunology.* 2009 Jul;127(3):345-53.
122. Matsumura Y, Kobayashi T, Ichiyama K, Yoshida R, Hashimoto M, Takimoto T, et al. Selective expansion of foxp3-positive regulatory T cells and immunosuppression by suppressors of cytokine signaling 3-deficient dendritic cells. *J Immunol.* 2007 Aug 15;179(4):2170-9.
123. Ilarregui JM, Croci DO, Bianco GA, Toscano MA, Salatino M, Vermeulen ME, et al. Tolerogenic signals delivered by dendritic cells to T cells through a galectin-1-driven immunoregulatory circuit involving interleukin 27 and interleukin 10. *Nat Immunol.* 2009 Sep;10(9):981-91.
124. Ghiringhelli F, Puig PE, Roux S, Parcellier A, Schmitt E, Solary E, et al. Tumor cells convert immature myeloid dendritic cells into TGF-beta-secreting cells inducing CD4+CD25+ regulatory T cell proliferation. *J Exp Med.* 2005 Oct 3;202(7):919-29.

125. Larmonier N, Marron M, Zeng Y, Cantrell J, Romanoski A, Sepassi M, et al. Tumor-derived CD4(+)CD25(+) regulatory T cell suppression of dendritic cell function involves TGF-beta and IL-10. *Cancer Immunol Immunother.* 2007 Jan;56(1):48-59.
126. Steinman RM, Hawiger D, Nussenzweig MC. Tolerogenic dendritic cells. *Annu Rev Immunol.* 2003;21:685-711.
127. Sumimoto H, Imabayashi F, Iwata T, Kawakami Y. The BRAF-MAPK signaling pathway is essential for cancer-immune evasion in human melanoma cells. *J Exp Med.* 2006 Jul 10;203(7):1651-6.
128. Gabrilovich DI, Chen HL, Girgis KR, Cunningham HT, Meny GM, Nadaf S, et al. Production of vascular endothelial growth factor by human tumors inhibits the functional maturation of dendritic cells. *Nat Med.* 1996 Oct;2(10):1096-103.
129. Bhardwaj A, Sethi G, Vadhan-Raj S, Bueso-Ramos C, Takada Y, Gaur U, et al. Resveratrol inhibits proliferation, induces apoptosis, and overcomes chemoresistance through down-regulation of STAT3 and nuclear factor-kappaB-regulated antiapoptotic and cell survival gene products in human multiple myeloma cells. *Blood.* 2007 Mar 15;109(6):2293-302.
130. Ahn KS, Sethi G, Sung B, Goel A, Ralhan R, Aggarwal BB. Guggulsterone, a farnesoid X receptor antagonist, inhibits constitutive and inducible STAT3 activation through induction of a protein tyrosine phosphatase SHP-1. *Cancer Res.* 2008 Jun 1;68(11):4406-15.
131. Otero DC, Poli V, David M, Rickert RC. Cutting edge: inherent and acquired resistance to radiation-induced apoptosis in B cells: a pivotal role for STAT3. *J Immunol.* 2006 Nov 15;177(10):6593-7.
132. Al Zaid Siddiquee K, Turkson J. STAT3 as a target for inducing apoptosis in solid and hematological tumors. *Cell Res.* 2008 Feb;18(2):254-67.
133. Hirano T, Nakajima K, Hibi M. Signaling mechanisms through gp130: a model of the cytokine system. *Cytokine Growth Factor Rev.* 1997 Dec;8(4):241-52.
134. Reich NC, Liu L. Tracking STAT nuclear traffic. *Nat Rev Immunol.* 2006 Aug;6(8):602-12.
135. Shuai K, Liu B. Regulation of JAK-STAT signalling in the immune system. *Nat Rev Immunol.* 2003 Nov;3(11):900-11.
136. Levy DE, Darnell JE, Jr. Stats: transcriptional control and biological impact. *Nat Rev Mol Cell Biol.* 2002 Sep;3(9):651-62.
137. Becker S, Groner B, Muller CW. Three-dimensional structure of the Stat3beta homodimer bound to DNA. *Nature.* 1998 Jul 9;394(6689):145-51.
138. Vinkemeier U, Cohen SL, Moarefi I, Chait BT, Kuriyan J, Darnell JE, Jr. DNA binding of in vitro activated Stat1 alpha, Stat1 beta and truncated Stat1: interaction between NH2-terminal domains stabilizes binding of two dimers to tandem DNA sites. *Embo J.* 1996 Oct 15;15(20):5616-26.
139. John S, Vinkemeier U, Soldaini E, Darnell JE, Jr., Leonard WJ. The significance of tetramerization in promoter recruitment by Stat5. *Mol Cell Biol.* 1999 Mar;19(3):1910-8.

140. Bromberg J, Darnell JE, Jr. The role of STATs in transcriptional control and their impact on cellular function. *Oncogene*. 2000 May 15;19(21):2468-73.
141. Ma J, Cao X. Regulation of Stat3 nuclear import by importin alpha5 and importin alpha7 via two different functional sequence elements. *Cell Signal*. 2006 Aug;18(8):1117-26.
142. Sekimoto T, Imamoto N, Nakajima K, Hirano T, Yoneda Y. Extracellular signal-dependent nuclear import of Stat1 is mediated by nuclear pore-targeting complex formation with NPI-1, but not Rch1. *Embo J*. 1997 Dec 1;16(23):7067-77.
143. Shuai K, Horvath CM, Huang LH, Qureshi SA, Cowburn D, Darnell JE, Jr. Interferon activation of the transcription factor Stat91 involves dimerization through SH2-phosphotyrosyl peptide interactions. *Cell*. 1994 Mar 11;76(5):821-8.
144. Wen Z, Zhong Z, Darnell JE, Jr. Maximal activation of transcription by Stat1 and Stat3 requires both tyrosine and serine phosphorylation. *Cell*. 1995 Jul 28;82(2):241-50.
145. Heinrich PC, Behrmann I, Haan S, Hermanns HM, Muller-Newen G, Schaper F. Principles of interleukin (IL)-6-type cytokine signalling and its regulation. *Biochem J*. 2003 Aug 15;374(Pt 1):1-20.
146. Kamimura D, Ishihara K, Hirano T. IL-6 signal transduction and its physiological roles: the signal orchestration model. *Rev Physiol Biochem Pharmacol*. 2003;149:1-38.
147. Boulanger MJ, Chow DC, Brevnova EE, Garcia KC. Hexameric structure and assembly of the interleukin-6/IL-6 alpha-receptor/gp130 complex. *Science*. 2003 Jun 27;300(5628):2101-4.
148. Muller-Newen G. The cytokine receptor gp130: faithfully promiscuous. *Sci STKE*. 2003 Sep 23;2003(201):PE40.
149. Davis S, Aldrich TH, Valenzuela DM, Wong VV, Furth ME, Squinto SP, et al. The receptor for ciliary neurotrophic factor. *Science*. 1991 Jul 5;253(5015):59-63.
150. Ihle JN. Janus kinases in cytokine signalling. *Philos Trans R Soc Lond B Biol Sci*. 1996 Feb 29;351(1336):159-66.
151. Kurth I, Horsten U, Pflanz S, Timmermann A, Kuster A, Dahmen H, et al. Importance of the membrane-proximal extracellular domains for activation of the signal transducer glycoprotein 130. *J Immunol*. 2000 Jan 1;164(1):273-82.
152. Stahl N, Boulton TG, Farruggella T, Ip NY, Davis S, Witthuhn BA, et al. Association and activation of Jak-Tyk kinases by CNTF-LIF-OSM-IL-6 beta receptor components. *Science*. 1994 Jan 7;263(5143):92-5.
153. Tanner JW, Chen W, Young RL, Longmore GD, Shaw AS. The conserved box 1 motif of cytokine receptors is required for association with JAK kinases. *J Biol Chem*. 1995 Mar 24;270(12):6523-30.
154. Haan C, Heinrich PC, Behrmann I. Structural requirements of the interleukin-6 signal transducer gp130 for its interaction with Janus kinase 1: the receptor is crucial for kinase activation. *Biochem J*. 2002 Jan 1;361(Pt 1):105-11.
155. Sengupta TK, Talbot ES, Scherle PA, Ivashkiv LB. Rapid inhibition of interleukin-6 signaling and Stat3 activation mediated by mitogen-activated protein kinases. *Proc Natl Acad Sci U S A*. 1998 Sep 15;95(19):11107-12.

156. Terstegen L, Gatsios P, Bode JG, Schaper F, Heinrich PC, Graeve L. The inhibition of interleukin-6-dependent STAT activation by mitogen-activated protein kinases depends on tyrosine 759 in the cytoplasmic tail of glycoprotein 130. *J Biol Chem*. 2000 Jun 23;275(25):18810-7.
157. Gerhartz C, Heesel B, Sasse J, Hemmann U, Landgraf C, Schneider-Mergener J, et al. Differential activation of acute phase response factor/STAT3 and STAT1 via the cytoplasmic domain of the interleukin 6 signal transducer gp130. I. Definition of a novel phosphotyrosine motif mediating STAT1 activation. *J Biol Chem*. 1996 May 31;271(22):12991-8.
158. Shuai K, Stark GR, Kerr IM, Darnell JE, Jr. A single phosphotyrosine residue of Stat91 required for gene activation by interferon-gamma. *Science*. 1993 Sep 24;261(5129):1744-6.
159. Tomida M, Heike T, Yokota T. Cytoplasmic domains of the leukemia inhibitory factor receptor required for STAT3 activation, differentiation, and growth arrest of myeloid leukemic cells. *Blood*. 1999 Mar 15;93(6):1934-41.
160. Qin HR, Kim HJ, Kim JY, Hurt EM, Klarmann GJ, Kawasaki BT, et al. Activation of signal transducer and activator of transcription 3 through a phosphomimetic serine 727 promotes prostate tumorigenesis independent of tyrosine 705 phosphorylation. *Cancer Res*. 2008 Oct 1;68(19):7736-41.
161. Lufei C, Koh TH, Uchida T, Cao X. Pin1 is required for the Ser727 phosphorylation-dependent Stat3 activity. *Oncogene*. 2007 Dec 6;26(55):7656-64.
162. Aziz MH, Manoharan HT, Church DR, Dreckschmidt NE, Zhong W, Oberley TD, et al. Protein kinase Cepsilon interacts with signal transducers and activators of transcription 3 (Stat3), phosphorylates Stat3Ser727, and regulates its constitutive activation in prostate cancer. *Cancer Res*. 2007 Sep 15;67(18):8828-38.
163. Wiederkehr-Adam M, Ernst P, Muller K, Bieck E, Gombert FO, Ottl J, et al. Characterization of phosphopeptide motifs specific for the Src homology 2 domains of signal transducer and activator of transcription 1 (STAT1) and STAT3. *J Biol Chem*. 2003 May 2;278(18):16117-28.
164. O'Shea JJ, Kanno Y, Chen X, Levy DE. Cell signaling. Stat acetylation--a key facet of cytokine signaling? *Science*. 2005 Jan 14;307(5707):217-8.
165. Suntharalingam M, Wenthe SR. Peering through the pore: nuclear pore complex structure, assembly, and function. *Dev Cell*. 2003 Jun;4(6):775-89.
166. Pemberton LF, Paschal BM. Mechanisms of receptor-mediated nuclear import and nuclear export. *Traffic*. 2005 Mar;6(3):187-98.
167. Pranada AL, Metz S, Herrmann A, Heinrich PC, Muller-Newen G. Real time analysis of STAT3 nucleocytoplasmic shuttling. *J Biol Chem*. 2004 Apr 9;279(15):15114-23.
168. Liu L, McBride KM, Reich NC. STAT3 nuclear import is independent of tyrosine phosphorylation and mediated by importin-alpha3. *Proc Natl Acad Sci U S A*. 2005 Jun 7;102(23):8150-5.
169. Bhattacharya S, Schindler C. Regulation of Stat3 nuclear export. *J Clin Invest*. 2003 Feb;111(4):553-9.

170. Herrmann A, Vogt M, Monnigmann M, Clahsen T, Sommer U, Haan S, et al. Nucleocytoplasmic shuttling of persistently activated STAT3. *J Cell Sci.* 2007 Sep 15;120(Pt 18):3249-61.
171. Jain N, Zhang T, Kee WH, Li W, Cao X. Protein kinase C delta associates with and phosphorylates Stat3 in an interleukin-6-dependent manner. *J Biol Chem.* 1999 Aug 20;274(34):24392-400.
172. Fu AK, Fu WY, Ng AK, Chien WW, Ng YP, Wang JH, et al. Cyclin-dependent kinase 5 phosphorylates signal transducer and activator of transcription 3 and regulates its transcriptional activity. *Proc Natl Acad Sci U S A.* 2004 Apr 27;101(17):6728-33.
173. Yue P, Turkson J. Targeting STAT3 in cancer: how successful are we? *Expert Opin Investig Drugs.* 2009 Jan;18(1):45-56.
174. Chatterjee M, Honemann D, Lentzsch S, Bommert K, Sers C, Herrmann P, et al. In the presence of bone marrow stromal cells human multiple myeloma cells become independent of the IL-6/gp130/STAT3 pathway. *Blood.* 2002 Nov 1;100(9):3311-8.
175. Militi S, Chiapparino C, Testa U, Carminati P, De Santis R, Serlupi-Crescenzi O. Role of IL-6 and CD23 in the resistance to growth arrest and apoptosis in LCL41 B lymphoma cells. *Cytokine.* 2005 Aug 21;31(4):314-23.
176. Wang LH, Kirken RA, Erwin RA, Yu CR, Farrar WL. JAK3, STAT, and MAPK signaling pathways as novel molecular targets for the tyrphostin AG-490 regulation of IL-2-mediated T cell response. *J Immunol.* 1999 Apr 1;162(7):3897-904.
177. Yadav A, Kalita A, Dhillon S, Banerjee K. JAK/STAT3 pathway is involved in survival of neurons in response to insulin-like growth factor and negatively regulated by suppressor of cytokine signaling-3. *J Biol Chem.* 2005 Sep 9;280(36):31830-40.
178. Ferrajoli A, Faderl S, Van Q, Koch P, Harris D, Liu Z, et al. WP1066 disrupts Janus kinase-2 and induces caspase-dependent apoptosis in acute myelogenous leukemia cells. *Cancer Res.* 2007 Dec 1;67(23):11291-9.
179. Iwamaru A, Szymanski S, Iwado E, Aoki H, Yokoyama T, Fokt I, et al. A novel inhibitor of the STAT3 pathway induces apoptosis in malignant glioma cells both in vitro and in vivo. *Oncogene.* 2007 Apr 12;26(17):2435-44.
180. Pardanani A, Hood J, Lasho T, Levine RL, Martin MB, Noronha G, et al. TG101209, a small molecule JAK2-selective kinase inhibitor potently inhibits myeloproliferative disorder-associated JAK2V617F and MPLW515L/K mutations. *Leukemia.* 2007 Aug;21(8):1658-68.
181. Kotha A, Sekharam M, Cilenti L, Siddiquee K, Khaled A, Zervos AS, et al. Resveratrol inhibits Src and Stat3 signaling and induces the apoptosis of malignant cells containing activated Stat3 protein. *Mol Cancer Ther.* 2006 Mar;5(3):621-9.
182. Li T, Wang W, Chen H, Li T, Ye L. Evaluation of anti-leukemia effect of resveratrol by modulating SATA3 signaling. *Int Immunopharmacol.* 2010 Jan;10(1):18-25.

183. Nam S, Buettner R, Turkson J, Kim D, Cheng JQ, Muehlbeyer S, et al. Indirubin derivatives inhibit Stat3 signaling and induce apoptosis in human cancer cells. *Proc Natl Acad Sci U S A*. 2005 Apr 26;102(17):5998-6003.
184. Jing N, Tweardy DJ. Targeting Stat3 in cancer therapy. *Anticancer Drugs*. 2005 Jul;16(6):601-7.
185. Blaskovich MA, Sun J, Cantor A, Turkson J, Jove R, Sebt SM. Discovery of JSI-124 (cucurbitacin I), a selective Janus kinase/signal transducer and activator of transcription 3 signaling pathway inhibitor with potent antitumor activity against human and murine cancer cells in mice. *Cancer Res*. 2003 Mar 15;63(6):1270-9.
186. Graness A, Poli V, Goppelt-Struebe M. STAT3-independent inhibition of lysophosphatidic acid-mediated upregulation of connective tissue growth factor (CTGF) by cucurbitacin I. *Biochem Pharmacol*. 2006 Jun 28;72(1):32-41.
187. Mackenzie GG, Queisser N, Wolfson ML, Fraga CG, Adamo AM, Oteiza PI. Curcumin induces cell-arrest and apoptosis in association with the inhibition of constitutively active NF-kappaB and STAT3 pathways in Hodgkin's lymphoma cells. *Int J Cancer*. 2008 Jul 1;123(1):56-65.
188. Deng J, Grande F, Neamati N. Small molecule inhibitors of Stat3 signaling pathway. *Curr Cancer Drug Targets*. 2007 Feb;7(1):91-107.
189. Dhillon N, Aggarwal BB, Newman RA, Wolff RA, Kunnumakkara AB, Abbruzzese JL, et al. Phase II trial of curcumin in patients with advanced pancreatic cancer. *Clin Cancer Res*. 2008 Jul 15;14(14):4491-9.
190. Wung BS, Hsu MC, Wu CC, Hsieh CW. Resveratrol suppresses IL-6-induced ICAM-1 gene expression in endothelial cells: effects on the inhibition of STAT3 phosphorylation. *Life Sci*. 2005 Dec 12;78(4):389-97.
191. Yu LJ, Wu ML, Li H, Chen XY, Wang Q, Sun Y, et al. Inhibition of STAT3 expression and signaling in resveratrol-differentiated medulloblastoma cells. *Neoplasia*. 2008 Jul;10(7):736-44.
192. Kim JE, Kim HS, Shin YJ, Lee CS, Won C, Lee SA, et al. LYR71, a derivative of trimeric resveratrol, inhibits tumorigenesis by blocking STAT3-mediated matrix metalloproteinase 9 expression. *Exp Mol Med*. 2008 Oct 31;40(5):514-22.
193. Sparano JA, Moulder S, Kazi A, Coppola D, Negassa A, Vahdat L, et al. Phase II trial of tipifarnib plus neoadjuvant doxorubicin-cyclophosphamide in patients with clinical stage IIB-IIIC breast cancer. *Clin Cancer Res*. 2009 Apr 15;15(8):2942-8.
194. Turkson J, Ryan D, Kim JS, Zhang Y, Chen Z, Haura E, et al. Phosphotyrosyl peptides block Stat3-mediated DNA binding activity, gene regulation, and cell transformation. *J Biol Chem*. 2001 Nov 30;276(48):45443-55.
195. Turkson J, Kim JS, Zhang S, Yuan J, Huang M, Glenn M, et al. Novel peptidomimetic inhibitors of signal transducer and activator of transcription 3 dimerization and biological activity. *Mol Cancer Ther*. 2004 Mar;3(3):261-9.
196. Vultur A, Cao J, Arulanandam R, Turkson J, Jove R, Greer P, et al. Cell-to-cell adhesion modulates Stat3 activity in normal and breast carcinoma cells. *Oncogene*. 2004 Apr 8;23(15):2600-16.

197. Buerger C, Nagel-Wolfrum K, Kunz C, Wittig I, Butz K, Hoppe-Seyler F, et al. Sequence-specific peptide aptamers, interacting with the intracellular domain of the epidermal growth factor receptor, interfere with Stat3 activation and inhibit the growth of tumor cells. *J Biol Chem*. 2003 Sep 26;278(39):37610-21.
198. Nagel-Wolfrum K, Buerger C, Wittig I, Butz K, Hoppe-Seyler F, Groner B. The interaction of specific peptide aptamers with the DNA binding domain and the dimerization domain of the transcription factor Stat3 inhibits transactivation and induces apoptosis in tumor cells. *Mol Cancer Res*. 2004 Mar;2(3):170-82.
199. Song H, Wang R, Wang S, Lin J. A low-molecular-weight compound discovered through virtual database screening inhibits Stat3 function in breast cancer cells. *Proc Natl Acad Sci U S A*. 2005 Mar 29;102(13):4700-5.
200. Chen CL, Loy A, Cen L, Chan C, Hsieh FC, Cheng G, et al. Signal transducer and activator of transcription 3 is involved in cell growth and survival of human rhabdomyosarcoma and osteosarcoma cells. *BMC Cancer*. 2007;7:111.
201. Siddiquee K, Zhang S, Guida WC, Blaskovich MA, Greedy B, Lawrence HR, et al. Selective chemical probe inhibitor of Stat3, identified through structure-based virtual screening, induces antitumor activity. *Proc Natl Acad Sci U S A*. 2007 May 1;104(18):7391-6.
202. Schust J, Sperl B, Hollis A, Mayer TU, Berg T. Stattic: a small-molecule inhibitor of STAT3 activation and dimerization. *Chem Biol*. 2006 Nov;13(11):1235-42.
203. Hao W, Hu Y, Niu C, Huang X, Chang CP, Gibbons J, et al. Discovery of the catechol structural moiety as a Stat3 SH2 domain inhibitor by virtual screening. *Bioorg Med Chem Lett*. 2008 Sep 15;18(18):4988-92.
204. Jing N, Li Y, Xu X, Sha W, Li P, Feng L, et al. Targeting Stat3 with G-quartet oligodeoxynucleotides in human cancer cells. *DNA Cell Biol*. 2003 Nov;22(11):685-96.
205. Jing N, Li Y, Xiong W, Sha W, Jing L, Tweardy DJ. G-quartet oligonucleotides: a new class of signal transducer and activator of transcription 3 inhibitors that suppresses growth of prostate and breast tumors through induction of apoptosis. *Cancer Res*. 2004 Sep 15;64(18):6603-9.
206. Jing N, Sha W, Li Y, Xiong W, Tweardy DJ. Rational drug design of G-quartet DNA as anti-cancer agents. *Curr Pharm Des*. 2005;11(22):2841-54.
207. Weerasinghe P, Garcia GE, Zhu Q, Yuan P, Feng L, Mao L, et al. Inhibition of Stat3 activation and tumor growth suppression of non-small cell lung cancer by G-quartet oligonucleotides. *Int J Oncol*. 2007 Jul;31(1):129-36.
208. Jing N, Zhu Q, Yuan P, Li Y, Mao L, Tweardy DJ. Targeting signal transducer and activator of transcription 3 with G-quartet oligonucleotides: a potential novel therapy for head and neck cancer. *Mol Cancer Ther*. 2006 Feb;5(2):279-86.
209. Leong PL, Andrews GA, Johnson DE, Dyer KF, Xi S, Mai JC, et al. Targeted inhibition of Stat3 with a decoy oligonucleotide abrogates head and neck cancer cell growth. *Proc Natl Acad Sci U S A*. 2003 Apr 1;100(7):4138-43.

210. Xi S, Gooding WE, Grandis JR. In vivo antitumor efficacy of STAT3 blockade using a transcription factor decoy approach: implications for cancer therapy. *Oncogene*. 2005 Feb 3;24(6):970-9.
211. Zhang X, Zhang J, Wang L, Wei H, Tian Z. Therapeutic effects of STAT3 decoy oligodeoxynucleotide on human lung cancer in xenograft mice. *BMC Cancer*. 2007;7:149.
212. Sun X, Zhang J, Wang L, Tian Z. Growth inhibition of human hepatocellular carcinoma cells by blocking STAT3 activation with decoy-ODN. *Cancer Lett*. 2008 Apr 18;262(2):201-13.
213. Conte MS, Bandyk DF, Clowes AW, Moneta GL, Seely L, Lorenz TJ, et al. Results of PREVENT III: a multicenter, randomized trial of edifoligide for the prevention of vein graft failure in lower extremity bypass surgery. *J Vasc Surg*. 2006 Apr;43(4):742-51; discussion 51.
214. Turkson J, Zhang S, Mora LB, Burns A, Sebti S, Jove R. A novel platinum compound inhibits constitutive Stat3 signaling and induces cell cycle arrest and apoptosis of malignant cells. *J Biol Chem*. 2005 Sep 23;280(38):32979-88.
215. Turkson J, Zhang S, Palmer J, Kay H, Stanko J, Mora LB, et al. Inhibition of constitutive signal transducer and activator of transcription 3 activation by novel platinum complexes with potent antitumor activity. *Mol Cancer Ther*. 2004 Dec;3(12):1533-42.
216. Weidler M, Rether J, Anke T, Erkel G. Inhibition of interleukin-6 signaling by galiellalactone. *FEBS Lett*. 2000 Oct 27;484(1):1-6.
217. Hellsten R, Johansson M, Dahlman A, Dizeyi N, Sterner O, Bjartell A. Galiellalactone is a novel therapeutic candidate against hormone-refractory prostate cancer expressing activated Stat3. *Prostate*. 2008 Feb 15;68(3):269-80.
218. Borghouts C, Kunz C, Delis N, Groner B. Monomeric recombinant peptide aptamers are required for efficient intracellular uptake and target inhibition. *Mol Cancer Res*. 2008 Feb;6(2):267-81.
219. Mirabelli CK, Bennett CF, Anderson K, Crooke ST. In vitro and in vivo pharmacologic activities of antisense oligonucleotides. *Anticancer Drug Des*. 1991 Dec;6(6):647-61.
220. Juliano R, Bauman J, Kang H, Ming X. Biological barriers to therapy with antisense and siRNA oligonucleotides. *Mol Pharm*. 2009 May-Jun;6(3):686-95.
221. Epling-Burnette PK, Liu JH, Catlett-Falcone R, Turkson J, Oshiro M, Kothapalli R, et al. Inhibition of STAT3 signaling leads to apoptosis of leukemic large granular lymphocytes and decreased Mcl-1 expression. *J Clin Invest*. 2001 Feb;107(3):351-62.
222. Grandis JR, Drenning SD, Zeng Q, Watkins SC, Melhem MF, Endo S, et al. Constitutive activation of Stat3 signaling abrogates apoptosis in squamous cell carcinogenesis in vivo. *Proc Natl Acad Sci U S A*. 2000 Apr 11;97(8):4227-32.
223. Chan JH, Lim S, Wong WS. Antisense oligonucleotides: from design to therapeutic application. *Clin Exp Pharmacol Physiol*. 2006 May-Jun;33(5-6):533-40.
224. Tamm I, Dorken B, Hartmann G. Antisense therapy in oncology: new hope for an old idea? *Lancet*. 2001 Aug 11;358(9280):489-97.

225. Lai SY, Koppikar P, Thomas SM, Childs EE, Egloff AM, Seethala RR, et al. Intratumoral epidermal growth factor receptor antisense DNA therapy in head and neck cancer: first human application and potential antitumor mechanisms. *J Clin Oncol*. 2009 Mar 10;27(8):1235-42.
226. Konnikova L, Kotecki M, Kruger MM, Cochran BH. Knockdown of STAT3 expression by RNAi induces apoptosis in astrocytoma cells. *BMC Cancer*. 2003 Sep 17;3:23.
227. Zhou W, Grandis JR, Wells A. STAT3 is required but not sufficient for EGF receptor-mediated migration and invasion of human prostate carcinoma cell lines. *Br J Cancer*. 2006 Jul 17;95(2):164-71.
228. Kunigal S, Lakka SS, Sodadasu PK, Estes N, Rao JS. Stat3-siRNA induces Fas-mediated apoptosis in vitro and in vivo in breast cancer. *Int J Oncol*. 2009 May;34(5):1209-20.
229. de Fougerolles A, Vornlocher HP, Maraganore J, Lieberman J. Interfering with disease: a progress report on siRNA-based therapeutics. *Nat Rev Drug Discov*. 2007 Jun;6(6):443-53.
230. Haupenthal J, Baehr C, Zeuzem S, Piiper A. RNase A-like enzymes in serum inhibit the anti-neoplastic activity of siRNA targeting polo-like kinase 1. *Int J Cancer*. 2007 Jul 1;121(1):206-10.
231. Merkel OM, Librizzi D, Pfestroff A, Schurrat T, Behe M, Kissel T. In vivo SPECT and real-time gamma camera imaging of biodistribution and pharmacokinetics of siRNA delivery using an optimized radiolabeling and purification procedure. *Bioconjug Chem*. 2009 Jan;20(1):174-82.
232. Gilmore IR, Fox SP, Hollins AJ, Akhtar S. Delivery strategies for siRNA-mediated gene silencing. *Curr Drug Deliv*. 2006 Apr;3(2):147-5.
233. Muruve DA. The innate immune response to adenovirus vectors. *Hum Gene Ther*. 2004 Dec;15(12):1157-66.
234. Zaiss AK, Muruve DA. Immune responses to adeno-associated virus vectors. *Curr Gene Ther*. 2005 Jun;5(3):323-31.
235. Kohn DB, Sadelain M, Glorioso JC. Occurrence of leukaemia following gene therapy of X-linked SCID. *Nat Rev Cancer*. 2003 Jul;3(7):477-88.
236. Uprichard SL. The therapeutic potential of RNA interference. *FEBS Lett*. 2005 Oct 31;579(26):5996-6007.
237. Kennedy D. Breakthrough of the year. *Science*. 2002 Dec 20;298(5602):2283.
238. Behlke MA. Progress towards in vivo use of siRNAs. *Mol Ther*. 2006 Apr;13(4):644-70.
239. Grayson AC, Doody AM, Putnam D. Biophysical and structural characterization of polyethylenimine-mediated siRNA delivery in vitro. *Pharm Res*. 2006 Aug;23(8):1868-76.
240. Li SD, Chono S, Huang L. Efficient gene silencing in metastatic tumor by siRNA formulated in surface-modified nanoparticles. *J Control Release*. 2008 Feb 18;126(1):77-84.
241. Kim SH, Jeong JH, Lee SH, Kim SW, Park TG. Local and systemic delivery of VEGF siRNA using polyelectrolyte complex micelles for effective treatment of cancer. *J Control Release*. 2008 Mar 14.

242. Kim WJ, Chang CW, Lee M, Kim SW. Efficient siRNA delivery using water soluble lipopolymer for anti-angiogenic gene therapy. *J Control Release*. 2007 Apr 23;118(3):357-63.
243. Kramer M, Stumbe JF, Grimm G, Kaufmann B, Kruger U, Weber M, et al. Dendritic polyamines: simple access to new materials with defined treelike structures for application in nonviral gene delivery. *Chembiochem*. 2004 Aug 6;5(8):1081-7.
244. Jensen DM, Cun D, Maltesen MJ, Frokjaer S, Nielsen HM, Foged C. Spray drying of siRNA-containing PLGA nanoparticles intended for inhalation. *J Control Release*. 2009 Oct 16.
245. Godbey WT, Wu KK, Mikos AG. Poly(ethylenimine) and its role in gene delivery. *J Control Release*. 1999 Aug 5;60(2-3):149-60.
246. Boussif O, Lezoualc'h F, Zanta MA, Mergny MD, Scherman D, Demeneix B, et al. A versatile vector for gene and oligonucleotide transfer into cells in culture and in vivo: polyethylenimine. *Proc Natl Acad Sci U S A*. 1995 Aug 1;92(16):7297-301.
247. Demeneix B, Behr JP. Polyethylenimine (PEI). *Adv Genet*. 2005;53:217-30.
248. Bologna JC, Dorn G, Natt F, Weiler J. Linear polyethylenimine as a tool for comparative studies of antisense and short double-stranded RNA oligonucleotides. *Nucleosides Nucleotides Nucleic Acids*. 2003 May-Aug;22(5-8):1729-31.
249. Urban-Klein B, Werth S, Abuharbeid S, Czubyko F, Aigner A. RNAi-mediated gene-targeting through systemic application of polyethylenimine (PEI)-complexed siRNA in vivo. *Gene Ther*. 2005 Mar;12(5):461-6.
250. Aigner A. Gene silencing through RNA interference (RNAi) in vivo: strategies based on the direct application of siRNAs. *J Biotechnol*. 2006 Jun 25;124(1):12-25.
251. Grzelinski M, Urban-Klein B, Martens T, Lamszus K, Bakowsky U, Hobel S, et al. RNA interference-mediated gene silencing of pleiotrophin through polyethylenimine-complexed small interfering RNAs in vivo exerts antitumoral effects in glioblastoma xenografts. *Hum Gene Ther*. 2006 Jul;17(7):751-66.
252. Kim SH, Jeong JH, Lee SH, Kim SW, Park TG. PEG conjugated VEGF siRNA for anti-angiogenic gene therapy. *J Control Release*. 2006 Jun 3.
253. Godbey WT, Wu KK, Mikos AG. Size matters: molecular weight affects the efficiency of poly(ethylenimine) as a gene delivery vehicle. *J Biomed Mater Res*. 1999 Jun 5;45(3):268-75.
254. Kim SH, Mok H, Jeong JH, Kim SW, Park TG. Comparative evaluation of target-specific GFP gene silencing efficiencies for antisense ODN, synthetic siRNA, and siRNA plasmid complexed with PEI-PEG-FOL conjugate. *Bioconjug Chem*. 2006 Jan-Feb;17(1):241-4.
255. Schiffelers RM, Ansari A, Xu J, Zhou Q, Tang Q, Storm G, et al. Cancer siRNA therapy by tumor selective delivery with ligand-targeted sterically stabilized nanoparticle. *Nucleic Acids Res*. 2004;32(19):e149.

256. Wang DA, Narang AS, Kotb M, Gaber AO, Miller DD, Kim SW, et al. Novel branched poly(ethylenimine)-cholesterol water-soluble lipopolymers for gene delivery. *Biomacromolecules*. 2002 Nov-Dec;3(6):1197-207.
257. Mahato RI, Lee M, Han S, Maheshwari A, Kim SW. Intratumoral delivery of p2CMVmIL-12 using water-soluble lipopolymers. *Mol Ther*. 2001 Aug;4(2):130-8.
258. Yockman JW, Maheshwari A, Han SO, Kim SW. Tumor regression by repeated intratumoral delivery of water soluble lipopolymers/p2CMVmIL-12 complexes. *J Control Release*. 2003 Feb 21;87(1-3):177-86.
259. Jain RA. The manufacturing techniques of various drug loaded biodegradable poly(lactide-co-glycolide) (PLGA) devices. *Biomaterials*. 2000 Dec;21(23):2475-90.
260. Bala I, Hariharan S, Kumar MN. PLGA nanoparticles in drug delivery: the state of the art. *Crit Rev Ther Drug Carrier Syst*. 2004;21(5):387-422.
261. Mundargi RC, Babu VR, Rangaswamy V, Patel P, Aminabhavi TM. Nano/micro technologies for delivering macromolecular therapeutics using poly(D,L-lactide-co-glycolide) and its derivatives. *J Control Release*. 2008 Feb 11;125(3):193-209.
262. Waeckerle-Men Y, Groettrup M. PLGA microspheres for improved antigen delivery to dendritic cells as cellular vaccines. *Adv Drug Deliv Rev*. 2005 Jan 10;57(3):475-82.
263. Jilek S, Merkle HP, Walter E. DNA-loaded biodegradable microparticles as vaccine delivery systems and their interaction with dendritic cells. *Adv Drug Deliv Rev*. 2005 Jan 10;57(3):377-90.
264. Kortylewski M, Swiderski P, Herrmann A, Wang L, Kowolik C, Kujawski M, et al. In vivo delivery of siRNA to immune cells by conjugation to a TLR9 agonist enhances antitumor immune responses. *Nat Biotechnol*. 2009 Oct;27(10):925-32.
265. Patil Y, Panyam J. Polymeric nanoparticles for siRNA delivery and gene silencing. *Int J Pharm*. 2009 Feb 9;367(1-2):195-203.
266. Murata N, Takashima Y, Toyoshima K, Yamamoto M, Okada H. Anti-tumor effects of anti-VEGF siRNA encapsulated with PLGA microspheres in mice. *J Control Release*. 2008 Mar 20;126(3):246-54.
267. Bouclier C, Moine L, Hillaireau H, Marsaud V, Connault E, Opolon P, et al. Physicochemical characteristics and preliminary in vivo biological evaluation of nanocapsules loaded with siRNA targeting estrogen receptor alpha. *Biomacromolecules*. 2008 Oct;9(10):2881-90.
268. Singh A, Nie H, Ghosh B, Qin H, Kwak LW, Roy K. Efficient modulation of T-cell response by dual-mode, single-carrier delivery of cytokine-targeted siRNA and DNA vaccine to antigen-presenting cells. *Mol Ther*. 2008 Dec;16(12):2011-21.
269. Hayun R, Shpungin S, Malovani H, Albeck M, Okun E, Nir U, et al. Novel involvement of the immunomodulator AS101 in IL-10 signaling, via the tyrosine kinase Fer. *Ann N Y Acad Sci*. 2007 Jan;1095:240-50.

CHAPTER TWO

PREPARATION AND CHARACTERIZATION OF siRNA POLYPLEXES OF LIPID-MODIFIED POLYETHYLENIMINES

A version of this chapter has been published in

Molecular Pharmaceutics 2009; 6(1):121-33

Aws Alshamsan, Azita Haddadi, Vanessa Incani, John Samuel,
Afsaneh Lavasanifar, and Hasan Uludağ

&

Presented as a poster in Canadian Society for Pharmaceutical Sciences (CSPS)

Montréal, Québec Canada, May 30-June 2, 2007

2.1 INTRODUCTION

RNA interference (RNAi) is a new technology that carries a promising therapeutic potential. In 2001, this post-transcriptional phenomenon was proven to exist as a defense mechanism in mammalian cells (1); it was shown that a double-stranded RNA of 21-23 nucleotides, known as small-interfering RNA (siRNA), mediated RNAi and effectively silenced target genes (2). Upon its introduction to cytosol, siRNA binds with specific proteins to conform the RNA-induced silencing complex (RISC) (3). RISC mediates the unwinding of siRNA duplex generating an oligonucleotide that binds to the target mRNA in a complementary manner. The resulting dsRNA gets cleaved by RISC and eventually destroyed by the intracellular machinery (4-6). Since its discovery, siRNA has been developed as a screening tool for cancer studies (7-9), and has been evaluated as a potential therapeutic agent for a variety of nucleic acid-based diseases such as HIV (10), Hepatitis C (11), and cancer (12, 13). siRNA has been employed to downregulate angiogenic and tumor-associated factors *in vitro* and *in vivo* (14). It was shown to inhibit the expression of Ki-67 and proliferation in human renal carcinoma cells (HRCC) (15). Inhibition of proliferation and induction of apoptosis of HRCC was achieved by anti-telomerase siRNA (16).

However, developing a stable and efficient delivery system is a major challenge for therapeutic applications of siRNA (17, 18). Optimum delivery strategy aims to reduce off-target effects, to improve siRNA pharmacokinetic and biodistribution after administration, and to promote efficient gene silencing (19). Viral vectors for siRNA delivery are associated with several drawbacks, such as

the possibility of uncontrolled cell proliferation of transduced cells (20), immune reactions to viral particles (21), and inflammation of the transduced tissue (22). Therefore, nonviral delivery systems are considered more favorable in therapy because of their reduced safety concerns and the relatively more convenient preparation techniques (23-26).

In this study, we examined the potential of hydrophobically-modified PEIs for stable condensation of siRNA in polyelectrolyte complexes and their ability to deliver siRNA to B16 melanoma cells *in vitro*. PEI is a cationic polymer that is used extensively in gene delivery studies (27); it is an attractive carrier for intracellular gene delivery because of its well-established ability to condense nucleic acids via electrostatic interaction between the anionic phosphate in the nucleic acid backbone and the cationic primary, secondary, and tertiary amines of the polymer (27, 28). PEI was shown to be effective in condensing and delivering siRNA to target mRNA *in vitro* and *in vivo* (29, 30). It was able to transfer functionally active siRNA to a variety of cell types including cancer cells (31). PEI-complexed siRNAs were shown to promote antitumoral effect in U87 orthotopic mouse glioblastoma model growing intracranially (32). A significant reduction in tumor growth was observed after intraperitoneal administration of PEI-siRNA complexes in mouse model targeting the c-erbB2/neu (HER-2) receptor (30). Additionally, PEI complexes of polyethylene glycol (PEG)-siRNA conjugates targeting vascular endothelial growth factor (VEGF) showed over 95% effective silencing of VEGF expression in PC-3 cells (33). The efficacy of PEI-

mediated siRNA delivery, however, was shown to be dependent on the structure and molecular weight of the PEI used in the formulation (34).

The relative simplicity in modifying PEI backbone can generate delivery systems that are target specific and possibly less toxic than native PEI. In a recent study, grafting PEG-folate residues to PEI was shown to efficiently deliver functionally-active siRNA into KB cells, a cell line originally derived from mouth epidermal carcinoma that highly express folate receptors (35). In addition, targeting cancer neovasculature *in vivo* and efficient silencing of vascular endothelial growth factor receptor-2 (VEGFR-2) was achieved by PEI nanoparticles that were decorated with Arg-Gly-Asp (RGD) peptides (36). Hydrophobic modification of PEI to improve cell membrane interactions is an alternative approach for siRNA delivery, as compared to receptor-specific modifications. One study have demonstrated that attaching cholesterol to PEI backbone promoted siRNA stability in water-soluble lipopolyplexes and inhibited VEGF expression in PC-3 cells *in vitro*, and ultimately induced tumor regression *in vivo* (37). PEI-cholesterol conjugates were also shown to enhance intracellular uptake of DNA and improve transfection efficiency (38). This system was effective for intratumoral delivery *in vivo* as well (39, 40). These results highlight the importance of lipid components in cationic polymers for efficient siRNA delivery. Based on this reasoning, we conducted this study to further investigate the beneficial effect of hydrophobic modifications by grafting simpler aliphatic lipids to PEI. By using PEIs modified with endogenous lipids, we investigated the complexation of the chosen polymers with a model siRNA and assessed their

capability to deliver siRNA intracellularly to B16 melanoma cells. An additional target-specific siRNA against integrin $\alpha(v)$ were used to evaluate functional siRNA delivery in this study. Our results indeed showed that PEIs modified with aliphatic lipids provide an improved model for siRNA-delivery.

2.2 MATERIALS and METHODS

2.2.1 Materials

Branched PEI (25 kDa), triethylamine (TEA), octanoyl chloride (CA, 99%), stearoyl chloride (StA, 98.5%), oleoyl chloride (OA, 99%), and linoleoyl chloride (LA, 99%) were obtained from SIGMA (St. Louis, MO). Anhydrous ethyl ether and dichloromethane (DCM) were purchased from Fisher Scientific (Fairlawn, NJ). Deuterated chloroform ($CDCl_3$) and water (D_2O) used as 1H -NMR solvent were from Cambridge Isotope Laboratories (Andover, MA) and ALDRICH (Milwaukee, WI), respectively. 3-(4,5-Dimethylthiazol-2-yl)-2,5-diphenyltetrazolium bromide (MTT) was obtained from SIGMA (St. Louis, MO). Fetal Bovine Serum (FBS) was obtained from HyClone (Logan, UT). INTERFERinTM and jetPEITM were purchased from Polyplus-Transfection (New York, NY). LipofectamineTM 2000 was purchased from Invitrogen Corporation (Carlsbad, CA), and MetafecteneTM was obtained from Biontix Laboratories (Munich, Germany). 4',6-diamidino-2-phenylindole (DAPI) was purchased from Invitrogen Molecular Probes (OR, USA). Sequenced siRNA targeting mouse integrin $\alpha(v)$, was purchased from Ambion:

(sense: 5'-GGCCUUGAAGUGUACCCUATT-3',

antisense: 5'-UAGGGUACACUUCAAGGCCAG-3').

The scrambled siRNAs used as a model siRNA were *Silencer*[®] Negative Control #1 siRNA (Catalogue #AM4635) and *Silencer*[®] FAM[™] labeled Negative Control #1 siRNA (Catalogue #AM4620), both purchased from Ambion (Austin, TX).

2.2.2 Cell Culture

B16.F10 cell line was grown and propagated in Dulbecco's modified Eagle's medium (DMEM) supplemented with 10% FBS at 37 °C and humidified 5% CO₂. The cell line was kindly provided by Dr. Mavanur Suresh, Faculty of Pharmacy and Pharmaceutical Sciences, University of Alberta.

2.2.3 Synthesis and Characterization of Lipid-Modified Polymers

A previously described procedure (41) was used to prepare the lipid-substituted PEIs (PEI-CA, PEI-StA, PEI-OA, PEI-LA) by N-acylation of the corresponding lipid chlorides with PEI (Table 2.1) at fatty acid:ethylenimine ratios of 1:15 and 1:86. Briefly, to obtain lipid-substituted PEI, 50 mg of PEI was dissolved in DCM 2.5 mL under N₂ at room temperature. After addition of 2 μL TEA, the desired fatty acid was dissolved in 2.5 mL DCM and gradually added to the PEI solution over a 30-min period. The solution was stirred for 12 hours under N₂. Excess of ethyl ether was added to precipitate and wash (x3) the polymer product, which was then dried under vacuum overnight at room temperature. The composition of the reaction products was determined by a 300 MHz ¹H-NMR spectroscope (Bruker 300 AM; Billerica, MA). The proton shifts

specific for fatty acids (~0.8 ppm; terminal -CH₃) and PEI (~2.5-2.8 ppm; -HN-CH₂-CH₂-NH-) were integrated, normalized for the number of protons in each peak, and used to obtain the lipid substitutions on polymers.

2.2.4 Determination of siRNA Condensation by Gel Retardation Assay

In sterile eppendorf tubes, serially diluted polymers ranging from 62.5 ng to 2 μg were added to 2 μg of siRNA in RNase-free water and incubated for 30 min at 37 °C. 3 μL of 6x sample buffer (50% glycerol, 1% bromophenol blue, and 1% xylene cyanol FF in Tris-Borate-EDTA (TBE) buffer) was then added to each sample. We then prepared 2% agarose gel by dissolving 2.4 g agarose powder in 120 ml TBE buffer and microaving the mixute for 2 min to allow for complete dissolution. Thereafter, EtBr was added to a final concentration of 0.2% mg/mL. The samples were then loaded onto the gel prior to electrophoresis. Electrophoresis was performed at 130 V and ~ 52 mA for 15 min. The resulting gels were photographed under UV-illumination. The pictures were digitized and analyzed with Scion image analysis software to determine the mean density of siRNA band. The binding percentage was calculated based on the relative intensity of siRNA in each well to reference wells of naked siRNA without any polymer. Each polymer was tested at least in 2 independent experiments.

2.2.5 Polyanion Competition Assay

The relative ability of complexes to release siRNA was measured after a challenge with the competing polyanion heparin (42). Complexes were formed in

1:1 polymer:siRNA mass ratios after incubating 2 µg of polymer and siRNA for 30 min, and then were incubated with 3.12, 6.25, 12.5, 25, 50, and 100 µg of heparin sulfate at 37 °C for 1 hour. The samples were run on agarose gel as described earlier. Results were presented as an average of at least 2 independent experiments.

2.2.6 Zeta Potential Measurement

Complexes of each polymer were formed at various polymer:siRNA mass ratios using 2 µg of siRNA. Zeta potential of each complex formulation ranging from 0.125:1 to 1:1 polymer:siRNA mass ratios was tested in water by 3 serial measurements using Zetasizer 3000 (Malvern, UK).

2.2.7 Serum Stability Studies

Naked siRNA (2 µg) was incubated with either 10% or 25% FBS at 37 °C. Samples were analyzed after 1, 4, and 24 hours of serum incubation by agarose gel electrophoresis to determine the percentage of intact siRNA. To determine the protective effect of the polymers, complexes were prepared in several polymer:siRNA mass ratios, ranging from 0.03125:1 to 1:1, and incubated with 25% FBS for 24 hours. Samples were then incubated for 1 hour with 100 µg of heparin to ensure complete release of siRNA from the formulations, and then analyzed for intact-siRNA percentage by agarose gel electrophoresis as described earlier. The results represent an average of at least 3 independent experiments.

2.2.8 Uptake of siRNA by B16 Melanoma Cells

In these experiments, 6-carboxyfluorescein (FAM)-labeled siRNA was formulated in the complexes. 1.4 µg of siRNA was incubated with serially diluted amounts of the polymers ranging from 175 ng to 1.4 µg in 50 µl PBS for 30 min at 37 °C. B16 murine melanoma cells (5×10^4) in 6-well plates were incubated with these complexes where each formulation contains 100 nM of siRNA.

In one study, to evaluate the complexes' ability to deliver several concentrations of siRNA, 24-well plates were used to incubate B16 cells with several concentrations of the complexes.

When commercial transfection agents were used to deliver a dose range of siRNA, sterile eppendorf tubes containing 1.4 µg of siRNA in RNase-free water were mixed with equal amounts of Lipofectamine™ 2000 or Metafectene™ for 20 min at room temperature. Moreover, 4 µL of jetPEI™ or INTERFERin™ were mixed with 1.4 µg siRNA for 20 min at room temperature. Thereafter, serial dilutions of the formulations were prepared in PBS and incubated with B16 cells in 24-well plates for 24 hours at 37°C. Percentage of siRNA-positive cells was determined by fluorescence activated cell sorting (FACS). For this, 10,000 cells (events) of each sample were acquired on a Becton–Dickinson FACSort™ flow cytometer (Franklin Lakes, NJ) and the data was analyzed with CellQuest™ software. At least duplicates of each sample were tested.

Intracellular uptake of siRNA was observed by Laser Scanning Confocal Microscopy (LSCM). After growing to 50% confluence, B16 cells were incubated with naked or formulated siRNA for 3 hours at 37 °C. The cells were then washed

three times with PBS and fixed with 2% paraformaldehyde solution in PBS for 10 min. To stain the nuclei, fixed B16 cells were washed with PBS then DAPI was added for 5 min. The cells were examined using a confocal microscope Zeiss 510 LSMNLO (Carl Zeiss; Jena, Germany) with identical settings for each confocal analysis.

2.2.9 siRNA-Mediated Inhibition of Integrin $\alpha(v)$

To evaluate functional siRNA silencing, we used a validated siRNA against integrin $\alpha(v)$. In 12-well plates, 5×10^5 B16 melanoma cells were incubated with 50, 100, and 200 nM of siRNA either naked or in formulations with 1:1 polymer:siRNA mass ratios at 37 °C. Identical formulations with scrambled siRNA were used as controls. After 36 hours, cells were washed and incubated for 30 min at 4 °C with 0.5 μ l of mAb against integrin $\alpha(v)$ (clone RMV-7; Santa Cruz Biotechnology, USA). Cells were washed three times with FACS buffer (5% FBS in PBS) to remove excess antibody. For labeling, 0.5 μ l of a secondary FITC-labeled antibody (Santa Cruz Biotechnology, USA) was added and the samples were incubated for 30 min at 4 °C. Then, cells were washed three times with FACS buffer and the levels of protein expression on cell surface were determined by flow cytometry.

2.2.10 Cytotoxicity Study

Polymer cytotoxicity was tested on B16 cells grown in 96-well flat-bottomed microplates. Serial dilutions of each polymer were prepared in PBS and

5 μ l of polymer solutions were added to 100 μ l of culture medium in each well. Total polymer concentration in each well ranged from 0.35 to 2.8 μ g/mL. The plates were incubated for 3, 12, 24, 48, and 72 h for assessment of viability. Each well was then incubated with 100 μ L of (0.5mg/mL) MTT solution in culture medium for 2 hours. The formed crystals were dissolved by adding 300 μ L of isopropyl alcohol to each well and gentle shaking for 30 min. Optical density was measured at 550 nm using a micoplate reader. The results were converted into % viability by using the absorbance from untreated sample as a reference (100%), and expressing the absorbances obtained from the treatment groups as a percentage of the reference value. The results were summarized as mean \pm SD of 7 replicates for each sample.

2.2.11 Statistical Analysis

The data were analyzed for statistical significance ($p < 0.05$) by One-Way ANOVA. Where indicated, the results were summarized as mean \pm SD.

2.3 RESULTS

2.3.1 siRNA Condensation by Oleic- and Stearic-acid Modified PEI

The hydrophobically-modified polymers, prepared by grafting lipid moieties on PEI backbone by N-acylation (41), were expected to possess sufficient cationic charge to neutralize the anionic charge of an siRNA. To assess the polymers' ability to condense siRNA, gel retardation assay was used to

analyze the complexes of siRNA with the native PEI or PEI derivatives (Table 2.1).

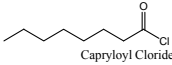
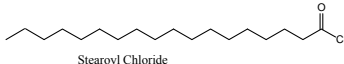
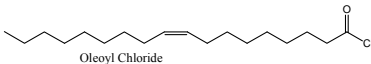
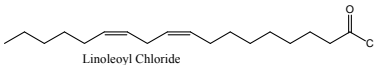
Polymer	Fatty-Acid Substitute	Substitution Level (Lipid/PEI)
PEI-CA1	 Capryloyl Chloride	28.14
PEI-CA2		10.47
PEI-StA1	 Stearoyl Chloride	2.63
PEI-StA2		1.89
PEI-OA1	 Oleoyl Chloride	4.57
PEI-OA2		2.1
PEI-LA1	 Linoleoyl Chloride	6.04
PEI-LA2		5.55

Table 2.1 PEI substitution with fatty acid chains

As shown in Figure 2.1A, complete condensation of siRNA could be achieved with all polymers, including PEI, at $\sim 0.4:1$ polymer:siRNA ratio. The condensation ability of the derivatives PEI-OA1 and PEI-StA2 were shown to be more efficient than the parent PEI, as indicated by a left shift in binding vs. concentration curves in Figure 2.1A. While $\sim 0.087:1$ mass ratio of PEI:siRNA was needed to achieve 50% siRNA binding, PEI-OA1 and PEI-StA2 required 0.026:1 and 0.019:1 polymer:siRNA ratios, respectively. Accordingly, PEI-OA1 and PEI-StA2 were chosen for further analysis due to their better siRNA binding capability.

To evaluate the stability of the formulations, siRNA complexes of PEI, PEI-OA1, and PEI-StA2 were prepared at polymer:siRNA mass ratio of 1:1 to ensure complete condensation of siRNA by the polymers (Figure 2.1B). Upon addition of serially-diluted heparin, 50% of siRNA was displaced from PEI complexes at heparin:polymer mass ratio of ~ 8.5 . However, with PEI-OA1, a heparin:polymer mass ratio of ~ 9.45 was needed to reach the 50% siRNA displacement value. PEI-StA2 complexes were even more stable, since a ratio of ~ 18.7 was needed to displace 50% of siRNA from the formulation. Complete dissociation of siRNA from all complexes was observed when the ratio of heparin:polymer reached 50. These findings were in line with the relatively higher siRNA binding of the hydrophobically-modified polymers compared to the unmodified PEI.

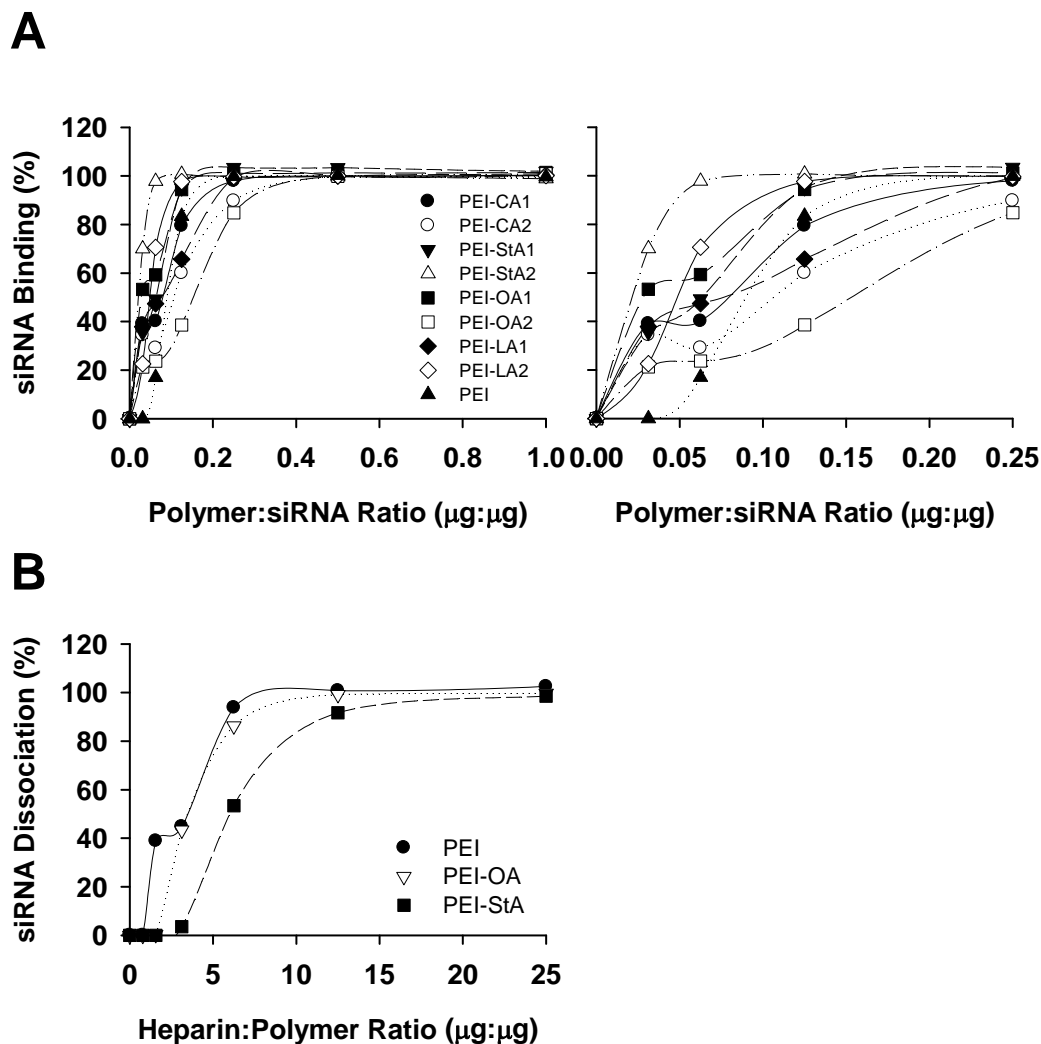


Figure 2.1 Assessment of siRNA complexation by gel migration assay. **(A)** The indicated polymers at different concentrations were incubated with a fixed amount of siRNA for 30 min at 37°C, and the complexes were run on agarose gel. The amount of naked siRNA in each sample was calculated by densitometry and siRNA Binding (%) was calculated accordingly. siRNA Binding (%) was plotted as a function of polymer concentration and sigmoidal curve fits were added for each polymer. PEI-OA1 and PEI-StA2 showed higher binding efficiency than the parent PEI, given by lower concentrations required for 50% binding of the siRNA. An expanded region of the original graph is plotted. **(B)** Displacement of siRNA from complexes by heparin competition. Complexes of 1:1 polymer:siRNA ratios were incubated for 1 hour at 37 °C with increasing concentrations of heparin sulfate, and the amount of free siRNA was determined by gel migration assay to obtain the extent of dissociation. PEI-StA complexes (filled squares) showed maximum stability in the presence of heparin.

2.3.2 Zeta Potential of siRNA-Complexes

Zeta potential analysis was carried out for the complexes at polymer:siRNA ratios of 1:1, 0.5:1, 0.25:1, and 0.125:1. The results (Figure 2.2) were consistent with the gel retardation assay where full complexation between siRNA and polymers was detected in all formulations at 0.25:1, 0.5:1 and 1:1 ratios. With PEI, the complexes displayed increasing net surface charge proportional to the increasing polymer ratio in the formulations. Although the hydrophobically-modified complexes did not show a uniform increase in surface charge, the polymers provided a sufficient net cationic charge on the particles at the polymer:siRNA mass ratios greater than 0.25:1. It was interesting to note that the modified polymers gave an increased cationic nature to the complexes at the lowest polymer:siRNA ratio, again indicating better binding of the polymers to siRNA after hydrophobic modification.

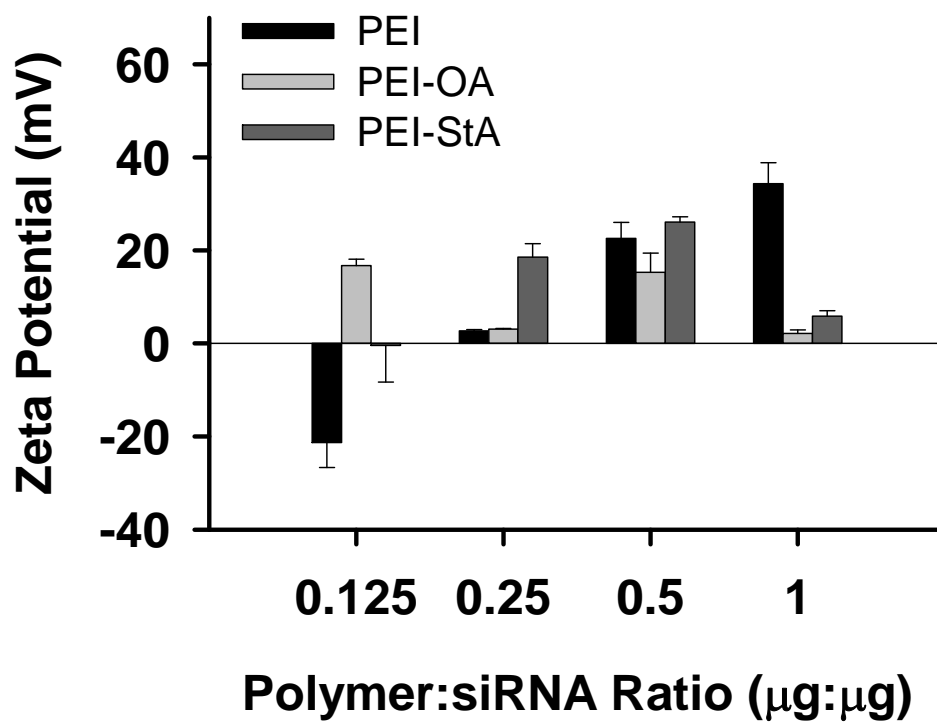


Figure 2.2 Determination of net surface charge by zeta potential analysis. The complexes were prepared at the indicated 4 different polymer:siRNA ratios and their zeta potential was determined. The bars represent the averages of 3 different measurements (\pm SD).

2.3.3 Protection of siRNA in Complexes from Degradation in Serum

Since siRNA is highly sensitive to degradation by nucleases (43), the protective effect of the complexes against siRNA degradation was assessed in serum. We first investigated the kinetics of naked siRNA degradation in 10% and 25% FBS at 37 °C. As shown in Figure 2.3A, siRNA was completely degraded in 10% FBS after 24 hours of incubation, while 4 hours were sufficient for 25% FBS to completely degrade siRNA. When the complexes of different polymer:siRNA mass ratios were incubated in 25% FBS for 24 hours, siRNA was fully recoverable and was protected from FBS degradation (Figure 2.3B) at polymer:siRNA ratios starting from 0.125:1. At the lower ratios 0.0625:1 and 0.03125:1, PEI-OA1 and PEI-StA2 demonstrated a significant protective effect for siRNA compared to parent PEI. The percentages of intact siRNA in PEI-OA1 and PEI-StA2 complexes were ~72 and ~97%, respectively, compared to only 29% in the case of PEI complexes at 0.0625:1 ratio.

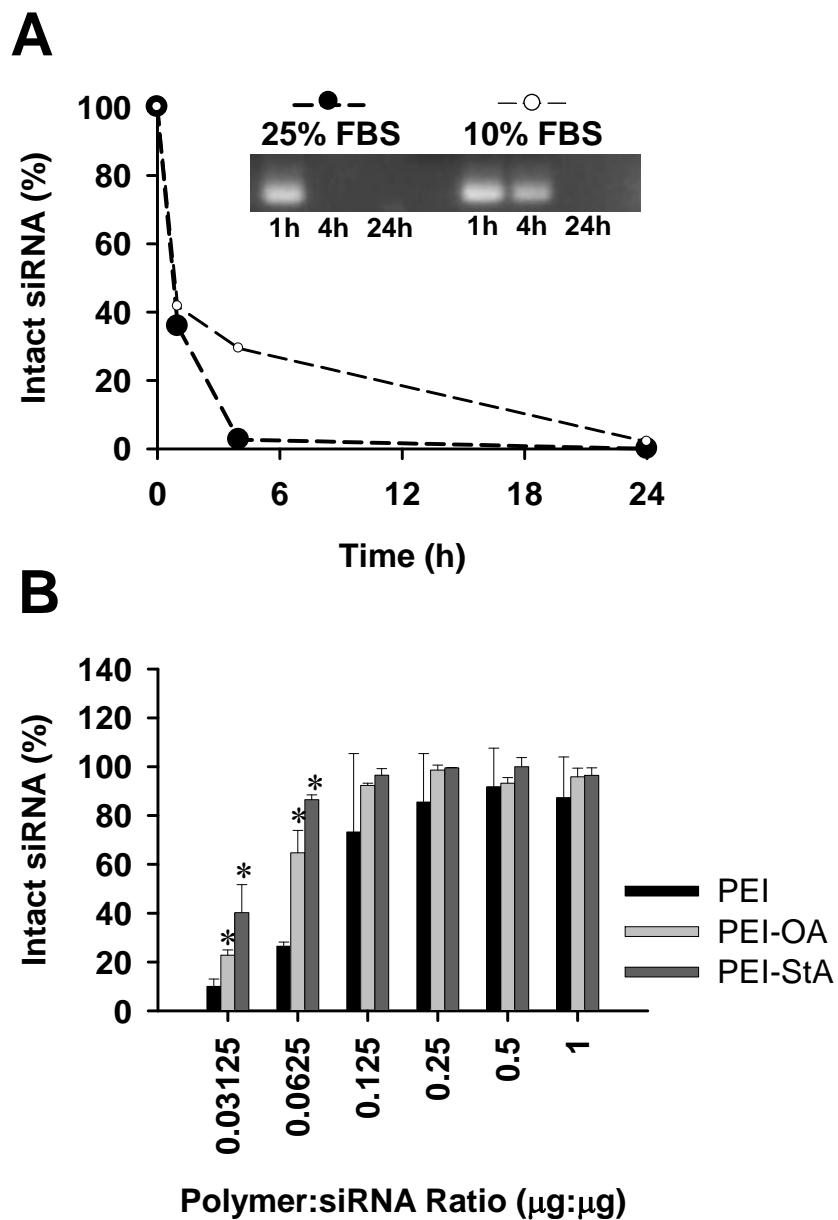


Figure 2.3 Determination of siRNA stability in presence of serum. **(A)** A fixed amount of naked siRNA was incubated with 10% and 25% FBS-containing medium for 1, 4 and 24 hours, and the amount of intact siRNA was determined by gel migration assay. Control refers to siRNA incubated in the absence of serum. Densitometry was used to calculate the amount of intact siRNA remaining after the incubation period and the intact siRNA remaining was plotted as a function of time in 25% FBS (filled circles) and 10% FBS (open circles). **(B)** siRNA/polymer complexes, at various polymer:siRNA ratios, were incubated in 25% FBS for 24 hours and the amount of intact siRNA was determined by gel migration assay and densitometry. Bars show the mean \pm SD of intact siRNA obtained at different polymer:siRNA ratios for 3 different measurements (*; $p < 0.05$). The modified polymers gave a higher amount of intact siRNA at low polymer:siRNA ratios

2.3.4 Uptake of siRNA Complexes by B16 Melanoma Cells

Naked siRNA uptake by B16 cells was determined *in vitro*. B16 cells were treated with increasing concentrations of naked siRNA (1-100 nM) for 24 hours. Our results indicate that the percentage of siRNA-positive cells increased in a concentration-dependent fashion, but only ~5% of the cells displayed significant uptake when incubated with naked siRNA in the absence of any carriers (data not shown). However, when formulated at 1:1 siRNA:polymer ratios, over 98% of B16 cells were positive for siRNA with all polymers, PEI, PEI-OA1, and PEI-StA2 (data not shown). A time-course study of siRNA uptake was then investigated to better characterize the uptake pattern. As shown in Figure 2.4A, the percentage of siRNA-positive cells with naked siRNA was significant within 30 min of incubation and reached ~20%. It peaked after 1 hour reaching 37% and then declined to less than 5% after 24 hours of incubation. When cellular uptake of siRNA in 1:1 complexes was assessed, significant increase in the percentage of siRNA-positive cells was detected as compared to naked siRNA reaching over 50% within 30 min of incubation. After 1 hour, PEI and PEI-OA1 complexes associated with ~90% of the cells, while PEI-StA2 complex was significantly higher reaching over 96% of the cells. Unlike naked siRNA, the percentage of siRNA-positive cells peaked after 4 hours of incubation with the PEI and PEI-StA2 complexes while all complexes sustained this high level after 24 hours of incubation.

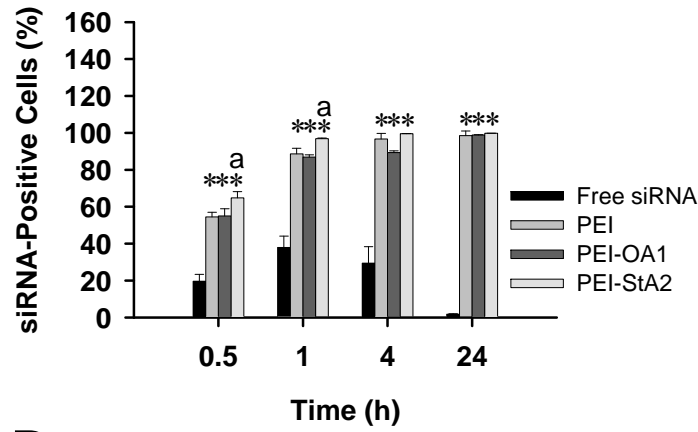
Since flow cytometry can not discriminate whether the siRNA was cell-surface bound or internalized, we used confocal microscopy to localize siRNA in

B16 cells (Figure 2.4B). We chose a time point (3 hours) where the percentage of siRNA-positive cells was submaximal based on flow cytometry data. The results of the confocal microscopy indicated the presence of the polymeric complexes of siRNA to enter B16 cells after 3 hours of incubation, as evident by sequestration of complexes (green dots in Figure 2.4B, due to FAM-labeled siRNA) in the cytoplasm, possibly inside endosomes, and their localization around the nucleus (blue structures, due to DAPI staining). At this time point, there was no indication of naked siRNA inside the B16 cells. Confocal microscopy did not indicate any qualitative differences among the three polymers (PEI, PEI-OA1, and PEI-StA2) used for complex formation. These results were consistent with our flow cytometry results, showing strong effect of the polymers to deliver the siRNA intracellularly. A discrepancy between the confocal microscopy results (indicated no uptake at 3 hours) and flow cytometry results (indicated some uptake at 4 hours), however, was present for naked siRNA (see Discussion on this issue).

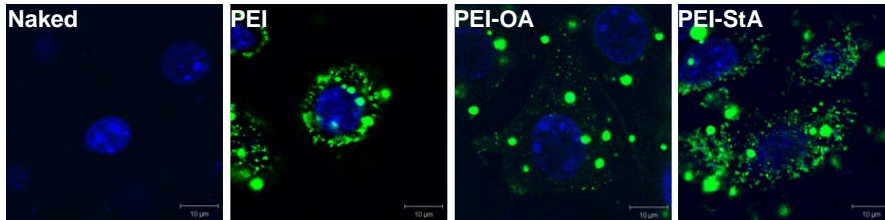
The ability of the hydrophobically-modified PEIs to deliver a dose range of siRNA to B16 cells was compared to commercially available transfecting reagents including: INTERFERin™, which was specifically designed for siRNA delivery, jetPEI™, which was used to transfect HepG2 cells with antisense RNA (44), Lipofectamine™ 2000, which demonstrated significant siRNA-mediated inhibition of tumor growth in human gastric carcinoma *in vitro* (45), and Metafectene™, which was used to mediate siRNA-silencing of PCNA gene in leukemic cell line (46). All polymer formulations were prepared at mass ratios of 1:1; for INTERFERin™ and jetPEI™, the manufacturer's recommendations were

followed for the amount of polymer used in the formulation. B16 cells were pulsed with serially diluted complexes for 24 hours where siRNA concentration in the formulations ranged from 1.56 to 50 nM. As shown in Figure 2.4C, when 25 nM of siRNA were delivered, PEI-OA1 and PEI-StA2 complexes demonstrated ~1.6-fold and ~3-fold increase in the percentage of siRNA-positive cells than the parent PEI, respectively. At 50 nM siRNA, ~1.3-fold and ~2-fold increase the percentage of siRNA-positive cells was observed with PEI-OA1 and PEI-StA2 compared to parent PEI. At this concentration, PEI-OA1 also showed significant increase in the percentage of siRNA-positive cells which was ~2.6-fold higher than MetafecteneTM and ~4.3-fold higher than jetPEITM. Similarly, PEI-StA2 demonstrated ~4-fold increase in the percentage of siRNA-positive cells than MetafecteneTM and ~6-fold higher than jetPEITM. PEI-StA2 was also found to be as efficient as LipofectamineTM 2000 for siRNA delivery to B16 cell line. INTERFERinTM was the most effective delivery vehicle at all concentrations of siRNA. When compared to INTERFERinTM, PEI-StA2 was only ~1.6-fold less efficient in cellular uptake while PEI showed at least 3-fold reduction in cell uptake.

A



B



C

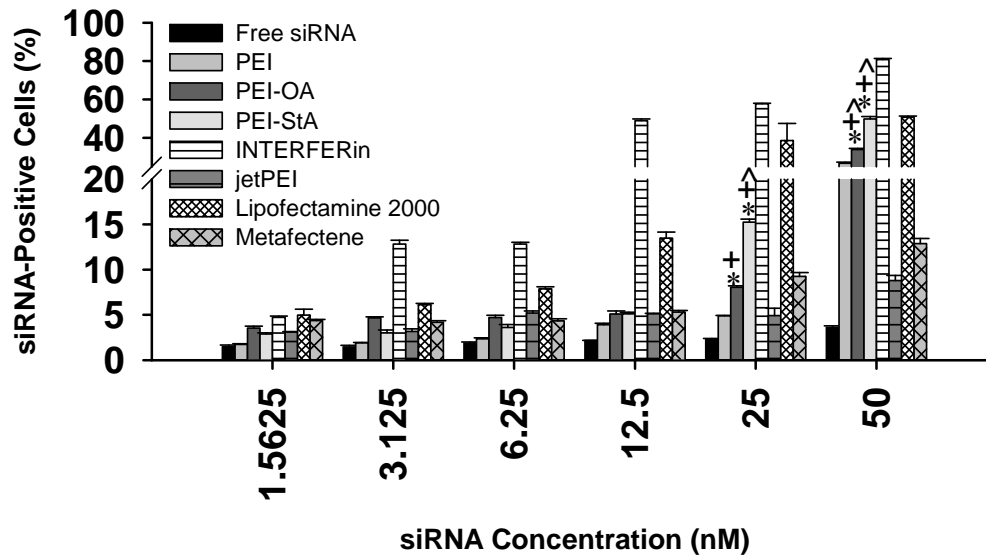


Figure 2.4 Cellular uptake of siRNA complexes by B16 cells. **(A)** Determination of siRNA-positive B16 cells over time by FACS. The study was conducted using 100 nM FAM-siRNA either naked or in 1:1 complexes with the polymers. Cells incubated with siRNA for indicated periods of time were harvested and analyzed in FACS. Percentage of siRNA-positive cells of complexed siRNA with the polymers was found to be significantly higher than the naked siRNA (a; $p < 0.05$). PEI-StA2 complexes showed significantly higher increase in siRNA-positive cells compared to the PEI complexes, at early time points (*; $p < 0.05$). Data are shown as the average \pm SD of 3 experiments. **(B)** Confocal microscopy analysis of intracellular siRNA when B16 cells were incubated with 100 nM naked FAM-siRNA or siRNA complexed with PEI, PEI-OA, and PEI-StA. Nuclei (blue) are stained with 4',6-diamidino-2-phenylindole (DAPI) and the scale bar for each image is 10 μ m. Note the lack of siRNA for cells incubated with naked siRNA, unlike cells incubated with complexes that yielded distinct particles associated with the cells. **(C)** Delivery of siRNA by hydrophobically-modified polymers and other commercially available carriers to B16 cells. siRNA complexes with the polymers were prepared at 1:2 polymer:siRNA ratios. Serially diluted complexes of 1:1 polymer:siRNA ratios were incubated in 24-well plates with B16 cells for 24 hours. Significant increase in siRNA-positive cells was noticed with hydrophobically-modified PEIs compared to PEI, (*; $p < 0.05$), jetPEITM, (+; $p < 0.05$), and MetafecteneTM, (^; $p < 0.05$). Data are shown as an average \pm SD of 3 experiments.

2.3.5 Effect of Polymer Ratio in Complexes on siRNA Delivery

In order to investigate the effect of polymer content on siRNA delivery, siRNA complexes were formulated with polymer:siRNA mass ratios of 1:1, 0.5:1, 0.25:1, and 0.125:1. As shown in Figure 2.5, reducing the polymer ratio in the formulation resulted in proportional reduction in the percentage of siRNA-positive cells. At 0.5:1 ratio, siRNA delivery by PEI-OA1 and PEI-StA2 complexes was shown to be 1.4-fold and 2.4-fold less than PEI, respectively. Further drop in polymeric content results in further reduction in the percentage of siRNA-positive cells. At ratios lower than 0.25:1, the percentage of siRNA-positive cells was comparable in all groups including naked siRNA. These results indicate that although complete siRNA condensation was achieved at 0.25:1 polymer:siRNA ratio with PEI, PEI-OA1, and PEI-StA2, higher polymer ratios are required in the formulation to achieve better siRNA delivery.

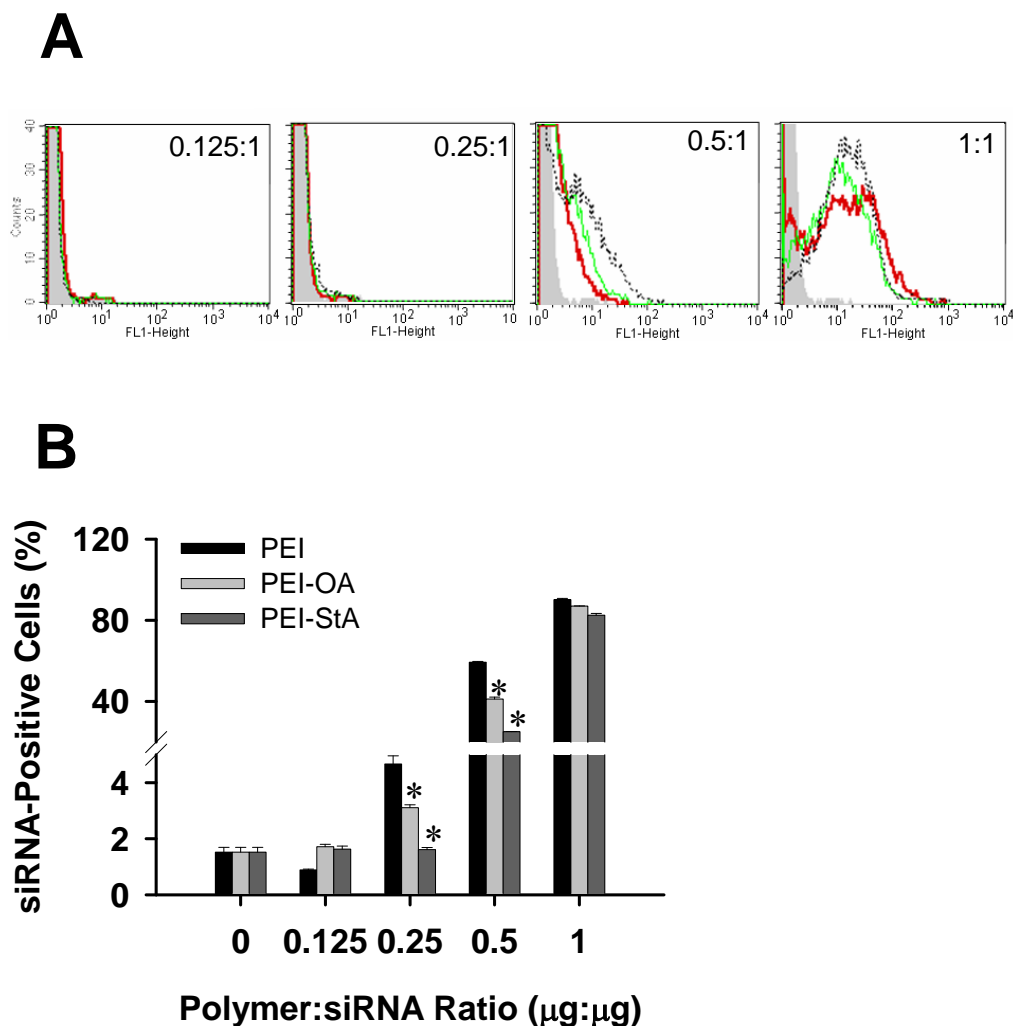


Figure 2.5 Effect of polymer:siRNA ratio on siRNA delivery. Complexes were prepared at the indicated polymer:siRNA ratios, incubated with the cells for 24 hours, and siRNA uptake was subsequently determined by FACS. The study was done using 100 nM siRNA in each sample. **(A)** Changes in FACS histograms indicative of siRNA-positive cells as a function of polymer:siRNA ratios (indicated in the upper right corner of each histogram). Shaded areas represent background, dotted lines represent PEI complexed group, green lines represent PEI-OA complexed group, and red lines represent PEI-StA complexed group. **(B)** Bars represent quantitative analysis of FACS histograms in **(A)** to obtain percentage of cells positive for the siRNA. Data are shown as an average \pm SD of 3 experiments (*; $p < 0.05$).

2.3.6 Knockdown of Integrin $\alpha(v)$ by siRNA Using Modified PEIs

We examined the ability of hydrophobically-modified PEIs to obtain functional siRNA silencing of integrin $\alpha(v)$ subunit on B16 cells. As shown in Figure 2.6A, all siRNA complexes significantly decreased surface expression of integrin $\alpha(v)$ compared to naked siRNA. Moreover, hydrophobic modification seemed to further enhance siRNA silencing over parent PEI; PEI-OA1 formulation mediated up to 27% reduction in surface expression of integrin $\alpha(v)$, while PEI-StA2 formulation mediated up to 45% reduction in integrin $\alpha(v)$ surface expression compared to parent PEI. At 50 nM siRNA, PEI-StA2 complexes gave marginal yet significant silencing of integrin $\alpha(v)$ as compared to PEI-OA1, but such a difference was not evident at the 100 and 200 nM siRNA doses. A scrambled siRNA, used as a control in this study, did not cause any reduction of surface integrin $\alpha(v)$ levels by naked siRNA or the corresponding siRNA complexes (Figure 2.6B).

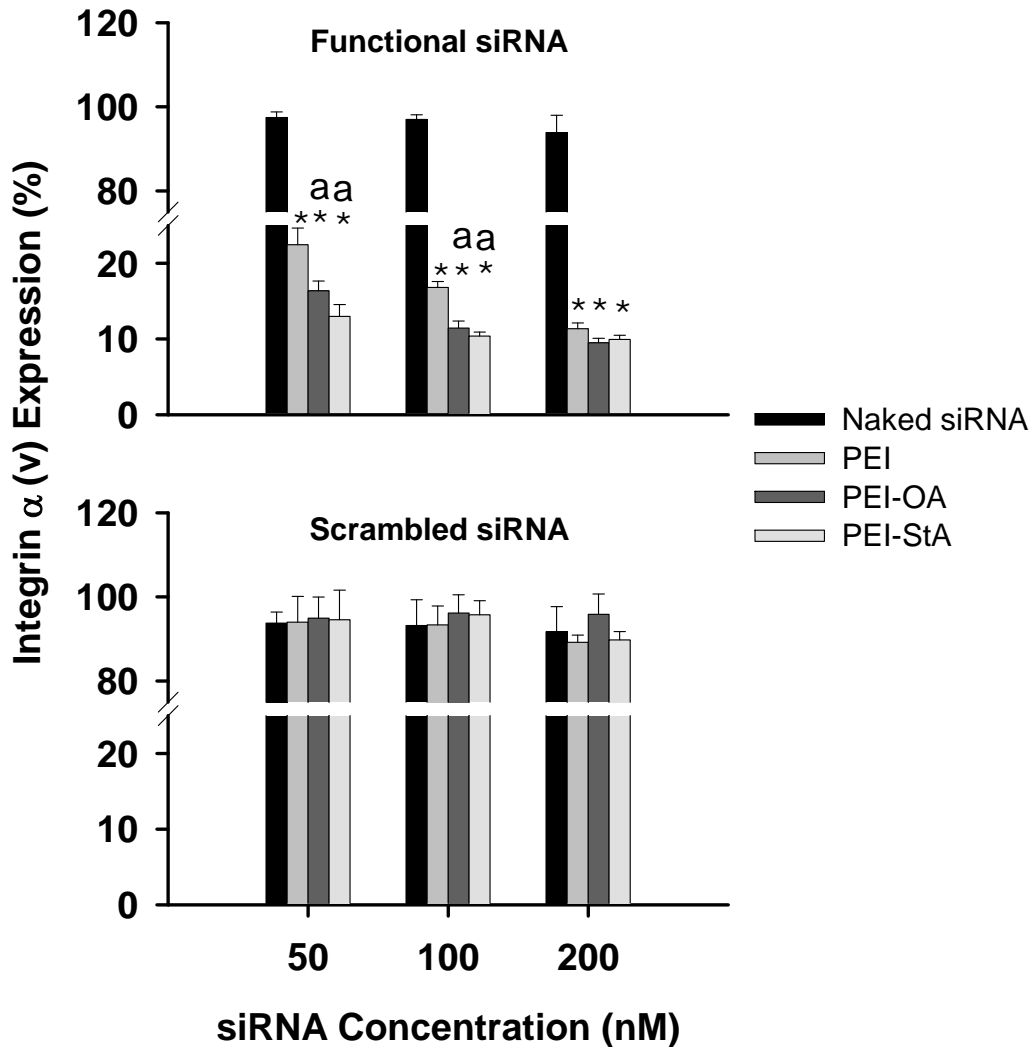


Figure 2.6 Inhibition of integrin $\alpha(v)$ expression by siRNA complexes in B16 cells exposed to three doses of siRNA. Increasing concentrations of (A) an siRNA targeting murine integrin $\alpha(v)$ or (B) a scrambled siRNA were incubated with B16 cells either naked or in complexes of 1:1 polymer:siRNA ratios for 36 hours. Significant inhibition of integrin $\alpha(v)$ expression was noticed with all complexes compared to naked siRNA (a; $p < 0.05$). Significant difference was also present between the hydrophobically-modified PEIs compared to PEI (*; $p < 0.05$), and between PEI-StA and PEI-OA at 50 nM siRNA (a; $p < 0.05$). Data are shown as an average of 3 experiments (\pm SD).

2.3.7 Cytotoxicity Studies

The cytotoxic effect of the polymers on B16 cells was assessed by the MTT assay. Cytotoxicity studies were conducted to explore whether the polymer concentrations used for siRNA delivery had any indirect effect on siRNA uptake due to disruption of cell viability. After 72 hours of incubation, the results revealed that PEI, PEI-OA1, and PEI-StA2 were not toxic to B16 cells at the polymer concentrations (<3 µg/ml) used in this study (Figure 2.7A). The cytotoxicity of the highest concentration was further examined by MTT assay over time and no significant changes in cell viability were noted over 72 hours (Figure 2.7B).

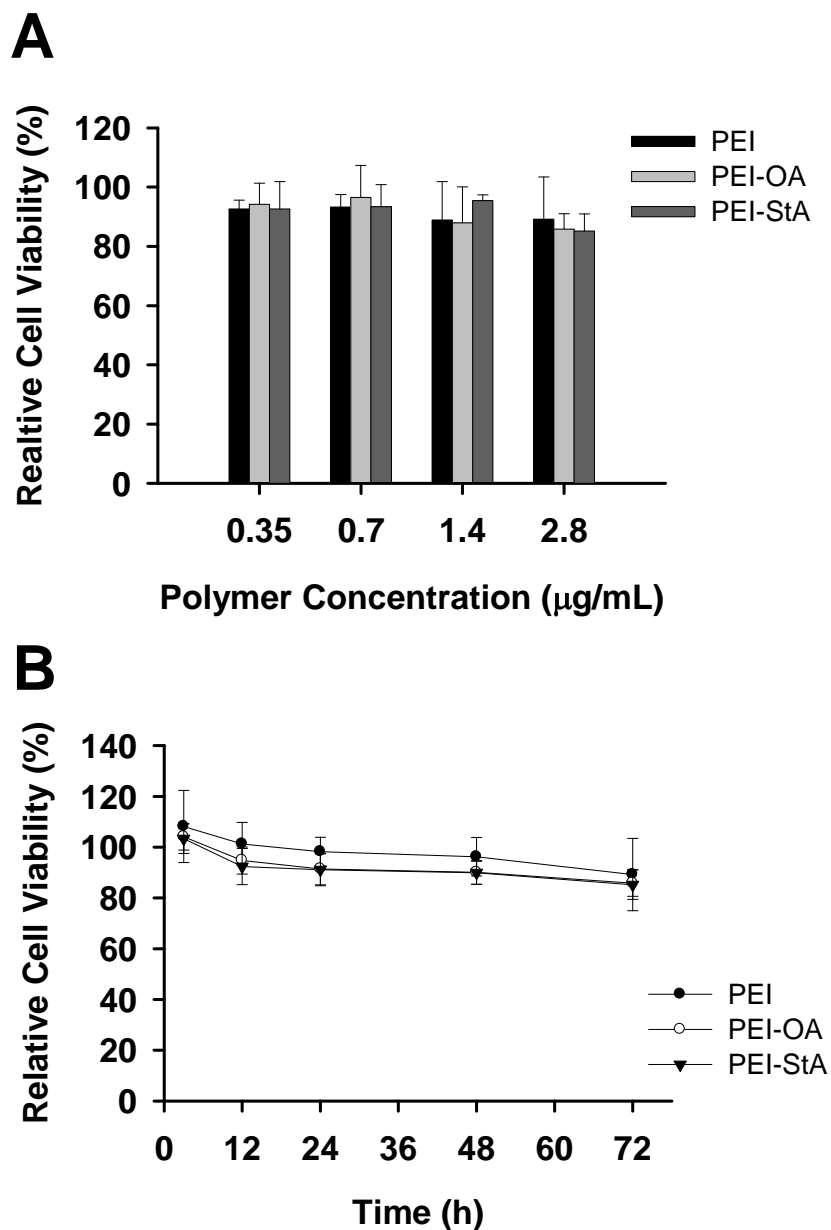


Figure 2.7 Cytotoxicity study for assessment of toxic effect of the siRNA complexes on B16 cells. The complexes were prepared at polymer:siRNA ratio of 1:1. **(A)** Complexes at polymer concentrations of 0.35 to 2.8 mg/mL were incubated with the cells for 72 hours. **(B)** Complexes at polymer concentration of 2.8 µg/mL were incubated with the cells over a period of 72 hours. This concentration is at least 2-time higher than the polymer concentration used in cellular uptake studies. Percentage of relative cell viability was determined by the MTT assay. Data are shown as mean (\pm SD) of 7 replicates for each sample.

2.4 DISCUSSION

siRNA-based therapy is a promising approach for cancer treatment (12, 13). It has been demonstrated that targeting laryngeal cancer cells with siRNA induced early or late stage apoptosis (47). Moreover, growth of laryngeal cancer has been inhibited *in vivo* when targeted with siRNA (48). However, successful siRNA delivery has always been one of the major challenges to the therapeutic applications of siRNA in clinic (49). The therapeutic potential of siRNA is abrogated by low cellular uptake and poor stability profile; these negative consequences have affected the anticipated move of siRNA-based therapeutics from bench to bedside. Therefore, there has been an increasing interest in developing suitable systems for siRNA delivery (30-33, 35, 36).

In our studies, we evaluated the ability of hydrophobically-modified derivatives of branched PEI (25 kDa) to condense, protect, and successfully deliver siRNA to B16 melanoma cells *in vitro*. Our findings demonstrated that PEI-OA1 and PEI-StA2 were able to condense siRNA at lower concentrations as compared to PEI (Figure 2.1A), indicating better binding affinity. This has been confirmed by siRNA displacement using the polyanion heparin (Figure 2.1B). Yet, we expect that the electrostatic interaction might not be the only mechanism by which hydrophobically-modified PEI form complexes with siRNA. In fact, based on our zeta potential results (Figure 2.2), the expected increase in the net surface charge proportional to polymer ratio was observed only with the PEI complexes. With modified PEIs, we attributed the variability in surface charge, in spite of the increasing polymer ratio in the formulation, to the relatively flexible three-dimensional conformation of the grafted fatty acids. The flexibility of the

fatty acids is able to create a non-uniform surface charge distribution on the particle, leading to unpredictable response in an electric field. Although we did not expect to see a reduction in zeta potential with increasing polymer content, this could be explained by the concomitant increment of the non-cationic fatty acid content. Therefore, we suggest that the flexibility of the aliphatic fatty acids could also allow for physical encapsulation of siRNA, which may explain the superior condensing and protective effect of the modified polymers over PEI in spite of variable zeta potentials. The hydrophobically-modified complexes, nevertheless, demonstrated a net cationic surface charge which was sufficient for successful cell uptake. This was confirmed by the efficient siRNA delivery by hydrophobically-modified PEIs compared to naked siRNA, which was evident in our confocal microscopy study (Figure 2.4B). Confocal microscopy, more so than the flow cytometry, revealed the beneficial effect of polymers on siRNA; no uptake was visible for naked siRNA with confocal microscopy, whereas some uptake was evident from flow cytometry. Differences in sample preparation procedures, possible quenching of fluorescence in confocal microscopy (as observed by Li, S.D. et al. (50)), or non-specific association of siRNA with cells under flow conditions, might have led to such a difference. Although exact reasons for such a difference are unknown in our studies, an independent study also noted some differences between the two methods using the analysis of viral binding and uptake (51).

The time-dependent decline noted in the percentage of siRNA-positive cells after incubation with naked siRNA might be attributed in part to the

instability of naked siRNA in culture medium (Figure 2.4A). This gradual reduction in the percentage of siRNA-positive cells from 37% after 1 hour of incubation to ~2% after 24 hours of incubation was consistent with the serum degradation profile after siRNA incubation with 10% FBS where the levels of siRNA declined from 41% after 1 hour of incubation to 2% after 24 hours of incubation (Figure 2.3A). A recent study has related the loss of siRNA activity after incubation with serum to RNase A-like enzymes (43). Hauptenthal et al. clearly demonstrated that the anti-tumor activity of siRNA directed against Polo-like kinase 1 was lost after 2 hours of incubation with human serum at 37 °C; this effect was prevented by the addition of RNaseOUT™, which is a potent inhibitor for RNase A (43). On the other hand, the prolonged siRNA delivery and persistent percentage of siRNA-positive cells achieved with siRNA complexes could be also explained by the polymer-protective effect from serum degradation (Figure 2.4A). Others have addressed the protective effect of polymers on siRNA. It was reported that almost complete degradation of siRNA occurred after 8 hours of incubation in 50% FBS, while micellar formulation of PEG-conjugated siRNA in PEI was able to protect the siRNA from degradation even after 48 hours of incubation (33). In addition, it was shown that siRNA degradation in 20% FBS could occur as soon as 30 min of incubation, while cholesterol-conjugated PEI efficiently protected siRNA from degradation (37). The protective effect of polymer complexation against nucleases will be vital after systemic administration of siRNA. Cholesterol conjugation to branched PEI (1.8 kDa) also showed significant increase in siRNA uptake by PC-3 cells compared to

unmodified PEI and promote anti-angiogenic effect *in vitro* and *in vivo* (37). Although a relatively higher polymeric ratio was required in this system to achieve successful siRNA delivery, these results strongly support our findings where hydrophobic modification of PEI improved siRNA delivery to target cells. Although PEI-StA2 complexes did not possess higher positive charge than PEI complexes at the experimental conditions used for cell uptake, they were found to demonstrate a significant increase in the percentage of siRNA-positive cells within the first hour of incubation compared to parent PEI (Figure 2.4A). Yet, when the ratio of PEI-StA2 was reduced in the formulation (Figure 2.5), the percentage of siRNA-positive cells was significantly less than parent PEI. This indicated that excess polymer might be important for siRNA delivery, since it is shown from gel retardation assay, zeta potential analysis, and serum stability studies that polymer:siRNA mass ratio of 0.25:1 was enough for siRNA condensation to occur. This has been previously noticed with DNA, when Derouazi et al. reported that although complete DNA condensation by branched PEI (25 kDa) was detected at N/P ratio of 2, successful gene transfer was only observed at N/P of 6 or more, reaching optimum transfection level at N/P of 13 (52). Presumably, excess polymer enhances the plasma membrane permeability directly, and/or prevents undesirable binding of the complexes to anionic surfaces that might cause loss of the particles.

Consistent with our findings on siRNA condensation, PEI-OA1 and PEI-StA2 demonstrated a significant improvement in delivering a range of siRNA doses as compared to parent PEI. Others have also shown that lipid component in

polymers positively influenced siRNA delivery, for example by the cholesterol-substituted PEI in PC-3 cells (37). Behr and colleagues demonstrated that cationic lipoplexes can promote siRNA delivery to the brain at picomolar level which was significantly higher than linear PEI (53). We also found that the lipid-containing commercially available transfecting agents, INTERFERinTM and LipofectamineTM 2000 are more efficient in delivering siRNA than jetPEITM and MetafecteneTM. We presumed that the hydrophobic moieties could enhance complex-plasma membrane interactions, which may facilitate endocytosis process in turn. Furthermore, the superior ability to condense, protect, and deliver siRNA that was obtained with PEI-StA2 might be related to the chemical structure of stearic acid. The free-rotation property of the saturated carbon atoms in stearic acid was expected to give the molecule more flexibility to move inward or project outward the complex. Hence, it was not surprising to find PEI-StA2 showing the highest siRNA binding, protection, and delivery among the PEI derivatives.

Our results on integrin $\alpha(v)$ inhibition *in vitro* were consistent with the findings on siRNA delivery by flow cytometry. Integrin $\alpha(v)$ is an attractive target for cancer therapy since it forms a larger subunit of many integrins which are directly involved in tumor angiogenesis, growth, survival, proliferation, invasion, migration and metastasis (54). Integrin $\alpha(v)$ was found to be involved in mediating melanoma tumorigenicity in human (55) and was also associated with higher metastatic ability of murine melanoma B16.F10 cells (56). We found that the polymeric formulations mediate siRNA silencing of integrin $\alpha(v)$ *in vitro* in a dose-dependent manner compared to naked siRNA, while scrambled siRNA had

no silencing effect either naked or formulated. Although both PEI-OA1 and PEI-StA2 showed higher silencing effect of siRNA compared to PEI, PEI-StA2 still provided a significant enhancement of siRNA silencing at a 50 nM concentration over PEI-OA1. This may be due to the higher stability of the formulation provided by PEI-StA2 (Figure 2.1B) and better protection from nuclease degradation (Figure 2.3B). Therefore, it is feasible that PEI-StA2 may exert this better efficiency through mediating siRNA protection and stability in the endosomal compartment, which allow for a higher amount of intact siRNA to reach the cytoplasm; the fact that both modified polymers were equipotent at higher siRNA concentrations (100 and 200 nM) may support this hypothesis. The reasons behind this issue, however, remain to be explored. Moreover, attempts to target integrin $\alpha(v)$ in melanoma using monoclonal antibodies have clearly demonstrated that blocking integrin $\alpha(v)$ on tumor cells directly mediated antitumor effects which was not due to the known antiangiogenic effect of integrin $\alpha(v)$ antagonists (54, 57-59). A recent study by Cao et al. used siRNA targeting integrin $\alpha(v)$ in combination with radiotherapy as a strategy for breast cancer therapy, since they noted an upregulation of integrin $\alpha(v)\beta(3)$ expression on MDA-MB-435 cells after irradiation, leading to radioresistance as compared to integrin $\alpha(v)\beta(3)$ -negative MCF-7 breast cancer cells. The authors found that siRNA treatment was able to effectively reduce integrin $\alpha(v)$ and integrin $\alpha(v)\beta(3)$ expression and increase the radiosensitivity of MDA-MB-435 cells (60). This collective experience indicated that the functional reduction of cell surface integrin $\alpha(v)$ by hydrophobically-modified PEIs might be an important target for

clinical applications. Our future studies will focus on exploring this aspect of the siRNA delivery by hydrophobically-modified PEIs.

We consider these polymers promising for therapeutic application, especially that they showed no signs of toxicity over prolonged time of incubation (Figure 2.7). Although it was reported that up to 50% reduction in cell viability occurred in mouse fibroblasts after 24 hours of incubation with 10 $\mu\text{g/mL}$ of PEI (61), our systems did not display significant toxicity presumably due to (i) the intrinsic resistance of B16 melanoma cells, or (ii) lower concentrations used in our system. The concentrations used in our toxicity assessment were based on concentrations found to be effective for siRNA delivery in our hands. The toxicity issue is not critical for cancerous cells, since toxicity on the target cells will actually be a beneficial effect in addition to the specific siRNA therapy. The toxicity issue, however, is critical for normal cells since the latter will inevitably get exposed to siRNA/polymer complexes after administration, and complexes that can provide good cellular internalization without directly affecting cell viability will lead to more tolerable formulations. Further studies are planned on this issue where the toxicity of the proposed hydrophobic PEIs will be evaluated at higher concentrations.

2.5 REFERENCES

1. Elbashir SM, Harborth J, Lendeckel W, Yalcin A, Weber K, Tuschl T. Duplexes of 21-nucleotide RNAs mediate RNA interference in cultured mammalian cells. *Nature*. 2001 May 24;411(6836):494-8.
2. Elbashir SM, Lendeckel W, Tuschl T. RNA interference is mediated by 21- and 22-nucleotide RNAs. *Genes Dev*. 2001 Jan 15;15(2):188-200.
3. Kawasaki H, Taira K, Morris KV. siRNA induced transcriptional gene silencing in mammalian cells. *Cell Cycle*. 2005 Mar;4(3):442-8.
4. Tang G. siRNA and miRNA: an insight into RISCs. *Trends Biochem Sci*. 2005 Feb;30(2):106-14.
5. Caplen NJ, Mousses S. Short interfering RNA (siRNA)-mediated RNA interference (RNAi) in human cells. *Ann N Y Acad Sci*. 2003 Dec;1002:56-62.
6. Schutze N. siRNA technology. *Mol Cell Endocrinol*. 2004 Jan 15;213(2):115-9.
7. Sachse C, Echeverri CJ. Oncology studies using siRNA libraries: the dawn of RNAi-based genomics. *Oncogene*. 2004 Nov 1;23(51):8384-91.
8. Luo Q, Kang Q, Song WX, Lu HH, Luo X, An N, et al. Selection and validation of optimal siRNA target sites for RNAi-mediated gene silencing. *Gene*. 2007 Jun 15;395(1-2):160-9.
9. Fuchs U, Borkhardt A. The application of siRNA technology to cancer biology discovery. *Adv Cancer Res*. 2007;96:75-102.
10. Chakraborty C. Potentiality of small interfering RNAs (siRNA) as recent therapeutic targets for gene-silencing. *Curr Drug Targets*. 2007 Mar;8(3):469-82.
11. Wilson JA, Richardson CD. Future promise of siRNA and other nucleic acid based therapeutics for the treatment of chronic HCV. *Infect Disord Drug Targets*. 2006 Mar;6(1):43-56.
12. Storvold GL, Andersen TI, Perou CM, Frengen E. siRNA: a potential tool for future breast cancer therapy? *Crit Rev Oncog*. 2006 Jul;12(1-2):127-50.
13. Cejka D, Losert D, Wacheck V. Short interfering RNA (siRNA): tool or therapeutic? *Clin Sci (Lond)*. 2006 Jan;110(1):47-58.
14. Lu PY, Xie FY, Woodle MC. Modulation of angiogenesis with siRNA inhibitors for novel therapeutics. *Trends Mol Med*. 2005 Mar;11(3):104-13.
15. Zheng JN, Ma TX, Cao JY, Sun XQ, Chen JC, Li W, et al. Knockdown of Ki-67 by small interfering RNA leads to inhibition of proliferation and induction of apoptosis in human renal carcinoma cells. *Life Sci*. 2006 Jan 11;78(7):724-9.
16. Zheng JN, Sun YF, Pei DS, Liu JJ, Chen JC, Li W, et al. Inhibition of proliferation and induction of apoptosis in human renal carcinoma cells by anti-telomerase small interfering RNAs. *Acta Biochim Biophys Sin (Shanghai)*. 2006 Jul;38(7):500-6.
17. Dev KK. Using RNAi in the clinic. *IDrugs*. 2006 Apr;9(4):279-82.
18. Hede K. Blocking cancer with RNA interference moves toward the clinic. *J Natl Cancer Inst*. 2005 May 4;97(9):626-8.
19. Thomas M, Lu JJ, Chen J, Klibanov AM. Non-viral siRNA delivery to the lung. *Adv Drug Deliv Rev*. 2007 Mar 30;59(2-3):124-33.

20. Kohn DB, Sadelain M, Glorioso JC. Occurrence of leukaemia following gene therapy of X-linked SCID. *Nat Rev Cancer*. 2003 Jul;3(7):477-88.
21. Zaiss AK, Muruve DA. Immune responses to adeno-associated virus vectors. *Curr Gene Ther*. 2005 Jun;5(3):323-31.
22. Muruve DA. The innate immune response to adenovirus vectors. *Hum Gene Ther*. 2004 Dec;15(12):1157-66.
23. Uprichard SL. The therapeutic potential of RNA interference. *FEBS Lett*. 2005 Oct 31;579(26):5996-6007.
24. Kennedy D. Breakthrough of the year. *Science*. 2002 Dec 20;298(5602):2283.
25. Behlke MA. Progress towards in vivo use of siRNAs. *Mol Ther*. 2006 Apr;13(4):644-70.
26. Putnam D, Doody A. RNA-interference effectors and their delivery. *Crit Rev Ther Drug Carrier Syst*. 2006;23(2):137-64.
27. Demeneix B, Behr JP. Polyethylenimine (PEI). *Adv Genet*. 2005;53:217-30.
28. Boussif O, Lezoualc'h F, Zanta MA, Mergny MD, Scherman D, Demeneix B, et al. A versatile vector for gene and oligonucleotide transfer into cells in culture and in vivo: polyethylenimine. *Proc Natl Acad Sci U S A*. 1995 Aug 1;92(16):7297-301.
29. Bologna JC, Dorn G, Natt F, Weiler J. Linear polyethylenimine as a tool for comparative studies of antisense and short double-stranded RNA oligonucleotides. *Nucleosides Nucleotides Nucleic Acids*. 2003 May-Aug;22(5-8):1729-31.
30. Urban-Klein B, Werth S, Abuharbeid S, Czubayko F, Aigner A. RNAi-mediated gene-targeting through systemic application of polyethylenimine (PEI)-complexed siRNA in vivo. *Gene Ther*. 2005 Mar;12(5):461-6.
31. Aigner A. Gene silencing through RNA interference (RNAi) in vivo: strategies based on the direct application of siRNAs. *J Biotechnol*. 2006 Jun 25;124(1):12-25.
32. Grzelinski M, Urban-Klein B, Martens T, Lamszus K, Bakowsky U, Hobel S, et al. RNA interference-mediated gene silencing of pleiotrophin through polyethylenimine-complexed small interfering RNAs in vivo exerts antitumoral effects in glioblastoma xenografts. *Hum Gene Ther*. 2006 Jul;17(7):751-66.
33. Kim SH, Jeong JH, Lee SH, Kim SW, Park TG. PEG conjugated VEGF siRNA for anti-angiogenic gene therapy. *J Control Release*. 2006 Nov 28;116(2):123-9.
34. Grayson AC, Doody AM, Putnam D. Biophysical and structural characterization of polyethylenimine-mediated siRNA delivery in vitro. *Pharm Res*. 2006 Aug;23(8):1868-76.
35. Kim SH, Mok H, Jeong JH, Kim SW, Park TG. Comparative evaluation of target-specific GFP gene silencing efficiencies for antisense ODN, synthetic siRNA, and siRNA plasmid complexed with PEI-PEG-FOL conjugate. *Bioconjug Chem*. 2006 Jan-Feb;17(1):241-4.

36. Schiffelers RM, Ansari A, Xu J, Zhou Q, Tang Q, Storm G, et al. Cancer siRNA therapy by tumor selective delivery with ligand-targeted sterically stabilized nanoparticle. *Nucleic Acids Res.* 2004;32(19):e149.
37. Kim WJ, Chang CW, Lee M, Kim SW. Efficient siRNA delivery using water soluble lipopolymer for anti-angiogenic gene therapy. *J Control Release.* 2007 Apr 23;118(3):357-63.
38. Wang DA, Narang AS, Kotb M, Gaber AO, Miller DD, Kim SW, et al. Novel branched poly(ethylenimine)-cholesterol water-soluble lipopolymers for gene delivery. *Biomacromolecules.* 2002 Nov-Dec;3(6):1197-207.
39. Mahato RI, Lee M, Han S, Maheshwari A, Kim SW. Intratumoral delivery of p2CMVmIL-12 using water-soluble lipopolymers. *Mol Ther.* 2001 Aug;4(2):130-8.
40. Yockman JW, Maheshwari A, Han SO, Kim SW. Tumor regression by repeated intratumoral delivery of water soluble lipopolymers/p2CMVmIL-12 complexes. *J Control Release.* 2003 Feb 21;87(1-3):177-86.
41. Incani V, Tunis E, Clements BA, Olson C, Kucharski C, Lavasanifar A, et al. Palmitic acid substitution on cationic polymers for effective delivery of plasmid DNA to bone marrow stromal cells. *J Biomed Mater Res A.* 2007 May;81(2):493-504.
42. Merdan T, Callahan J, Petersen H, Kunath K, Bakowsky U, Kopeckova P, et al. Pegylated polyethylenimine-Fab' antibody fragment conjugates for targeted gene delivery to human ovarian carcinoma cells. *Bioconjug Chem.* 2003 Sep-Oct;14(5):989-96.
43. Haupenthal J, Baehr C, Zeuzem S, Piiper A. RNase A-like enzymes in serum inhibit the anti-neoplastic activity of siRNA targeting polo-like kinase 1. *Int J Cancer.* 2007 Jul 1;121(1):206-10.
44. Liang SJ, Xiao WL, Mu DZ, Wu HN, Wang XJ. [IL-1beta antisense RNA enhanced sensitivity of HepG2 cells to NK cell mediated cytotoxicity.]. *Xi Bao Yu Fen Zi Mian Yi Xue Za Zhi.* 2007 Aug;23(8):719-22.
45. Miao GY, Lu QM, Zhang XL. Downregulation of survivin by RNAi inhibits growth of human gastric carcinoma cells. *World J Gastroenterol.* 2007 Feb 28;13(8):1170-4.
46. Merkerova M, Bruchova H, Brdicka R. [Specific silencing of PCNA gene expression in leukemic cell lines using siRNA]. *Cas Lek Cesk.* 2005;144(7):472-5.
47. Gao LF, Xu DQ, Wen LJ, Zhang XY, Shao YT, Zhao XJ. Inhibition of STAT3 expression by siRNA suppresses growth and induces apoptosis in laryngeal cancer cells. *Acta Pharmacol Sin.* 2005 Mar;26(3):377-83.
48. Gao LF, Wen LJ, Yu H, Zhang L, Meng Y, Shao YT, et al. Knockdown of Stat3 expression using RNAi inhibits growth of laryngeal tumors in vivo. *Acta Pharmacol Sin.* 2006 Mar;27(3):347-52.
49. Gilmore IR, Fox SP, Hollins AJ, Akhtar S. Delivery strategies for siRNA-mediated gene silencing. *Curr Drug Deliv.* 2006 Apr;3(2):147-5.
50. Li SD, Chono S, Huang L. Efficient gene silencing in metastatic tumor by siRNA formulated in surface-modified nanoparticles. *J Control Release.* 2008 Feb 18;126(1):77-84.

51. Pizzato M, Marlow SA, Blair ED, Takeuchi Y. Initial binding of murine leukemia virus particles to cells does not require specific Env-receptor interaction. *J Virol.* 1999 Oct;73(10):8599-611.
52. Derouazi M, Girard P, Van Tilborgh F, Iglesias K, Muller N, Bertschinger M, et al. Serum-free large-scale transient transfection of CHO cells. *Biotechnol Bioeng.* 2004 Aug 20;87(4):537-45.
53. Hassani Z, Lemkine GF, Erbacher P, Palmier K, Alfama G, Giovannangeli C, et al. Lipid-mediated siRNA delivery down-regulates exogenous gene expression in the mouse brain at picomolar levels. *J Gene Med.* 2005 Feb;7(2):198-207.
54. Nemeth JA, Nakada MT, Trikha M, Lang Z, Gordon MS, Jayson GC, et al. Alpha-v integrins as therapeutic targets in oncology. *Cancer Invest.* 2007 Oct;25(7):632-46.
55. Felding-Habermann B, Mueller BM, Romerdahl CA, Cheresh DA. Involvement of integrin alpha V gene expression in human melanoma tumorigenicity. *J Clin Invest.* 1992 Jun;89(6):2018-22.
56. Ratheesh A, Ingle A, Gude RP. Pentoxifylline Modulates Cell Surface Integrin Expression and Integrin Mediated Adhesion of B16F10 Cells to Extracellular Matrix Components. *Cancer Biol Ther.* 2007 Aug 3;6(11).
57. Mitjans F, Meyer T, Fittschen C, Goodman S, Jonczyk A, Marshall JF, et al. In vivo therapy of malignant melanoma by means of antagonists of alphav integrins. *Int J Cancer.* 2000 Sep 1;87(5):716-23.
58. Chen Q, Manning CD, Millar H, McCabe FL, Ferrante C, Sharp C, et al. CNTO 95, a fully human anti alphav integrin antibody, inhibits cell signaling, migration, invasion, and spontaneous metastasis of human breast cancer cells. *Clin Exp Metastasis.* 2007 Dec 5.
59. Trikha M, Zhou Z, Nemeth JA, Chen Q, Sharp C, Emmell E, et al. CNTO 95, a fully human monoclonal antibody that inhibits alphav integrins, has antitumor and antiangiogenic activity in vivo. *Int J Cancer.* 2004 Jun 20;110(3):326-35.
60. Cao Q, Cai W, Li T, Yang Y, Chen K, Xing L, et al. Combination of integrin siRNA and irradiation for breast cancer therapy. *Biochem Biophys Res Commun.* 2006 Dec 22;351(3):726-32.
61. Fischer D, Li Y, Ahlemeyer B, Krieglstein J, Kissel T. In vitro cytotoxicity testing of polycations: influence of polymer structure on cell viability and hemolysis. *Biomaterials.* 2003 Mar;24(7):1121-31.

CHAPTER THREE

siRNA SILENCING OF STAT3 IN MURINE MELANOMA MODEL

A version of this chapter has been published in

Biomaterials 2010 Feb;31(6):1420-8

Aws Alshamsan, Samar Hamdy, John Samuel,
Ayman O.S. El-Kadi, Afsaneh Lavasanifar, and Hasan Uludağ

&

Presented as a poster in Nano Drug Delivery Symposium (NanoDDS) Toronto,
Ontario, Canada, November 3-5, 2008

&

Presented as an oral talk in 13th Canadian Society for Pharmaceutical Sciences
(CSPS) Annual Symposium, Vancouver, British Columbia, Canada, June 2-5,

2010

3.1 INTRODUCTION

Persistent activation of signal transducer and activator of transcription 3 (STAT3) has been associated with a vast number of solid and blood tumors and was linked to several malignant properties including tumor survival, proliferation, angiogenesis, and immune evasion (1). STAT3 is a downstream protein that becomes activated by phosphorylation of a single tyrosine (Y⁷⁰⁵) in response to cytokine and growth factor receptor stimulations (2). This persistent activation of STAT3 was associated with persistent activation of tyrosine kinases including src kinases, growth factor receptors with intrinsic kinase activity, and Janus kinases (JAKs) (3). Upon activation, STAT3 dimerizes through reciprocal phosphotyrosine-SH2 interaction. The formed dimers translocate to the nucleus and bind to STAT-specific sites on the promoters of target genes to induce the transcription of proteins that have critical role in regulating cell survival and proliferation (e.g. c-Myc, cyclin D1, and Bcl-family proteins) (2). Since the original discovery of the association of constitutive STAT3 with malignant transformation (4), research outcomes summarized four criteria carried by constitutively active STAT3 that make this molecule an attractive target for downregulation in cancer therapy: (i) hyperactivity in a large percentage of cells in different tumor types, (ii) mediating various malignant properties, (iii) susceptibility to inhibitors, and (iv) the dependence of tumor cells on STAT3 for survival more than normal cells (5). However, although targeting STAT3 signaling pathway has been achieved by several modalities (e.g. upstream inhibition of cytokine and growth factors (6, 7), inhibition of STAT3 dimerization

(8), inhibition of STAT3/STAT3 nuclear translocation (9) and inhibition of DNA binding activity (10)), low progress has been made for therapeutic application of STAT3 inhibition (11). It is possible that due to cytotoxicity and lack of specificity of pharmacological inhibitors, the progress of STAT3 inhibitors from bench to bedside did not match the anticipations. Hence, small interfering RNA (siRNA) has emerged as an attractive modality with a promising therapeutic potential for treating many nucleic acid-based diseases such as cancer (12).

The siRNA delivery has been shown to be effective in downregulating STAT3 expression in several tumor cells. Inhibition of STAT3 gene expression has led to suppression of growth and induction of apoptosis of Hep2 laryngeal cancer cell line after transfection with DNA plasmid encoding for anti-STAT3 siRNA using OligofectamineTM (13). Another study has reported that the delivery of siRNA by LipofectamineTM 2000 for STAT3 silencing can induce apoptosis in astrocytoma cells (14). However, the use of these carriers is limited for *in vitro* application due to carrier-associated toxicity *in vivo* (15). Therefore, developing an optimum delivery system for siRNA remains the main obstacle for efficient RNA interference (RNAi)-based therapeutics. The delivery strategy should maintain siRNA stability under physiological conditions, improve pharmacokinetics and biodistribution, and enhance siRNA potency while reducing potential off-target effects of siRNA (16). In this regard, conventional viral vectors used for nucleic acids delivery are associated with several drawbacks, *in vivo*, including possibility of uncontrolled cell proliferation of transfected cells, immune reactions to viral particles and inflammation of the transduced tissue (17-

19). On the other hand, non-viral delivery systems are preferred over their viral counterparts for therapeutic applications due to their acceptable safety profile and polymeric carriers in particular are attractive since they are amenable for optimal design via chemical modification techniques (20-23). The polymeric carrier polyethylenimine (PEI) is an attractive carrier for intracellular delivery of siRNA. Because of its high cationic charge density, PEI possesses the ability to effectively condense nucleic acids by electrostatic interaction between the anionic phosphates in the siRNA backbone and the cationic amines in the polymer (24). It demonstrated effective siRNA delivery *in vitro* and *in vivo* to several cell types including cancerous cells (reviewed in (25)). The work of Urban-Klein et. al. signified the therapeutic applicability of PEI as a delivery system for siRNA-based cancer therapy (26). Using siRNA targeting c-erbB2/neu (HER2) receptor, the authors demonstrated marked reduction in tumor growth following systemic (intraperitoneal, i.p.) administration of the PEI/siRNA complex to mice bearing subcutaneous ovarian carcinoma xenograft (26). However, it is worth noting that the vehicle used in this study was a linear low-molecular-weight PEI. This explains the high N/P ratio needed in this study to achieve the desired complexation. Such carrier with lower cationic charge density compared to branched high-molecular-weight PEI (25 kDa) would end up with larger particle size upon nucleic acid compaction resulting in lower transfection efficiency (27). In contrast, branched PEI (25 kDa) is more effective systems for nucleic acids delivery than the linear counterpart (28). The smaller particles produced (nano-sized) enhances the transfection efficiency, and the higher complexation ability

(lower N/P ratio) is thought to reduce the need for both the polymeric material and the nucleic acid for biological functionality and, therefore, implies more specificity. However, this higher efficiency is also associated with higher cytotoxicity (28). Nonetheless, it is also possible to manipulate PEI backbone in order to enhance its condensation and transfection properties and to reduce associated cytotoxicity.

We recently developed improved polymeric systems for siRNA delivery to B16 melanoma cells based on stearic acid (StA) substitution on PEI backbone, where such a modification led to better protection of siRNA integrity in biological milieu and also improved the siRNA delivery into the cytoplasm (29). An enhanced silencing was obtained when this StA-derivative was used to deliver siRNA against α_v integrin. The latter served as a model target for demonstrating the feasibility of silencing and our previous studies were restricted to an *in vitro* culture system. In this study, we further evaluated the StA-substituted PEI carrier for siRNA-mediated downregulation of STAT3 in B16 melanoma cells, since recent data suggested that STAT3 was directly required for the initiation and promotion of mouse skin tumorigenesis (30). The molecular and cellular consequences of such a STAT3 inhibition in tumor cells were determined based on identified targets (IL-6 and VEGF secretion) and the studies were extended to a B16 tumor model in order to explore the effectiveness of the proposed carrier *in vivo* for the first time.

3.2 MATERIALS and METHODS

3.2.1 Materials

Branched PEI (25 kDa), triethylamine (TEA), 3-(4,5-dimethylthiazol-2-yl)-2,5-diphenyltetrazolium bromide (MTT), dimethyl sulfoxide (DMSO), and stearyl chloride (98.5%) were obtained from Sigma-Aldrich (St. Louis, MO). Anhydrous ethyl ether and dichloromethane (DCM) were purchased from Fisher Scientific (Fairlawn, NJ). Fetal Bovine Serum (FBS) was obtained from HyClone (Logan, UT). Dulbecco's Modified Eagle's Medium (DMEM), L-glutamine, and gentamicin were purchased from Gibco-BRL (Burlington, ON, Canada). Mouse IL-6 ELISA kit was purchased from e-Biosciences (San Diego, CA). Mouse VEGF Quantikine ELISA Kit was purchased from R&D Systems (Minneapolis, MN). Sequence-specific siRNA targeting murine STAT3 mRNA was purchased from Ambion (Austin, TX) (sense: 5'-GGACGACUUUGAUUUCAACTt-3', antisense: 5'-GUUGAAAUCAAGUCGUCCtg-3'). The scrambled siRNAs Silencer[®] Negative Control #1 siRNA (Catalogue #AM4635) and Silencer[®] FAM[™] labeled Negative Control #1 siRNA (Catalogue #AM4620), both purchased from Ambion (Austin, TX). Caspase 3 Assay Kit, Nonidet P-40, Protease Inhibitor Cocktails, and 4-Nitrophenyl phosphate were purchased Sigma-Aldrich (St. Louis, MO). SK-MEL-28 + IFN- γ Cell Lysate, anti-phosphotyrosine (Y⁷⁰⁵) STAT3 monoclonal antibody, and anti-actin antibody (I-19) were purchased from Santa Cruz Biotechnology (Santa Cruz, CA). ECL Plus[™] detection kit was purchased from GE Healthcare Life Sciences (Piscataway, NJ).

3.2.2 Cells and Animals

Murine B16.F10 cells were grown and propagated in DMEM supplemented with 10% FBS at 37 °C following the recommended propagation conditions of the American Type Culture Collection (ATCC). Male C57Bl/6 mice were purchased from the Jackson Laboratory (Bar Harbor, ME, USA). All experiments were performed in accordance with the University of Alberta guidelines for the care and use of laboratory animals. All experiments were performed using 4-6 week old male mice.

3.2.3 Preparation and Characterization of siRNA Complexes

As previously described, PEI-StA was prepared by N-acylation of PEI with stearyl chloride and characterized as described in (31). Thereafter, complexes of desired siRNA concentrations were prepared as previously described in (29) by incubating equal weights of siRNA and PEI or PEI-StA in RNase-free water for 30 min at 37 °C. Particle sizes were determined by employing dynamic light scattering methodology and ζ -potentials were determined for each siRNA complex in water by 3 serial measurements using Zetasizer 3000 (Malvern, UK).

3.2.4 STAT3 Knockdown by siRNA Complexes

For STAT3 targeting, polymer:siRNA complexes (1:1) were prepared at final siRNA concentrations of 6.25, 12.5, 25, 50, 100 and 200 nM. Thereafter, in 24-well plates, 1×10^5 B16 melanoma cells were incubated with the designated

complexes at 37 °C. 200 nM naked STAT3 siRNA and identical complexes of 200 nM of scrambled siRNA were used as controls. To remove uninternalized complexes, B16 medium was replaced after 8 h. Then, tumor supernatants were collected at 36 h and levels of IL-6 and VEGF were determined by ELISA. Moreover, cells were lysed and phosphorylated stat3 (p-stat3) levels were detected by Western blot (details in section 3.2.5). Optical intensity of p-stat3 band was quantified and normalized to actin protein band using ImageJ software (W. Rasband (2005) National Institutes of Health, Bethesda, MD, <http://rsb.info.nih.gov/ij>). Simultaneously, cancer cell viability was determined by MTT assay following 36 h of incubation with identical siRNA complexes.

3.2.5 Western Blot

Cells were collected and washed twice with ice-cold PBS. Then, sample tubes were imbedded in ice and cells were lysed in lysis buffer containing 30 mM HEPES (pH 7.5), 2 mM Na₃VO₄, 25 mM NaF, 2 mM EGTA, 2% Nonidet P-40, 1:100 protease inhibitor cocktails, 0.5 mM DTT and 6.4 mg/mL phosphatase substrate 4-nitrophenyl phosphate. Cell lysates were centrifuged for 20 seconds at 16,000×g. Thereafter, NaCl was added to samples to final concentration of 420 mM and cell lysates were centrifuges for 20 min at 16,000×g and supernatant was transferred to new tubes and pellets were discarded. Total protein extract was determined by Micro BCA Protein Assay kit. Equal amounts of protein (20 µg) were mixed with equal volumes of loading buffer (0.5 M Tris-HCl pH 6.8, 20% glycerol, 10% SDS, 1.5% bromophenol blue, 5% β-mercaptoethanol). Samples

were dipped in boiling water for 5 min then loaded on 8% SDS-PAGE gel. Electrophoresis was conducted in running buffer (25 mM Tris base, 192 mM glycine, 0.1% SDS). For the first 30 min, the run was conducted under 60 v then it was increased to 120 v for 90 min. Proteins were then transferred into activated PVDF membrane in transfer buffer (1L contains: 200 mL methanol 2.4 g Tris base, 14.2 g glycine, 0.1 g SDS) at 140 v for 2 h. Thereafter, the membrane was incubated overnight at 4° C with blocking buffer containing 5% skimmed milk and 0.5% bovine serum albumin (BSA) in Tris-Buffer Saline containing 0.1% (v/v) Tween-20 (TBS-T). Then, membranes were thoroughly washed in TBS-T and then probed with anti-phosphotyrosine (Y⁷⁰⁵) STAT3 monoclonal antibody at (1:500) dilution for 2 h. The membrane was then washed 5 times (5 minutes per wash) with TBS-T under gentle shaking. Then, goat anti-mouse polyclonal Ab at (1:50,000) was added to the membranes in blocking buffer and kept in room temperature for 90 min under gentle shaking. The membrane was then washed 5 times (5 minutes per wash) with TBS-T under gentle shaking and developed using ECL Plus™ detection kit. For loading control, the membrane was incubated with stripping solution (100 mM β-mercaptoethanol in TBS-T) at 37 °C for 30 min. The membrane was washed, blocked, and probed with anti-actin antibody (I-19) at dilution (1:1000) as mentioned above.

3.2.6 MTT Assay

B16 cells, grown in 96-well flat-bottomed microplates, were treated as indicated. Thereafter, 100 μL of MTT solution in culture medium (0.5 mg/mL)

was added to each well for 2 h. The formed formazan crystals were dissolved by adding 200 μ L of DMSO to each well and kept under gentle shaking for 30 min. Optical density was measured at 550 nm using a microplate reader (Powerwave with KC Junior software; Bio-Tek, Winooski, VT). The results were converted into % viability relative to untreated sample.

In another study, B16 cells in 96-well plates were challenged with a daily dose of 50 nM siRNA PEI and PEI-StA complexes for 3 consecutive days. Media was refreshed 8 h after each incubation to remove uninternalized complexes and MTT assay was carried out for 5 days from the first dose to assess cellular viability. Media was refreshed every day in all groups during this experiment.

3.2.7 Caspase 3 Activity Study

The Caspase 3 activity was measured as an indicator for apoptosis. For that purpose, B16 cells were treated with 50 nM siRNA in PEI or PEI-StA for 24 h. Using Caspase 3 Assay Kit, cells were normalized for 10^5 cells per treatment group, lysed, and placed in designated wells in 96-well flat-bottomed microplates. Provided Caspase 3 inhibitor (Ac-DEVD-CHO) and Caspase 3 substrate (Ac-DEVD-pNA) were then added to designated wells according to the manufacturer's instructions. Optical density was measured at 405 nm using microplate reader and Caspase 3 activity was calculated based on p-Nitroaniline calibration curve.

3.2.8 STAT3 silencing *in vivo*

For tumor establishment, 0.75×10^6 B16 cells, isolated from confluent culture and suspended in normal saline, were inoculated subcutaneously in the upper left flank of male C57Bl/6 mice. After 10 days, 500 pmol of STAT3-targeting or scrambled (non-targeting) siRNAs complexes in normal saline were administered to randomly-assigned groups (5 mice per group) by intratumoral (i.t.) injections on daily basis for 4 consecutive days. Untreated control group received daily i.t. injections of normal saline. Tumor dimensions were measured by vernier caliber once a day during treatment period. The longest diameter and the perpendicular shorter diameter were multiplied to obtain tumor area (mm^2). Thereafter, mice were euthanized 1 day after the final treatment dose and tumor samples were immediately isolated and weighed. Consequently, isolated tumors were crushed between two slides in sterile PBS to form uniform cell suspension. Tumor supernatants were obtained after centrifugation at $10,000 \times g$. Protein content in tumor supernatant was normalized using Micro BCA Protein Assay kit and analyzed for IL-6 and VEGF using corresponding ELISAs. Cellular part was lysed and analyzed for STAT3 activation and Caspase 3 activity as described above.

3.2.9 Data Analysis

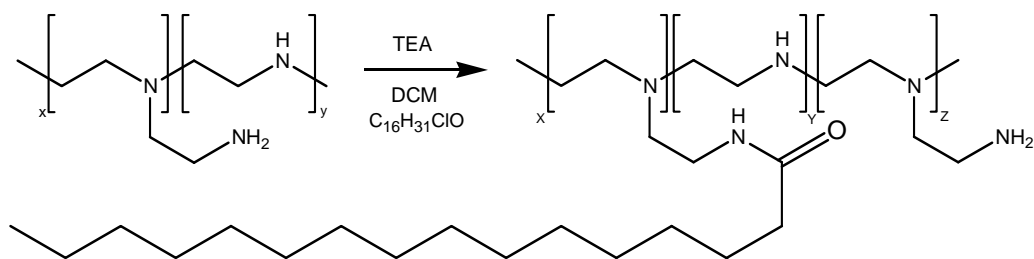
IC_{50} for STAT3 knockdown was calculated using four parameter logistic function (SigmaPlot for Windows, Version 10.0). The data were analyzed for

statistical significance ($p < 0.05$) by one-way ANOVA; Post-Hoc Scheffé's test was conducted to determine level of significance (SPSS for Windows, Version 16.0).

3.3 RESULTS

3.3.1 Characterization of siRNA Complexes

The average hydrodynamic diameter and ζ -potential of the siRNA complexes with PEI and PEI-StA are summarized in Figure 3.1. Both complexes formed ~110 nm structures with no significant differences in diameter. The complexes displayed positive net surface charge, where the complexes with the unmodified PEI showed 4.9-fold higher ζ -potential value than the PEI-StA complexes.



Polyplex	Diameter (nm)	ζ Potential (mV)
PEI	112 ± 21	34.3 ± 4.5
PEI-StA	110 ± 2	5.8 ± 1.2

Figure 3.1 Fatty acid attachment on PEI backbone and characteristics of the siRNA complexes. Table represents the size and zeta potential of polymer:siRNA (1:1) complexes in averages of 3 different measurements (\pm SD).

3.3.2 STAT3 Knockdown by siRNA Complexes

To evaluate the ability of complexes for STAT3 knockdown, B16 melanoma cells were targeted with siRNA doses ranging from 6.25 to 200 nM. The knockdown of the active protein, p-stat3, was dependant on the siRNA dose (Figure 3.2A). Levels of p-stat3 after incubation with PEI-StA complex were found to be 55.8% lower than that of PEI at 50 nM siRNA. At 100 nM siRNA, PEI-StA complexes also showed up to 42.2% reduction in p-stat3 levels compared to the PEI complexes. At 200 nM siRNA, there was no significant difference among the two polymers in spite of further p-stat3 reduction. It is worth noting that 25 nM siRNA was sufficient for PEI-StA complex to reach significant reduction in p-stat3 level. The observed knockdown is considered specific since 200 nM of scrambled siRNA did not show any significant reduction in p-stat3 levels (not shown). The IC_{50} of STAT3 knockdown was calculated based on the data in Figure 3.2A. PEI-StA complexes had an IC_{50} value of 19.0 ± 3.0 nM for p-stat3 knockdown, significantly lower than that of PEI complexes (94.3 ± 23.7 nM; $p < 0.05$).

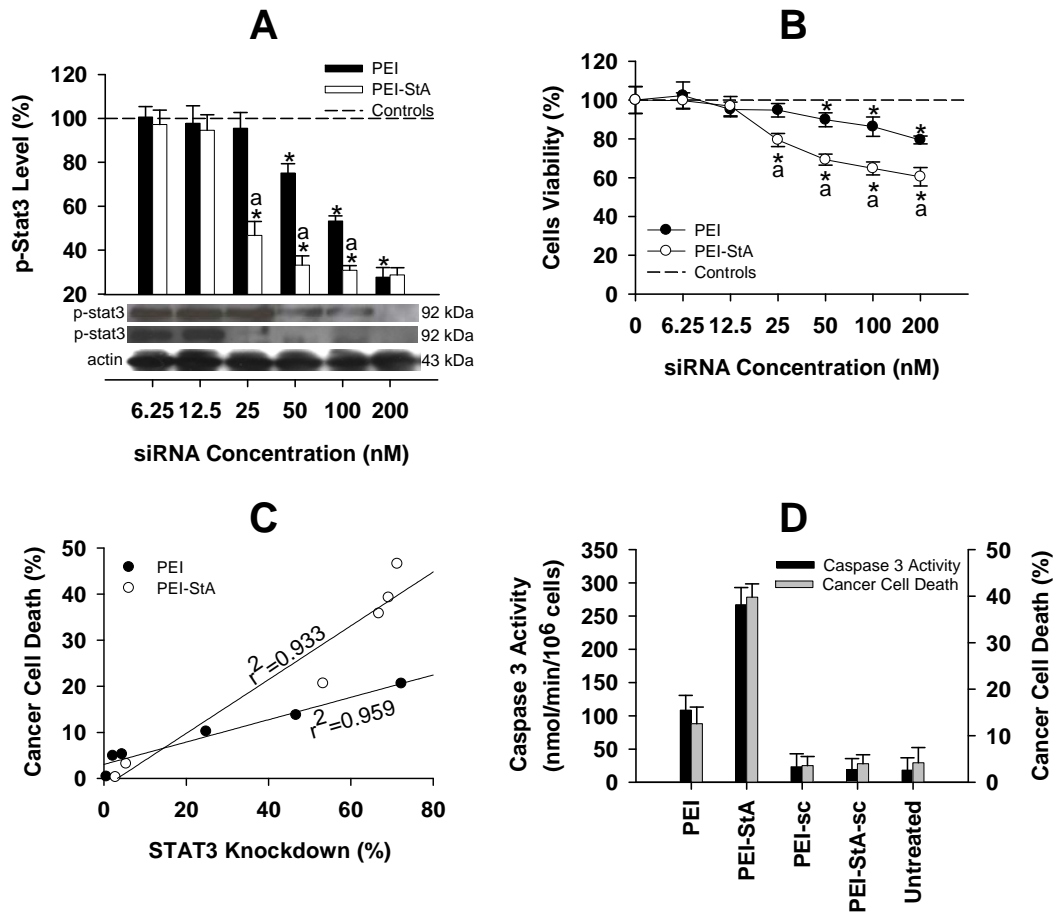


Figure 3.2 STAT3 knockdown by siRNA complexes in vitro. (A) Western blot analysis showing a dose-dependent reduction in p-stat3 signal using actin as loading control. Bars represent expression of p-stat3 upon the designated siRNA treatment. Data are shown as the average \pm SD of 4 experiments. (B) Percentage of cell viability was determined relative to untreated control by MTT assay. Data are shown as mean (\pm SD) of 7 replicates for each sample. (C) Correlation between p-stat3 knockdown and cancer cell death was determined by linear regression. Correlation co-efficient (r^2) for each set is expressed on the trend line of best fit. (D) Correlation between Caspase 3 activity (black bars) and cell death % (grey bars). PEI-StA caused higher apoptosis as compared to control (*; $p < 0.05$) and PEI (a; $p < 0.05$). Data are shown as mean (\pm SD) of 3 experiments. Where shown, dashed line represents controls including: 200 nM of naked siRNA or identical complexes of scrambled siRNA. Statistical significance was determined compared to control (*; $p < 0.05$) and PEI (a; $p < 0.05$).

3.3.3 Effect of STAT3 Knockdown on B16 Survival *in vitro*

To examine B16 cells survival following STAT3 knockdown, we measured cell viability using the MTT assay. After 36 h of incubation with the complexes, a dose-dependent cytotoxicity was obtained with all complexes (Figure 3.2B). At siRNA concentration of 50 nM, both complexes caused significant cytotoxicity of B16 melanoma cells, but cell viability was 18.5% lower after treatment with PEI-StA2 complexes as compared to that of PEI complexes. These results were consistent with the Western blot analysis. The possibility of non-specific cell death was tested using 200 nM of scrambled siRNA complexes and there were no significant changes in cell viability compared to untreated control. A strong correlation between the siRNA-mediated p-stat3 knockdown (data from Figure 3.2A) and B16 cell death (data from Figure 3.2B) was observed with all complexes, where the correlation coefficients (r^2) were 0.933 and 0.959 for PEI and PEI-StA complexes (Figure 3.2C).

In order to confirm apoptosis, Caspase 3 activity was measured after treatment with 50 nM siRNA (Figure 3.2D). While controls showed basal Caspase 3 activity, PEI complexes resulted in up to 6-fold increased Caspase 3 activities as compared to the untreated cells. When PEI-StA was used, Caspase 3 activity reached to 14.9 folds more than the untreated control. Consistent with our cytotoxicity results, Caspase 3 activity with the PEI-StA complexes was found to be ~ 2.5 times higher than that with PEI complexes. With formulations of scrambled siRNA using both polymers, no significant difference was noticed compared to untreated cells.

We then investigated the changes in cell viability after STAT3 silencing with fixed daily dose of siRNA (Figure 3.3). The B16 cells were incubated with 50 nM fresh siRNA complexes of PEI or PEI-StA every 24 h for 3 consecutive days, and cell viability was measured for 7 days. After 24 h, PEI-StA complexes caused 39.7% decrease in cancer cell viability, which was statistically better than what achieved by PEI complexes (12.6% reduction in cell viability). The second dose allowed for dramatic reduction in cell viability where PEI-StA complexes caused 73.9% decrease in cell viability as compared to only 23.9% reduction caused by PEI complexes. A third dose of PEI complexes further reduced cell viability by 30.6%, but with PEI-StA complexes reduction in cell viability was remarkably more reaching over 84.7% cell death. After treatment removal, cells started to regain viability and continued to grow back. A similar study was carried out with identical formulations of scrambled siRNA where no significant changes in cancer cell viability were noticed.

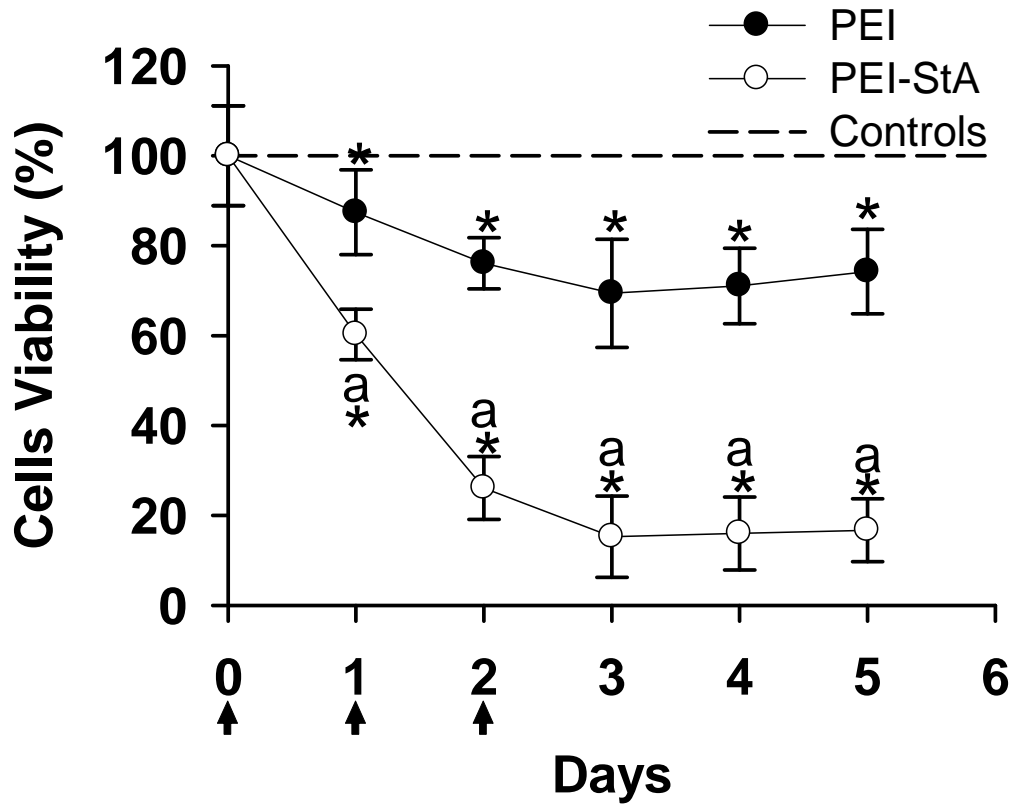


Figure 3.3 Effect of multiple administrations of 50 nM siRNA complexes on B16 viability in vitro. B16 cell viability is dramatically reduced by daily supplementation of anti-STAT3 siRNA in PEI and PEI-StA complexes. PEI-StA gave higher cell death as compared to control (*; $p < 0.05$) and PEI (a; $p < 0.05$). Data are shown as the average (\pm SD) of 3 independent experiments.

3.3.4 *In vitro* Cytokine Secretion by B16 Cells

To examine changes in the cytokine profile of B16 cells following STAT3 knockdown, B16 supernatants were collected after designated treatments and analyzed for IL-6 and VEGF. At 36 h after incubation, there was an increase in IL-6 secretion as a function of siRNA concentration used for STAT3 knockdown (Figure 3.4A). Unlike the PEI complexes, PEI-StA complexes mediated a significant increase in IL-6 levels at 25 nM siRNA. At this concentration, p-stat3 level was also significantly lower compared to the PEI complexes. Both polymers showed significant increase in IL-6 secretion at 50 nM siRNA; however, IL-6 concentration after treatment with PEI-StA complexes was 42.7% higher than the PEI complexes. Further increase in IL-6 levels was observed at 100 nM, where PEI-StA complexes produced higher IL-6 levels (33.4% higher than that of PEI complexes). The highest concentration of IL-6 was achieved at 200 nM with both polymers.

A dose-dependent decrease in VEGF concentration in B16 supernatant was observed following 36 h of siRNA treatment (Figure 3.4B). Consistent with the previous Western blot data, a significant reduction in VEGF level was detected at 25 nM siRNA with the PEI-StA complexes, but not with PEI complexes. Although all complexes significantly reduced VEGF secretion at 50 nM, PEI-StA mediated a higher reduction in VEGF level compared to PEI complexes. A more profound reduction in VEGF concentration was detected at 100 nM siRNA, where PEI-StA accounted for 27.2% decrease in measured VEGF concentration compared to the PEI complexes.

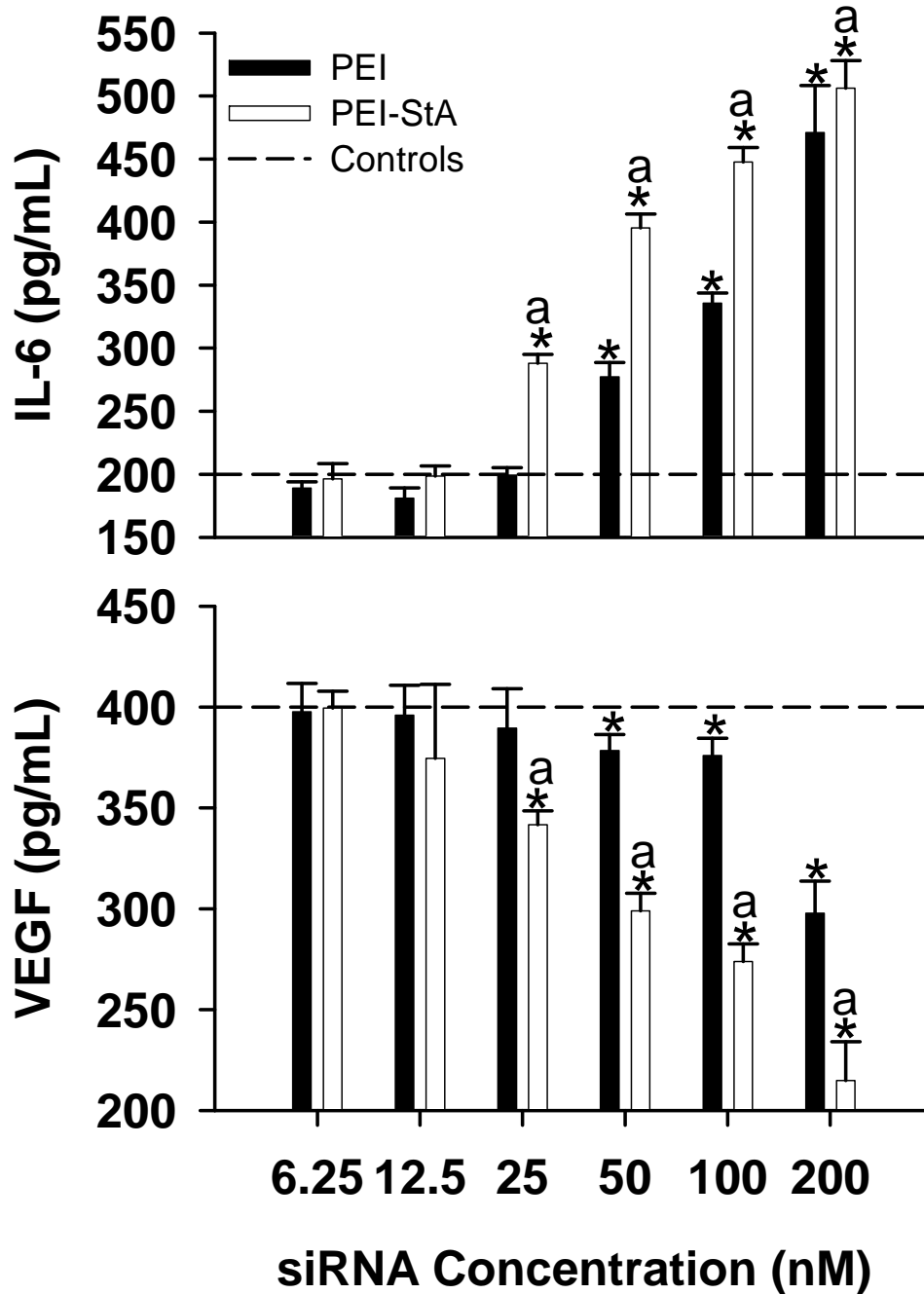
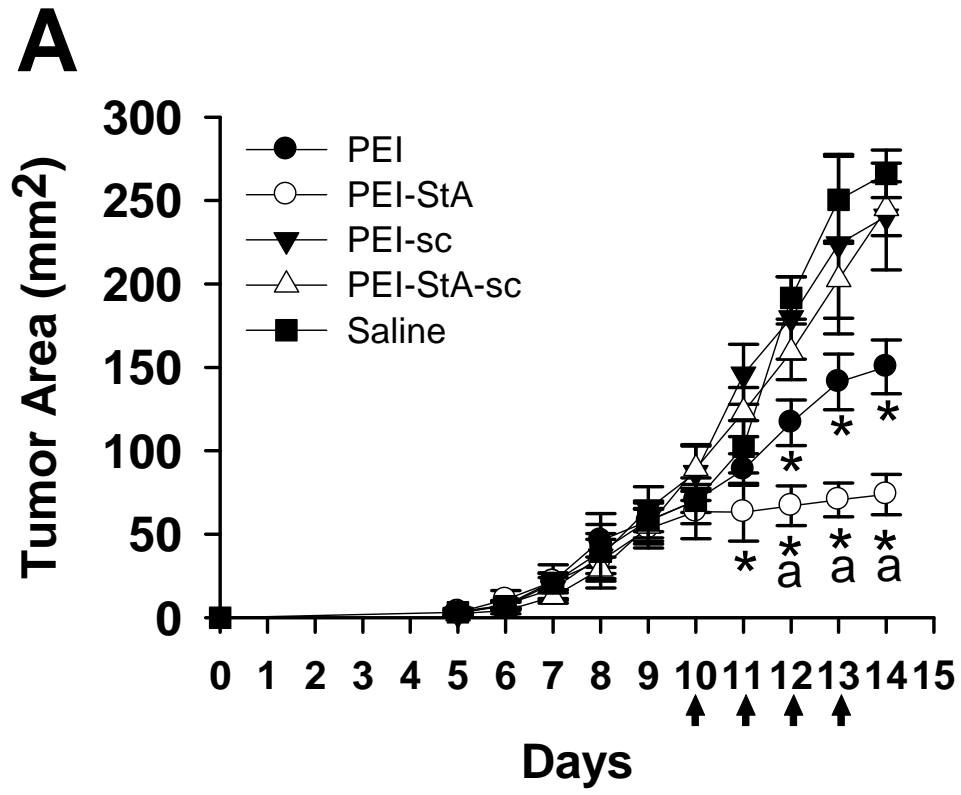


Figure 3.4 Analysis of cytokine profile after STAT3 knockdown in vitro. Cytokine levels measured by ELISA were plotted in bar graphs for IL-6 (top) and VEGF (bottom) where PEI-StA showed significant induction of IL-6 production and decrease in VEGF levels as compared to control (*; $p < 0.05$) and PEI (a; $p < 0.05$). Dashed line represents controls which include 200 nM of naked siRNA or identical complexes of scrambled siRNA. Data are shown as the average (\pm SD) of 3 measurements.

3.3.5 Effect of STAT3 Knockdown on B16 Tumor *in vivo*

To assess changes in tumor area after siRNA silencing of STAT3, we administered siRNA complexes intratumorally to an already established B16 tumor model. The results showed significant retardation in tumor growth after 4 days of administration of STAT3- siRNA by PEI-StA as compared to PEI (Figure 3.5A). Scrambled siRNA complexes did not show any significant difference from untreated control at any point throughout the study. By the end of the study, tumor area for animals treated by PEI-StA/siRNA complexes was 2 fold smaller than those treated with PEI/siRNA complexes (Figure 3.5A). Comparing the weights of isolated tumors, only STAT3-specific siRNA complexes showed significant reduction in tumor weight as compared to the controls (Figure 3.5B). Nevertheless, siRNA delivery with the PEI-StA showed a 38% reduction in tumor weight as compared to the delivery with PEI. A superior antitumor effect of STAT3-specific PEI-StA complexes over PEI and other controls was also evident visually at the time of sacrifices (Figure 3.5B).



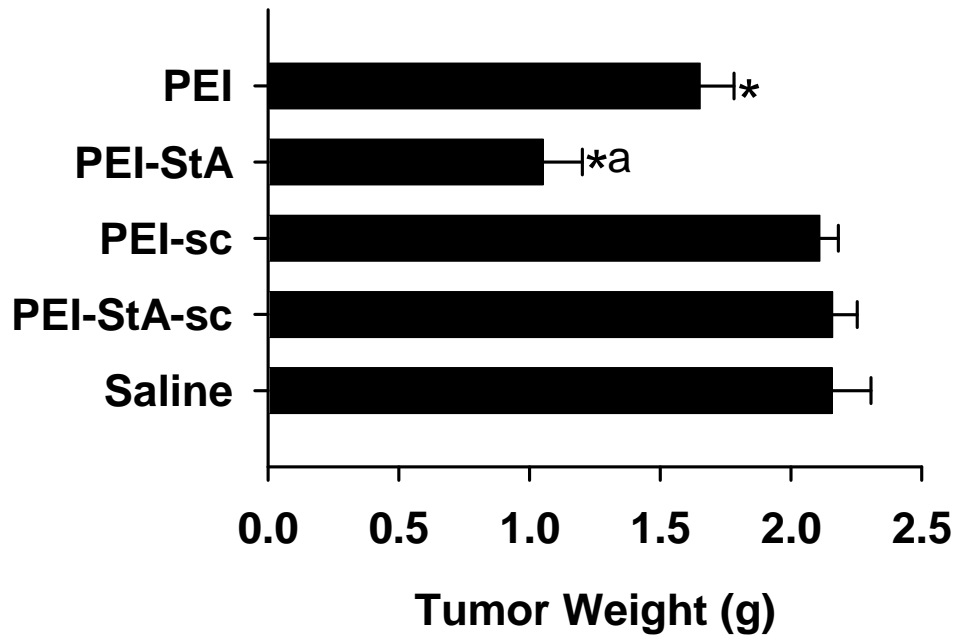
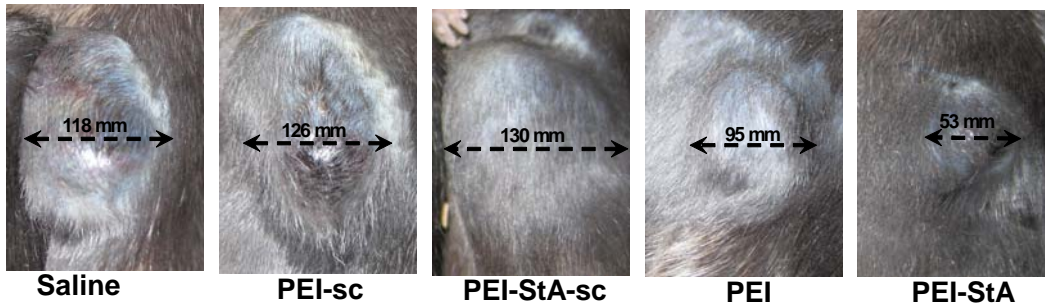
B**C**

Figure 3.5 Effect of siRNA complexes on tumor growth *in vivo*. (A) Male C57Bl/6 mice (5 per group) with established B16 tumors were injected with 500 pmol siRNA complexes for 4 days intratumorally. Tumor size was measured daily. The mean tumor area (\pm SE) for each group was plotted versus time. PEI-StA shows higher retardation in tumor growth as compared to control (*; $p < 0.05$) and PEI (a; $p < 0.05$). (B) Tumor weight was measured at the endpoint of the study. Bars represent mean weight (\pm SE) of the isolated tumors from each group. (C) Pictures representative for mice in each group at the endpoint of the study.

The western blot analysis of tumor homogenates showed that PEI-StA complexes were able to successfully reduce p-stat3 levels by ~41% and 60 % lower than what achieved by PEI complexes and untreated control, respectively (Figure 3.6A). This significant inhibition in p-stat3 was accompanied by a significant increase in Caspase 3 activity in PEI-StA treated groups, which was 2-fold and 22-fold higher than the PEI complex treated and the untreated control groups, respectively (Figure 3.6B). In agreement with the *in vitro* data, IL-6 level was significantly higher in PEI-StA/siRNA treated tumors, with 2-fold and 6-fold increase as compared to the PEI/siRNA treatment and the untreated control groups, respectively (Figure 3.6C). Consistently, VEGF level after PEI-StA/siRNA treatment was 3-fold and 5-fold less than the PEI/siRNA treatment and the untreated control groups, respectively (Figure 3.6D).

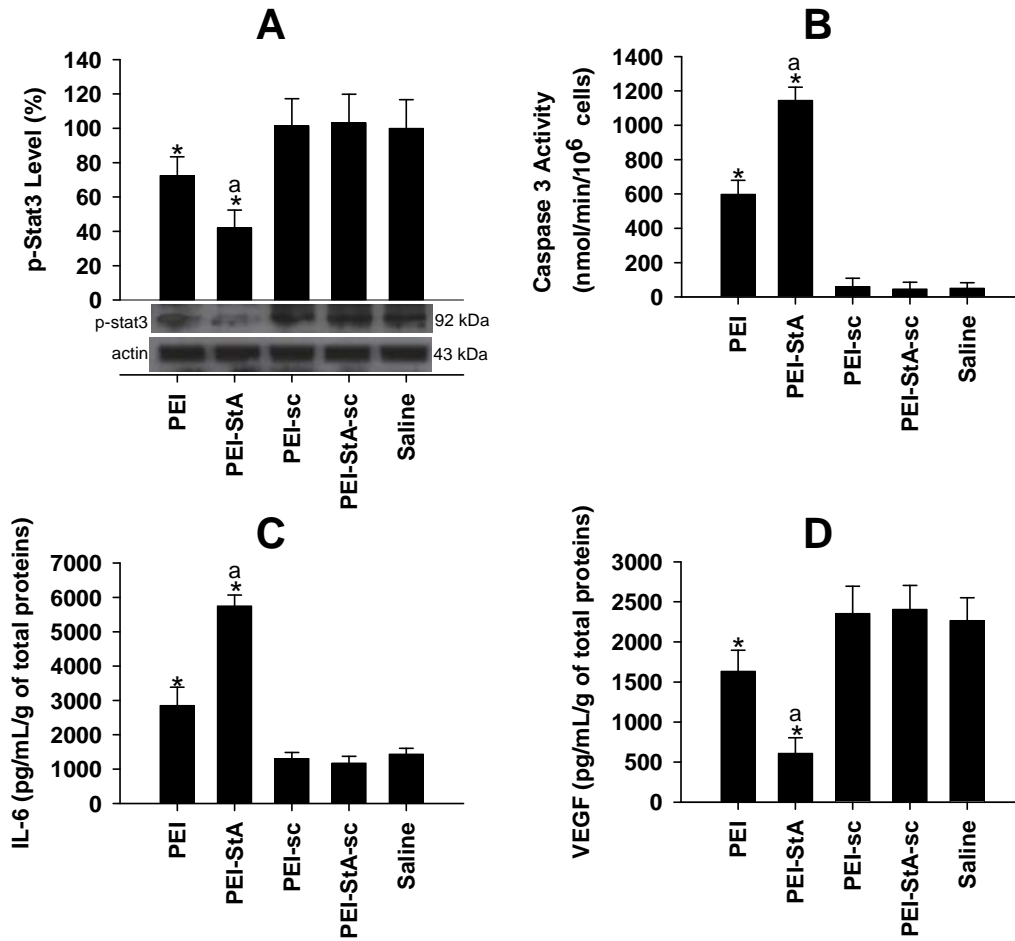


Figure 3.6 Molecular analysis of tumor following siRNA administration in vivo. (A) p-STAT3 was detected in 20 μ g of collected cell lysate from each treatment group by Western blot. Data are shown as the average (\pm SD) of 4 measurements. (B) Caspase 3 activity was measured in each treatment group. Data represent the mean of 6 measurements (\pm SD). (C) & (D) Levels of IL-6 and VEGF, respectively, in tumors from each treatment group as determined by ELISA. Data represent the mean (\pm SD) of at least 3 measurements. Significance levels are indicated by (*; $p < 0.05$) as compared to control and (a; $p < 0.05$) as compared to PEI.

3.4 DISCUSSION

The first direct evidence suggesting a critical role of STAT3 in cancer growth emerged when it was shown that down-regulation of STAT3 in cell lines derived from patients with squamous cell carcinoma of the head and neck (SCCHN) reduced the proliferation of SCCHN cells (32). Further molecular investigation on multiple-myeloma cells separated from bone-marrow aspirates, and on U266 myeloma cell line provided evidence for STAT3 contribution in survival and malignant progression of multiple myeloma (33). Furthermore, in a study involving prostate cancer patients, 82% of tumor specimens obtained by radical prostatectomy showed elevated levels of STAT3 compared with matched non-tumor prostate tissues (34). STAT3 was also found to be essential for leptin-induced survivin expression in breast cancer cells (35). Recently, studies on melanoma patients also suggested that tyrosine-phosphorylated STAT3 is a biomarker for atypical nevi progression and a potential target for chemoprevention of melanoma (36). Subsequent studies revealed that STAT3 is also persistently activated in other solid and hematological malignancies in human (reviewed in (37, 38)). Finally, interruption of the STAT3 signaling pathway in solid and hematological tumors were proposed to serve as a promising strategy for cancer therapy (39). For instance, in a study where both JAK and STAT3 were inhibited, a reduced tumor invasion and an increased apoptosis were noted in a human colorectal cancer model (40). Additionally, in a phase I/II clinical trial, tipifarnib (a farnesyl transferase inhibitor) was administered to patients with breast cancer in combination with doxorubicin and cyclophosphamide (41). The

authors found that p-STAT3 was inhibited in patients upon tipifarnib treatment, which produced higher pathologic complete response rate than chemotherapy alone. This collective experience clearly indicated STAT3 inhibition to be a promising approach for control of tumor growth and regression.

Several modalities have been employed to achieve effective STAT3 inhibition (11, 39). Peptides and peptidomimetics were introduced as inhibitors of STAT3 dimerization (8), but the effectiveness of these molecules was limited by the poor cellular permeability and insufficient stability profile. Small molecular inhibitors of STAT3 such as JSI-124 (cucurbitacin I) were shown to induce cell death and inhibit cell growth of transformed murine fibroblasts and human breast cancer (6). However, non-specific toxicity limited the clinical application of JSI-124. At effective JAK2/STAT3 inhibitory concentration, JSI-124 was shown to profoundly affect actin cytoskeleton via STAT3-independent mechanism in both cancerous and non-cancerous cells (42). More tolerable natural agents such as curcumin were reported to exert STAT3 inhibitory action in cancer (43). It was shown that curcumin inhibition of STAT3 phosphorylation is time dependent, where complete suppression of p-STAT3 was achieved after 4 h (10). However, the relatively high curcumin concentration used in these studies (40-50 μ M) raised a concern for its potential non-specific effects. A Phase II clinical trial investigating the anti-cancer potential of curcumin in prostate cancer patients indicated low bioavailability of curcumin when administered orally (44). Overall, since the inhibitory effect of small molecular weight agents on STAT3 is suggested to be indirect through disrupting upstream components in STAT3

signaling pathway (11), potential side effects and toxicities at levels required for STAT3 inhibition along with solubility, bioavailability and biological stability problems limit clinical application of these compounds.

RNA interference has been examined for STAT3 inhibition in cancer as a more specific modality. This strategy can be used as a direct STAT3 inhibitory approach, as well as serving as a complimentary means to reduce the required dose of inhibitors of STAT3 function. However, the therapeutic potential of siRNA is hindered by its poor cellular internalization and biological instability (45). Development of efficient and safe delivery systems that can correct these properties of siRNA will be paramount for its clinical application. Numerous non-viral carriers have been investigated for siRNA delivery, such as PEI, cationic liposomes, polyelectrolyte complex micelles, water soluble lipopolymers, and polycationic dendrimers. The knockdown of STAT3 by siRNA inducing apoptosis in astrocytoma cell lines has been achieved by high siRNA doses (20-60 μ M) using OligofectamineTM as carrier (14). Moreover, STAT3 knockdown by siRNA at 100 nM using LipofectamineTM 2000 was shown to induce apoptosis and limit invasiveness and motility of human prostate cancer cells *in vitro* (46). High siRNA doses used in such studies raises the concern for off-target effects. Besides, application of mentioned carriers has been associated with cellular toxicity limiting their *in vivo* application (15).

In this manuscript, we report on a potent siRNA polyplex that achieved efficient down-regulation of STAT3 at a relatively low siRNA concentration (~25 nM) (Figure 3.2A) and inhibited tumor growth both *in vitro* (Figure 3.2B) and *in*

in vivo (Figure 3.6A). This polyplex was based on StA attachment to branched PEI (25 kDa), which was recently reported to form complexes with siRNA, interact with B16 melanoma cells *in vitro* and reduce the expression of $\alpha(v)$ integrin in those cells (29). We evaluated this system for STAT3 targeting as a cancer therapeutic modality *in vitro* and *in vivo*. The dependence of B16 melanoma cells on STAT3 activity for their survival has been previously established (47). Our findings demonstrate that both polymers effectively pack siRNA into polyelectrolyte complexes suitable for cell internalization. However, cellular association of siRNA is higher when packed by PEI-StA as compared to PEI (not shown). The higher degree of siRNA protection in serum by PEI-StA might contribute to this effect (29). Others have also shown that siRNA protection from serum degradation is associated with better cellular distribution. The work of Kim et. al. showed that almost complete degradation of naked siRNA could occur after 8 h of incubation in 50% FBS; however, micelles of PEG-conjugated siRNA/PEI complexes were able to protect the siRNA even after 48 h of incubation (48). In the presence of serum, cellular uptake of these micelles by human prostate carcinoma cells (PC-3) was shown to be higher than siRNA/PEI complexes used in that study, which indicates improved stability (49). Moreover, we also found that the higher cellular association is correlated with higher siRNA silencing efficacy. Although both complexes were equipotent in STAT3 knockdown at 200 nM siRNA, PEI-StA yielded significant silencing effect and enhanced cancerous cell death at siRNA concentrations as low as 25 nM. This is expected to be beneficial to reduce possible siRNA off-target effects as a consequence of the

reduced dose. Secondly, lower polymer contents were needed for siRNA complexation when PEI-StA was used in comparison to PEI. Therefore, application of PEI-StA as the siRNA complexing agent may help to minimize potential inherent toxicity of PEI against non-target cells. In this regard, several approaches have been followed in literature to reduce PEI-associated cell toxicity while retaining transfecting efficacy including PEGylation (50, 51) and disulfide cross-linkage of PEI (52). Although non-specific toxicity of the polymers could complicate the interpretation of our results, the dose-dependent reduction in cancer cell viability observed in this study was unlikely to be due to non-specific polymer cytotoxicity, since; (i) the noted cell death after STAT3 knockdown by siRNA is shown to be an apoptotic rather than a necrotic event (i.e., cytotoxic effect of polymers is usually mediated via necrosis) and (ii) at the highest siRNA concentration used in this study (i.e., highest polymeric amount) were proven not to be toxic on B16 cells (29).

The *in vitro* B16 cell death was highly correlated with STAT3 knockdown efficiency (Figure 3.4C). It is worth noting that 50% inhibition in cancer cell survival *in vitro* was only achieved by PEI-StA complex after daily administration of siRNA complexes (Figure 3.3). This is not surprising because of the temporary nature of siRNA interference owing to its degradation by intracellular nucleases, which can be compensated by the daily supplementation of siRNA complexes. Such information was valuable in scheduling our *in vivo* study where daily administration of anti-STAT3 siRNA complexes for 4 days significantly suppressed tumor growth rate (Figure 3.5A). Although no reduction in the

originally treated tumor mass was noted, groups treated with PEI and in particular PEI-StA/STAT3 siRNA complexes, demonstrated remarkable inhibition in tumor growth and significant induction of apoptosis *in vivo* compared to scrambled siRNA complexes and untreated controls (Figure 3.6B).

Upon STAT3 knockdown, an increase in IL-6 production and a decrease in VEGF production by B16 cells were detected *in vitro* (Figure 3.4A and B) and *in vivo* (Figure 3.6C and D). IL-6 is a pleiotropic cytokine with paradoxical effects. In some cases, IL-6 promotes tumor growth, while exerting anti-tumoral activity in other cases, and being used for the treatment of malignancies such as melanoma (53). This paradox is partly due two opposing transcription factors activated by the IL-6 signaling, namely STAT3 and STAT1 (54). In many cancer types, IL-6 constitutively activates STAT3, whereas STAT1 activation by IL-6 seems to be transient and inefficient especially when compared to its activation by interferon alpha (IFN- α) and interferon gamma (IFN- γ) (55). Interestingly, in the absence of STAT3, IL-6 causes a drastic and prolonged activation of STAT1, and induces the same spectrum of genes that are induced by IFN- γ with similar kinetics and response (56). Such an effect would directly translate into suppression of B16 cell growth (57). Therefore, we argue that one reason for the noted cancer regression after STAT3 knockdown in this study is perhaps the anti-tumoral effect of IL-6 that is reminiscent of the IFN- γ effect. Moreover, the expression of IL-6 is known to be induced by IFN- γ (58) and NF κ B activity (59). Upon IL-6 expression, STAT3 strongly inhibits IFN expression (60) and suppresses NF κ B activity (61). Therefore, when STAT3 is downregulated, it is

logical to expect an induction in IL-6 production. Our results showed a dose-dependent increase in IL-6 secretion *in vitro* associated with STAT3 knockdown. Similarly, we detected an enhanced production of IL-6 in the isolated tumor tissue (Figure 3.6C) where STAT3 is downregulated (Figure 3.6A). An independent group has also reported similar observation where induction of IL-6 production was detected in B16 melanoma cells *in vivo* after STAT3 targeting by anti-sense oligonucleotide (62). In contrast to our findings, another study reported a reduction of IL-6 mRNA in B16.F10 after interrupting STAT3 signaling (9). The reason behind this discrepancy is unclear to us, but we note that the approach used by these authors to suppress STAT3 activity was by suppression of STAT3 nuclear translocation by decoy oligonucleotide with no inhibition of cytoplasmic levels of STAT3. The presence of STAT3 in the cytoplasm raises the possibility of STAT3 inhibition on NF κ B (63). Recently, it was suggested that STAT3 could interact with p65 subunit to form a novel complex that suppresses P-NF κ B activity (64). In our siRNA-based approach as well as in the anti-sense oligonucleotide approach (62), intracellular protein levels of STAT3 was reduced, which minimized the negative effect on NF κ B and, hence, promoted the IL-6 production. However, because IL-6 is also produced *in vivo* by components of the immune systems, we cannot attribute all IL-6 secretion solely to tumor cells. A more detailed analysis of the infiltrating immune cells to the tumor mass and the possible anti-tumoral immune response is discussed in Chapter 4.

The reduction in the VEGF levels as a result of STAT3 knockdown was expected since VEGF gene expression was shown to be upregulated by STAT3

(65). Beside its role for tumoral angiogenesis, the importance of VEGF for B16 survival has been demonstrated (66). Considering the well established relationship between the VEGF expression, tumor vascularization and cancer survival, we expect the regression in tumor growth *in vivo* after STAT3 inhibition was due to both its direct effects on cancer cell survival and its anti-angiogenic effect on tumor tissue mass. However, we could not rule out the possibility of B16 cell death due to reduced expression of other antiapoptotic proteins as a result of STAT3 knockdown. It has been demonstrated that STAT3 upregulates the expression of several antiapoptotic proteins such as Bcl-2, Bcl-xL, and Mcl-1 (39) and the inhibition of STAT3 activity results in an increased sensitivity to apoptosis (67). Moreover, the detrimental effects of STAT3 disruption on B16 survival has been linked to inhibition in Bcl-xL expression (67). It will be important to elucidate the role of other intracellular proteins involved upon STAT3 inhibition, and this may identify better therapeutic targets.

3.5 REFERENCES

1. Jing N, Tweardy DJ. Targeting Stat3 in cancer therapy. *Anticancer Drugs*. 2005 Jul;16(6):601-7.
2. Turkson J, Jove R. STAT proteins: novel molecular targets for cancer drug discovery. *Oncogene*. 2000;19:6613 - 26.
3. Buettner R, Mora LB, Jove R. Activated STAT Signaling in Human Tumors Provides Novel Molecular Targets for Therapeutic Intervention. *Clin Cancer Res*. 2002;8:945–54.
4. Yu CL, Meyer DJ, Campbell GS, Larner AC, Carter-Su C, Schwartz J, et al. Enhanced DNA-binding activity of a Stat3-related protein in cells transformed by the Src oncoprotein. *Science*. 1995 Jul 7;269(5220):81-3.
5. Yu H, Jove R. The STATs of Cancer — New Molecular Targets Come of Age. *Nat Rev Cancer*. 2004;4:97-105.
6. Blaskovich MA, Sun J, Cantor A, Turkson J, Jove R, Sebt SM. Discovery of JSI-124 (cucurbitacin I), a selective Janus kinase/signal transducer and activator of transcription 3 signaling pathway inhibitor with potent antitumor activity against human and murine cancer cells in mice. *Cancer Res*. 2003 Mar 15;63(6):1270-9.
7. Bharti AC, Donato N, Aggarwal BB. Curcumin (diferuloylmethane) inhibits constitutive and IL-6-inducible STAT3 phosphorylation in human multiple myeloma cells. *J Immunol*. 2003 Oct 1;171(7):3863-71.
8. Turkson J, Ryan D, Kim JS, Zhang Y, Chen Z, Haura E, et al. Phosphotyrosyl peptides block Stat3-mediated DNA binding activity, gene regulation, and cell transformation. *J Biol Chem*. 2001 Nov 30;276(48):45443-55.
9. Liu X, Li J, Zhang J. STAT3-decoy ODN inhibits cytokine autocrine of murine tumor cells. *Cell Mol Immunol*. 2007 Aug;4(4):309-13.
10. Deng J, Grande F, Neamati N. Small molecule inhibitors of Stat3 signaling pathway. *Curr Cancer Drug Targets*. 2007 Feb;7(1):91-107.
11. Yue P, Turkson J. Targeting STAT3 in cancer: how successful are we? *Expert Opin Investig Drugs*. 2009 Jan;18(1):45-56.
12. Cejka D, Losert D, Wacheck V. Short interfering RNA (siRNA): tool or therapeutic? *Clin Sci (Lond)*. 2006 Jan;110(1):47-58.
13. Gao LF, Xu DQ, Wen LJ, Zhang XY, Shao YT, Zhao XJ. Inhibition of STAT3 expression by siRNA suppresses growth and induces apoptosis in laryngeal cancer cells. *Acta Pharmacol Sin*. 2005 Mar;26(3):377-83.
14. Konnikova L, Kotecki M, Kruger MM, Cochran BH. Knockdown of STAT3 expression by RNAi induces apoptosis in astrocytoma cells. *BMC Cancer*. 2003 Sep 17;3:23.
15. Omid Y, Hollins AJ, Benboubetra M, Drayton R, Benter IF, Akhtar S. Toxicogenomics of non-viral vectors for gene therapy: a microarray study of lipofectin- and oligofectamine-induced gene expression changes in human epithelial cells. *J Drug Target*. 2003 Jul;11(6):311-23.
16. Thomas M, Lu JJ, Chen J, Klibanov AM. Non-viral siRNA delivery to the lung. *Adv Drug Deliv Rev*. 2007 Mar 30;59(2-3):124-33.

17. Kohn DB, Sadelain M, Glorioso JC. Occurrence of leukaemia following gene therapy of X-linked SCID. *Nat Rev Cancer*. 2003 Jul;3(7):477-88.
18. Zaiss AK, Muruve DA. Immune responses to adeno-associated virus vectors. *Curr Gene Ther*. 2005 Jun;5(3):323-31.
19. Muruve DA. The innate immune response to adenovirus vectors. *Hum Gene Ther*. 2004 Dec;15(12):1157-66.
20. Uprichard SL. The therapeutic potential of RNA interference. *FEBS Lett*. 2005 Oct 31;579(26):5996-6007.
21. Kennedy D. Breakthrough of the year. *Science*. 2002 Dec 20;298(5602):2283.
22. Behlke MA. Progress towards in vivo use of siRNAs. *Mol Ther*. 2006 Apr;13(4):644-70.
23. Putnam D, Doody A. RNA-interference effectors and their delivery. *Crit Rev Ther Drug Carrier Syst*. 2006;23(2):137-64.
24. Demeneix B, Behr JP. Polyethylenimine (PEI). *Adv Genet*. 2005;53:217-30.
25. Aigner A. Gene silencing through RNA interference (RNAi) in vivo: strategies based on the direct application of siRNAs. *J Biotechnol*. 2006 Jun 25;124(1):12-25.
26. Urban-Klein B, Werth S, Abuharbeid S, Czubayko F, Aigner A. RNAi-mediated gene-targeting through systemic application of polyethylenimine (PEI)-complexed siRNA in vivo. *Gene Ther*. 2005 Mar;12(5):461-6.
27. Lungwitz U, Breunig M, Blunk T, Gopferich A. Polyethylenimine-based non-viral gene delivery systems. *Eur J Pharm Biopharm*. 2005 Jul;60(2):247-66.
28. Godbey WT, Wu KK, Mikos AG. Size matters: molecular weight affects the efficiency of poly(ethylenimine) as a gene delivery vehicle. *J Biomed Mater Res*. 1999 Jun 5;45(3):268-75.
29. Alshamsan A, Haddadi A, Incani V, Samuel J, Lavasanifar A, Uludag H. Formulation and Delivery of siRNA by Oleic Acid and Stearic Acid Modified Polyethylenimine. *Mol Pharm*. 2009 Feb 2;6(1):121-33.
30. Kataoka K, Kim DJ, Carbajal S, Clifford JL, DiGiovanni J. Stage-specific disruption of Stat3 demonstrates a direct requirement during both the initiation and promotion stages of mouse skin tumorigenesis. *Carcinogenesis*. 2008 Jun;29(6):1108-14.
31. Incani V, Tunis E, Clements BA, Olson C, Kucharski C, Lavasanifar A, et al. Palmitic acid substitution on cationic polymers for effective delivery of plasmid DNA to bone marrow stromal cells. *J Biomed Mater Res A*. 2007 May;81(2):493-504.
32. Grandis JR, Drenning SD, Chakraborty A, Zhou MY, Zeng Q, Pitt AS, et al. Requirement of Stat3 but not Stat1 activation for epidermal growth factor receptor-mediated cell growth in vitro. *J Clin Invest*. 1998 Oct 1;102(7):1385-92.
33. Catlett-Falcone R, Landowski TH, Oshiro MM, Turkson J, Levitzki A, Savino R, et al. Constitutive Activation of Stat3 Signaling Confers Resistance to Apoptosis in Human U266 Myeloma Cells. *Immunity*. 1999;10:105-15.
34. Mora LB, Buettner R, Seigne J, Diaz J, Ahmad N, Garcia R, et al. Constitutive activation of Stat3 in human prostate tumors and cell lines: direct

inhibition of Stat3 signaling induces apoptosis of prostate cancer cells. *Cancer Res.* 2002 Nov 15;62(22):6659-66.

35. Jiang H, Yu J, Guo H, Song H, Chen S. Upregulation of survivin by leptin/STAT3 signaling in MCF-7 cells. *Biochem Biophys Res Commun.* 2008 Mar 28;368(1):1-5.

36. Wang W, Edington HD, Rao UN, Jukic DM, Wang H, Shipe-Spotloe JM, et al. STAT3 as a biomarker of progression in atypical nevi of patients with melanoma: dose-response effects of systemic IFNalpha therapy. *J Invest Dermatol.* 2008 Aug;128(8):1997-2002.

37. Yu H, Jove R. The STATs of cancer--new molecular targets come of age. *Nat Rev Cancer.* 2004 Feb;4(2):97-105.

38. Darnell JE. Validating Stat3 in cancer therapy. *Nat Med.* 2005 Jun;11(6):595-6.

39. Al Zaid Siddiquee K, Turkson J. STAT3 as a target for inducing apoptosis in solid and hematological tumors. *Cell Res.* 2008 Feb;18(2):254-67.

40. Xiong H, Zhang ZG, Tian XQ, Sun DF, Liang QC, Zhang YJ, et al. Inhibition of JAK1, 2/STAT3 signaling induces apoptosis, cell cycle arrest, and reduces tumor cell invasion in colorectal cancer cells. *Neoplasia.* 2008 Mar;10(3):287-97.

41. Sparano JA, Moulder S, Kazi A, Coppola D, Negassa A, Vahdat L, et al. Phase II trial of tipifarnib plus neoadjuvant doxorubicin-cyclophosphamide in patients with clinical stage IIB-IIIC breast cancer. *Clin Cancer Res.* 2009 Apr 15;15(8):2942-8.

42. Graness A, Poli V, Goppelt-Struebe M. STAT3-independent inhibition of lysophosphatidic acid-mediated upregulation of connective tissue growth factor (CTGF) by cucurbitacin I. *Biochem Pharmacol.* 2006 Jun 28;72(1):32-41.

43. Mackenzie GG, Queisser N, Wolfson ML, Fraga CG, Adamo AM, Oteiza PI. Curcumin induces cell-arrest and apoptosis in association with the inhibition of constitutively active NF-kappaB and STAT3 pathways in Hodgkin's lymphoma cells. *Int J Cancer.* 2008 Jul 1;123(1):56-65.

44. Dhillon N, Aggarwal BB, Newman RA, Wolff RA, Kunnumakkara AB, Abbruzzese JL, et al. Phase II trial of curcumin in patients with advanced pancreatic cancer. *Clin Cancer Res.* 2008 Jul 15;14(14):4491-9.

45. Gilmore IR, Fox SP, Hollins AJ, Akhtar S. Delivery strategies for siRNA-mediated gene silencing. *Curr Drug Deliv.* 2006 Apr;3(2):147-5.

46. Zhou W, Grandis JR, Wells A. STAT3 is required but not sufficient for EGF receptor-mediated migration and invasion of human prostate carcinoma cell lines. *Br J Cancer.* 2006 Jul 17;95(2):164-71.

47. Niu G, Shain KH, Huang M, Ravi R, Bedi A, Dalton WS, et al. Overexpression of a dominant-negative signal transducer and activator of transcription 3 variant in tumor cells leads to production of soluble factors that induce apoptosis and cell cycle arrest. *Cancer Res.* 2001 Apr 15;61(8):3276-80.

48. Kim SH, Jeong JH, Lee SH, Kim SW, Park TG. PEG conjugated VEGF siRNA for anti-angiogenic gene therapy. *J Control Release.* 2006 Nov 28;116(2):123-9.

49. Kim SH, Jeong JH, Lee SH, Kim SW, Park TG. Local and systemic delivery of VEGF siRNA using polyelectrolyte complex micelles for effective treatment of cancer. *J Control Release*. 2008 Jul 14;129(2):107-16.
50. Veisheh O, Kievit FM, Gunn JW, Ratner BD, Zhang M. A ligand-mediated nanovector for targeted gene delivery and transfection in cancer cells. *Biomaterials*. 2009 Feb;30(4):649-57.
51. Malek A, Czubayko F, Aigner A. PEG grafting of polyethylenimine (PEI) exerts different effects on DNA transfection and siRNA-induced gene targeting efficacy. *J Drug Target*. 2008 Feb;16(2):124-39.
52. Breunig M, Lungwitz U, Liebl R, Goepferich A. Breaking up the correlation between efficacy and toxicity for nonviral gene delivery. *Proc Natl Acad Sci U S A*. 2007 Sep 4;104(36):14454-9.
53. Hsiao YW, Liao KW, Chung TF, Liu CH, Hsu CD, Chu RM. Interactions of host IL-6 and IFN-gamma and cancer-derived TGF-beta1 on MHC molecule expression during tumor spontaneous regression. *Cancer Immunol Immunother*. 2008 Jul;57(7):1091-104.
54. Rakemann T, Niehof M, Kubicka S, Fischer M, Manns MP, Rose-John S, et al. The designer cytokine hyper-interleukin-6 is a potent activator of STAT3-dependent gene transcription in vivo and in vitro. *J Biol Chem*. 1999 Jan 15;274(3):1257-66.
55. Haan S, Keller JF, Behrmann I, Heinrich PC, Haan C. Multiple reasons for an inefficient STAT1 response upon IL-6-type cytokine stimulation. *Cell Signal*. 2005 Dec;17(12):1542-50.
56. Costa-Pereira AP, Tininini S, Strobl B, Alonzi T, Schlaak JF, Is'harc H, et al. Mutational switch of an IL-6 response to an interferon-gamma-like response. *Proc Natl Acad Sci U S A*. 2002 Jun 11;99(12):8043-7.
57. Kakuta S, Tagawa Y, Shibata S, Nanno M, Iwakura Y. Inhibition of B16 melanoma experimental metastasis by interferon-gamma through direct inhibition of cell proliferation and activation of antitumour host mechanisms. *Immunology*. 2002 Jan;105(1):92-100.
58. Costanzo C, Piacentini G, Vicentini L, Armenante F, Mazzi P, Savio C, et al. Cell-specific differences in the regulation of IL-6 expression by PMA. *Biochem Biophys Res Commun*. 1999 Jul 14;260(3):577-81.
59. Libermann TA, Baltimore D. Activation of interleukin-6 gene expression through the NF-kappa B transcription factor. *Mol Cell Biol*. 1990 May;10(5):2327-34.
60. Kortylewski M, Kujawski M, Herrmann A, Yang C, Wang L, Liu Y, et al. Toll-like receptor 9 activation of signal transducer and activator of transcription 3 constrains its agonist-based immunotherapy. *Cancer Res*. 2009 Mar 15;69(6):2497-505.
61. Nishinakamura H, Minoda Y, Saeki K, Koga K, Takaesu G, Onodera M, et al. An RNA-binding protein alphaCP-1 is involved in the STAT3-mediated suppression of NF-kappaB transcriptional activity. *Int Immunol*. 2007 May;19(5):609-19.

62. Wang T, Niu G, Kortylewski M, Burdelya L, Shain K, Zhang S, et al. Regulation of the innate and adaptive immune responses by Stat-3 signaling in tumor cells. *Nat Med.* 2004 Jan;10(1):48-54.
63. Yu Z, Zhang W, Kone BC. Signal transducers and activators of transcription 3 (STAT3) inhibits transcription of the inducible nitric oxide synthase gene by interacting with nuclear factor kappaB. *Biochem J.* 2002 Oct 1;367(Pt 1):97-105.
64. Yang J, Stark GR. Roles of unphosphorylated STATs in signaling. *Cell Res.* 2008 Apr;18(4):443-51.
65. Chen Z, Han ZC. STAT3: a critical transcription activator in angiogenesis. *Med Res Rev.* 2008 Mar;28(2):185-200.
66. Ghosh S, Maity P. Augmented antitumor effects of combination therapy with VEGF antibody and cisplatin on murine B16F10 melanoma cells. *Int Immunopharmacol.* 2007 Dec 15;7(13):1598-608.
67. Niu G, Heller R, Catlett-Falcone R, Coppola D, Jaroszeski M, Dalton W, et al. Gene therapy with dominant-negative Stat3 suppresses growth of the murine melanoma B16 tumor in vivo. *Cancer Res.* 1999 Oct 15;59(20):5059-63.

CHAPTER FOUR

BYSTANDER IMMUNE RESPONSE IN STAT3-SILENCED MELANOMA

A version of this chapter has been published in

J Pharm Pharmaceut Sci. 2010; 13(1) 21-26

Aws Alshamsan, Samar Hamdy, Saswati Das, Afsaneh Lavasanifar, John Samuel,
and Ayman O. S. El-Kadi

& submitted to

Cancer. 2010;

Aws Alshamsan, Samar Hamdy, Azita Haddadi, John Samuel,
Ayman O.S. El-Kadi, Hasan Uludağ, and Afsaneh Lavasanifar

&

Presented as a poster in

Faculty of Pharmacy and Pharmaceutical Sciences Research and Development

Day, Edmonton, Alberta, Canada, October, 2005

&

The 37th Annual Meeting and Exposition of the Controlled Release Society,

Portland, Oregon, USA, July 10-14, 2010

4.1 INTRODUCTION

Immune evasion is a hallmark of cancer progression and development (1, 2). One of the major strategies that allow tumors to evade immune detection and eradication is through persistent activation of signal transducer and activator of transcription 3 (STAT3) (3-6). This downstream protein is a transcription factor that becomes activated in response to cytokine and growth factor receptor stimulation; forming dimers and translocating to the nucleus upon activation. In a variety of tumor cells, activated STAT3 promotes the transcription of genes responsible for cell survival and proliferation, angiogenesis, metastasis, as well as immune escape (7, 8). For immune escape property, STAT3 involvement appears at two levels: the cell intrinsic level and the cell extrinsic level. The cell intrinsic mechanisms encompass changes in cancer cells that have resulted from persistently active STAT3. For instance, constitutively active STAT3 suppresses the production of the chemokines RANTES and IP-10 that are responsible for T-cell recruitment (3). Another example is the downregulation of the tumor-cell-surface expression of Fas receptor (CD95), which is a proapoptotic receptor involved in cytotoxic T lymphocyte (CTL)-dependant cytotoxicity (9). The cell extrinsic level is orchestrated by the ability of STAT3 to mediate a cross-talk between cancer and immune cells (10-12). In this scenario, tumor-derived factors (TDFs) produced by STAT3-activated tumors, induce the activation of STAT3 in multiple subsets of innate and adaptive immune cells (11, 13). Upon STAT3 hyperactivity, innate immune cells such as natural killer (NK) cells, tumor-associated macrophages (TAM), NKT cells, and neutrophils lose their ability to

inhibit tumors and their effective production of immunostimulatory molecules (11). Dendritic cells (DCs), which are the most potent antigen presenting cells (APCs), are also negatively influenced by STAT3 hyperactivation. The immunosuppressive milieu induces the production of immunosuppressive TDFs that further inhibit DC maturation and results in the inhibition of Th1-type immune response and CTL cytotoxicity (3). Thus, in the presence of cancer, DC malfunction causes an immunological paralysis and potentiation of cancer progression (5, 14). Therefore, breaking this cycle of tolerance by targeting persistently-active STAT3 in tumors is essential to reactivate the immune system for a robust anti-tumor response in an otherwise immunosuppressive microenvironment.

RNA interference (RNAi) induced by small interfering RNA (siRNA) provides a very specific and effective modality to downregulate protein expression at the mRNA level (15). Despite great potential, siRNA technology suffers from fundamental drawbacks such as low biological stability, poor cell permeability, and unfavorable pharmacokinetic and biodistribution profile that hinder its progress from bench to bedside (16). Therefore, it is essential to develop a delivery system that optimally delivers siRNA to its site of action while retaining its silencing activity (17).

We have recently developed a polymeric system for siRNA delivery to B16 melanoma cells based on stearic acid (StA) substitution on polyethylenimine (PEI) backbone, where such modification led to a better siRNA stability in biological milieu, effective downregulation of STAT3 at low siRNA doses,

leading to the inhibition of B16 cell growth both *in vitro* and *in vivo* (18). Moreover, a reduction in the level of vascular endothelial growth factor (VEGF), an increase in interleukin-6 (IL-6) production, and a rise in Caspase 3 activity in isolated tumor mass upon siRNA intervention was noted (18). This chapter sheds the light on the intratumoral trafficking and activity of immune cells, including DCs, following STAT3 downregulation in tumor cells by its siRNA/PEI-StA complexes.

Also, in this chapter, we examined the possible discrepancy in immune response of DCs coming from different sources i.e. primary culture of bone-marrow derived DCs and DC.24 cell lines, which have been used in literature in order to study TDF effects on DC maturation and STAT3 activation *in vitro*.

4.2 MATERIALS and METHODS

4.2.1 Materials

Branched PEI (25 kDa), triethylamine (TEA), 3-(4,5-dimethylthiazol-2-yl)-2,5-diphenyltetrazolium bromide (MTT), dimethyl sulfoxide (DMSO), and stearoyl chloride (98.5%) were obtained from Sigma-Aldrich (St. Louis, MO). Anhydrous ethyl ether and dichloromethane (DCM) were purchased from Fisher Scientific (Fairlawn, NJ). Fetal Bovine Serum (FBS) was obtained from HyClone (Logan, UT). Dulbecco's Modified Eagle's Medium (DMEM), RPMI-1640, L-glutamine, and gentamicin were purchased from Gibco-BRL (Burlington, ON, Canada). Mouse IL-2, IL-12, TNF- α , and IFN- γ ELISA kit was purchased from e-Biosciences (San Diego, CA). Sequence-specific siRNA targeting murine STAT3 mRNA was purchased from Ambion (Austin, TX) (sense: 5'-GGACGACUUUGAUUUCAACt-3', antisense: 5'-GUUGAAAUCAAGUCGUCCtg-3'). The scrambled siRNAs Silencer[®] Negative Control #1 siRNA (Catalogue #AM4635) and Silencer[®] FAM[™] labeled Negative Control #1 siRNA (Catalogue #AM4620), both purchased from Applied Biosystems (Foster City, CA). Caspase 3 Assay Kit, Nonidet P-40, Protease Inhibitor Cocktails, and 4-Nitrophenyl phosphate were purchased Sigma-Aldrich (St. Louis, MO). Anti-phosphotyrosine (Y⁷⁰⁵) STAT3 monoclonal antibody, anti-STAT3 antibody and anti-Actin antibody (I-19) were purchased from Santa Cruz Biotechnology (Stanta Cruz, CA). ECL Plus[™] detection kit was purchased from GE Healthcare Life Sciences (Piscataway, NJ). Anti-mouse CD3 (FITC labeled), CD4 (phycoerythrin (PE)-Cy5 labeled), CD8 (PE-Cy5 labeled), NK1.1 (PE

labeled), CD11c (FITC labeled), CD86 (PE labeled), and CD40 (PE-Cy5 labeled) mAbs, or corresponding isotype controls, were purchased from BD Biosciences (Mississauga, ON, Canada). EasySep[®] Negative Selection kit for T cells isolation was purchased from Stemcell Technologies (Vancouver, BC).

4.2.2 Preparation of siRNA Complexes

PEI-StA was prepared by N-acylation of PEI with stearoyl chloride and characterized as described in (19). Then, in sterile eppendorf tubes, equal amounts (in μg) of siRNA and PEI or PEI-StA in PBS were incubated for 30 minutes at 37 °C as previously described (18). Samples were freshly prepared before each administration.

4.2.3 Assessing the Effect of Media from Untreated and siRNA Treated B16 Cells on *in vitro* DC Maturation and Function

4.2.3.1 Cell Culture

Primary DC culture was generated from bone marrow precursor of C57BL/6 mice femurs and propagated in complete RPMI-1640 in presence of GM-CSF as previously described (20). In brief, femur bone was removed from dissected mouse in aseptic technique and all tissue was removed from the intact bone structure. Then, the femur was dipped in 70% ethanol pool for 1 min to reduce contamination. Carefully, each tip of the femur was cut by scissors just below the joint. After that, insulin needle was carefully inserted into one end and 1 mL PBS was used to flush the bone marrow using a syringe into 50 mL sterile tubes. This

process was repeated until the exterior color of the bone become completely white. Thereafter, the flushed bone marrow was filtered through a mesh to preclude particulate matter. Then, filtrate was suspended in sterile PBS and centrifuged at 500 g for 5 min. Cells were counted using hemocytometer and 2×10^6 cells were seeded in Petri dishes in 10 mL growth media. At day 3, another 10 mL growth media was added; at day 6, 10 mL was replaced by fresh growth media. The purity of the DC population on day 7 was found to be between 70-75% based on the expression of CD11c on the semi-adherent and non-adherent cell populations.

DC2.4 cell line, obtained from Dr. Kenneth Rock (University of Massachusetts, Worcester, MA), was propagated in complete RPMI-1640 with 10% FBS.

B16.F10 cell line was provided by Dr. Mavanur Suresh (University of Alberta, Edmonton, AB), and NIH 3T3 cell line was obtained from ATCC (Manassas, VA). Both cell lines were propagated in DMEM with 10% FBS. To generate tumor-conditioned medium from B16.F10 (B16-CM), confluent B16.F10 cells were incubated in fresh serum-free DMEM medium for 24 h. Thereafter, the medium was collected and centrifuged.

Then, primary DC culture or DC2.4 culture was exposed to B16-CM for 24 h where final concentration of B16-CM was 50%. FBS was corrected to 10% in each culture. Then p-STAT3 level was detected in each cell type by Western blot, and maturation level was assessed by CD86 and CD40 expression (details below).

4.2.3.2 Treatments

4.2.3.2.1 B16.F10 Treatment

For STAT3 targeting, siRNA complexes were prepared at final siRNA concentrations of 50 nM. Thereafter, in 24-well plates, 1×10^5 B16 melanoma cells were incubated with the designated complexes at 37 °C. Identical complexes scrambled siRNA as well as untreated B16 cells were used as controls. To remove uninternalized complexes, B16 medium was replaced after 8 h. Then, cells were lysed and levels of p-STAT3 as well as total STAT3 were detected by Western blot as described in chapter 3. Optical intensity of p-STAT3 band was quantified and normalized to Actin protein band using ImageJ software (W. Rasband (2005) National Institutes of Health, Bethesda, MD, <http://rsb.info.nih.gov/ij>). Simultaneously, on 96-well plate, cancer cell viability was determined by MTT assay and Caspase 3 Activity assay following 36 h of incubation with siRNA complexes.

4.2.3.2.2 DC Treatment

Malfunctioned DCs at day 7 were generated by exposure to tumor-conditioned media from B16.F10 melanoma culture (B16-CM) for 24 h. Murine B16.F10 cells were grown and propagated in DMEM media supplemented with 10% FBS at 37 °C and 5% CO₂. After confluence, B16 cells were incubated with serum-free media for 24 h. This media was collected and grouped according to the designated treatment into: anti-STAT3 siRNA complexes treated (B16-CM/PEI and B16-

CM/PEI-StA), scrambled siRNA complexes treated (B16-CM/PEI-sc and B16-CM/PEI-StA-sc), and untreated B16-CM. Thereafter, conditioned medium from each treatment group was added to a primary DC culture reaching final B16-CM concentration of 50%. FBS was then supplemented to 10% final concentration in culture. After that, DC phenotypic maturation was evaluated by surface expression of CD40 and CD86 as analyzed by fluorescence activated cell sorting (FACS). Moreover, mixed lymphocytes reaction (MLR) was performed as described below to assess DC function as indicated by their capability to stimulate allogenic T cell proliferation.

4.2.3.3 Western Blot

Cells were washed twice with ice-cold PBS, then lysed in a buffer containing 30 mM HEPES (pH 7.5), 2 mM Na₃VO₄, 25 mM NaF, 2 mM EGTA, 2% Nonidet P-40, 1:100 protease inhibitor cocktails, 0.5 mM DTT and 6.4 mg/mL phosphatase substrate 4-nitrophenyl phosphate. Cell lysates were centrifuged for 20 seconds at 16,000×g. Thereafter, NaCl was added to samples to final concentration of 420 mM and cell lysates were centrifuges for 20 min at 16,000×g and supernatant was transferred to new tubes and pellets were discarded. Total protein extract was determined by Micro BCA Protein Assay. Equal amounts of protein (20 µg) were loaded on 8% SDS-PAGE. Proteins were then transferred into PVDF membrane and were probed with anti-phosphotyrosine (Y⁷⁰⁵) STAT3 mAb. Stripped membranes were probed with anti-STAT3 Ab and anti-Actin Ab (I-19).

Membranes were developed using ECL Plus™ detection kit as described in chapter 3.

4.2.3.4 MTT Assay

B16 cells, grown in 96-well flat-bottomed microplates, were treated as indicated. Thereafter, 100 µL of MTT solution in culture medium (0.5 mg/mL) was added to each well for 2 h. The formed formazan crystals were dissolved by adding 200 µL of DMSO to each well and kept in gentle shaking for 30 min to ensure complete dissolution. Optical density was measured at 550 nm using a microplate reader (Powerwave with KC Junior software; Bio-Tek, Winooski, VT). The results were converted into (%) viability relative to untreated sample.

4.2.3.5 Caspase 3 Activity Assay

The Caspase 3 activity was measured as an indicator for apoptosis. For that purpose, B16 cells were treated with 50 nM siRNA in PEI or PEI-StA for 24 h. Using Caspase 3 Assay Kit, cells were normalized for 10⁵ cells per treatment group, lysed, and placed in designated wells in 96-well flat-bottomed microplates. Provided Caspase 3 inhibitor (Ac-DEVD-CHO) and Caspase 3 substrate (Ac-DEVD-pNA) were then added to designated wells according to the manufacturer's instructions. Optical density was measured at 405 nm using microplate reader and Caspase 3 activity was calculated based on p-Nitroaniline calibration curve.

4.2.3.6 FACS Analysis

For phenotypic maturation studies, 1×10^5 DC primary cultures were washed with PBS and suspended in FACS buffer (PBS with 5% FBS). Then, cells were incubated with 0.5 μ l CD16 mAbs for 30 min at 4° C. Then, cells were incubated with 0.25 μ l fluorescence-labeled CD86 and CD40 mAbs or corresponding isotype controls and kept in 4°C for 30 min. After that, cells were washed 3 times with FACS buffer and centrifuged at $10,000 \times g$ for 4 min to remove excess mAbs. All samples were finally acquired on a Becton-Dickinson FACSort and analyzed by Cell-Quest software.

4.2.3.7 Mixed Lymphocyte Reaction

T cells were obtained from spleen of Balb/c mice Jackson Laboratory (Bar Harbor, ME, USA). Spleen was crushed between two slides and T cells were purified using EasySep[®] Negative Selection kit according to manufacturer's instructions. Purified T cells were cocultured in flat-bottomed 96-well plates with irradiated DCs in a ratio of (2:1) in 37°C and 5% CO₂. Thereafter, [³H]-thymidine was added during the last 18 hours of a 3 day coculture and the T-cell proliferation measured by [³H]-thymidine incorporation in counts per minute. Corresponding IL-2 secretion was determined by ELISA in a 96-well microplate using a microplate reader (Powerwave with KC Junior software; Bio-Tek, Winooski, VT) at OD of 450 nm with reference set at 570 nm. All samples were analyzed in at least triplicates.

4.2.4 Assessing the Effect of Anti-STAT3 siRNA Complex Treatment of B16 Tumors on Immune Response *in vivo*

4.2.4.1 Tumor Establishment and Treatment

All experiments were performed in accordance with the University of Alberta guidelines for the care and use of laboratory animals using 4-6 week old male mice. Male C57Bl/6 mice were purchased from the Jackson Laboratory (Bar Harbor, ME, USA). B16 tumor was established as described earlier in (18) (chapter 3). In brief, 0.75×10^6 B16 cells were inoculated subcutaneously in the upper left flank of male C57Bl/6 mice. After 10 days, 500 pmol of STAT3-targeting siRNA complexes (PEI and PEI-StA) or scrambled siRNA complexes (PEI-sc and PEI-StA-sc) in normal saline were administered to randomly-assigned groups (5 to 7 mice per group) by intratumoral (i.t.) injections on daily basis for 4 days. siRNA complexes were freshly prepared before each administration as described previously in (18) (chapter 3). Additional control group received daily i.t. injections of normal saline without any formulation.

4.2.4.2 Assessing tumor growth and STAT3 expression

Tumor dimensions were measured by vernier caliper after 1 day of the final treatment dose. Tumor volume was calculated as:

$$\text{Tumor Volume (mm}^3\text{)} = \frac{\text{Longest Diameter} \times \text{Perpendicular Diameter}^2}{2}$$

Thereafter, mice were euthanized tumor samples were immediately isolated and crushed between two slides to form uniform cell suspension and analyzed for STAT3 expression by Western blot as described in chapter 3.

4.2.4.3 Evaluating the Immunological Profile in Tumor Milieu

Supernatants of each tumor sample were analyzed for protein content by Micro BCA Protein Assay kit, normalized, and analyzed for IL-12, TNF- α , and IFN- γ using corresponding ELISA kit as mentioned earlier. Furthermore, immune cells were evaluated for cell percentage and activation level by FACS as previously mentioned. For that purpose, each cell suspension was incubated with anti-mouse CD3, CD4, CD8, NK1.1, CD11c, CD86, and CD40 mAbs, or corresponding isotype controls and kept in 4°C for 30 min. Then, cells were washed 3 times with FACS buffer to remove excess mAbs and 1×10^6 cells were finally acquired from each sample on a Becton-Dickinson FACSsort and analyzed by Cell-Quest software.

4.2.4.4 Evaluation of DC Functionality following siRNA Treatment in vivo

To assess DC functionality in tumor-bearing mice following STAT3 knockdown, MLR was conducted. Splenocytes from each treatment group were isolated, irradiated, and cocultured with purified T cells from Balb/c mice in 37°C and 5% CO₂. T-cell proliferation was measured as described earlier. Similarly, IL-2 level in each sample was measured by ELISA as described earlier.

4.2.5 Data Analysis

The data were analyzed for statistical significance ($p < 0.05$) by one-way ANOVA; Post-Hoc Scheffé's test was conducted to determine level of significance (SPSS for Windows, Version 16.0).

4.3 RESULTS

4.3.1 Comparison between Primary DCs and DC Cell Line (DC2.4)

Intracellular levels of phosphorylated STAT3 (p-stat3) were determined in BMDCs and DC2.4 by Western blot. Upon exposure to B16-CM, intracellular p-stat3 level remarkably increased in BMDCs when compared to untreated BMDCs, which only showed basal p-stat3 level (Figure 4.1A). In addition, conditioned medium of NIH 3T3 did not induce p-stat3 levels in DCs. Moreover, when LPS was used to stimulate BMDCs, p-stat3 was highly expressed with and especially without B16-CM exposure. On the other hand, Western blot analysis indicated elevated basal level of p-stat3 in untreated DC2.4 culture compared to untreated BMDCs. Although this was slightly induced by LPS, B16-CM remarkably reduced p-stat3 levels in the presence or absence of LPS (Figure 4.1A). In all groups, no remarkable difference in total stat3 expression was noticed.

Flow cytometry was employed to detect the surface maturation markers CD86 and CD40 on BMDCs and DC2.4 upon exposure to B16-CM. In BMDCs, both CD86 and CD40 expression was reduced after B16-CM exposure compared to untreated control. LPS was able to induce BMDCs maturation as evidenced by high expression of CD86 and CD40. However, pretreatment with B16-CM reduced the ability of LPS to induce BMDC maturation (Figure 4.1B). In contrast, exposure of DC2.4 to B16-CM did not reduce maturation markers expression (Figure 4.1B). On the contrary, B16-CM seems to further induce CD86 and CD40 expression in DC2.4 cells in comparison to LPS.

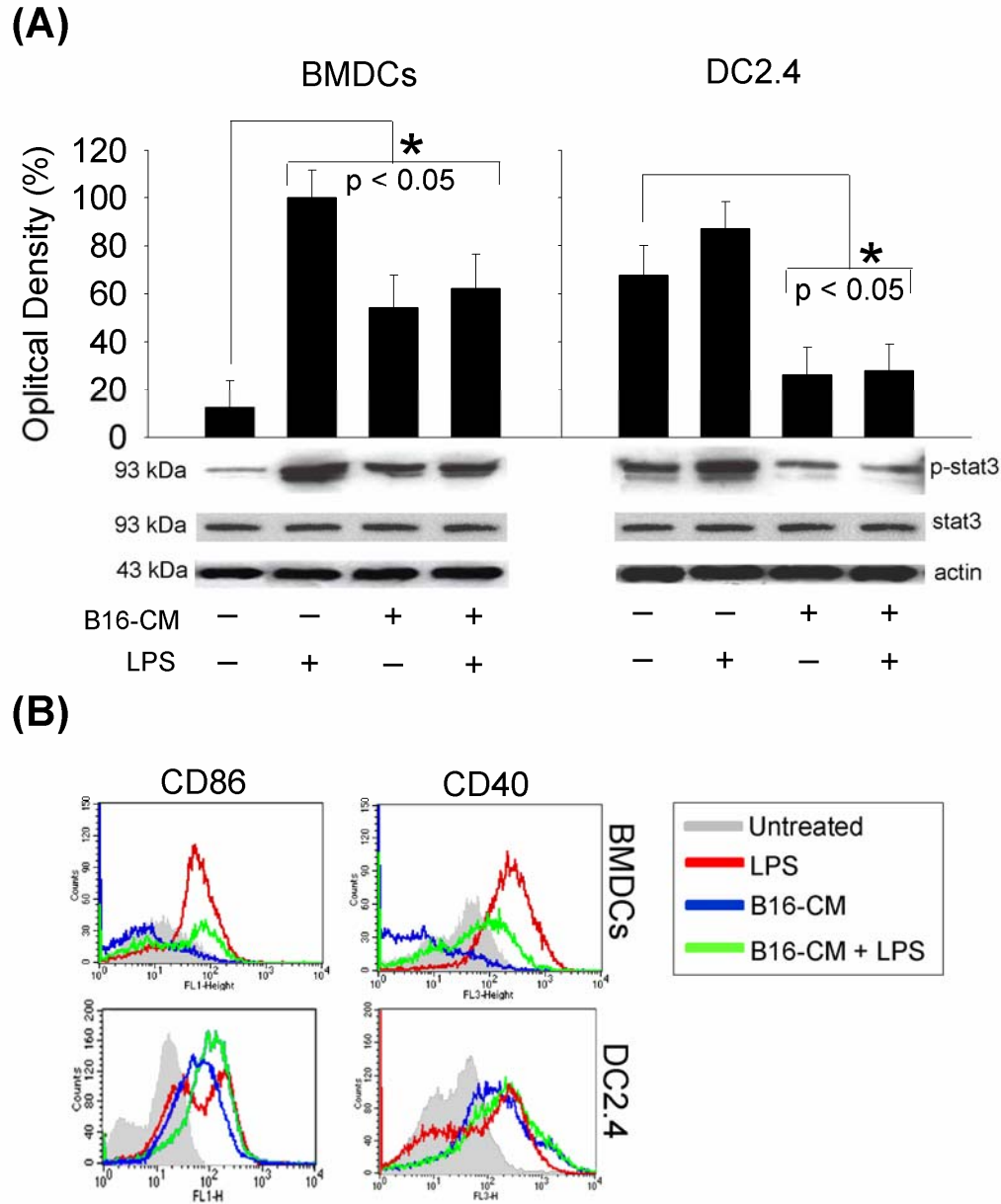


Figure 4.1 Effects of B16-CM on STAT3 activation and DC maturation. **(A)** Detection of p-stat3 level in BMDCs (left panel) and DC2.4 (right panel) by Western blot. Data represent the mean of 4 independent experiments \pm SD. Optical intensity of p-stat3 band was quantified and normalized to actin protein band using ImageJ software (W. Rasband (2005) National Institutes of Health, Bethesda, MD, <http://rsb.info.nih.gov/ij>). This software accounts for band density, width, thickness, and background. Test-to-loading control ratio was calculated and presented as bar graphs. **(B)** Flow cytometry histogram of CD86 and CD40 expression by BMDCs and DC2.4. Acquisition was performed at least twice and normalized to 10^4 events per run per sample

4.3.2 STAT3 Knockdown in B16 by siRNA Induces DC Maturation and Activation *in vitro*

The results of this study demonstrated that the immunosuppressive effect of B16-CM on DCs can be reversed by silencing STAT3 in B16 cells prior to DC exposure. Targeting B16 cells with anti-STAT3 siRNA in PEI and PEI-StA complexes caused a significant knockdown of STAT3 expression in a specific manner (Figure 4.2A and B). This corresponded to cytotoxic effect on B16 cancer cells as shown by up to 30% reduction cell viability (Figure 4.2C) and over 2 folds induction in the activity of the apoptotic protein Caspase 3 (Figure 4.2D). The exposure of DCs to B16-CM from B16 cells in which STAT3 was silenced by PEI or PEI-StA/siRNA complexes induced phenotypic DC maturation indicated by the significantly higher surface expression of CD86 and CD40 as compared to controls (Figure 4.3). For both markers, the surface expression was higher by B16-CM/PEI-StA treatment where it allowed for an induction reaching 89% for CD86 and 66% for CD40 higher than that of B16-CM/PEI. Consistently, DC activity, characterized by their ability in recognition and priming of allogenic T cells, was also restored following STAT3 silencing in B16 cells (Figure 4.3). T cells cocultured with DCs from B16-CM/PEI or B16-CM/PEI-StA groups showed a significant increase in their proliferation compared to controls (Figure 4.4A). Similar to the phenotypic DC maturation results, DCs showed enhanced functionality when exposed to B16-CM/PEI-StA as compared to B16-CM/PEI. It is worth noting that IL-2 that is concomitantly secreted from T cells during their proliferation followed a similar pattern where its maximum level was detected

after T cell-coculture with DCs from B16-CM/PEI-StA group (Figure 4.4B). This is consistent with our FACS results since DCs exposed to B16-CM/PEI-StA showed a significantly higher expression of costimulatory molecules compared to that of B16-CM/PEI (data from Figure 4.3).

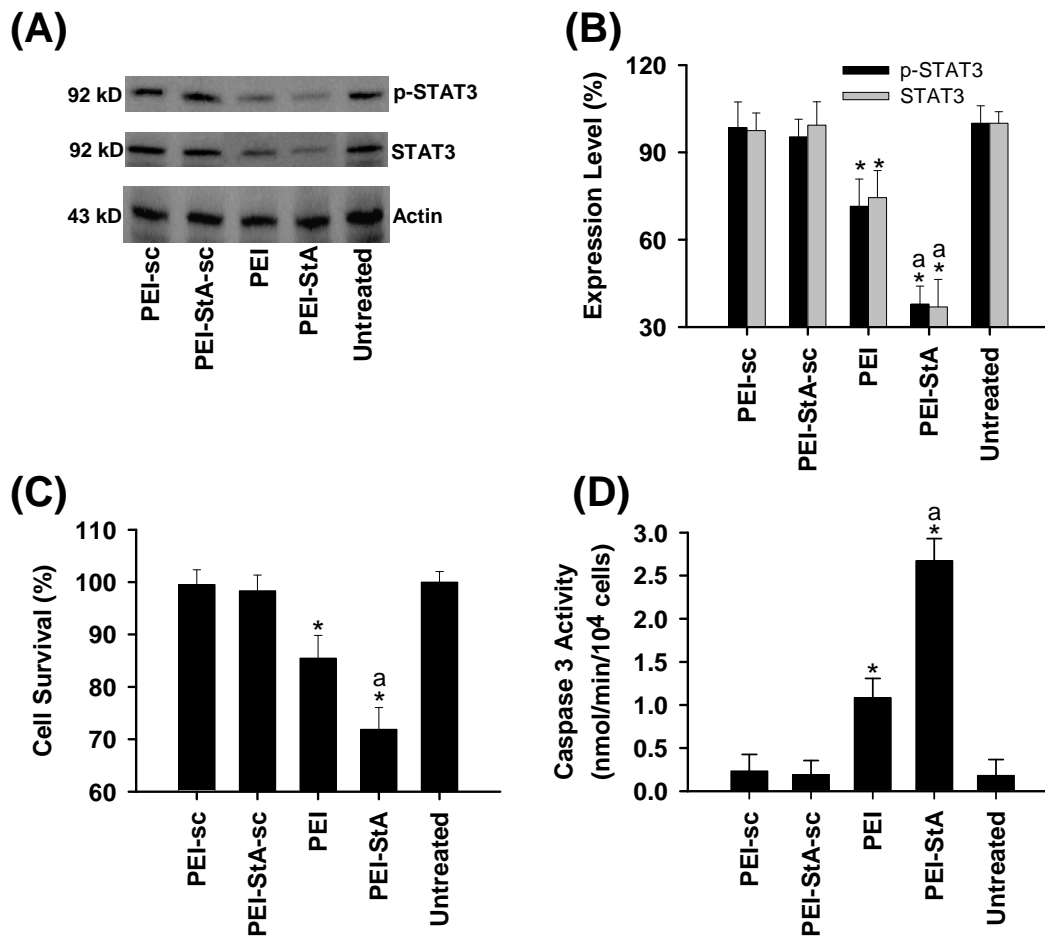


Figure 4.2 B16.F10 cell death following STAT3 knockdown by PEI and PEI-StA complexes *in vitro*. Confluent B16 cells were incubated with 50 nM anti-STAT3 siRNA delivered by PEI or PEI-StA complexes. Identical complexes of scrambled siRNA as well as untreated B16 cells were used as controls. **(A)** Western blot analysis showing expression level of p-STAT3, STAT3, and Actin loading control. **(B)** Bands optical intensities of p-STAT3 (black bars) and STAT3 (grey bars) were quantified and normalized to Actin bands using ImageJ software (W. Rasband (2005) National Institutes of Health, Bethesda, MD, <http://rsb.info.nih.gov/ij>). The software provides optical densities that are normalized for width, thickness, and background. Data are shown as the average \pm SD of 4 experiments. **(C)** Percentage of cell viability was determined relative to untreated control by MTT assay. Data are shown as mean (\pm SD) of 7 replicates for each sample. **(D)** Caspase 3 activity after designated treatment was calculated as the difference in the rates of substrate cleavage in the samples with and without specific caspase 3 inhibitor and expressed as (nmol/min/10⁴ cells). Data are shown as mean (\pm SD) of 8 replicates for each sample. Statistical significance was determined compared to control (*; $p < 0.05$) and PEI (a; $p < 0.05$).

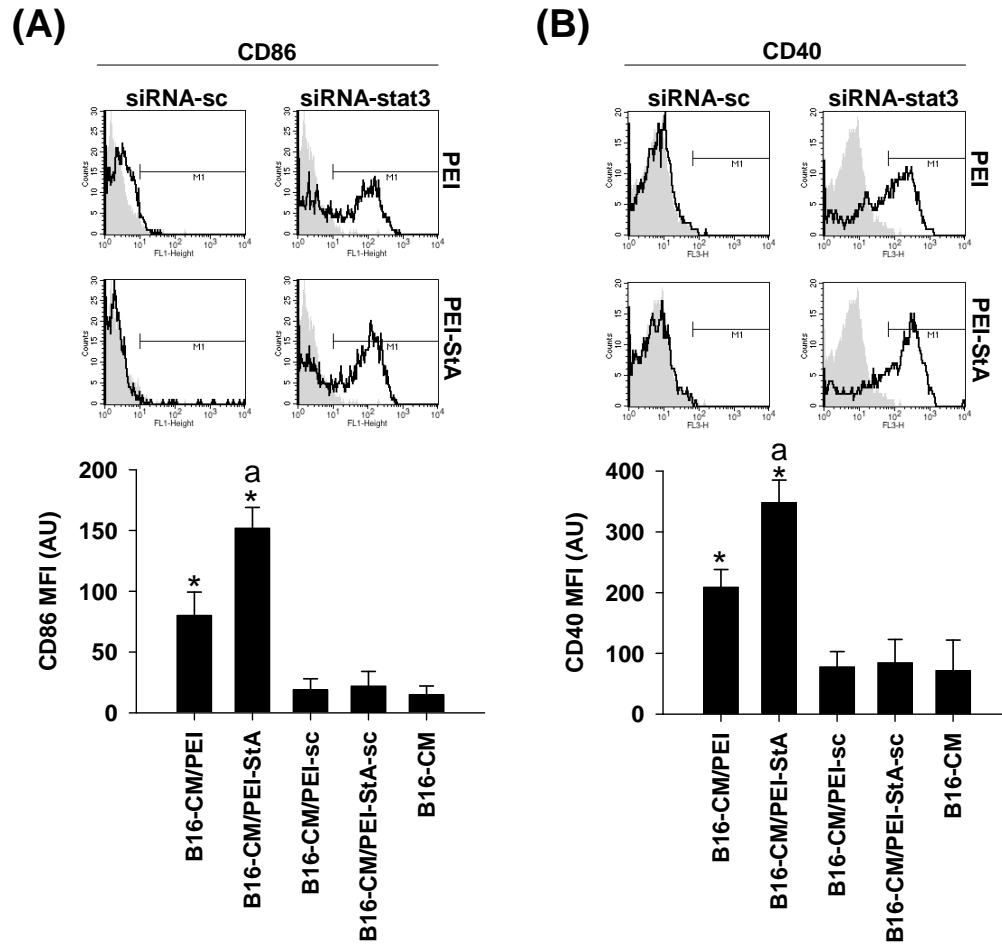


Figure 4.3 Restoration of DC phenotypic maturation *in vitro*. Primary DC cultures in day 7 were incubated with B16-CM of B16 culture that was treated with anti-STAT3 siRNA or scrambled (sc) siRNA complexes of PEI or PEI-StA for 24 h. FACS analysis of CD86 expression (A) or CD40 expression (B) on DC surface. Histograms indicate a shift in the fluorescence signal only following STAT3 knockdown in B16. Black lines indicate DCs exposed to B16-CM from siRNA-treated groups (whether anti-STAT3 or sc) while gray shade indicates DCs exposed to untreated B16-CM control. Bar graphs show mean fluorescence intensity (MFI) values after each treatment where B16-CM/PEI-StA gives more MFI signals than controls (*; $p < 0.05$) and B16-CM/PEI (a; $p < 0.05$) for both CD86 and CD40. Data was presented as average of 3 different measurements (\pm SD).

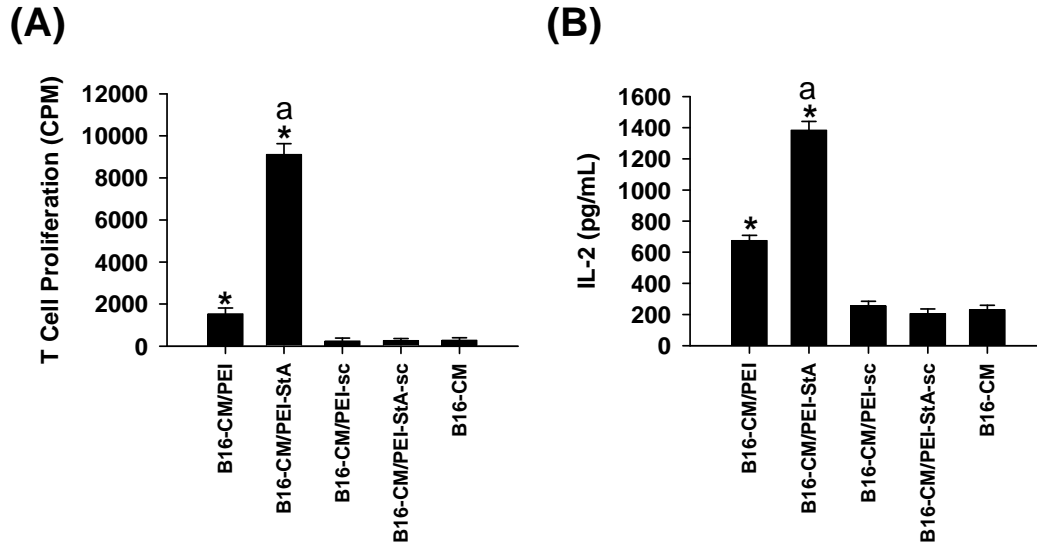


Figure 4.4 Allogenic MLR following STAT3 silencing *in vitro*. **(A)** Bars represent level of T cell proliferation. DCs incubated with B16-CM/PEI-StA allowed for higher alloreactivity compared to controls (*; $p < 0.05$) and B16-CM/PEI (a; $p < 0.05$). **(B)** Bars represent IL-2 levels secreted from T cells upon proliferation. IL-2 secretion, measured by ELISA, was highly correlated with T cell proliferation where B16-CM/PEI-StA gave a significantly higher result compared to controls (*; $p < 0.05$) and B16-CM/PEI (a; $p < 0.05$). All data are shown as mean (\pm SD) of at least triplicates for each sample.

4.3.3 Tumor Regression following STAT3 Knockdown *in vivo*

Tumor growth study following STAT3 knockdown in B16 tumors by siRNA revealed significant tumor regression of the treated tumor masses as compared to controls as a result of STAT3 knockdown (Figure 4.5). STAT3 expression *in vivo*, measured in isolated tumors one day following final treatment dose, was significantly reduced upon siRNA administration by PEI and PEI-StA complexes reaching 25% and 55% less than saline-treated control, respectively (Figure 4.4A and 4.5B). Tumor growth rate was significantly reduced following STAT3 knockdown (Figure 4.5C). PEI-StA complexes allowed for 6.2 times reduction in tumor growth compared to saline-treated control. PEI-StA complexes were also 3 times more effective in reducing tumor growth as compared to parent PEI complexes. Moreover, tumor volume analysis confirmed uniformity of treatment and response as indicated by close adherence of subjects in each group to the group average (Figure 4.5D). Tumor volume dramatically dropped from $\sim 390 \text{ mm}^3$ in the untreated group to $\sim 170 \text{ mm}^3$ in case of PEI complexes. It is worth noting that further reduction in tumor volume was noticed with PEI-StA complexes as it reached $\sim 42 \text{ mm}^3$ as measured after 24 h of final treatment dose. This is consistent with our previous findings where the stearic-acid derivative of PEI increased both stability and potency of siRNA *in vitro* and *in vivo* (18, 21). Besides, the anti-tumor effect was better in each single subject of the PEI-StA group as compared to PEI group indicating the potency provided by the lipid-modified formulation.

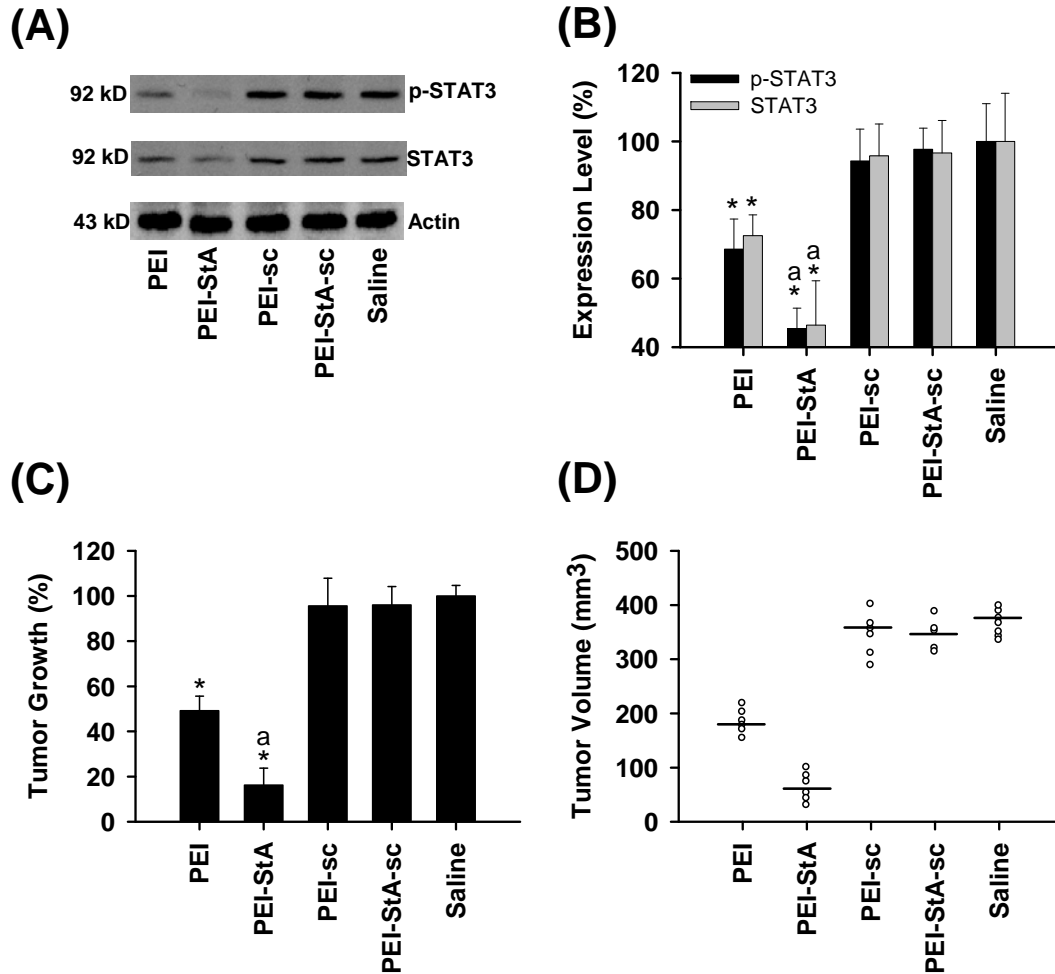


Figure 4.5 Tumor regression following STAT3 knockdown by siRNA complexes. B16 cells were inoculated subcutaneously. Scrambled or anti-STAT3 siRNA were administered by i.t. route from day 10 to day 13. At day 14, tumor dimensions were taken tumor volume was calculated for each subject. Isolated tumors from each groups were lysed for Western blot analysis. **(A)** Western blot analysis showing expression level of p-STAT3, STAT3, and Actin loading control. **(B)** Bands optical intensities of p-STAT3 (black bars) and STAT3 (grey bars) were quantified and normalized to Actin bands using ImageJ software. Data are shown as the average \pm SD of 4 experiments. **(C)** Bars represent (%) of tumor growth following designated treatments. PEI-StA complexes significantly reduced tumor growth as compared to saline-treated control (*; $p < 0.05$) and PEI-treated group (a; $p < 0.05$). Data are shown as the average (\pm SE) of 5 to 7 measurements. **(D)** Value of tumor volume was plotted for each subject and presented as open circles. Median of each designated group was indicated as crossing horizontal short lines.

4.3.4 Induction of DC Activation *in vivo* following STAT3 Knockdown in B16 Tumor

To evaluate DC infiltration and activation, FACS analysis was performed for DC lineage marker CD11c and activation markers CD86 and CD40 in tumor cell suspensions following designated treatments of B16 tumors. Our results demonstrate up to ~ 4-fold increase in DC infiltration in B16 tumor mass upon STAT3 knockdown (Figure 4.6A). However, no statistically-significant difference was noted between PEI and PEI-StA treatment groups. In PEI and PEI-StA groups, further analysis of DC population showed an increase in the surface expression of both CD86 and CD40 reaching up to 35% and 48% higher than scrambled siRNA and saline control treatments (Figure 4.6B). PEI-StA complexes of STAT3 siRNA also allowed for an increase in CD86 and CD40 expression that was 16% higher than that of PEI complexes. Moreover, ELISA analysis of tumor supernatants indicated the production of high levels of proinflammatory cytokines IL-12 and TNF- α after STAT3 knockdown (Figure 4.6C). The results clearly show that PEI-StA complexes allowed for significant increase in TNF- α and IL-12 production that was 38% and 129% higher than what was measured with PEI complexes, respectively.

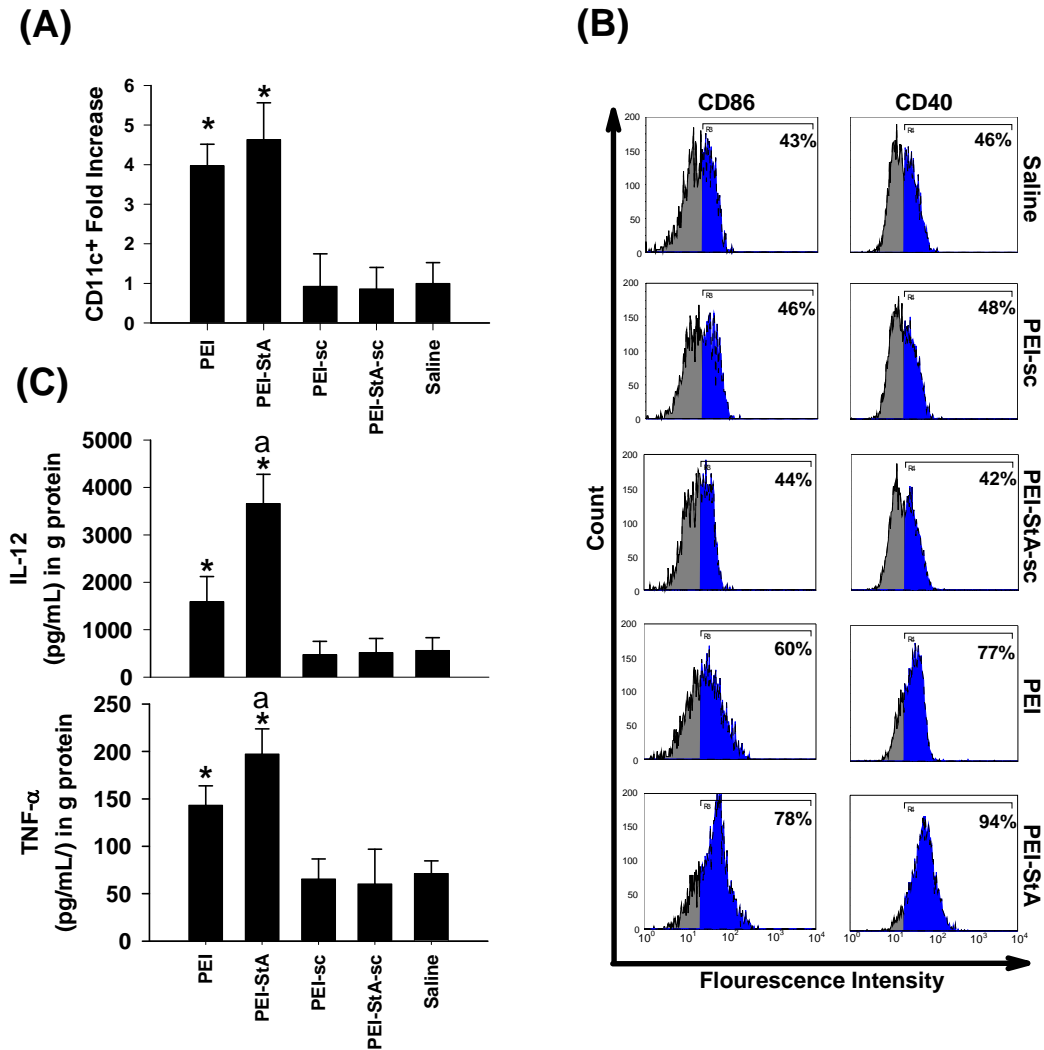


Figure 4.6 DC tumor infiltration, activation, and cytokine production *in vivo*. Tumor samples were isolated and crushed between two slides into uniform cell suspensions. Cellular component as well as supernatant of each group was analyzed by FACS and ELISA, respectively. **(A)** Fold-increase of CD11c⁺ cells presented as bar graphs. Tumor treated with anti-STAT3 siRNA complexes showed higher DC infiltration as compared to controls (*; $p < 0.05$). Data are shown as the average (\pm SD) of 3 measurements. **(B)** FACS analysis histograms designated for DC activation markers CD86 and CD40. DCs were more activated following intratumoral delivery of anti-STAT3 siRNA by PEI-StA complexes as compared to that of PEI complexes treatment. Percentage of cells of the gated population is indicated in the upper right corner of each histogram, n-gate and out-of-gate cells were separated by vertical lines. **(C)** Cytokine levels measured in tumor-sample supernatants by ELISA were plotted in bar graphs for IL-12 and TNF- α . PEI-StA polyplexes of anti-STAT3 siRNA showed significant induction of both cytokines as compared to control groups (*; $p < 0.05$) and PEI group (a; $p < 0.05$). Data are shown as the average (\pm SD) of 3 measurements.

4.3.5 Alloreactivity of DCs from Tumor-Bearing Mice

To evaluate the functional maturation of DCs after STAT3 knockdown *in vivo*, MLR between irradiated splenocytes from tumor-bearing and allogenic T cells was conducted. As shown in Figure 4.7A, high allogenic T cell proliferation was recorded after coculture with splenocytes from the STAT3 knockdown groups treated with PEI and PEI-StA complexes. In addition, the measured counts per minute (CPM) was 1.5 times higher in PEI-StA group than PEI. This was in agreement with our previous FACS results where PEI-StA induced the highest expression of costimulatory molecules on DC surface *in vivo* (data from Figure 4.6B). Consistently, IL-2 production concomitant to T cell proliferation in PEI-StA group was around double of that for the PEI group (Figure 4.7B). These results indicate more distal effects of local intratumoral silencing of STAT3 in B16 tumor by siRNA complexes particularly those of PEI-StA.

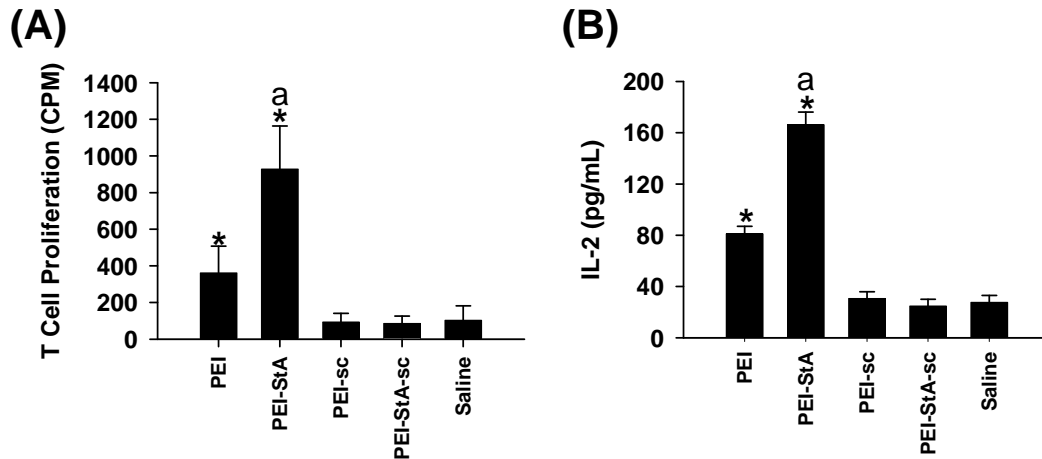


Figure 4.7 Allogenic MLR following STAT3 silencing *in vivo*. Splenocytes from tumor-bearing mice were collected, irradiated, and cocultured with allogenic T cells. **(A)** Bars represent level of T cell proliferation. Splenocytes isolated from mice that were treated with PEI-StA allowed for higher alloreactivity compared to controls (*; $p < 0.05$) and PEI (a; $p < 0.05$). **(B)** Bars represent IL-2 levels secreted from T cells upon proliferation. IL-2 secretion, measured by ELISA, was highly correlated with T cell proliferation where PEI-StA gave a significantly higher result compared to controls (*; $p < 0.05$) and PEI (a; $p < 0.05$). All data are shown as mean (\pm SD) of 5 replicates for each sample.

4.3.6 Tumor Infiltration of T Cells following STAT3 Knockdown

FACS analysis was conducted in tumor cell suspensions for CD3 expression, the signaling part of the T cell receptor (TCR) complex. As shown in Figure 4.8A, STAT3 knockdown in B16 tumor allowed for a profound lymphocyte infiltration into tumor mass reaching over 3 and 5 fold increase with PEI and PEI-StA groups compared to saline control, respectively. The results also demonstrate a significant increase in the tumor-infiltrating lymphocytes (TIL) following administration of PEI-StA complexes that was 67% higher than that of PEI. Differential analysis of CD3⁺ population indicates an increase in CD4⁺ T helper cells, CD8⁺ cytotoxic T cells, and NKT cells (Figure 4.8B). Moreover, since activated T cells produce IFN- γ , we measured the level of this cytokine in tumor cell supernatant. The ELISA results detected a significant production of IFN- γ following STAT3 knockdown, where PEI-StA allowed for ~ 48% higher cytokine level than PEI treatment. This immunostimulatory profile strongly suggests a role of the immune response in the anti-tumoral effect recorded with siRNA-mediated STAT3 knockdown in B16 cells.

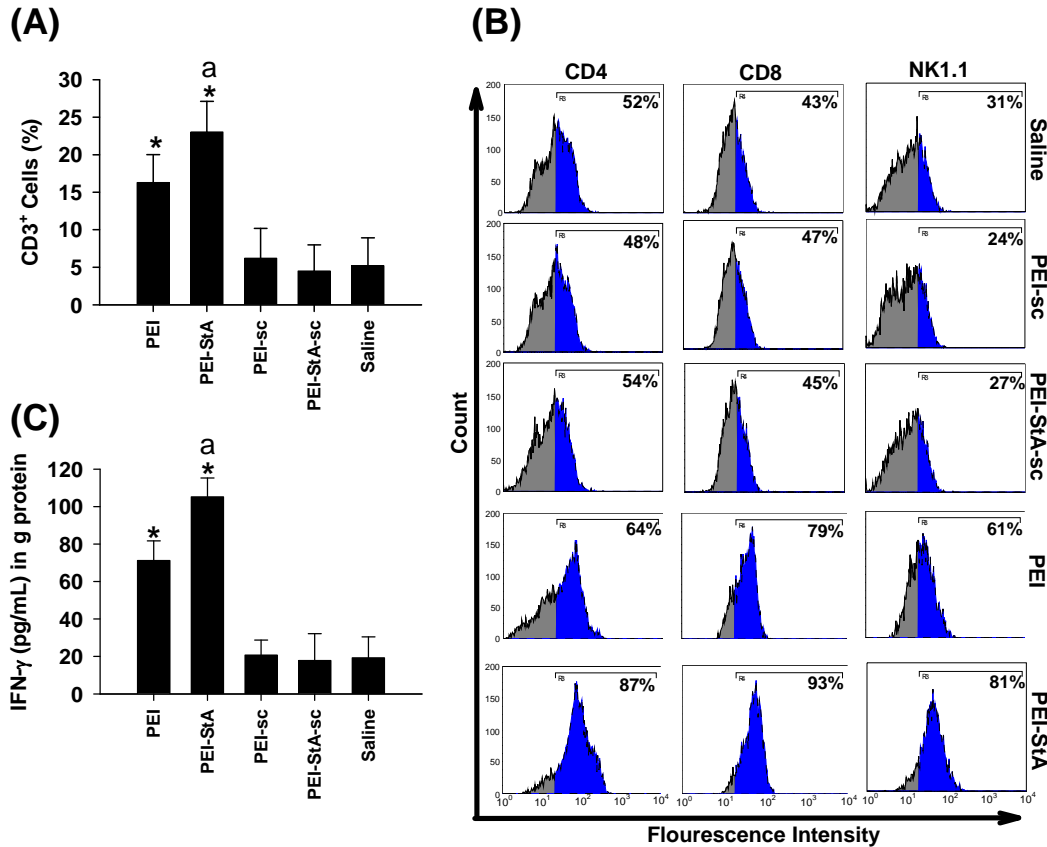


Figure 4.8 Evaluation of tumor-infiltrating lymphocytes, *in vivo*, and determination of cytokine profile in tumor milieu. **(A)** Fold-increase of CD3⁺ cells was presented as bar graphs. Tumor treated with anti-STAT3 siRNA complexes showed higher lymphocytes infiltration as compared to controls (*; $p < 0.05$) and PEI complexes (a; $p < 0.05$). Data are shown as the average (\pm SD) of 3 measurements. **(B)** FACS analysis for differential lymphocyte population makers CD4, CD8, and NK1.1. Histograms of designated treatment groups demonstrate that in PEI-StA complexes more infiltration was detected for CD4⁺ helper T cells, CD8⁺ CTL, and NKT cells as compared to PEI. Percentage of cells of the gated population is indicated in the upper right corner of each histogram, while cells population in-gate and out-of-gate were separated by vertical line in each histogram. **(C)** Cytokine levels measured by ELISA were plotted in bar graphs for IFN- γ where PEI-StA showed significant induction in cytokine production as compared to control (*; $p < 0.05$) and PEI complexes (a; $p < 0.05$). Data are shown as the average (\pm SD) of 3 measurements.

4.4. DISCUSSION

Compelling evidence has accumulated supporting the promise of interrupting STAT3 signaling pathway as a strategy for cancer therapy in solid and hematological tumors (reviewed in (22)). Recent studies on melanoma patients suggested that tyrosine-phosphorylated STAT3 is a valid biomarker for atypical nevi progression (23). Moreover, activated STAT3 was found to have permanent DNA-binding activity in primary human melanoma samples, but not normal skin samples from the same patients (24). Hence, STAT3 was considered a potential target for chemoprevention and treatment of melanoma. Furthermore, numerous studies showed that targeting STAT3 in melanoma tumor models leads to the induction of tumor regression (25), inhibition of angiogenesis (26), prevention of metastasis (27), as well as activation of immune response (3, 4). Since constitutively-activated STAT3 in tumors would negatively influence multiple subsets of immune cells, it is logical to expect an induction of the immune response following STAT3 disruption in tumors. In fact, such effect is not thought to be totally associated with direct STAT3 disruption in immune cells, as they were not intended for manipulation, but rather a consequence for the anti-STAT3 effect in tumor cells i.e. a bystander effect.

Bystander effects as a result of STAT3 inhibition were first described in B16 murine melanoma transfected with dominant-negative form of STAT3 (28). In that study, unpredicted cytotoxicity was noted in neighboring tumor cells that never received the dominant-negative treatment. Subsequent studies in this focus have isolated three possible mechanisms following STAT3 inhibition by which

bystander effects could be mediated: (i) production of soluble factors that induce tumor apoptosis (29), (ii) suppressed angiogenesis as determined by VEGF downregulation (26), and (iii) involvement of innate and adaptive anti-tumor immune response as indicated by the production of proinflammatory mediators and infiltration of macrophages, neutrophils, and T cells in the tumor mass (3, 10). The later gained special focus of the scientific community as a widely-progressing area of research today comprises chemo- and immunotherapy of cancer (30).

We have recently showed that siRNA-mediated STAT3 silencing in B16.F10 via intratumoral administration of siRNA/PEI complexes results in a remarkable tumor regression (18). Along with direct tumor apoptosis, molecular investigation in that study revealed two possible bystander effects: increase in IL-6 and decrease in VEGF levels in tumor microenvironment (18). We hypothesized that the anti-tumor activity observed subsequent to STAT3 knockdown is partly owed to the breakdown of immunosuppressive microenvironment leading to improvements in DC maturation, immune cell activation and trafficking to the tumor. The validity of this hypothesis was investigated in the current study through assessing the bystander immune response following STAT3 knockdown in B16 melanoma cells *in vitro* and *in vivo* using siRNA complexes of PEI and its stearic-acid derivative. In our approach to evaluate the immunological picture after siRNA intervention, we focused on three aspects: the level of immune cell maturation and activation, percentage of TIL, and cytokine profiles in tumor milieu.

DCs are professional APCs that form a crucial link between innate and adaptive immune system. In normal situations, DCs recognize antigens from normal, microbial, or tumoral origins (31). These antigens get processed and presented in the context of major histocompatibility complex (MHC) class I and II to be recognized by CD8⁺ and CD4⁺ T cells, respectively (32). Nevertheless, DCs must provide three signals in order to activate naïve T cells: antigen presentation in the context of MHC class I and II (signal 1), co-stimulation provided by molecules such as CD86 and CD40 that interact with their ligands on T cell surface (signal 2), and cytokine stimulation (signal 3) to polarize T cells toward intended response, e.g. anti-tumoral response. However, tumors secrete factors that inhibit DC differentiation and maturation and eventually evade the adaptive immune response through this strategy (4). Therefore we wanted to develop an *in vitro* model to mimic this effect. Primary DCs are isolated cells that have not been genetically modified. On the contrary, DC2.4 cells were infected with retrovirus encoding *myc* and *raf* genes in order to immortalize the cell line (33). Since STAT3 is required for the expression of *myc* in myeloid monocytes (34), this explains, at least in part, the high constitutive level of p-stat3 in untreated DC2.4 lysate. Moreover, unlike the scenario in BMDCs, failure of B16-CM to further induce p-stat3 in DC2.4 confirms the independence of STAT3 hyperactivation in DC2.4 from exogenous inducers such as cytokines or growth factors. The reason for the reduction seen in p-stat3 after DC2.4 exposure to B16-CM is unclear to us. Nevertheless, mere detection of p-STAT3 upregulation does not conclusively reflect DC maturation status. As we and others have shown, STAT3 is also

activated in mature DCs upon stimulation by LPS. Therefore, we evaluated DC-maturation surface markers in order to assess the influence of STAT3 activation by B16-CM on DC maturation. Our flow cytometry studies demonstrated distinct phenotypic maturation profiles between BMDCs and DC2.4 cell line. Untreated DC2.4 expresses higher levels of CD86 and CD40 expression than BMDCs, indicating a more mature status. As mentioned earlier, the fact that DC2.4 cells were infected with retrovirus encoding *myc* and *raf* for immortalization may contributed to the induced maturation (33). The use of retrovirus vectors in that process could trigger inflammatory signals in DCs as a result of viral component recognition by TLR-3 or TLR-7 in DC endosome. Therefore, it is not surprising to see reduction in DC maturation in response to B16-CM exposure only with BMDCs. Furthermore, it was only with BMDCs that the ability of B16-CM to reduce LPS stimulation was noticed, while DC2.4 exposure to B16-CM neither reduced basal expression of CD86 and CD40 nor mitigated LPS stimulation. This is consistent with the previous observation from Western blot analysis since STAT3 should provoke an anti-inflammatory state and render DCs immature. However, further studies are needed to shed the light on the molecular reasons of the noticed inconsistency between the two models. Taken together, these findings preclude DC2.4 cell line as an *in vitro* model to study cancer-mediated immunosuppression.

Moreover, DC malfunction due to TDFs is documented in melanoma patients (4). Therefore, we conducted an *in vitro* study where DCs were exposed to B16-CM with or without siRNA treatment (Figures 2 and 3). Our *in vitro* study

indicates: (i) phenotypical and functional maturation of DCs can be restored after cancer cell manipulation with STAT3 siRNA complexes. (ii) The level of DC activation is correlated with the level of STAT3 knockdown in B16 cells. We show that DC alloreactivity (Figure 4.3) was noticed only with groups that showed higher expression of the costimulatory molecules CD86 and CD40 (Figure 4.2). This is an important observation since it proves that B16-CM treated DCs became functional after siRNA manipulation of B16 cells. The CD86 and CD40 molecules on DC surface interact with CD28 and CD40 ligand (CD40L) on T cell surface. Such interaction is beneficial for both DCs and T cells where stimulation of CD28 stabilizes CD40L on T cells and stimulation of CD40 on DCs increases their expression of CD86 molecules (35, 36). Therefore, functional and phenotypic maturation of DCs are both required for naïve T cell activation. Moreover, we noticed that STAT3 knockdown of B16 cells with PEI-StA complexes of siRNA leads to higher phenotypic and functional maturation of DCs. This is consistent with our previous results where PEI-StA complexes were more potent in STAT3 knockdown and caused higher cell-killing effect on B16 cells (18). One reason for the superior effect of PEI-StA complexes reflected on DC activation is the exponential nature of B16 cell death. It has been suggested that B16 apoptosis after STAT3 disruption involves the production of soluble factors such as TNF-related apoptosis-inducing ligand (TRAIL), which induces tumor cell death (29, 37). Such effect has shown to improve anti-tumoral function of DCs *in vitro* and *in vivo* (38). Nevertheless, detailed analysis of B16-CM is still needed to pinpoint factors responsible for DC activation. These proof-of-concept

results demonstrate that manipulation of STAT3 in tumor cell culture has a positive effect on DC activation.

Similar effect was noticed after STAT3 knockdown *in vivo*. The recorded B16 tumor regression (Figure 4.4) was associated with DC activation (Figure 4.5 and 4.6) and lymphocytes infiltration (Figure 4.7). Consistent with our previous findings, STAT3 silencing by siRNA/PEI-StA complexes was superior to that of PEI owing to the higher protective effect of PEI-StA toward siRNA (18). Consequently, we observed a significant infiltration of CD11c⁺ DCs in tumor tissue (Figure 4.5A). However, we also noted a comparable DC infiltration for groups treated with PEI and PEI-StA complexes. Such picture is quite logical *in vivo* due to the fact that DCs traffic out of the site of antigen encounter to the spleen and draining lymph node in order to present the antigen to naïve T cells (39). Considering the fact that DC influx and efflux in and out of tumor mass is a continuous process while the FACS analysis was performed in a specific time point, the difference in DC infiltration between the two formulations is irrelevant. In this case a more important factor is the level of DC activation. Here we noticed an advantage for PEI-StA over PEI in CD86 and CD40 expression (Figure 4.5B) as well as levels of proinflammatory cytokines IL-12 and TNF- α (Figure 4.5C). DCs are known to produce IL-12 and TNF- α upon capturing tumor antigen (40). The production of IL-12 was recently found to be an absolute requirement for Th1-type immune response that leads to CTL anti-tumor response (41). TNF- α was also shown to enhance DC maturation and promote anti-tumor immune response (42). The DC activation results were corroborated with our MLR study.

Here we show that upon STAT3 knockdown *in vivo*, DCs in the spleens of tumor-bearing mice showed more alloreactivity with allogenic T cells (Figure 4.6). The noted advantage of PEI-StA group supports our argument that activated DCs home to secondary lymphoid organs as more indicative results are demonstrated in those organs. Moreover, we find the results of clinical significance since some evidence showed that peripheral blood DCs induce lower allogenic MLR in a study done on 32 breast-cancer patients (43). Hence, high MLR outcome can be considered a positive indicator of the therapeutic approach.

Furthermore, high level of TIL was recorded after tumor regression following STAT3 knockdown was proved by the high level of CD3⁺ cells (Figure 4.7A). In that population, the superiority of PEI-StA treatment was noted by the induced infiltration of CD4⁺ T cells, CD8⁺ T cells, and NKT cells (Figure 4.7B). This high presence of TIL indicates three incidents in this study: stimulation of an innate immune response following tumor regression, imminent DC activation after siRNA intervention as T cell immune response is a latent response, and finally the noted tumor regression is also mediated by CTL response. The latter is explained by the ~ 4-fold reduction in tumor volume after PEI-StA administration compared to PEI. Moreover, IFN- γ was positively correlated with TIL level (Figure 4.7C). This proinflammatory cytokines is produced by activated CD4⁺ T cells, CD8⁺ CTL, NK cells, and NKT cells and plays a crucial role in anti-tumor immunity (44). In fact, IFN- γ production is directly related to suppression of B16 cell growth (45). Moreover, the results of *in vivo* DC activation (data from Figure 4.5) highly correlates with these result as the production of IL-12 by DCs and

other phagocytes is known to induce IFN- γ production (41). TNF- α was demonstrated to induce T cell activation as well (42). However, it is also important to know that our siRNA complexes may not have an exclusive effect on cancer cells. *In vivo*, the siRNA complexes might have directly affected immune cells as well as cancer cells. This is a therapeutically relevant approach, as blocking STAT3 in tumor as well as immune cells can produce a synergistic anti-tumor effect (10). Such effect was evidenced by the elegant work of Hua Yu's group where the authors demonstrated the requirement of immune cells for tumor regression using tumor-bearing mouse model with Stat3^{-/-} hematopoietic system (6). Taken together, the collective picture of our work proves that manipulation of tumoral STAT3 is crucial for the generation of robust innate and adaptive immune responses. Appropriately designed delivery systems can enhance the potency and functional activities of STAT3 siRNA leading to more effective cancer therapy approaches.

4.5 REFERENCES

1. Hanahan D, Weinberg RA. The hallmarks of cancer. *Cell*. 2000 Jan 7;100(1):57-70.
2. Pardoll D. Does the immune system see tumors as foreign or self? *Annu Rev Immunol*. 2003;21:807-39.
3. Wang T, Niu G, Kortylewski M, Burdelya L, Shain K, Zhang S, et al. Regulation of the innate and adaptive immune responses by Stat-3 signaling in tumor cells. *Nat Med*. 2004 Jan;10(1):48-54.
4. Kortylewski M, Jove R, Yu H. Targeting STAT3 affects melanoma on multiple fronts. *Cancer Metastasis Rev*. 2005 Jun;24(2):315-27.
5. Cheng F, Wang HW, Cuenca A, Huang M, Ghansah T, Brayer J, et al. A critical role for Stat3 signaling in immune tolerance. *Immunity*. 2003 Sep;19(3):425-36.
6. Kortylewski M, Kujawski M, Wang T, Wei S, Zhang S, Pilon-Thomas S, et al. Inhibiting Stat3 signaling in the hematopoietic system elicits multicomponent antitumor immunity. *Nat Med*. 2005 Dec;11(12):1314-21.
7. Buettner R, Mora LB, Jove R. Activated STAT Signaling in Human Tumors Provides Novel Molecular Targets for Therapeutic Intervention. *Clin Cancer Res*. 2002;8:945-54.
8. Hirano T, Ishihara K, Hibi M. Roles of STAT3 in mediating the cell growth, differentiation and survival signals relayed through the IL-6 family of cytokine receptors. *Oncogene*. 2000 May 15;19(21):2548-56.
9. Ivanov VN, Bhoumik A, Krasilnikov M, Raz R, Owen-Schaub LB, Levy D, et al. Cooperation between STAT3 and c-jun suppresses Fas transcription. *Mol Cell*. 2001 Mar;7(3):517-28.
10. Kortylewski M, Yu H. Stat3 as a potential target for cancer immunotherapy. *J Immunother*. 2007 Feb-Mar;30(2):131-9.
11. Kortylewski M, Yu H. Role of Stat3 in suppressing anti-tumor immunity. *Curr Opin Immunol*. 2008 Apr;20(2):228-33.
12. Yu H, Kortylewski M, Pardoll D. Crosstalk between cancer and immune cells: role of STAT3 in the tumour microenvironment. *Nat Rev Immunol*. 2007 Jan;7(1):41-51.
13. Xu Q, Briggs J, Park S, Niu G, Kortylewski M, Zhang S, et al. Targeting Stat3 blocks both HIF-1 and VEGF expression induced by multiple oncogenic growth signaling pathways. *Oncogene*. 2005 Aug 25;24(36):5552-60.
14. Nefedova Y, Nagaraj S, Rosenbauer A, Muro-Cacho C, Sebt SM, Gabrilovich DI. Regulation of dendritic cell differentiation and antitumor immune response in cancer by pharmacologic-selective inhibition of the janus-activated kinase 2/signal transducers and activators of transcription 3 pathway. *Cancer Res*. 2005 Oct 15;65(20):9525-35.
15. Cejka D, Losert D, Wacheck V. Short interfering RNA (siRNA): tool or therapeutic? *Clin Sci (Lond)*. 2006 Jan;110(1):47-58.
16. Hede K. Blocking cancer with RNA interference moves toward the clinic. *J Natl Cancer Inst*. 2005 May 4;97(9):626-8.

17. Thomas M, Lu JJ, Chen J, Klibanov AM. Non-viral siRNA delivery to the lung. *Adv Drug Deliv Rev.* 2007 Mar 30;59(2-3):124-33.
18. Alshamsan A, Hamdy S, Samuel J, El-Kadi AO, Lavasanifar A, Uludag H. The induction of tumor apoptosis in B16 melanoma following STAT3 siRNA delivery with a lipid-substituted polyethylenimine. *Biomaterials.* 2010 Feb;31(6):1420-8.
19. Incani V, Tunis E, Clements BA, Olson C, Kucharski C, Lavasanifar A, et al. Palmitic acid substitution on cationic polymers for effective delivery of plasmid DNA to bone marrow stromal cells. *J Biomed Mater Res A.* 2007 May;81(2):493-504.
20. Lutz MB, Kukutsch N, Ogilvie AL, Rossner S, Koch F, Romani N, et al. An advanced culture method for generating large quantities of highly pure dendritic cells from mouse bone marrow. *J Immunol Methods.* 1999 Feb 1;223(1):77-92.
21. Alshamsan A, Haddadi A, Incani V, Samuel J, Lavasanifar A, Uludag H. Formulation and delivery of siRNA by oleic acid and stearic acid modified polyethylenimine. *Mol Pharm.* 2009 Jan-Feb;6(1):121-33.
22. Al Zaid Siddiquee K, Turkson J. STAT3 as a target for inducing apoptosis in solid and hematological tumors. *Cell Res.* 2008 Feb;18(2):254-67.
23. Wang W, Edington HD, Rao UN, Jukic DM, Wang H, Shipe-Spotloe JM, et al. STAT3 as a biomarker of progression in atypical nevi of patients with melanoma: dose-response effects of systemic IFNalpha therapy. *J Invest Dermatol.* 2008 Aug;128(8):1997-2002.
24. Niu G, Bowman T, Huang M, Shivers S, Reintgen D, Daud A, et al. Roles of activated Src and Stat3 signaling in melanoma tumor cell growth. *Oncogene.* 2002 Oct 10;21(46):7001-10.
25. Niu G, Heller R, Catlett-Falcone R, Coppola D, Jaroszeski M, Dalton W, et al. Gene therapy with dominant-negative Stat3 suppresses growth of the murine melanoma B16 tumor in vivo. *Cancer Res.* 1999 Oct 15;59(20):5059-63.
26. Niu G, Wright KL, Huang M, Song L, Haura E, Turkson J, et al. Constitutive Stat3 activity up-regulates VEGF expression and tumor angiogenesis. *Oncogene.* 2002 Mar 27;21(13):2000-8.
27. Xie TX, Wei D, Liu M, Gao AC, Ali-Osman F, Sawaya R, et al. Stat3 activation regulates the expression of matrix metalloproteinase-2 and tumor invasion and metastasis. *Oncogene.* 2004 Apr 29;23(20):3550-60.
28. Catlett-Falcone R, Landowski TH, Oshiro MM, Turkson J, Levitzki A, Savino R, et al. Constitutive Activation of Stat3 Signaling Confers Resistance to Apoptosis in Human U266 Myeloma Cells. *Immunity.* 1999;10:105-15.
29. Niu G, Shain KH, Huang M, Ravi R, Bedi A, Dalton WS, et al. Overexpression of a dominant-negative signal transducer and activator of transcription 3 variant in tumor cells leads to production of soluble factors that induce apoptosis and cell cycle arrest. *Cancer Res.* 2001 Apr 15;61(8):3276-80.
30. Rass K, Hassel JC. Chemotherapeutics, chemoresistance and the management of melanoma. *G Ital Dermatol Venereol.* 2009 Feb;144(1):61-78.
31. Segura E, Villadangos JA. Antigen presentation by dendritic cells in vivo. *Curr Opin Immunol.* 2009 Feb;21(1):105-10.

32. Trombetta ES, Mellman I. Cell biology of antigen processing in vitro and in vivo. *Annu Rev Immunol.* 2005;23:975-1028.
33. Shen Z, Reznikoff G, Dranoff G, Rock KL. Cloned dendritic cells can present exogenous antigens on both MHC class I and class II molecules. *J Immunol.* 1997 Mar 15;158(6):2723-30.
34. Shamsasenjan K, Otsuyama K, Abroun S, Iqbal MS, Mahmoud MS, Asaoku H, et al. IL-6-induced activation of MYC is responsible for the down-regulation of CD33 expression in CD33⁺ myeloma cells. *Int J Hematol.* 2009 Apr;89(3):310-8.
35. Yang Y, Wilson JM. CD40 ligand-dependent T cell activation: requirement of B7-CD28 signaling through CD40. *Science.* 1996 Sep 27;273(5283):1862-4.
36. Johnson-Leger C, Christensen J, Klaus GG. CD28 co-stimulation stabilizes the expression of the CD40 ligand on T cells. *Int Immunol.* 1998 Aug;10(8):1083-91.
37. Sheridan JP, Marsters SA, Pitti RM, Gurney A, Skubatch M, Baldwin D, et al. Control of TRAIL-induced apoptosis by a family of signaling and decoy receptors. *Science.* 1997 Aug 8;277(5327):818-21.
38. Schumacher LY, Vo DD, Garban HJ, Comin-Anduix B, Owens SK, Dissette VB, et al. Immunosensitization of tumor cells to dendritic cell-activated immune responses with the proteasome inhibitor bortezomib (PS-341, Velcade). *J Immunol.* 2006 Apr 15;176(8):4757-65.
39. Martin-Fontecha A, Lanzavecchia A, Sallusto F. Dendritic cell migration to peripheral lymph nodes. *Handb Exp Pharmacol.* 2009(188):31-49.
40. Onishi H, Kuroki H, Matsumoto K, Baba E, Sasaki N, Kuga H, et al. Monocyte-derived dendritic cells that capture dead tumor cells secrete IL-12 and TNF-alpha through IL-12/TNF-alpha/NF-kappaB autocrine loop. *Cancer Immunol Immunother.* 2004 Dec;53(12):1093-100.
41. Trinchieri G. Interleukin-12 and the regulation of innate resistance and adaptive immunity. *Nat Rev Immunol.* 2003 Feb;3(2):133-46.
42. Brunner C, Seiderer J, Schlamp A, Bidlingmaier M, Eigler A, Haimerl W, et al. Enhanced dendritic cell maturation by TNF-alpha or cytidine-phosphate-guanosine DNA drives T cell activation in vitro and therapeutic anti-tumor immune responses in vivo. *J Immunol.* 2000 Dec 1;165(11):6278-86.
43. Gabrilovich DI, Corak J, Ciernik IF, Kavanaugh D, Carbone DP. Decreased antigen presentation by dendritic cells in patients with breast cancer. *Clin Cancer Res.* 1997 Mar;3(3):483-90.
44. Schoenborn JR, Wilson CB. Regulation of interferon-gamma during innate and adaptive immune responses. *Adv Immunol.* 2007;96:41-101.
45. Kakuta S, Tagawa Y, Shibata S, Nanno M, Iwakura Y. Inhibition of B16 melanoma experimental metastasis by interferon-gamma through direct inhibition of cell proliferation and activation of antitumor host mechanisms. *Immunology.* 2002 Jan;105(1):92-100.

CHAPTER FIVE

STAT3 SILENCING IN DENDRITIC CELLS BY PLGA NANOPARTICLES of siRNA POLYPLEXES

A version of this chapter has been published in

Molecular Pharmaceutics 2010 (In Press)

Aws Alshamsan, Azita Haddadi, Samar Hamdy, John Samuel, Ayman O. S. El-

Kadi, Hasan Uludağ, and Afsaneh Lavasanifar

&

Presented as a poster in AAPS Annual Meeting and Exposition Exhibitor

Information, Los Angeles, California, USA, November 12-18, 2009

5.1 INTRODUCTION

Dendritic cells (DCs) are professional antigen presenting cells (APCs) that serve as sentinels against internal and external pathogens in most peripheral tissues (1-3). Typically, when immature DCs (imDCs) encounter antigens, they get activated and transformed into mature DCs (mDCs) that express high levels of major histocompatibility complex (MHC) class-I and class-II, co-stimulatory molecules, as well as proinflammatory cytokines (4, 5). These mDCs migrate to secondary lymphoid organs where they activate naïve mature CD4⁺ and CD8⁺ T cells (6, 7). However, in tumor microenvironment, DCs cannot exert their proper function due to the state of immune tolerance enforced by tumor milieu (8). One mechanism by which tumors abrogate DC function is through the constitutive activation of signal transducer and activator of transcription 3 (STAT3) (9).

STAT3 is a transcription factor that becomes activated in response to cytokine and growth factor receptor stimulation (10). For activation, STAT3 monomers get phosphorylated on critical tyrosine residues (Y⁷⁰⁵) by Janus Kinases (JAKs). Thereafter, monomers of phosphorylated-STAT3 (p-STAT3) dimerize through reciprocal phosphotyrosine-SH2 interaction and translocate to the nucleus where they bind to STAT-specific sites on the promoter region of the target genes (10). In tumor cells, many tumor-derived factors (TDFs) are induced by the transcriptional activity p-STAT3 such as vascular endothelial growth factor (VEGF), interleukin-6 (IL-6), and IL-10 (11). The secretion of these TDFs in tumor milieu leads to further induction of p-STAT3 in several tumor-exposed immune cells including DCs (11). This hyperactive STAT3 forces DCs to remain

immature and malfunctioned expressing low levels of MHC class-I/II, costimulatory molecules, and proinflammatory cytokines (12, 13). Therefore, DCs lose their ability to polarize T cells toward T helper type 1 (Th1) and cytotoxic T lymphocyte (CTL) response, which is needed for anti-tumoral immunity (14). In fact, numerous studies strongly indicated the negative-regulatory role of JAK/STAT3 pathway on DC maturation, which has been systematically evidenced *in vivo* (15-17). As a result, the anti-tumor activity mediated by DCs gets profoundly harnessed (9, 11, 18-21). Hence, the disruption of tumor-induced hyperactive p-STAT3 in DCs is considered as an attractive strategy for cancer immunotherapy.

Several modalities have been employed to study anti-tumor immune responses following STAT3 inhibition in DCs. Pioneer studies focused on the inhibition of JAKs as a mean for STAT3 activity disruption. In fact, targeted disruption of STAT3 signaling in APCs using AG490, a known inhibitor of JAK1 and JAK2, resulted in the priming of antigen-specific CD4⁺ T cells in response to an otherwise tolerogenic stimulus *in vivo* (16). Consistently, the work of Gabrilovich and colleagues on the JAK2/STAT3 inhibitor JSI-124 (cucurbitacin I) demonstrated a dramatic activation of imDCs generated in the presence of TDFs as well as in control medium (17). The outcomes from STAT3 disruption data in DCs support the use of this approach for therapeutic applications. However, due to the incomplete understanding of the mechanism of inhibition by which these agents act, as well as the apparently generalized upstream action and the associated non-specific toxicities of these pharmacological inhibitors, clinical

applications of AG490 or JSI-124 were not possible (22). Therefore, the need is imminent for specific STAT3 inhibition strategies.

Recently, RNA interference (RNAi) emerged as a specific and effective modality to downregulate protein expression at the mRNA level (23). This technology is based on introducing a small interfering RNA (siRNA) in the cytoplasm where it integrates into RNA-induced silencing complex (RISC) that cleaves the mRNA of interest specifically (24). However, due to low biological stability, poor cell permeability, and unfavorable pharmacokinetic and biodistribution profile, the progress of siRNA from bench to bedside was significantly hindered (25). Hence, it is important to develop an optimum siRNA delivery strategy (26). In this regard, we have previously developed siRNA delivery systems based on lipid modification of polyethylenimine (PEI) (27). We have shown that attachment of stearic-acid molecules on PEI backbone (PEI-StA) enhances the protective effect of PEI against degradation of complexed siRNA in serum (27). Moreover, the anti-STAT3 activity of the PEI and PEI-StA polyplexes was proven in B16 melanoma cells *in vitro* and *in vivo* where PEI-StA, in particular, enhanced the silencing potency of STAT3 siRNA and promoted its anti-cancer activity (28). Moreover, STAT3 knockdown in B16 tumor by siRNA/PEI-StA complexes induced a bystander anti-tumor immune response evidenced by high infiltration and activation levels of DCs, CD4⁺, CD8⁺ and NKT cells into tumor mass (29). However, knockdown of STAT3 in DC directly with anti-STAT3 siRNA has not been investigated. In this study we evaluate this approach by designing a delivery system based on physical encapsulation of

siRNA/PEI or siRNA/PEI-StA complexes in poly(D,L-lactic-co-glycolic acid) (PLGA) nanoparticles (NPs) (Figure 5.1). The incorporation of siRNA polyplexes into PLGA NPs improves the toxicity profile of PEI and enhance cellular uptake (30). To our knowledge, for the first time we provide evidence that PLGA NPs of STAT3 siRNA could restore DC maturation and functionality after exposure to tumor factors while masking the PEI-associated toxicity.

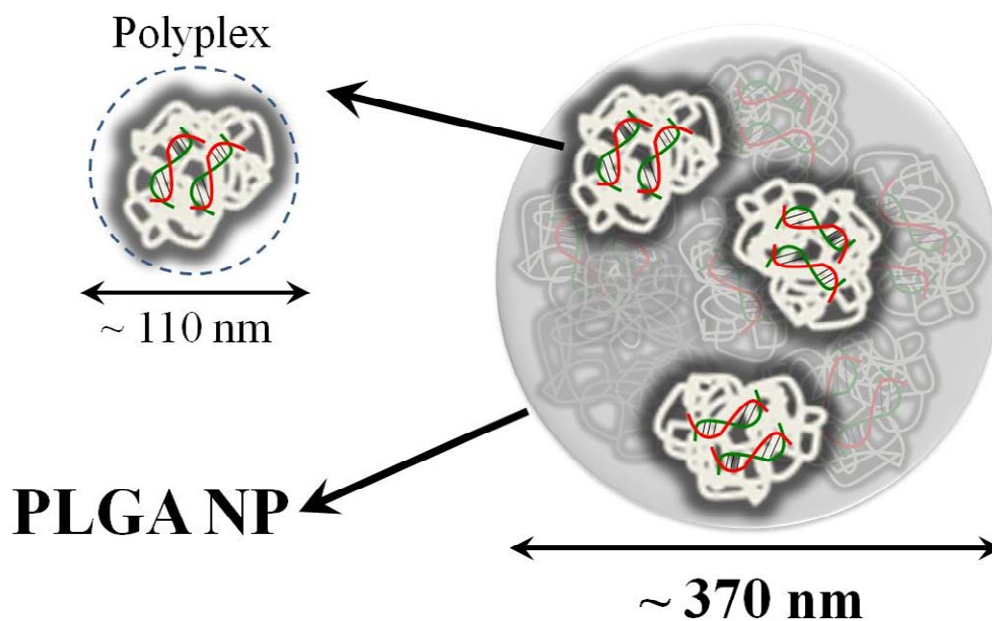


Figure 5.1 Schematic diagram showing components of PLGA-P or PLGA-PS nanoparticulate formulation with relative sizes to the polyplexes counterparts.

5.2 MATERIALS AND METHODS

5.2.1 Materials

Branched PEI (25 kDa), triethylamine (TEA), 3-(4,5-dimethylthiazol-2-yl)-2,5-diphenyltetrazolium bromide (MTT), dimethyl sulfoxide (DMSO), and stearoyl chloride (98.5%) were obtained from Sigma-Aldrich (St. Louis, MO). Polyvinyl alcohol (PVA), carboxylic-acid terminated PLGA polymers (monomer ratio 50:50, MW ~7 kDa) was purchased from Absorbable Polymers International (Pelham, AL, USA). Anhydrous ethyl ether and dichloromethane (DCM) were purchased from Fisher Scientific (Fairlawn, NJ). Fetal Bovine Serum (FBS) was obtained from HyClone (Logan, UT). Dulbecco's Modified Eagle's Medium (DMEM), RPMI-1640, L-glutamine, and gentamicin were purchased from Gibco-BRL (Burlington, ON, Canada). Mouse TNF- α ELISA kit was purchased from e-Biosciences (San Diego, CA). Sequence-specific siRNA targeting murine STAT3 mRNA was purchased from Ambion (Austin, TX) (sense: 5'-GGACGACUUUGAUUUCAACTt-3', antisense: 5'-GUUGAAAUCAAGUCGUCctg-3'). The scrambled Silencer[®] Negative Control #1 siRNA (Catalogue #AM4635) and Silencer[®] FAM[™] labeled Negative Control #1 siRNA (Catalogue #AM4620), both purchased from Ambion (Austin, TX). LysoTracker[®] Red DND-99 and ProLong[®] Gold Antifade with DAPI were purchased from invitrogen[™] (Burlington, ON). Anti-mouse CD86 (PE labeled) mAb was purchased from BD Biosciences (Mississauga, ON, Canada). EasySep[®] Negative Selection kit for T cells isolation was purchased from Stemcell Technologies (Vancouver, BC). Anti-phosphotyrosine (Y⁷⁰⁵) STAT3 monoclonal antibody, anti-STAT3 antibody and anti-Actin antibody (I-19) were purchased

from Santa Cruz Biotechnology (Santa Cruz, CA). ECL Plus™ detection kit was purchased from GE Healthcare Life Sciences (Piscataway, NJ).

5.2.2 Preparation of Primary DC Culture

Primary DC culture was generated from bone marrow precursor of C57BL/6 mice femurs and propagated in complete RPMI-1640 in presence of GM-CSF as previously described (31). The purity of the DC population on day 7 was found to be between 70-75% based on the expression of CD11c on the semi-adherent and non-adherent cell populations. To increase DC purity, semi-adherent and non-adherent cells were isolated from primary culture on day 6 by thorough suspension in growth medium. Cells were centrifuged and resuspended in fresh complete RPMI-1640 in the presence of GM-CSF and then transferred to new cell culture plates 24 h prior to any manipulation. After this process, 95 % of cells were confirmed to be positive for CD11c.

5.2.3 Preparation of PLGA NPs of siRNA Complexes

PEI-StA was prepared by N-acylation of PEI with stearoyl chloride and characterized as described in (32). Then, in sterile eppendorf tubes, 12.5 µg of siRNA was added to equal amount of PEI or PEI-StA in 50 µL PBS and incubated for 30 minutes at 37 °C as previously described (27). Thereafter, the formed complexes were encapsulated into PLGA NPs by double-emulsion solvent evaporation method regularly used in our lab. In brief, a primary w/o emulsion is formed by emulsification of the first aqueous phase (PEI or PEI-StA polyplexes in

50 μ L PBS) with the organic phase (25 mg PLGA in 300 μ L DCM) using a microtip probe sonicator (Model XL2010, Heat Systems, Farmingdale, NY). The primary emulsion is further emulsified with a secondary aqueous phase (1 mL of 5% PVA in PBS) to form a secondary w/o/w emulsion. The resulting emulsion is transferred drop-wise to stirring 4 mL of double-deionized water to allow the removal of DCM by evaporation. After 3 hours, the NP suspension is washed three times at 4 °C (35000 \times g, 15 min) and freeze-dried.

5.2.4 Characterization of PLGA-P and PLGA-PS NPs

5.2.4.1 Surface Morphology, Particle Size, and Surface Charge Analysis

From freeze-dried stocks, PLGA-P or PLGA-PS suspensions of 1 mg/mL in water were prepared. Thereafter, aliquots of PLGA-P or PLGA-PS suspensions were aspirated and mounted on specimen stubs and sputter coated with Au/Pd in Hummer 6.2 Sputter Coater. After 24 h, samples were visualized by Scanning Electron Microscope XL30 (FEI Company, Hillsboro, OR, USA) and SEM images were taken. Other aliquots were used for size and surface charge analysis by dynamic light scattering (DLS) and zeta potential analysis, respectively, of 3 serial measurements using Zetasizer 3000 (Malvern, UK).

5.2.4.2 Determination of siRNA Content

Encapsulation efficiency (E.E.) and loading of siRNA in PLGA-P and PLGA-PS NPs was calculated by fluorescence spectroscopy and confirmed by gel retardation assay. FAM-labeled siRNA was complexed with PEI or PEI-StA and

then encapsulated in PLGA NPs as described above. Serial dilution of each sample were prepared and read at ($\lambda_{\text{ex}} = 484 \text{ nm}$ and $\lambda_{\text{em}} = 535 \text{ nm}$) in Baxter 96-well plate fluorescence reader (Chicago, IL). Blank PLGA NPs spiked with known serial concentrations of siRNA-polyplexes were used as calibration curve.

For gel retardation assay, PLGA-P and PLGA-PS were dissolved in chloroform. The solvent was evaporated under nitrogen and precipitants were suspended in RNase-Free water. Supernatant (containing siRNA + PEI or PEI-StA polyplexes) was incubated with 50 μg heparin at 37°C for 1 h to ensure that all siRNA is released in free form, as previously described in (27). The samples were then loaded onto 2% agarose gel containing 0.2% mg/mL EtBr and electrophoresis was performed under previously-described conditions (27). The resulting gel was photographed under UV-illumination. The pictures were digitized and analyzed with ImageJ software (W. Rasband (2005) National Institutes of Health, Bethesda, MD, <http://rsb.info.nih.gov/ij>) to determine the mean density of siRNA band. To determine the recovery of the extraction process, known amount of siRNA/polyplexes and empty PLGA NPs were added into chloroform, and the extraction procedure was performed as described above. Thereafter, E.E. % and siRNA loading (w/w) were calculated using the following equations:

$$E.E. \% = \frac{\text{Amount of loaded siRNA in } \mu\text{g}}{\text{Amount of total siRNA used in } \mu\text{g}} \times 100$$

$$siRNA \text{ Loading (w/w)} = \frac{\text{Amount of loaded siRNA in } \mu\text{g}}{\text{Amount of PLGA in mg}}$$

5.2.4.3 *In vitro* Release Study

Aliquots of 5 mg/mL of the suspended PLGA-P and PLGA-PS in PBS were placed in a 37 °C gently-shaking water bath. At designated time intervals, a set of triplicate samples was removed, and the supernatant was separated from the particles by centrifugation. Fluorescence spectroscopy was used to determine siRNA concentration as mentioned earlier. To determine the remaining siRNA in the precipitated portion, pellets were dissolved and run on agarose gel as described above.

5.2.5 Cytotoxicity Studies

DCs on day 7 were transferred to 6-well plates at cell density of 2×10^5 cells per well. Then, cells were subjected to scrambled siRNA treatment in PEI complexes, PEI-StA complexes, PLGA-P, or PLGA-PS for 24 h at 37°C. The treatment dose was calculated based on 10 µg/mL PEI or PEI-StA concentration in culture media. After designated treatments, cells were washed with PBS. Then, 1 mL of Trypan Blue in media (1:1 ratio) was added, and Trypan Blue exclusion was detected by Axio Observer Z1 Inverted Microscope (Carl Zeiss Canada Ltd., Toronto, ON) and visualized with Axio Vision 4.8 software.

To determine cell viability as a function of polyplex concentrations, MTT assay was carried out. Day 7 DCs were transferred to 96-well plate at cell density of 5,000 cells per well. Then, cells were incubated with PEI complexes, PEI-StA complexes, PLGA-P, or PLGA-PS for 24 h at 37°C. Thereafter, 100 µL of MTT solution in culture medium (0.5 mg/mL) was added to each well for 2 h. The

formed formazan crystals were dissolved by adding 200 μ L of DMSO to each well and kept under gentle shaking for 30 min. Optical density was measured at 550 nm using a microplate reader (Powerwave with KC Junior software; Bio-Tek, Winooski, VT). The results were converted into % viability by using the absorbance from untreated sample as a reference (100%), and expressing the absorbances obtained from the treatment groups as a percentage of the reference value.

5.2.6 Uptake of PLGA-P and PLGA-PS by DCs

DCs uptake of PLGA-P and PLGA-PS was determined by fluorescence microscopy. Day-7 DCs were transferred to 24-well plates and grown on cover slips for 24 h. Then, DCs were pulsed for 6 h at 37°C with PLGA-P and PLGA-PS encapsulating FAM-labeled scrambled siRNA (100 nM). Then, LysoTracker[®] Red DND-99 at concentration of 100 nM was added for 30 min. The cells were then washed three times with PBS and fixed with 2% paraformaldehyde solution in PBS for 10 minutes. Then, ProLong[®] Gold Antifade with DAPI was mounted to prevent photobleaching as well as to stain the nucleus. Samples were then visualized under with Axio Observer Inverted Microscope (Carl Zeiss Canada Ltd., Toronto, ON).

5.2.7 Treatment of Malfunctioned DCs

Malfunctioned DCs at day 7 were generated by exposure to tumor-conditioned media from B16.F10 melanoma culture (B16-CM) for 24 h as

previously described in (33) (chapter 4). In brief, murine B16.F10 cells were grown and propagated in DMEM media supplemented with 10% FBS at 37 °C and 5% CO₂. After confluence, B16 cells were incubated with serum-free media for 24 h. Thereafter, conditioned medium was added to a primary DC culture reaching final B16-CM concentration of 50%. FBS was then supplemented to 10% final concentration in culture. Then, DCs were pulsed with anti-STAT3 PLGA-P and PLGA-PS for 48 h. As controls, DCs treated with naked anti-STAT3 siRNA or PLGA-P and PLGA-PS of scrambled siRNA (PLGA-P-sc) and (PLGA-PS-sc) were used. Thereafter, STAT3 activation level in DCs was determined by Western blot, phenotypic maturation was assessed by analyzing CD86 expression by fluorescence activated cell sorting (FACS), TNF- α secretion was determined by ELISA, and DCs alloreactivity was assessed by mixed lymphocytes reaction (MLR).

5.2.7.1 Western Blot

After designated treatments, DCs were collected and washed twice with ice-cold PBS, then lysed in a buffer containing 30 mM HEPES (pH 7.5), 2 mM Na₃VO₄, 25 mM NaF, 2 mM EGTA, 2% Nonidet P-40, 1:100 protease inhibitor cocktails, 0.5 mM DTT and 6.4 mg/mL phosphatase substrate 4-nitrophenyl phosphate. Cell lysates were centrifuged for 20 seconds at 16,000 \times g (Eppendorf Centrifuge 5415C). Thereafter, NaCl was added to samples to final concentration of 420 mM and cell lysates were centrifuged for 20 min at 16,000 \times g and supernatant was transferred to new tubes and pellets were discarded. Total protein

extract was determined by Micro BCA Protein Assay kit. Equal amounts of protein (20 µg) were loaded on 8% SDS-PAGE gel. Proteins were then transferred into PVDF membrane and were probed with anti-phosphotyrosine (Y⁷⁰⁵) STAT3 monoclonal antibody (1:500). Stripped membranes were probed with polyclonal anti-STAT3 antibody (1:1000) or anti-actin antibody (I-19) (1:1000). Membranes were developed using ECL Plus[™] detection kit. Optical intensity of p-STAT3 band was quantified and normalized to actin protein band using ImageJ software (W. Rasband (2005) National Institutes of Health, Bethesda, MD, <http://rsb.info.nih.gov/ij>). The Western blot procedure was described in detail in chapter 3.

5.2.7.2 FACS Analysis

For phenotypic maturation studies, 1×10^5 DC primary cultures were washed with PBS and suspended in FACS buffer. Then, cells were incubated with CD86 mAbs or corresponding isotype controls and kept in 4°C for 30 min. After that, cells were washed 3 times with FACS buffer to remove excess mAbs and all samples were finally acquired on a Becton-Dickinson FACSsort and analyzed by Cell-Quest software.

5.2.7.3 ELISA Assay

After designated treatments, supernatants of DCs cultures were collected after centrifugation at 10,000×g for 5 min (Eppendorf Centrifuge 5415C). Then, several dilutions of supernatants were loaded in a 96-well plate pre-coated with

anti-TNF- α mAb. Sandwich ELISA was performed using mouse TNF- α ELISA kit according to the manufacturer's directions. The resulting color, proportional to TNF- α concentration, was read using a microplate reader (Powerwave with KC Junior software; Bio-Tek, Winooski, VT) at OD of 450 nm with reference set at 570 nm. Concentration was calculated from standard curve of authentic TNF- α sample provided by the manufacturer.

5.2.7.4 Mixed Lymphocytes Reaction

T cells were obtained from spleen of Balb/c mice Jackson Laboratory (Bar Harbor, ME, USA). Spleen was crushed between two slides and T cells were purified using EasySep[®] Negative Selection kit according to manufacturer's instructions. Purified T cells were cocultured in flat-bottomed 96-well plates with irradiated DCs in a ratio of (2:1) in 37°C and 5% CO₂. Thereafter, [³H]-thymidine was added during the last 18 hours of a 3 day coculture and the T-cell proliferation measured by [³H]-thymidine incorporation in counts per minute.

5.2.8 Data Analysis

The data were analyzed for statistical significance ($p < 0.05$) by one-way ANOVA; Post-Hoc Scheffé's test was conducted to determine level of significance (SPSS for Windows, Version 16.0).

5.3 RESULTS

5.3.1 Characterization of PLGA-P and PLGA-PS

Surface morphology, size distribution, and zeta potential analysis for PLGA-P and PLGA-PS is shown in Figure 5.2. Evaluation of NPs surface morphology by scanning electron microscopy (SEM) showed that PLGA-P and PLGA-PS form spherical structures with smooth surfaces. Size determination by DLS indicates that both PLGA-P and PLGA-PS conformed uniform populations evidenced by the Gaussian distribution of the hydrodynamic diameter histograms. PLGA-PS was slightly, but not significantly, larger than PLGA-P (the average hydrodynamic diameter for PLGA-P and PLGA-PS was 351 and 392 nm, respectively). Moreover, surface charge analysis indicated that PLGA-P and PLGA-PS displayed comparable negative surface charges reaching ~ -13 and -19 mV, respectively. The difference was not statistically significant.

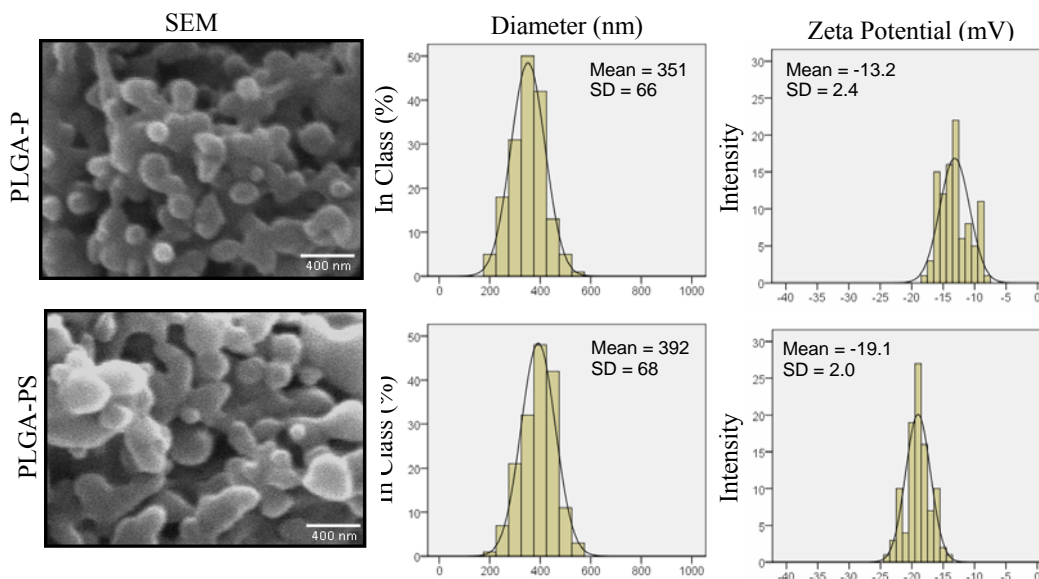


Figure 5.2 Characterization of PLGA-P and PLGA-PS NPs. SEM images (left panels) of dried samples showing spherical structures of smooth surfaces. Bar scale is 400 nm. Binning charts represent with Gaussian distribution histogram of hydrodynamic diameter of PLGA-P and PLGA-PS (middle panels). Mean \pm SD for each sample is presented in the upper corner of each panel. Mean hydrodynamic diameters of all NPs did not show any significant difference from each other. Gaussian distribution demonstrated no skewness indicating the uniformity of sample population. The data is representative of 10 reading cycles for 3 independent measurements. Binning chart histograms for zeta potential distribution (mV) (right panels) demonstrated no skewness indicating the uniformity of sample population. Mean \pm SD for each sample is presented in the upper corner of each panel. The data is representative of 10 reading cycles for 3 independent measurements.

Moreover, siRNA encapsulation efficiency and loading in PLGA-P and PLGA-PS was 26.3% and 43.9%, respectively (Table 5.1). This was also confirmed by gel retardation assay of extracted siRNA from each formulation where it reached 25.7% and 50.7% in PLGA-P and PLGA-PS, respectively (Figure 5.3). These results indicate a significant increase in siRNA E.E. in PLGA-PS by PEI-StA as compared to PLGA-P. Similarly, siRNA loading was significantly higher in PLGA-PS compared to PLGA-P reaching 3.8 ($\mu\text{g}/\text{mg}$) and 2.2 ($\mu\text{g}/\text{mg}$) of PLGA, respectively (Table 5.1).

Table 5.1. siRNA E.E. and Loading in PLGA-based NPs

Formulation	E.E. (%)	Loading ($\mu\text{g}/\text{mg}$)[*]
PLGA-P	26.31 \pm 5.96	2.2 \pm 0.4
PLGA-PS	43.98 \pm 6.07 ^a	3.8 \pm 0.3 ^a

^a Statistical significance at $p < 0.05$

* siRNA loading per 1 mg PLGA

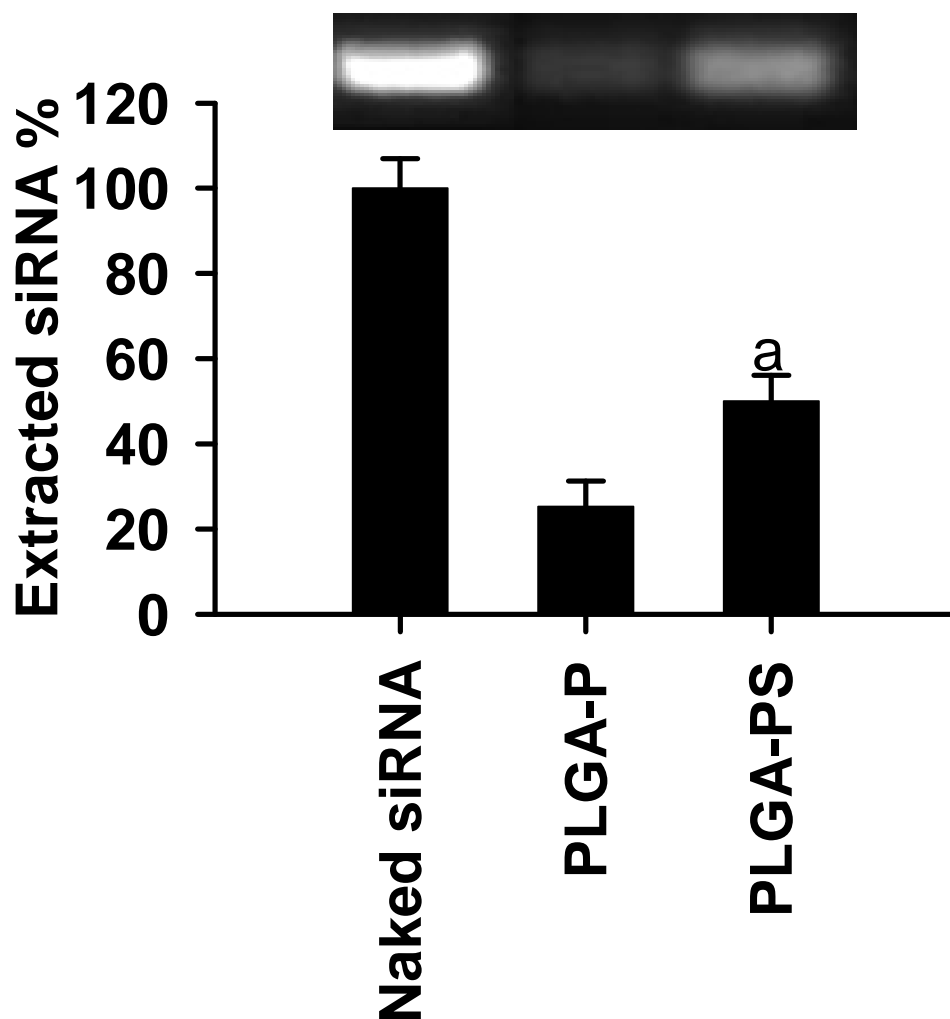


Figure 5.3 Gel retardation assay of free siRNA and extracted siRNA from PLGA-P and PLGA-PS. The pictures were digitized and analyzed with ImageJ software (W. Rasband (2005) National Institutes of Health, Bethesda, MD, <http://rsb.info.nih.gov/ij>) to determine the mean density of siRNA band. The results are plotted in the bar graph which represents the average \pm SD of at least 2 tests. Statistical significance (a; $p < 0.05$) compared to PLGA-P.

5.3.2 *In vitro* Release Profile of siRNA from PLGA-P and PLGA-PS

The cumulative release of siRNA from PLGA-P and PLGA-PS was sustained and followed a triphasic pattern characteristic for PLGA particulate systems (Figure 5.4A). A burst release of siRNA was seen for both PLGA-P and PLGA-PS reaching ~40% in the first 24 h. Thereafter, more sustained and continuous release was observed over a period of 6 days. Then, another climb in release was seen for both NPs until day 8. At this point, no significant difference in the percentage of siRNA released was observed. By the end of the 10 days, siRNA release was entering a plateau phase where the cumulative release of siRNA was significantly higher for PLGA-PS than that of PLGA-P, reaching almost 94 and 79%, respectively. The analysis of the entrapped siRNA in the NPs was in agreement with the released siRNA 8% and 24% siRNA was detected in PLGA-PS and PLGA-P, respectively, after 10 days (Figure 5.4B).

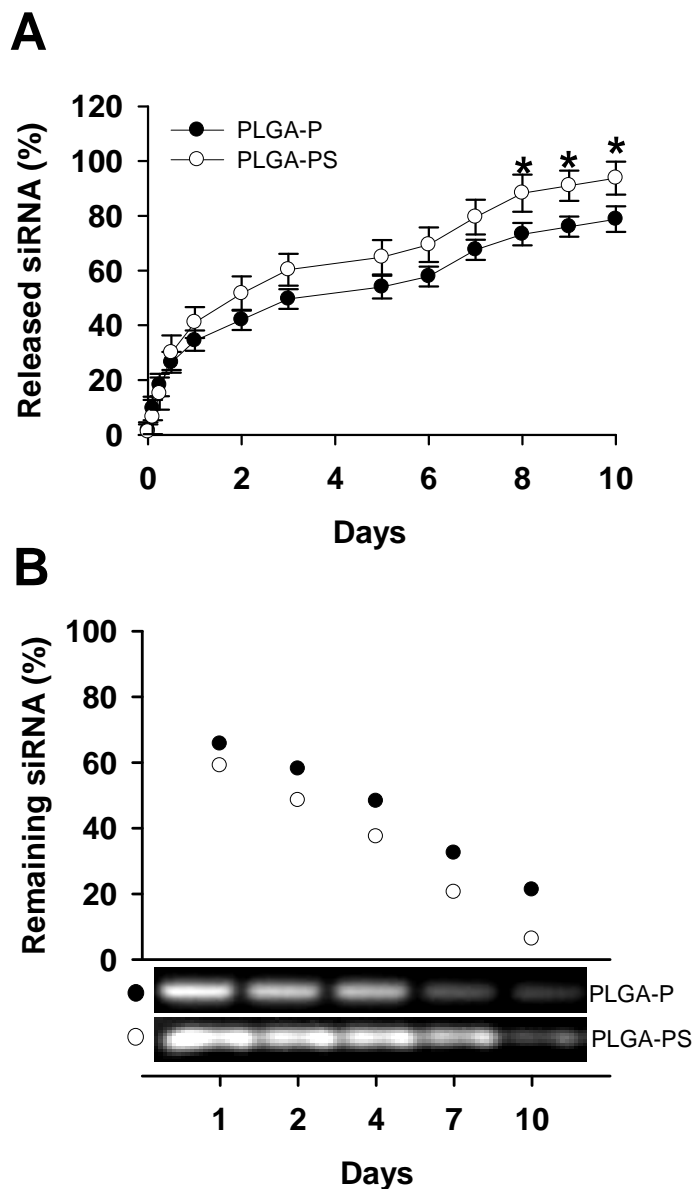


Figure 5.4 *In vitro* release of siRNA and NPs surface analysis. (A) *In vitro* release profile of FAM-siRNA in PBS detected over 10-day time period for PLGA-P (filled circles) and PLGA-PS (open circles). Significant increase in FAM-siRNA release rate was seen with PLGA-PS at days 8, 9, and 10 compared to PLGA-P (*; $p < 0.05$). Data was presented as average \pm SD of 3 different measurements. (B) Circles represent signals of remaining siRNA extracted from PLGA-P (filled circles) and PLGA-PS (open circles) as determined by gel retardation assay. Percentage of the remaining siRNA in each NPs set was calculated based on extracted siRNA at time 0 for each set. Reduction in entrapped siRNA with time confirms the release profile in (A).

5.3.3. Assessment of PLGA-P and PLGA-PS Cytotoxicity

In order to assess the cytotoxic effect of PLGA-P and PLGA-PS on DC primary culture compared to PEI and PEI-StA polyplexes that were not encapsulated in PLGA NPs, Trypan Blue assay and MTT assay were conducted to determine cell membrane integrity and metabolic activity, respectively (Figure 5.5). Only DCs incubated with PLGA-P and PLGA-PS retained their membrane integrity and adequately excluded the Trypan Blue dye. On the contrary, direct application of PEI and PEI-StA polyplexes caused cytoplasmic membrane disruption as evidenced by abundance of the Trypan Blue dye in DCs cytoplasmic compartment (Figure 5.5A). Furthermore, we conducted a concentration-dependent cytotoxicity study by MTT assay to determine the safety margins of each formulation. As shown in Figure 5.5B, no cytotoxic effect was noticed at concentrations less than 5 $\mu\text{g/mL}$ with all formulations. Only after that concentration, reduction in DC viability started to appear with PEI and PEI-StA polyplexes. Moreover, this toxic effect was of a concentration-dependent manner until it reached a plateau after 12.5 $\mu\text{g/mL}$ concentration. On the other hand, the PLGA-P and PLGA-PS NPs were less toxic than their polyplexes counterparts. No significant reduction in cell viability was noted with PLGA-P and PLGA-PS even at higher concentrations.

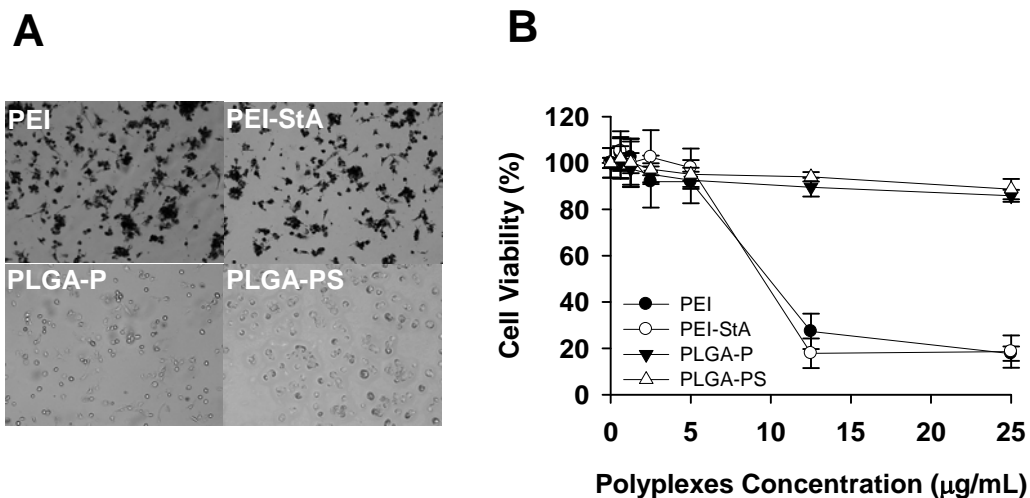


Figure 5.5 Cytotoxicity assessment of PLGA-P and PLGA-PS compared to PEI and PEI-StA polyplexes. (A) Trypan Blue exclusion test was performed for Day 7 DCs treated with 10 µg/mL of PEI or PEI-StA polyplexes (upper panels) and PLGA-P or PLGA-PS (lower panels). Trypan Blue was detected only with unencapsulated polyplexes, while with PLGA-P and PLGA-PS, DCs were able to exclude the Trypan Blue dye. (B) MTT assay was performed for DCs treated with increasing concentrations of polyplexes before and after PLGA encapsulation. Signs for cytotoxicity started to appear after 5 µg/mL concentration only with PEI (filled circles) and PEI-StA (open circles). No signs for toxicity were recorded with PLGA-P (filled triangles) and PLGA-PS (open triangles) even at higher concentrations. Data are shown as mean \pm SD of 7 replicates for each sample.

5.3.4 Cellular Uptake of PLGA-P and PLGA-PS by DCs

DC primary culture was incubated with PLGA-P and PLGA-PS encapsulating 100 nM siRNA for 6 h at 37°C. We chose this time point (6 h) as we have previously shown that around 80% of DCs could internalize PLGA NPs within 4-8 h (34). Our fluorescence microscopy results indicated the presence of the PLGA-P and PLGA-PS of FAM-siRNA (green color in Figure 5.6, due to FAM-labeled siRNA) in the cytoplasm. Some FAM-siRNA signals was shown to co-localize with LysoTracker[®] Red signals (orange color, due to overlay of the green signal from FAM-siRNA, and the red signal from LysoTracker[®] Red), which indicated the presence of PLGA-P and PLGA-PS inside the endosomes and in areas around the nuclei (blue structures, due to DAPI staining). No qualitative differences between the uptake of PLGA-P and PLGA-PS were indicated.

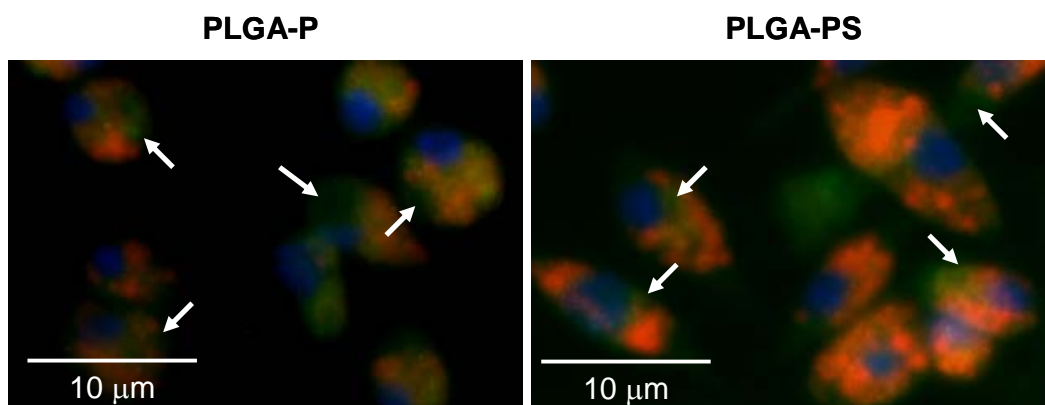


Figure 5.6 Cellular uptake of FAM-siRNA/PLGA-P and PLGA-PS by DCs. Fluorescence microscopy analysis of intracellular siRNA when DCs were incubated with 100 nM FAM-siRNA/PLGA-P and PLGA-PS (green fluorescence). Co-localization analysis was shown as orange color resulting from an overlay of FAM-siRNA and LysoTracker Red signal. Nuclei (blue) are stained with 4',6-diamidino-2-phenylindole (DAPI) and the scale bar for each image is 10 μm. White arrows points out siRNA presence in the cytoplasm and peri-nuclear areas indicating successful endosomal escape.

5.3.5 Restoration of DC Functionality Following STAT3 Knockdown by siRNA NPs

We generated defective and tolerogenic DCs in which the STAT3 phosphorylation has been induced through exposure to conditioned medium of the STAT3-active melanoma cell line B16.F10 (33). The STAT3⁺ DCs were then treated with PLGA-P and PLGA-PS of anti-STAT3 siRNA (100 nM) for 48 h. Controls included using naked anti-STAT3 siRNA or identical formulations of scrambled siRNA. We assessed our intervention at four levels: the specific disruption of STAT3 signaling pathway, the induction of phenotypic DC maturation marker (CD86) expression, the induction of proinflammatory cytokine secretion (TNF- α), and the ability of DCs to activate the proliferation of allogenic T cells (Figure 5.7).

Western blot analysis demonstrated a significant reduction in phosphorylated and total STAT3 signals only by PLGA-P and PLGA-PS NPs of anti-STAT3 siRNA (Figure 5.7A). Compared to naked siRNA-treated DC group, p-STAT3 level was reduced by ~ 48% and 77% upon treatment with PLGA-P and PLGA-PS, respectively. More importantly, the noted inhibition in p-STAT3 level was specific since it was correlated with reduction in total STAT3 level as a result of siRNA silencing. Furthermore, PLGA-PS allowed for more profound siRNA silencing of STAT3 that was statistically significant as compared to PLGA-P ($p < 0.05$). No silencing effect was noticed with scrambled siRNA formulations (PLGA-P-sc or PLGA-PS-sc) indicating the specificity of our intervention.

The induction of p-STAT3 in DCs by B16-CM reduced their phenotypic maturation as we have previously demonstrated (33). The siRNA silencing of STAT3 in DCs restored surface expression of DC maturation marker CD86. As shown in Figure 5.7B, DC groups treated with PLGA-P and PLGA-PS expressed remarkably high levels of CD86. The mean fluorescence intensity (MFI) of the FACS histograms were 93 and 111 for cells treated with PLGA-P and PLGA-PS, respectively, as compared to only 33 in case of naked siRNA-treated DCs (Figure 5.7B). Scrambled siRNA formulations (PLGA-P-sc or PLGA-PS-sc) did not induce CD86 expression, which is in agreement with our Western blot results (data in Figure 5.7A).

This maturation picture was accompanied by a significant induction in TNF- α secretion by DCs treated with PLGA-P or PLGA-PS (Figure 5.7C). DCs treated with PLGA-P were shown to secrete TNF- α at levels that were 3.4 folds higher than what was recorded with naked siRNA-treated group. Treatment of DCs with PLGA-PS has led to the secretion of TNF- α at 5.7 folds higher than naked siRNA control treatment. In fact, TNF- α secretion upon treatment with PLGA-PS was even 1.7 folds higher than what followed PLGA-P treatment. This was consistent with our FACS analysis findings where CD86 expression was induced only after treatment with PLGA-P and, particularly, after treatment with PLGA-PS.

More importantly, this immunostimulatory picture was corroborated by the ability of DCs to induce allogenic T cells proliferation (Figure 5.7D). DCs treated with naked siRNA or PLGA-P-sc or PLGA-PS-sc were not able to interact

with allogenic T cells. However, PLGA-P or PLGA-PS that deliver functional anti-STAT3 siRNA, allowed DCs to significantly induce allogenic T cell proliferation. A 4.4 and 5.6 fold increase in the proliferation of T cells co-cultured with DCs treated with PLGA-P or PLGA-PS was observed, respectively (Figure 5.7D).

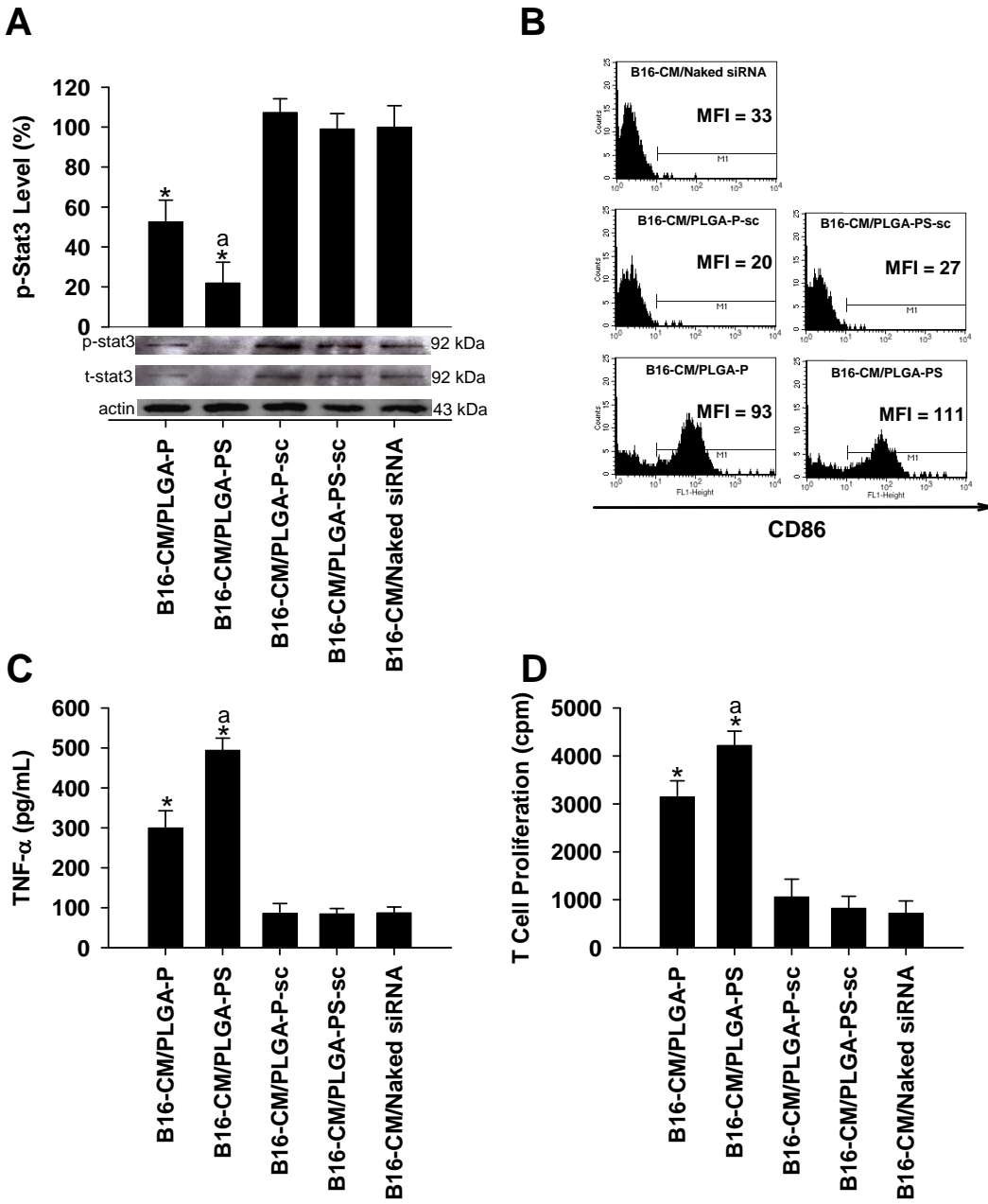


Figure 5.7 Evaluation of immunostimulatory potential of PLGA-P and PLGA-PS of STAT3 siRNA. Primary DC cultures in day 7 were incubated with B16-CM of B16 culture for 24 h. DCs were pulsed with anti-STAT3 PLGA-P and PLGA-PS for 48 h. (A) Western blot analysis showing expression level of p-STAT3, STAT3, and Actin loading control. Bands optical intensities of p-STAT3 (black bars) were quantified and normalized to Actin bands using ImageJ software (W. Rasband (2005) National Institutes of Health, Bethesda, MD, <http://rsb.info.nih.gov/ij>). The software provides optical densities that are normalized for width, thickness, and background. Data are shown as the average \pm SD of 4 experiments. Statistical significance was determined compared to control (*; $p < 0.05$) and PLGA-P (a; $p < 0.05$). (B) FACS analysis of CD86 expression. Histograms indicate a shift in the fluorescence signal only following STAT3 knockdown in DCs. mean fluorescence intensity (MFI) values after each treatment were reported for M1 population. M1 gate region indicates the inclusion area for CD86 expression where in-gate cells are considered positive for marker expression. (C) TNF- α cytokine levels measured in DC culture following STAT3 knockdown. Significant induction TNF- α cytokines secretion was noted with PLGA-PS as compared to control groups (*; $p < 0.05$) and PLGA-P group (a; $p < 0.05$). Data are shown as the average \pm SD of 3 measurements. (D) Allogenic MLR following STAT3 silencing in vitro. Treated DCs were collected, irradiated, and cocultured with allogenic T cells isolated from the spleen of Balb/c mouse. Bars represent level of T cell proliferation. DCs treated with PLGA-PS allowed for higher alloreactivity compared to controls (*; $p < 0.05$) and PLGA-P (a; $p < 0.05$).

5.4 DISCUSSION

In a variety of solid and hematological tumors, constitutive activation of STAT3 has been found to mediate numerous oncogenic properties such as cancer cells survival, proliferation, angiogenesis, metastasis, as well as immune escape (35-37). The latter is centrally driven by tumor-mediated inhibition of DC maturation (8, 14). For optimum immune response, mDCs must provide T cells with three signals: *Signal 1* which represents the antigen presentation in context of class I and class II MHC, *Signal 2* which is the co-stimulation provided by surface molecules such as CD80, CD86, and CD40 that interact with their ligands on T cell surface, and *Signal 3* which is the set of cytokines released by mDCs that polarizes T cells toward the intended response. Failure of DCs to conduct these stimulatory signals leads to a state of immune tolerance where T cells become inactive (38). In fact, robust anti-tumor immune response is governed by the capacity of mDCs to polarize T cells toward Th1/CTL response (14, 39). However, tumors tend to escape immune recognition and response by abrogating DC activation via p-STAT3 induction (8). This immunosuppressive/regulatory effect, caused by tumors, imposes a state of immunological paralysis and potentiates cancer progression (40). Therefore, inhibition of STAT3 signal in tumor-exposed DCs was shown to be of critical significance to break tumor-mediated immune tolerance and induce robust anti-tumor immune response (16).

Efficient inhibition of STAT3 signaling pathway in DCs was sought by the employment of various modalities such as pharmacological inhibition by AG490 and JSI-124 (17, 41). However, this approach is not suitable for clinical practice

due to the non-specific nature of these agents (22). The inhibitory effect of AG490 on JAK/STAT3 pathway has been recently shown to be through the inhibition of gp130 expression, which is the signaling chain in IL-6 receptor complex at which JAK docks to phosphorylate STAT3 (42). Other members of IL-6 family: cardiotrophin 1 (CT-1), leukemia inhibitory factor (LIF), ciliary neurotrophic factor (CNTF), oncostatin M (OSM), and IL-11, depend on gp130 for signal transduction (43). Therefore, the loss of gp130 basically eliminates multiple physiologically-critical events. Similarly, JSI-124 was shown to profoundly affect actin cytoskeleton via STAT3-independent mechanism at effective JAK2/STAT3 inhibitory concentration in both cancerous and non-cancerous cells (41). This non-specific action may highly account for JSI-124 cytotoxic effect. We have previously shown that PLGA NPs of chemically-conjugated JSI-124 can indeed reduce p-STAT3 level in B16-CM exposed DCs, and mitigate the deleterious effect of JSI-124 (44). Although the study provided important proof-of-concept results, we were interested in investigating a more clinically-relevant strategy. Therefore, we employed anti-STAT3 siRNA as a specific modality for STAT3 inhibition in B16-CM-exposed DCs.

We were able to load pre-complexed siRNA with PEI and PEI-StA in PLGA NPs i.e. PLGA-P and PLGA-PS, respectively. Characterization of PLGA-P and PLGA-PS for surface morphology demonstrated the formation of nanospheres of smooth surface and in a size range comparable to the hydrodynamic diameter measured by DLS that showed unimodal distributions for all NPs (Figure 5.2). Furthermore, despite the known cationic charge of PEI, the anionic surface charge

seen on PLGA-P and PLGA-PS surface could mostly be a covering effect due to the anionic density of the carboxylic-acid terminated PLGA. Masking the dense cationic charge in PLGA NPs may be the reason behind a significant reduction in the non-specific toxicity of PEI and PEI-StA polyplexes towards DCs when incorporated in PLGA NPs (Figure 5.5). The E.E. and loading of siRNA by PLGA-PS was significantly higher than that of PLGA-P (Table 1). This observation can be attributed to the intrinsically higher binding capacity of PEI-StA toward siRNA as compared to PEI (27).

The release profile indicates that complete siRNA release is dependent on PLGA NP degradation (Figure 5.4A). Moreover, the noted 40% burst release is mainly due to presence of siRNA polyplexes on or near the surfaces of PLGA NPs. Furthermore, since PEI and PEI-StA are relatively more hydrophilic compared to PLGA, they may induce formation of aqueous channels in the PLGA matrix (45, 46). The channels could then serve as outlets for siRNA diffusion. Such effect was reported with the release of oligonucleotides from PEI-containing PLGA microspheres, which was correlated with the amount of PEI added to the aqueous phase (45). Others have also reported similar pattern of siRNA release from PLGA NPs that incorporates PEI (46). We also noticed that siRNA release from PLGA-PS becomes faster than its release from PLGA-P, especially at the end of the release profile (Figure 5.4A). The reason behind this could be the higher electrostatic interaction between PEI polyplexes and PLGA than that of PEI-StA, which drives PEI polyplexes to remain attached to the PLGA matrix. This is an important observation as it implies that we can control the release of

siRNA by modifying the structure of the polyplexes. The faster release of siRNA from PLGA-PS may also be contributed to the higher loading of PEI-StA compared to PEI polyplexes in PLGA NPs.

PLGA-P and PLGA-PS were found not toxic to DCs compared to the cationic polyplexes alone (Figure 5.5). We attribute the significant reduction in PEI toxicity after incorporation into PLGA NPs to two factors: (i) participation of PLGA in preventing the surface exposure of the cationic charge as evidenced by our zeta potential analysis (Figure 5.2B); thus prevention of PEI-induced membrane disintegration, and (ii) the intrinsic safety of PLGA NPs since PLGA is an FDA-approved biodegradable polymer that had been widely used in several controlled-release drug products for human use and as a delivery system for DC (47, 48). Although it is arguable that the sustained release effect dictated by PLGA system may lower PEI toxicity below detection by reducing the exposure rate of PEI to the cells, we do not anticipate this profile to be the reason behind the noticed mitigation in PEI toxicity. In fact, the *in vitro* release pattern might not be exactly mirrored after cellular internalization where the NPs are exposed to variable pH ranges in different intracellular compartments, which would influence the release pattern. We argue that the considerable concealment of the cationic charge within the PLGA particles and the unique ability of PLGA NPs for endosomal escape (discussed below) could prevent membrane disintegration and the release of the cytotoxic lysosomal contents into the cytoplasm. Additionally, the improvement of PEI toxicity profile by incorporation into PLGA system has been also shown on other cell types indicating the reliability of the approach (30).

Moreover, it has been documented that PLGA particles did not significantly affect the viability of DCs even when DCs were loaded with large number of PLGA particles and even during PLGA degradation where acidic byproducts are formed (49).

The constructed NPs were successfully internalized by DCs (Figure 5.6). The fact that these particles fit in the preferable size for DC endocytosis (Figure 5.2) is one reason for the high intracellular signal (34). Moreover, it has been argued that the presence of PEI in the polymeric matrix of PLGA facilitates cellular uptake and enhances the transfection efficiency to some extent (30). Nonetheless, since the uptake study was performed on pure DC culture, it is hard to estimate the effectiveness of these NPs in preferentially targeting DCs. Determination of NPs uptake by DCs in the presence of other cells or *in vivo* studies is needed for clearer and more conclusive assessment. Our localization studies confirm the presence of our formulations in the endosomal compartments as indicated by the orange color resulting from the co-localization of FAM-siRNA/PLGA-P and PLGA-PS with the LysoTracker Red. Moreover, green fluorescence of siRNA was also detected in the cytoplasmic compartment, which is an indicative of an endosomal escape property of the particulate systems. A combination of two phenomena might be responsible for this property: (i) proton-sponge effect provided by the PEI system, and (ii) surface cationization of PLGA NPs in the acidic pH of secondary endosomes (50). The latter was also confirmed in PLGA NPs internalized by DCs, where endosomal escape mediated cross-presentation of exogenous antigens (51). Surface cationization of PLGA in acidic

pH was attributed to the transfer of excess protons from the bulk liquid to the NP surface or attributed to hydrogen bonding between carboxyl groups of PLGA and hydronium molecules in the acidic pH (50, 52).

The results of cell culture study indicates: (i) phenotypical and functional maturation of B16-CM-exposed DCs can be restored, *in vitro*, after DC incubation with anti-STAT3 siRNA PLGA-P and PLGA-PS. (ii) The level of DC activation is correlated with the level of STAT3 knockdown (Figures 5.7A and 5.7B). We show that DC alloreactivity (Figure 5.7D) was noticed only following STAT3 knockdown and the induction of the costimulatory molecules expression CD86 (Figure 5.7B). This is an important observation since it proves that siRNA was successfully unpacked at the site of action and encountered its cytoplasmic target. The CD86 on DC surface is known to interact with CD28. In turn, T cells provide stimulatory signal to DCs via CD40/CD40-ligand (CD40L) interaction. Such interaction is beneficial for both DCs and T cells where stimulation of CD28 stabilizes CD40L on T cells and stimulation of CD40 on DCs increases their expression of CD86 molecules (53, 54). Moreover, the remarkable secretion of the proinflammatory cytokine TNF- α from DCs upon STAT3 knockdown provides another evidence of restoring DCs function. When secreted by activated DCs, TNF- α was demonstrated to induce T cell activation and polarize T cells toward Th1/CTL response (55, 56). We attribute the collective picture of DC activation to STAT3 knockdown by siRNA and not merely to NP uptake by DCs. Endocytosis-induced DC maturation is debatable in literature and evidence that either confirm (57) or contradict (50, 58) this notion has been documented with

PLGA NPs. We take the latter position since our study show no effect of scrambled-siRNA NPs (PLGA-P-sc or PLGA-PS-sc) in restoring DC maturation, which strongly support the specificity of our approach where STAT3 knockdown is required for the observed effect. In fact, STAT3 inhibition in DCs was associated with the maturation process even without tumor exposure (17). Furthermore, the superior effect of PLGA-PS over PLGA-P in mediating siRNA silencing is most likely due to the ability of PEI-StA to protect siRNA from nuclease degradation to higher extent than PEI as we have previously demonstrated (27). However, using the proposed approach, *in vivo* studies for siRNA-mediated STAT3 knockdown in DCs are needed now to better evaluated the therapeutic potential of this formulation.

5.5 REFERENCES

1. Banchereau J, Steinman RM. Dendritic cells and the control of immunity. *Nature*. 1998 Mar 19;392(6673):245-52.
2. Stockwin LH, McGonagle D, Martin IG, Blair GE. Dendritic cells: immunological sentinels with a central role in health and disease. *Immunol Cell Biol*. 2000 Apr;78(2):91-102.
3. Shortman K, Liu YJ. Mouse and human dendritic cell subtypes. *Nat Rev Immunol*. 2002 Mar;2(3):151-61.
4. Steinman RM, Banchereau J. Taking dendritic cells into medicine. *Nature*. 2007 Sep 27;449(7161):419-26.
5. Steinman RM. Lasker Basic Medical Research Award. Dendritic cells: versatile controllers of the immune system. *Nat Med*. 2007 Oct;13(10):1155-9.
6. Kalinski P, Hilkens CM, Wierenga EA, Kapsenberg ML. T-cell priming by type-1 and type-2 polarized dendritic cells: the concept of a third signal. *Immunol Today*. 1999 Dec;20(12):561-7.
7. Trombetta ES, Mellman I. Cell biology of antigen processing in vitro and in vivo. *Annu Rev Immunol*. 2005;23:975-1028.
8. Yang L, Carbone DP. Tumor-host immune interactions and dendritic cell dysfunction. *Adv Cancer Res*. 2004;92:13-27.
9. Gabrilovich D. Mechanisms and functional significance of tumour-induced dendritic-cell defects. *Nat Rev Immunol*. 2004 Dec;4(12):941-52.
10. Turkson J, Jove R. STAT proteins: novel molecular targets for cancer drug discovery. *Oncogene*. 2000 Dec 27;19(56):6613-26.
11. Yu H, Kortylewski M, Pardoll D. Crosstalk between cancer and immune cells: role of STAT3 in the tumour microenvironment. *Nat Rev Immunol*. 2007 Jan;7(1):41-51.
12. Gabrilovich DI, Chen HL, Girgis KR, Cunningham HT, Meny GM, Nadaf S, et al. Production of vascular endothelial growth factor by human tumors inhibits the functional maturation of dendritic cells. *Nat Med*. 1996 Oct;2(10):1096-103.
13. Sumimoto H, Imabayashi F, Iwata T, Kawakami Y. The BRAF-MAPK signaling pathway is essential for cancer-immune evasion in human melanoma cells. *J Exp Med*. 2006 Jul 10;203(7):1651-6.
14. Kennedy R, Celis E. Multiple roles for CD4+ T cells in anti-tumor immune responses. *Immunol Rev*. 2008 Apr;222:129-44.
15. Park SJ, Nakagawa T, Kitamura H, Atsumi T, Kamon H, Sawa S, et al. IL-6 regulates in vivo dendritic cell differentiation through STAT3 activation. *J Immunol*. 2004 Sep 15;173(6):3844-54.
16. Cheng F, Wang HW, Cuenca A, Huang M, Ghansah T, Brayer J, et al. A critical role for Stat3 signaling in immune tolerance. *Immunity*. 2003 Sep;19(3):425-36.
17. Nefedova Y, Cheng P, Gilkes D, Blaskovich M, Beg AA, Sebt SM, et al. Activation of dendritic cells via inhibition of Jak2/STAT3 signaling. *J Immunol*. 2005 Oct 1;175(7):4338-46.

18. Imada K, Leonard WJ. The Jak-STAT pathway. *Mol Immunol*. 2000 Jan-Feb;37(1-2):1-11.
19. Kortylewski M, Yu H. Role of Stat3 in suppressing anti-tumor immunity. *Curr Opin Immunol*. 2008 Apr;20(2):228-33.
20. Vicari AP, Caux C, Trinchieri G. Tumour escape from immune surveillance through dendritic cell inactivation. *Semin Cancer Biol*. 2002 Feb;12(1):33-42.
21. Zou W. Immunosuppressive networks in the tumour environment and their therapeutic relevance. *Nat Rev Cancer*. 2005 Apr;5(4):263-74.
22. Yue P, Turkson J. Targeting STAT3 in cancer: how successful are we? *Expert Opin Investig Drugs*. 2009 Jan;18(1):45-56.
23. Cejka D, Losert D, Wacheck V. Short interfering RNA (siRNA): tool or therapeutic? *Clin Sci (Lond)*. 2006 Jan;110(1):47-58.
24. Kawasaki H, Taira K, Morris KV. siRNA induced transcriptional gene silencing in mammalian cells. *Cell Cycle*. 2005 Mar;4(3):442-8.
25. Hede K. Blocking cancer with RNA interference moves toward the clinic. *J Natl Cancer Inst*. 2005 May 4;97(9):626-8.
26. Thomas M, Lu JJ, Chen J, Klibanov AM. Non-viral siRNA delivery to the lung. *Adv Drug Deliv Rev*. 2007 Mar 30;59(2-3):124-33.
27. Alshamsan A, Haddadi A, Incani V, Samuel J, Lavasanifar A, Uludag H. Formulation and delivery of siRNA by oleic acid and stearic acid modified polyethylenimine. *Mol Pharm*. 2009 Jan-Feb;6(1):121-33.
28. Alshamsan A, Hamdy S, Samuel J, El-Kadi AO, Lavasanifar A, Uludag H. The induction of tumor apoptosis in B16 melanoma following STAT3 siRNA delivery with a lipid-substituted polyethylenimine. *Biomaterials*. 2010 Feb;31(6):1420-8.
29. Alshamsan A, Haddadi A, Hamdy S, Samuel J, El-Kadi AO, Uludag H, et al. Down-Modulation of STAT3 in B16 Melanoma by siRNA/Lipid-Substituted Polyethylenimine Complexes Induces Bystander Immune Response in vitro and in vivo. *Cancer*. 2010. (submitted).
30. Zhang XQ, Intra J, Salem AK. Comparative study of poly (lactic-co-glycolic acid)-poly ethyleneimine-plasmid DNA microparticles prepared using double emulsion methods. *J Microencapsul*. 2008 Feb;25(1):1-12.
31. Lutz MB, Kukutsch N, Ogilvie AL, Rossner S, Koch F, Romani N, et al. An advanced culture method for generating large quantities of highly pure dendritic cells from mouse bone marrow. *J Immunol Methods*. 1999 Feb 1;223(1):77-92.
32. Incani V, Tunis E, Clements BA, Olson C, Kucharski C, Lavasanifar A, et al. Palmitic acid substitution on cationic polymers for effective delivery of plasmid DNA to bone marrow stromal cells. *J Biomed Mater Res A*. 2007 May;81(2):493-504.
33. Alshamsan A, Hamdy S, Das S, Lavasanifar A, Samuel J, El-Kadi AO. Bone Marrow Derived Dendritic Cells are More Suitable than Dendritic Cell Line DC2.4 to Study Tumor-Mediated Suppression of DC Maturation through STAT3 Hyperactivation. *J Pharm Pharmaceut Sci*. 2010;13(1):21-6.

34. Elamanchili P, Diwan M, Cao M, Samuel J. Characterization of poly(D,L-lactic-co-glycolic acid) based nanoparticulate system for enhanced delivery of antigens to dendritic cells. *Vaccine*. 2004 Jun 23;22(19):2406-12.
35. Buettner R, Mora LB, Jove R. Activated STAT Signaling in Human Tumors Provides Novel Molecular Targets for Therapeutic Intervention. *Clin Cancer Res*. 2002;8:945-54.
36. Hirano T, Ishihara K, Hibi M. Roles of STAT3 in mediating the cell growth, differentiation and survival signals relayed through the IL-6 family of cytokine receptors. *Oncogene*. 2000 May 15;19(21):2548-56.
37. Yu H, Pardoll D, Jove R. STATs in cancer inflammation and immunity: a leading role for STAT3. *Nat Rev Cancer*. 2009 Nov;9(11):798-809.
38. Mueller DL. Mechanisms maintaining peripheral tolerance. *Nat Immunol*. 2010 Jan;11(1):21-7.
39. Knutson KL, Disis ML. Tumor antigen-specific T helper cells in cancer immunity and immunotherapy. *Cancer Immunol Immunother*. 2005 Aug;54(8):721-8.
40. Chaput N, Conforti R, Viaud S, Spatz A, Zitvogel L. The Janus face of dendritic cells in cancer. *Oncogene*. 2008 Oct 6;27(45):5920-31.
41. Graness A, Poli V, Goppelt-Strube M. STAT3-independent inhibition of lysophosphatidic acid-mediated upregulation of connective tissue growth factor (CTGF) by cucurbitacin I. *Biochem Pharmacol*. 2006 Jun 28;72(1):32-41.
42. Seo IA, Lee HK, Shin YK, Lee SH, Seo SY, Park JW, et al. Janus Kinase 2 Inhibitor AG490 Inhibits the STAT3 Signaling Pathway by Suppressing Protein Translation of gp130. *Korean J Physiol Pharmacol*. 2009 Apr;13(2):131-8.
43. Kishimoto T, Akira S, Narazaki M, Taga T. Interleukin-6 family of cytokines and gp130. *Blood*. 1995 Aug 15;86(4):1243-54.
44. Molavi O, Mahmud A, Hamdy S, Hung R, Samuel J, Lai R, et al. Development of a poly(D,L-lactic-co-glycolic acid) (PLGA) nanoparticle formulation of STAT3 inhibitor JSI-124: Implication for cancer immunotherapy. *Mol Pharm*. 2010 Apr 5;7(2):364-74.
45. De Rosa G, Quaglia F, La Rotonda MI, Appel M, Alphandary H, Fattal E. Poly(lactide-co-glycolide) microspheres for the controlled release of oligonucleotide/polyethylenimine complexes. *J Pharm Sci*. 2002 Mar;91(3):790-9.
46. Patil YB, Swaminathan SK, Sadhukha T, Ma L, Panyam J. The use of nanoparticle-mediated targeted gene silencing and drug delivery to overcome tumor drug resistance. *Biomaterials*. 2010 Jan;31(2):358-65.
47. Bala I, Hariharan S, Kumar MN. PLGA nanoparticles in drug delivery: the state of the art. *Crit Rev Ther Drug Carrier Syst*. 2004;21(5):387-422.
48. Waeckerle-Men Y, Groettrup M. PLGA microspheres for improved antigen delivery to dendritic cells as cellular vaccines. *Adv Drug Deliv Rev*. 2005 Jan 10;57(3):475-82.
49. Walter E, Dreher D, Kok M, Thiele L, Kiama SG, Gehr P, et al. Hydrophilic poly(DL-lactide-co-glycolide) microspheres for the delivery of DNA to human-derived macrophages and dendritic cells. *J Control Release*. 2001 Sep 11;76(1-2):149-68.

50. Panyam J, Zhou WZ, Prabha S, Sahoo SK, Labhasetwar V. Rapid endo-lysosomal escape of poly(DL-lactide-co-glycolide) nanoparticles: implications for drug and gene delivery. *Faseb J.* 2002 Aug;16(10):1217-26.
51. Shen H, Ackerman AL, Cody V, Giodini A, Hinson ER, Cresswell P, et al. Enhanced and prolonged cross-presentation following endosomal escape of exogenous antigens encapsulated in biodegradable nanoparticles. *Immunology.* 2006 Jan;117(1):78-88.
52. Makino K, Ohshima H, Kondo T. Transfer of protons from bulk solution to the surface of poly(L-lactide) microcapsules. *J Microencapsul.* 1986 Jul-Sep;3(3):195-202.
53. Johnson-Leger C, Christensen J, Klaus GG. CD28 co-stimulation stabilizes the expression of the CD40 ligand on T cells. *Int Immunol.* 1998 Aug;10(8):1083-91.
54. Yang Y, Wilson JM. CD40 ligand-dependent T cell activation: requirement of B7-CD28 signaling through CD40. *Science.* 1996 Sep 27;273(5283):1862-4.
55. Brunner C, Seiderer J, Schlamp A, Bidlingmaier M, Eigler A, Haimerl W, et al. Enhanced dendritic cell maturation by TNF-alpha or cytidine-phosphate-guanosine DNA drives T cell activation in vitro and therapeutic anti-tumor immune responses in vivo. *J Immunol.* 2000 Dec 1;165(11):6278-86.
56. Mariotti S, Sargentini V, Marcantonio C, Todero E, Teloni R, Gagliardi MC, et al. T-cell-mediated and antigen-dependent differentiation of human monocyte into different dendritic cell subsets: a feedback control of Th1/Th2 responses. *Faseb J.* 2008 Sep;22(9):3370-9.
57. Yoshida M, Babensee JE. Molecular aspects of microparticle phagocytosis by dendritic cells. *J Biomater Sci Polym Ed.* 2006;17(8):893-907.
58. Waeckerle-Men Y, Scandella E, Uetz-Von Allmen E, Ludewig B, Gillesen S, Merkle HP, et al. Phenotype and functional analysis of human monocyte-derived dendritic cells loaded with biodegradable poly(lactide-co-glycolide) microspheres for immunotherapy. *J Immunol Methods.* 2004 Apr;287(1-2):109-24.

CHAPTER SIX

GENERAL DISCUSSION, CONCLUSIONS, AND FUTURE DIRECTIONS

6.1 GENERAL DISCUSSION

The underlying mechanism(s) for cellular transformation and cancer progression is/are still debatable, and the therapeutic approaches currently used are still ineffective to completely eradicate the disease. According to the hypothesis of cancer immunoediting, cancer progression undergoes three phases. An elimination phase, where immune cells recognize and kill transformed cells; followed by a long equilibrium phase, where tumor cells persist but remain dormant against the immune pressure; and lastly an escape phase, where the balance is tilted toward tumor progression as a result of immune exhaustion or inhibition (1). In this process, STAT3 is an important player since it is involved in different scenarios of cancer immune escape mediated by both intrinsic and extrinsic factors, as well as sustaining tumor survival and proliferation. This is because STAT3 mediates the production of TDFs that are responsible for cancer progression and immunosuppression. These TDFs further induce STAT3 activation in multiple components of the immune system leading to weakened or abolished anti-tumor immunity. Therefore, STAT3 disruption is critical to induce tumor-killing effect and to reactive anti-tumor immune response.

The ultimate goal of this research project was to develop strategies with cancer-therapy potentials based on disrupting the abnormally-activated STAT3 in cancer cells and in cancer-exposed DCs. The choice of these two targets was based on the compelling evidence that STAT3 mediates a cross talk between cancer and immune cells (2-4). In this research we used B16.F10 murine

melanoma model since it has been shown that STAT3 targeting in melanoma tumor models leads to the induction of tumor regression (5), inhibition of angiogenesis (6), prevention of metastasis (7), as well as activation of immune response (5, 8). Because of the abundance of an arsenal of STAT3 inhibitors, which vary in their mechanisms of action and sub-cellular targets, we wanted to develop a modality that is as specific, efficient, and safe as possible. This is not an easy task because of the drawbacks associated with each modality involved in STAT3 disruption (discussed in Chapter 1). Since the unwanted and toxic effects of each agent are attributed to its degree of specificity, we decided to apply RNAi because this is the most specific modality to our knowledge if disease-causing proteins are to be targeted at the mRNA level (9, 10). Based on our knowledge of STAT3 role in cancer progression, we set three hypotheses for our research. First, STAT3 knockdown by siRNA in B16 cells leads to apoptosis *in vitro* and tumor regression *in vivo*; second, down-modulation of STAT3 by siRNA in tumor cells induces bystander immune response *in vitro* and *in vivo*; and third, STAT3 knockdown by siRNA induces phenotypic maturation and functional activation tumor-exposed DC. In order to test these hypotheses, we designed our experimental approach to meet specific objectives as follows.

Our first objective was to develop an efficient delivery system for siRNA (Chapter 2). As previously documented, the clinical applications of siRNA are hindered by serious, but virtually controllable, obstacles that we tried to address in this thesis. These hurdles (summarized in Figure 6.1) are mainly in regard of two

points: siRNA stability in serum and successful encounter of the target mRNA of interest (11). To circumvent such barriers that significantly diminish therapeutic potentials of siRNA, we focused on designing and evaluating delivery systems that would protect siRNA from degradation, deliver it successfully to the site of action, and improve its biological function.

Our siRNA delivery strategy was based on attaching free-fatty acids to the backbone of PEI (25 kDa): the gold standard for gene delivery (12). The rationale behind the fatty acids attachment was initially to enhance cellular uptake of exogenous nucleic acids through hydrophobic interaction with the phospholipid bilayer component of the cell membrane, and through other biomimetic mechanisms e.g. facilitated intracellular trafficking (13, 14). However, the introduction of lipid groups was found to be beneficial for siRNA delivery at multiple fronts: entrapment, stability, and delivery.

The attachment of fatty acids at different substitution levels, in most cases, enhanced the capacity of PEI to bind with siRNA, but with significant variability among the lipid-modified derivatives (Chapter 2, Figure 2.1) (15). Although we were not able to pinpoint a specific reason for this erratic response, we used an empirical approach as a screening method to choose the most effective lipid-modified PEI in siRNA entrapment. Nevertheless, based on our observations, we considered three factors to be possible participants to fatty-acid contribution in siRNA binding capacity of the derived PEIs. These factors are: fatty acid composition, chain length, and level of substitution.

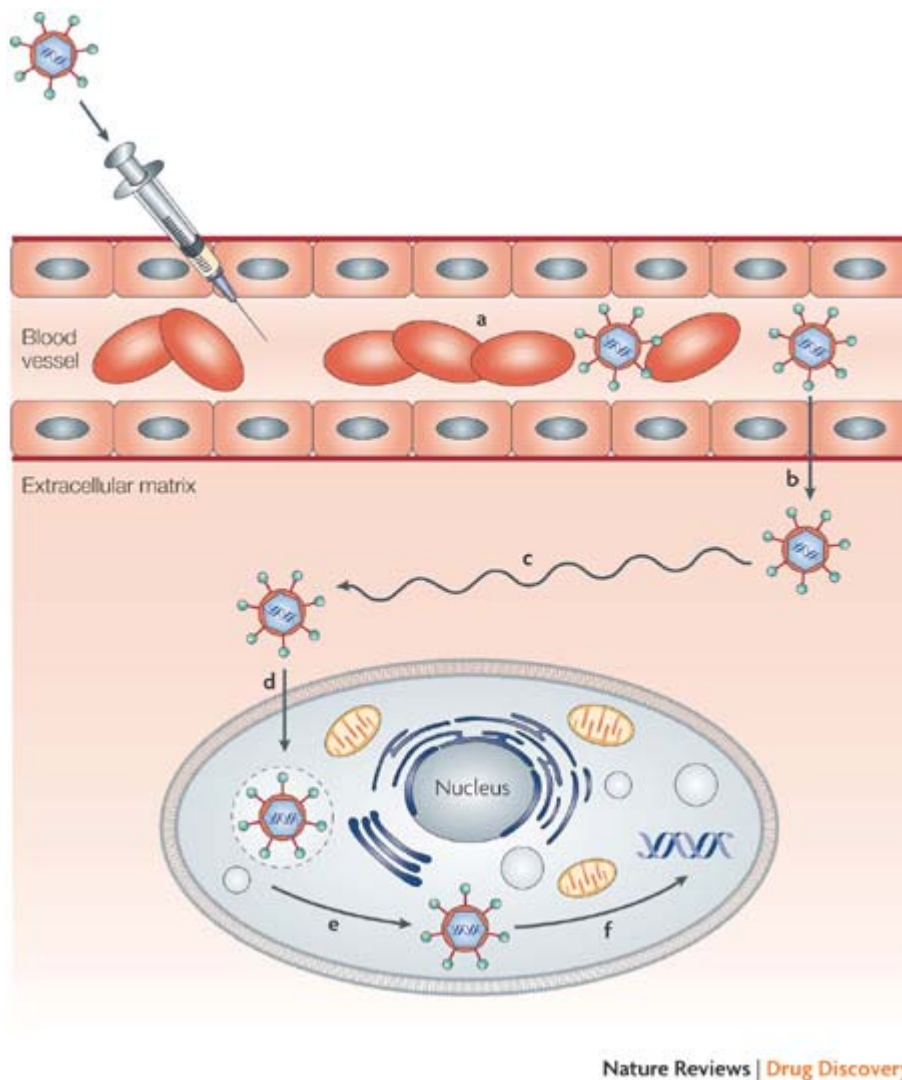


Figure 6.1 Adopted from (11). Physiological barriers to the systemic delivery of siRNA nanoparticles. An injected nanoparticle must avoid filtration, phagocytosis and degradation in the bloodstream (a); be transported across the vascular endothelial barrier (b); diffuse through the extracellular matrix (c); be taken up into the cell (d); escape the endosome (e); and unpackage and release the siRNA to the RNAi machinery (f).

Looking at the most potent fatty acid derivative worked in our hand, PEI-StA2, we can inductively suggest that an optimum point for maximal binding efficiency requires the attachment of saturated fatty acid that is not less than 18-carbon long. Of course we cannot stretch this statement into a conclusion; however, the evidence collected from direct comparison of the PEI derivatives compositions supports our argument. We have two saturated fatty-acid derivatives in this library, stearic acid (18 carbons) and caprylic acid (8 carbons). To reach comparable capacities, the substitution level of CA was over 10-times higher than StA (Chapter 2, Table 2.1) (15). This indicates the importance of the fatty acid chain length. In fact, in a study targeting hepatocytes with fatty-acid conjugated siRNA, the authors stated that fatty acids of chain lengths less than 18 carbons did not induce gene knockdown (16). Moreover, comparing the lipid composition of the three 18-carbon fatty acids in our library, we rank the binding efficiency of the derived PEIs as follows: stearic acid (saturated) > oleic acid (monounsaturated) > linoleic acid (polyunsaturated). This indicates that the presence of more double bonds throughout the fatty acid structure is counterproductive in spite of the substitution level. This is probably due to the increased rigidity of the three-dimensional structure dictated by the double bonds, as discussed in Chapter 2 (15). We proposed that the flexibility of StA could allow the molecule to flex inward and participate in physical encapsulation of siRNA on top of the electrostatic interaction with PEI (15). However, although counterintuitive, we found that higher substitution level of StA results in less siRNA binding capacity as compared to that of the lower substitution counterpart. To explain this paradox,

we find it plausible to argue that StA could interfere with the charge distribution in PEI and possibly mask some spots for electrostatic interaction with siRNA. Taken that siRNA entrapment by PEI-StA is a combination of electrostatic interaction with PEI backbone and physical loading by StA chains, the content of StA in the polymeric network could have an influence on either factors, where the net result of siRNA entrapment is ultimately affected. We support this argument by the inconsistency in zeta potential measurements at different polymer/siRNA ratio, where only polyplexes of undecorated PEI showed consistent increment in zeta potential but not the fatty-acid modified PEIs (Chapter 2, Figure 2.2) (15). Therefore, more physicochemical studies must be done to determine how these factors could contribute to siRNA binding/loading.

Another advantage of StA attachment is the addition of relative hydrophobicity to the polyplexes. This translated, along with intrinsic binding efficiency, into higher encapsulation of siRNA into PLGA NPs when DC targeting was intended (Chapter 5). Moreover, the hydrophobicity provided by PEI-StA may be one reason behind the higher cellular uptake by B16 melanoma cells (Chapter 2, Figure 2.4), especially at lower complexes concentration (15). As a paradigm, more cell uptake should translate into higher biological activity (17). Many have shown that addition of lipid to PEI chain enhances cell uptake of nucleic acids and their biological functions (18-21). Nevertheless, higher cellular uptake as a result of increased hydrophobicity is not the only reason behind the increased siRNA silencing efficiency noticed with PEI-StA system (15, 22, 23). A very important factor is the enhanced stability of siRNA in serum.

As we have previously shown, siRNA is very labile in serum (Chapter 2, Figure 2.3) (15). Given that siRNA is prone to nucleases degradation at multiple steps before encountering its target mRNA (24), we argue that the improved siRNA stability profile seen with PEI-StA is probably the major determinant in the noticed superiority of PEI-StA over PEI in mediating siRNA silencing. The orientation of StA in the polyplex matrix probably created a steric hindrance to serum nucleases. Adding this to the higher siRNA loading, PEI-StA could transfect cells with more functional siRNA molecules that are well protected (Figure 6.2). The collective contribution of StA, was translated in our optimization studies into more silencing effect of a biological target in B16.F10 cells (integrin α_v) (Chapter 2, Figure 2.6) (15).

After this step, our next objective was to determine the clinical relevance of our strategy by targeting STAT3, which is a key protein in cancer progression and immune escape (25), in B16.F10 murine melanoma cells (Chapter 3). To prove the efficacy of this system for STAT3 knockdown in cancer cells *in vitro* and *in vivo*, and to study the outcomes of STAT3 knockdown to evaluate the clinical relevance of the approach, we targeted B16 cells with STAT3 siRNA in PEI or PEI-StA. We found an association between cellular uptake level and siRNA silencing efficacy (Chapter 3) (23). However, we suggest that the improved serum stability provided by PEI-StA is the main reason for the profound increase in siRNA potency when delivered by PEI-StA as compared to PEI (23). Although we have not confirmed this, it is highly likely that PEI-StA may also

provide a prolonged intracellular effect as a result of higher entrapment efficiency of siRNA and low nuclease degradation. Therefore, such system, if optimized, could potentially overcome one major drawback of siRNA, which is the temporary nature of treatment. We tried to overcome this issue by administering repetitive doses of the polyplexes where we see remarkable anti-cancer effect *in vitro* and *in vivo* (Chapter 3) (23). However, optimizing the lipid content to develop a prolonged effect of the single dose would be very significant clinically. Since it is known that many cancer cells, including melanoma, depend on STAT3 for survival, prolonged STAT3 knockdown could switch the balance toward tumor eradication response (26). Our *in vitro* results were in agreement with the *in vivo* results where PEI-StA mediated more silencing effect of STAT3 siRNA than that of PEI. We attribute this to the higher cellular association of PEI-StA polyplexes as well as protective effect to siRNA from serum nucleases. These effects resulted in the reduction of the dose needed to mediate STAT3 silencing to as low as 25 nM *in vitro* (Chapter 3). In addition, we noticed that by a multiple-administration schedule, significant induction of B16 apoptosis takes place after STAT3 silencing by siRNA polyplexes *in vitro* and *in vivo* compared to scrambled siRNA complexes and saline-treated controls after 4 daily doses via i.t. route. This is also a confirmatory evidence for the temporary nature of siRNA intervention, which signify the need for the development of delivery systems with prolonged effect. Moreover, by these studies, we also validated the pivotal role of STAT3 in cancer progression and its potential as a target for cancer therapy. We showed a strong correlation between STAT3 silencing and cancer cell death *in*

vitro and *in vivo* that was proportional to the level of STAT3 knockdown, and specific to STAT3 inhibition since scrambled siRNA polyplexes did not induce any noticeable STAT3 silencing nor cytotoxicity on B16 cells (Chapter 3). Although this is an evidence for the specificity of our approach, it does not completely overrule possible non-specific cytotoxicity when other cell types are intended for targeting. Nonetheless, at least in the studied model, the observed results indicate clinical relevance since they suggest a specificity of the approach especially that mice treated scrambled-siRNA polyplexes did not exhibit any noticeable signs of toxicity. Furthermore, beside the direct correlation between STAT3 knockdown and cancer cell death, we also noticed changes in the tumor microenvironment particularly in the cytokine profiles, angiogenesis, and immune response. We have seen an induction in pro-apoptotic inflammatory cytokines in tumor microenvironment (22, 23). This switch toward more tumor-suppressing inflammatory response has a direct cancer-killing effect owing to the role of STAT3 in anti-apoptotic proteins overexpression (27), as well as indirect anti-tumor effect by possible triggering of immune cells activation (25). Additionally, we have seen a reduction in VEGF expression following STAT3 knockdown (Chapter 3) (23). This effect, as well, leads to cancer cell death directly since VEGFR has a role in tumor progression (28), and indirectly through anti-angiogenic effect (29). From this piece of information we conclude that the inhibition of STAT3 activity is of significant importance as a cancer therapy strategy since VEGF gene expression was shown to be upregulated by STAT3 (30).

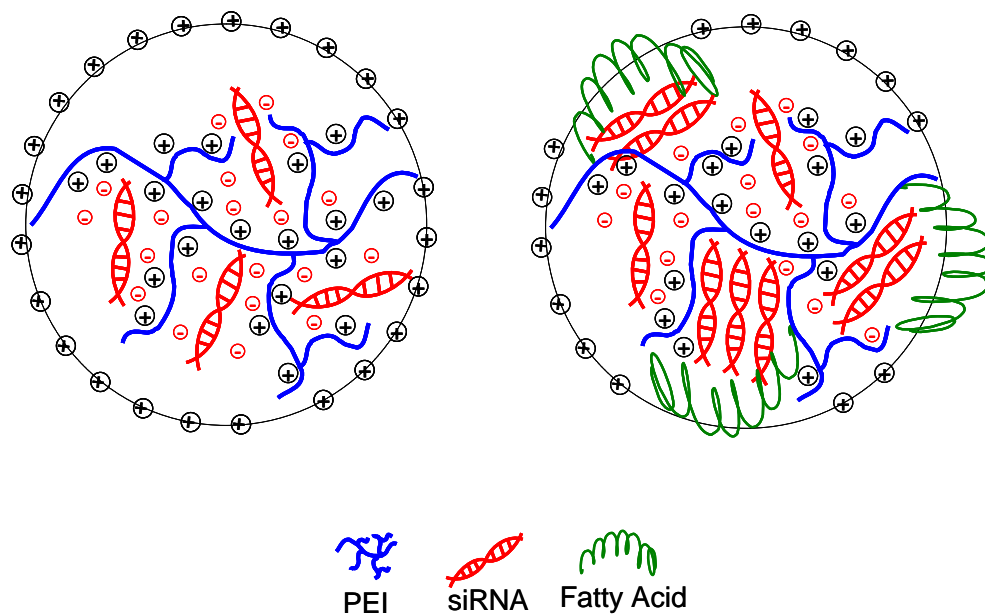


Figure 6.2 Possible roles of fatty acid chains in enhancing siRNA properties. The flexibility of fatty acid chains could allow for more encapsulation of siRNA and forces the molecule to remain relatively closer to the core. This adds a protective effect from serum degradation by preventing the access of nucleases to siRNA.

We also confirmed the observation that STAT3 inhibition in tumor cells leads to induction in IL-6 expression, where anti-tumor effect is amplified probably due to the IL-6-mediated STAT1 activation (Chapter 3). The activation of STAT1 by IL-6 is hindered in cancer cells due to STAT3 competition on the docking site on the gp130 chain (the signaling chain of the IL-6R), where STAT3 signal prevails. In absence of STAT3, however, STAT1 signal take place and leads to IFN- γ like effect on tumor cells (31).

From here, our next avenue was to determine whether STAT3 knockdown in tumor cells induces bystander immune response (Chapter 4). To evaluate this objective, we analyzed the tumor microenvironment for immune cells infiltration and activation, cytokine levels, as well as functionality of splenocytes from tumor-bearing mice before and after STAT3 knockdown. We noticed a creation of immune response suggesting a Th1 type response evidenced by remarkable infiltration of innate and adaptive immune cells in tumor mass as well as activation of tumor-exposed DCs *in vivo* following intratumoral STAT3 knockdown (Chapter 4) (22). Here also we noticed that the collective anti-tumor response was correlated to the degree of STAT3 knockdown by siRNA. In the CD3⁺ cell population studied in isolated tumors, the superiority of PEI-StA treatment was noted by the induced infiltration of CD4⁺ T cells, CD8⁺ T cells, and NKT cells. This is also indicative to the role of the delivery system in enhancing siRNA potency. In this regard, the effect is specific to STAT3 knockdown and not due to non-specific inflammatory responses since significant difference was seen

between STAT3 knockdown groups and scrambled-siRNA formulations, especially that IFN- γ secretion was only induced in STAT3-knockdown groups. Moreover, the T cells response seen is corroborated by the picture of DC activation following STAT3 knockdown in tumor, which is broken into three segments. First, we observed a significant infiltration of CD11c⁺ DCs in tumor tissue. Second, these DCs were mature as evidenced by CD86 and CD40 expression (Chapter 4 Figure 4.5B) as well as the high levels of Th1-type cytokines IL-12 and TNF- α (Chapter 4 Figure 4.5C). The third segment is the alloreactivity of DCs with Balb/c T cells. The alloreactivity of splenocytes isolated from tumor-bearing mice that were treated with STAT3-siRNA polyplexes indicates bystander immune response. Here also we noticed an advantage for PEI-StA over PEI, which is relative to the degree of STAT3 knockdown mediated by the polyplexes. This interplay created between DCs and T cells indicates the high potential of STAT3 knockdown in cancer immunotherapy, and also revalidates the role of STAT3 as a cross-talk mediator between cancer and immune cells.

In fact, those collective factors i.e. proinflammatory cytokines, anti-angiogenic effect, and cellular immune response, might have a significant role in the noticed tumor regression, (Chapter 3, Figure 3.5) and (Chapter 4, Figure 4.5) (22, 23), along with the direct effect of STAT3 knockdown on tumor cells survival. Therefore, it is hard to determine the direct role of STAT3 knockdown in tumor cells *in vivo*, devoid from the contribution of the other external factors. Probably, reevaluating this approach in Nude or SCID mice, where adaptive

immunity is lacking, may give an idea of the magnitude of direct STAT3 knockdown on tumor cell survival as well as the role contributed by the immune response following STAT3 knockdown in tumor cells. It is also important to know that our siRNA complexes may not have an exclusive effect on cancer cells. *In vivo*, the siRNA complexes might have directly affected immune cells as well as cancer cells. This is of clinical significance, as blocking STAT3 directly in immune cells can produce a synergistic anti-tumor effect to STAT3 knockdown in tumors (2). In fact, the requirement of immune cells for tumor regression has been proven using tumor-bearing mouse model with Stat3^{-/-} hematopoietic system (5).

Therefore, our next objective was to evaluate STAT3 knockdown by targeting STAT3 directly in tumor-exposed DCs with STAT3-siRNA polyplexes loaded in PLGA NPs (Chapter 5). We applied this approach because several studies strongly indicated the negative-regulatory role of JAK/STAT3 signaling pathway on DC maturation (32-34), and because PLGA NPs were extensively used in DCs targeting for immunotherapy strategies (35, 36). We found this strategy to carry three advantages: (i) preferential uptake by DCs, (ii) controlled-release property by hydrophobic modification of PEI and (iii) reduction of PEI-associated toxicity (Chapter 5). Encompassing these properties makes PLGA NPs optimum for DCs targeting especially when co-delivery of other agents is intended e.g. antigens, adjuvants, as well as when co-delivery with low molecular weight drugs is needed. In deed, our NPs were in the size range of preferential uptake by DCs (37). The uptake process might also be facilitated by the presence

of PEI-based polymers as noticed with PLGA microspheres of comparable construct (38). High cellular internalization is very important objective since siRNA suffers from poor cellular internalization, which is one reason preventing its emergence in clinical setting. By designing PLGA NPs that are readily internalized by DCs, not only RNAi can be mediated but also other payloads can be co-delivered with the siRNA for additive or synergistic effect. In fact, others have recently designed PLGA NPs that contain PEI, anti-p-glycoprotein siRNA, and paclitaxel to target multi-drug resistant tumor (39). Along with cell internalization, they have shown that targeting tumor cells with these PLGA NPs potentiated the cytotoxic effect of paclitaxel due to the controlled release pattern where siRNA was released prior to paclitaxel in order to downregulate p-gp and, therefore, sensitized tumor cells to the chemotherapeutic agent (39). This indicates the potential of PLGA/PEI systems to have temporal controlled-release component that is highly applicable when siRNA and low-molecular weight drugs are co-encapsulated, since the onset of protein downregulation is usually delayed compared to low-molecular weight inhibitors. Therefore, it is useful to release siRNA before the other agent. Our data adds that fatty-acid modification to PEI backbone seems to enhance siRNA release from PLGA matrix compared to unmodified PEI (Chapter 5). This opens a new avenue for tuning the release process of siRNA by hydrophobic modification of the cationic polymer. The biological impact of this property can be significant as we have noticed a superiority of PLGA-PS over PLGA-P in mediating effective STAT3 knockdown by siRNA within 48 h, *in vitro* (Chapter 5). For our purpose, we have shown that

direct knockdown of STAT3 in B16-CM-exposed DCs restores phenotypic and functional maturation of DCs. We noticed that STAT3 knockdown in B16-CM-exposed DCs by PLGA-based siRNA NPs induced multiple stimulatory effects in DCs: (i) phenotypic expression of maturation marker (CD86), (ii) secretion of Th1-type response cytokine TNF- α , and (iii) alloreactivity with T cells isolated from Balb/c mice. This is a significant step for cancer immunotherapy since cancer employs a state of immune tolerance that is considered a reason for cancer vaccine failure in clinical settings (40). Furthermore, the noted restoration of DCs functionality was comparable, at least *in vitro*, between the two cases when STAT3 was targeted in cancer cells (Chapter 4, Figure 4.3) or directly in DCs (Chapter 5, Figure 5.7). This is an evidence for the availability of the second approach to synergize or alternate the first approach, especially if cancer cells developed a resistance mechanism, which is not uncommon throughout the process of cancer treatment (41).

From our observations, we obtained two main remarks: first, the validity of tumor-induced STAT3 in DCs as a target for cancer immunotherapy. This also confirms previous results from our lab where targeting B16-CM-exposed DCs with PLGA NPs of chemically conjugated STAT3 inhibitor JSI-124 resorted DCs phenotypic and functional maturation (42). Second, the protective property of the fatty-acid modified PEI to siRNA is carried on even when polyplexes are integrated into another formulation. The clinical relevance of this observation is retaining the effectiveness of the PEI system could as a powerful transfecting vehicle for nucleic acids, while reducing its associated non-specific cytotoxicity,

which is the main reason stands against its use in clinical applications. Moreover, designing an effective, and non-toxic, delivery system for siRNA can serve as a template or a frame for different siRNA applications with other molecular targets.

It is also important to emphasize that the work presented in this thesis is limited to the model used. Subcutaneous inoculation of tumor cells generates tumor models that are criticized for not mimicking etiological pathogenicity of cancer in clinical setting. Currently, cancer researchers are attracted to spontaneous-tumor models for better understanding of tumor progression and more relevant therapeutic applications. Another limitation of our work is that siRNA polyplexes, in the current form, are only suitable for intratumoral application. These polyplexes cannot be administered intravenously because they are highly prone to non-specific binding with blood-stream components. We highlight this issue in more detail in section 6.3.1. Moreover, we targeted DCs with PLGA-P and PLGA-PS only *in vitro*. We haven't investigated the specificity of these NPs to be differentially internalized by DCs in presence of other cell populations. Also, application of these NPs *in vivo* is crucial for a better evaluation of this therapeutic strategy. In section 6.3.2, we discuss the latter point in further details.

6.2 CONCLUSIONS

We developed for non-toxic polymeric systems siRNA delivery to B16 melanoma cells based on hydrophobic modification of PEI. Substituting long-chain endogenous lipids (especially stearic acid) onto PEI contributed to

significantly better binding to siRNA, as well as better protection in a serum-containing medium. These two factors contributed to enhancement in siRNA delivery to the cells and promotion of target knockdown as compared to parent PEI. We found out that the presence of the hydrophobic moieties was indispensable to formulate stable and efficient delivery systems for siRNA, especially at low concentrations. The desired siRNAs were effectively delivered to almost all cells (>90%) in culture, and a resultant knockdown of molecular targets e.g. integrin α_v and more importantly STAT3.

The delivery system based on stearic-acid modification of PEI turned to significantly increased siRNA potency *in vitro* and *in vivo* and consequently has the potential to reduce off-target effects. Furthermore, the siRNA-mediated silencing of STAT3 in B16 melanoma cells was found to be able to break the state of immune tolerance employed by the tumor and induce bystander anti-tumor innate and adaptive immune response. We also found that the bystander effect is highly correlated to the siRNA silencing effect and the tumor-killing action. Such strategy carries a therapeutic potential and could be considered for combined chemo- and immunotherapy for cancer.

We have also developed a PLGA-based delivery system of siRNA by the aid of PEI and PEI-StA for STAT3 targeting in DCs. The formulation successfully mediated specific siRNA silencing with no signs of non-specific toxicities. Moreover, this approach showed a therapeutic potential by restoring DCs function that was compromised with B16-CM exposure. This strategy holds a promise for inclusion with other immunotherapeutic strategies such as cancer

vaccine and adjuvant therapy. Co-delivery of STAT3 siRNA with cancer vaccine to DCs in the same PLGA NPs might improve the success rate of cancer vaccines at clinical settings.

6.3 FUTURE DIRECTIONS

6.3.1 Development of a delivery system for systemic administration of siRNA

siRNA faces similar physiological barriers as DNA intended for gene therapy, which are mostly in regard to enzymatic degradation and inefficient accumulation in target cells i.e. sub-optimal transfection (43). Therefore, developing a delivery strategy for systemic administration is crucial for effective therapeutic plan.

To accumulate in solid tumors, the so-called Enhanced Permeability and Retention (EPR) effect can be exploited as a passive targeting strategy (44). The permeability concept is based on the leaky nature of solid tumors' vasculature. Most solid tumors express elevated levels of permeability factors such as bradykinin (45), nitric oxide (NO) (46, 47), peroxynitrite (ONOO^-) (48), and proteinaceous vascular permeability factor (VPF) (49, 50). This permeability results in the extravasation of plasma proteins as well as macromolecules and nanoparticles into tumor interstitial space. The extent of nanoparticles extravasation depends on the gap width between endothelial junctions, which has been reported in several tumor models to have a cut-off size of 380-780 nm (51, 52). Moreover, the retention concept is attributed to the fact that lymphatic clearance from tumor tissues is much slower than normal or inflamed tissues, which lead to macromolecules and nanoparticles retention in tumor site after extravasation (53). Therefore, nanoparticles circulation in blood stream must be long enough for the EPR effect to take place.

Although our polyplexes fall in the size range for EPR effect and were shown capable of siRNA protection from serum degradation, they cannot be used for intravenous administration as they are. The surface cationic charge of our polyplexes renders them prone to non-specific association with negatively charged components in the blood stream e.g. cell membranes and proteins. Moreover, they can be recognized by the reticular endothelial system (RES). This could significantly reduce circulation time for the polyplexes before extravagating through the leaky vasculature in tumor site, and enhance their clearance before showing a therapeutic benefit. To overcome this drawback, adding a stealth property by PEGylation could be helpful in prolonging polyplexes circulation to prevent RES clearance and increase the chance for the EPR effect (54, 55). The effectiveness of this approach has been proven by two methods: attachment of PEG to siRNA and then complexation with PEI (56), or attachment of PEG to PEI and then complexation with siRNA (57). Moreover, external PEG side chains could be used as attachment sites for active-targeting ligands. For instance, Folate-PEG-PEI systems have shown enhanced efficacy of siRNA when targeting that overexpress folate receptors (58-60).

Very recently, this first report has just appeared on phase I clinical trial involving systemic administration of siRNA against M2 subunit of ribonuclease reductase to melanoma patients using human transferrin protein (TF)-targeted PEGylated cyclodextrin-based polymeric nanoparticles (61). This study provided the first evidence of specific RNAi mediated by siRNA. It also signified the importance of EPR effect in NPs accumulation specifically in tumor tissues.

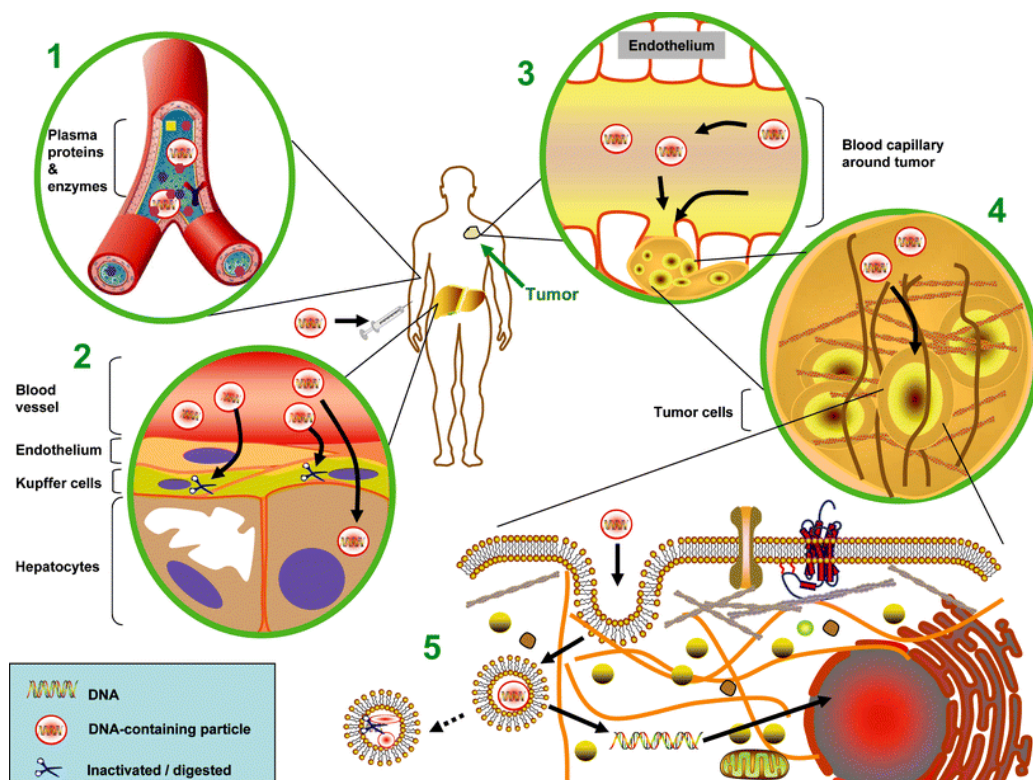


Figure 6.3 Illustration of barriers for i.v. gene delivery. Adopted from (43). DNA-containing NPs are injected intravenously into human body. Serum proteins may bind to the particles, crosslink them and increase the particle size. This can result in rapid particle elimination (Inset 1). The Kupffer cells (RES) may take up particles, leading to rapid NP elimination from circulation and decrease their access to the hepatocytes (Inset 2). Circulating NPs may extravasate in tumor tissue through the leaky tumor vessels (the EPR effect) (Inset 3). Particles then need to pass through the crowded extracellular matrix to contact the cell surface (Inset 4). When the particles are internalized into cells, DNA must escape from the endosome and find its way into the nucleus (Inset 5).

6.3.2 Applying STAT3 knockdown strategy in context of cancer vaccines

The weak qualitative and quantitative T cell responses and immunosuppressive tumor microenvironment that inhibits anti-tumor T cell activity at the effector phase are the two main reasons for the failure of current cancer vaccines in clinical trials (40, 62, 63). Therefore, in order to improve the response to cancer vaccines, immunotherapy strategies must be directed to activate robust and long-lasting anti-tumor immune responses. For this to happen, the ‘immunosuppressive milieu’ of the tumor microenvironment must be reversed.

We have shown that our strategy could reverse the tumor-mediated immune tolerance by STAT3 inhibition at the level of tumor microenvironment as well as the level of tumor-exposed DCs. Since DCs are considered the main target for cancer vaccines, STAT3 inhibitory modalities must be co-administered to the same cell population to reverse the deleterious effects of tumor milieu. Previously, we have shown that vaccination of mice bearing melanoma B16 tumors with PLGA NPs co-encapsulating the poorly immunogenic melanoma antigen, tyrosinase-related protein 2 (TRP2) along with Toll-like receptor (TLR) ligand (7-acyl lipid A) induces therapeutic anti-tumor effect characterized by highly activated TRP2-specific CD8⁺ CTL that were capable of IFN- γ secretion at lymph nodes and spleens of the vaccinated mice (64). This model provides a perfect framework to integrate our STAT3 siRNA systems where PLGA NPs co-encapsulate antigen/adjuvant for DC targeting, and the polyplexes applied directly on B16 tumor.

6.4 REFERENCES

1. Dunn GP, Old LJ, Schreiber RD. The three Es of cancer immunoediting. *Annu Rev Immunol.* 2004;22:329-60.
2. Kortylewski M, Yu H. Stat3 as a potential target for cancer immunotherapy. *J Immunother.* 2007 Feb-Mar;30(2):131-9.
3. Yu H, Kortylewski M, Pardoll D. Crosstalk between cancer and immune cells: role of STAT3 in the tumour microenvironment. *Nat Rev Immunol.* 2007 Jan;7(1):41-51.
4. Kortylewski M, Yu H. Role of Stat3 in suppressing anti-tumor immunity. *Curr Opin Immunol.* 2008 Apr;20(2):228-33.
5. Kortylewski M, Kujawski M, Wang T, Wei S, Zhang S, Pilon-Thomas S, et al. Inhibiting Stat3 signaling in the hematopoietic system elicits multicomponent antitumor immunity. *Nat Med.* 2005 Dec;11(12):1314-21.
6. Niu G, Wright KL, Huang M, Song L, Haura E, Turkson J, et al. Constitutive Stat3 activity up-regulates VEGF expression and tumor angiogenesis. *Oncogene.* 2002 Mar 27;21(13):2000-8.
7. Xie TX, Wei D, Liu M, Gao AC, Ali-Osman F, Sawaya R, et al. Stat3 activation regulates the expression of matrix metalloproteinase-2 and tumor invasion and metastasis. *Oncogene.* 2004 Apr 29;23(20):3550-60.
8. Wang T, Niu G, Kortylewski M, Burdelya L, Shain K, Zhang S, et al. Regulation of the innate and adaptive immune responses by Stat-3 signaling in tumor cells. *Nat Med.* 2004 Jan;10(1):48-54.
9. Lenz G. The RNA interference revolution. *Braz J Med Biol Res.* 2005 Dec;38(12):1749-57.
10. Kim DH, Rossi JJ. Strategies for silencing human disease using RNA interference. *Nat Rev Genet.* 2007 Mar;8(3):173-84.
11. Whitehead KA, Langer R, Anderson DG. Knocking down barriers: advances in siRNA delivery. *Nat Rev Drug Discov.* 2009 Feb;8(2):129-38.
12. Demeneix B, Behr JP. Polyethylenimine (PEI). *Adv Genet.* 2005;53:217-30.
13. Linder ME, Deschenes RJ. New insights into the mechanisms of protein palmitoylation. *Biochemistry.* 2003 Apr 22;42(15):4311-20.
14. Abbasi M, Uludag H, Incani V, Olson C, Lin X, Clements BA, et al. Palmitic acid-modified poly-L-lysine for non-viral delivery of plasmid DNA to skin fibroblasts. *Biomacromolecules.* 2007 Apr;8(4):1059-63.
15. Alshamsan A, Haddadi A, Incani V, Samuel J, Lavasanifar A, Uludag H. Formulation and delivery of siRNA by oleic acid and stearic acid modified polyethylenimine. *Mol Pharm.* 2009 Jan-Feb;6(1):121-33.
16. Wolfrum C, Shi S, Jayaprakash KN, Jayaraman M, Wang G, Pandey RK, et al. Mechanisms and optimization of in vivo delivery of lipophilic siRNAs. *Nat Biotechnol.* 2007 Oct;25(10):1149-57.
17. Felgner PL, Gadek TR, Holm M, Roman R, Chan HW, Wenz M, et al. Lipofection: a highly efficient, lipid-mediated DNA-transfection procedure. *Proc Natl Acad Sci U S A.* 1987 Nov;84(21):7413-7.

18. Kim WJ, Chang CW, Lee M, Kim SW. Efficient siRNA delivery using water soluble lipopolymer for anti-angiogenic gene therapy. *J Control Release*. 2007 Apr 23;118(3):357-63.
19. Mahato RI, Lee M, Han S, Maheshwari A, Kim SW. Intratumoral delivery of p2CMVmIL-12 using water-soluble lipopolymers. *Mol Ther*. 2001 Aug;4(2):130-8.
20. Wang DA, Narang AS, Kotb M, Gaber AO, Miller DD, Kim SW, et al. Novel branched poly(ethylenimine)-cholesterol water-soluble lipopolymers for gene delivery. *Biomacromolecules*. 2002 Nov-Dec;3(6):1197-207.
21. Yockman JW, Maheshwari A, Han SO, Kim SW. Tumor regression by repeated intratumoral delivery of water soluble lipopolymers/p2CMVmIL-12 complexes. *J Control Release*. 2003 Feb 21;87(1-3):177-86.
22. Alshamsan A, Haddadi A, Hamdy S, Samuel J, El-Kadi AO, Uludag H, et al. Down-Modulation of STAT3 in B16 Melanoma by siRNA/Lipid-Substituted Polyethylenimine Complexes Induces Bystander Immune Response in vitro and in vivo. *Biomaterials*. 2010. (submitted).
23. Alshamsan A, Hamdy S, Samuel J, El-Kadi AO, Lavasanifar A, Uludag H. The induction of tumor apoptosis in B16 melanoma following STAT3 siRNA delivery with a lipid-substituted polyethylenimine. *Biomaterials*. 2010 Feb;31(6):1420-8.
24. Hauptenthal J, Baehr C, Zeuzem S, Piiper A. RNase A-like enzymes in serum inhibit the anti-neoplastic activity of siRNA targeting polo-like kinase 1. *Int J Cancer*. 2007 Jul 1;121(1):206-10.
25. Yu H, Pardoll D, Jove R. STATs in cancer inflammation and immunity: a leading role for STAT3. *Nat Rev Cancer*. 2009 Nov;9(11):798-809.
26. Kim DJ, Chan KS, Sano S, Digiovanni J. Signal transducer and activator of transcription 3 (Stat3) in epithelial carcinogenesis. *Mol Carcinog*. 2007 Aug;46(8):725-31.
27. Real PJ, Sierra A, De Juan A, Segovia JC, Lopez-Vega JM, Fernandez-Luna JL. Resistance to chemotherapy via Stat3-dependent overexpression of Bcl-2 in metastatic breast cancer cells. *Oncogene*. 2002 Oct 31;21(50):7611-8.
28. Hatake K, Tokudome N, Ito Y. Next generation molecular targeted agents for breast cancer: focus on EGFR and VEGFR pathways. *Breast Cancer*. 2007;14(2):132-49.
29. Chen Z, Han ZC. STAT3: a critical transcription activator in angiogenesis. *Med Res Rev*. 2008 Mar;28(2):185-200.
30. Cascio S, Ferla R, D'Andrea A, Gerbino A, Bazan V, Surmacz E, et al. Expression of angiogenic regulators, VEGF and leptin, is regulated by the EGF/PI3K/STAT3 pathway in colorectal cancer cells. *J Cell Physiol*. 2009 Oct;221(1):189-94.
31. Costa-Pereira AP, Tininini S, Strobl B, Alonzi T, Schlaak JF, Is'harc H, et al. Mutational switch of an IL-6 response to an interferon-gamma-like response. *Proc Natl Acad Sci U S A*. 2002 Jun 11;99(12):8043-7.
32. Park SJ, Nakagawa T, Kitamura H, Atsumi T, Kamon H, Sawa S, et al. IL-6 regulates in vivo dendritic cell differentiation through STAT3 activation. *J Immunol*. 2004 Sep 15;173(6):3844-54.

33. Cheng F, Wang HW, Cuenca A, Huang M, Ghansah T, Brayer J, et al. A critical role for Stat3 signaling in immune tolerance. *Immunity*. 2003 Sep;19(3):425-36.
34. Nefedova Y, Cheng P, Gilkes D, Blaskovich M, Beg AA, Sebt SM, et al. Activation of dendritic cells via inhibition of Jak2/STAT3 signaling. *J Immunol*. 2005 Oct 1;175(7):4338-46.
35. Bala I, Hariharan S, Kumar MN. PLGA nanoparticles in drug delivery: the state of the art. *Crit Rev Ther Drug Carrier Syst*. 2004;21(5):387-422.
36. Waeckerle-Men Y, Groettrup M. PLGA microspheres for improved antigen delivery to dendritic cells as cellular vaccines. *Adv Drug Deliv Rev*. 2005 Jan 10;57(3):475-82.
37. Elamanchili P, Diwan M, Cao M, Samuel J. Characterization of poly(D,L-lactic-co-glycolic acid) based nanoparticulate system for enhanced delivery of antigens to dendritic cells. *Vaccine*. 2004 Jun 23;22(19):2406-12.
38. Zhang XQ, Intra J, Salem AK. Comparative study of poly (lactic-co-glycolic acid)-poly ethyleneimine-plasmid DNA microparticles prepared using double emulsion methods. *J Microencapsul*. 2008 Feb;25(1):1-12.
39. Patil YB, Swaminathan SK, Sadhukha T, Ma L, Panyam J. The use of nanoparticle-mediated targeted gene silencing and drug delivery to overcome tumor drug resistance. *Biomaterials*. 2010 Jan;31(2):358-65.
40. Rosenberg SA, Yang JC, Restifo NP. Cancer immunotherapy: moving beyond current vaccines. *Nat Med*. 2004 Sep;10(9):909-15.
41. Liu FS. Mechanisms of chemotherapeutic drug resistance in cancer therapy--a quick review. *Taiwan J Obstet Gynecol*. 2009 Sep;48(3):239-44.
42. Molavi O, Mahmud A, Hamdy S, Hung RW, Lai R, Samuel J, et al. Development of a Poly(d,l-lactic-co-glycolic acid) Nanoparticle Formulation of STAT3 Inhibitor JSI-124: Implication for Cancer Immunotherapy. *Mol Pharm*. 2010 Jan 26.
43. Li W, Szoka FC, Jr. Lipid-based nanoparticles for nucleic acid delivery. *Pharm Res*. 2007 Mar;24(3):438-49.
44. Maeda H, Wu J, Sawa T, Matsumura Y, Hori K. Tumor vascular permeability and the EPR effect in macromolecular therapeutics: a review. *J Control Release*. 2000 Mar 1;65(1-2):271-84.
45. Matsumura Y, Kimura M, Yamamoto T, Maeda H. Involvement of the kinin-generating cascade in enhanced vascular permeability in tumor tissue. *Jpn J Cancer Res*. 1988 Dec;79(12):1327-34.
46. Maeda H, Noguchi Y, Sato K, Akaike T. Enhanced vascular permeability in solid tumor is mediated by nitric oxide and inhibited by both new nitric oxide scavenger and nitric oxide synthase inhibitor. *Jpn J Cancer Res*. 1994 Apr;85(4):331-4.
47. Doi K, Akaike T, Horie H, Noguchi Y, Fujii S, Beppu T, et al. Excessive production of nitric oxide in rat solid tumor and its implication in rapid tumor growth. *Cancer*. 1996 Apr 15;77(8 Suppl):1598-604.
48. Wu J, Akaike T, Hayashida K, Okamoto T, Okuyama A, Maeda H. Enhanced vascular permeability in solid tumor involving peroxynitrite and matrix metalloproteinases. *Jpn J Cancer Res*. 2001 Apr;92(4):439-51.

49. Senger DR, Galli SJ, Dvorak AM, Perruzzi CA, Harvey VS, Dvorak HF. Tumor cells secrete a vascular permeability factor that promotes accumulation of ascites fluid. *Science*. 1983 Feb 25;219(4587):983-5.
50. Senger DR, Perruzzi CA, Feder J, Dvorak HF. A highly conserved vascular permeability factor secreted by a variety of human and rodent tumor cell lines. *Cancer Res*. 1986 Nov;46(11):5629-32.
51. Yuan F, Dellian M, Fukumura D, Leunig M, Berk DA, Torchilin VP, et al. Vascular permeability in a human tumor xenograft: molecular size dependence and cutoff size. *Cancer Res*. 1995 Sep 1;55(17):3752-6.
52. Hobbs SK, Monsky WL, Yuan F, Roberts WG, Griffith L, Torchilin VP, et al. Regulation of transport pathways in tumor vessels: role of tumor type and microenvironment. *Proc Natl Acad Sci U S A*. 1998 Apr 14;95(8):4607-12.
53. Noguchi Y, Wu J, Duncan R, Strohal J, Ulbrich K, Akaike T, et al. Early phase tumor accumulation of macromolecules: a great difference in clearance rate between tumor and normal tissues. *Jpn J Cancer Res*. 1998 Mar;89(3):307-14.
54. Klibanov AL, Maruyama K, Torchilin VP, Huang L. Amphipathic polyethyleneglycols effectively prolong the circulation time of liposomes. *FEBS Lett*. 1990 Jul 30;268(1):235-7.
55. Podesta JE, Kostarelos K. Chapter 17 - Engineering cationic liposome siRNA complexes for in vitro and in vivo delivery. *Methods Enzymol*. 2009;464:343-54.
56. Kim SH, Jeong JH, Lee SH, Kim SW, Park TG. Local and systemic delivery of VEGF siRNA using polyelectrolyte complex micelles for effective treatment of cancer. *J Control Release*. 2008 Jul 14;129(2):107-16.
57. de Wolf HK, Snel CJ, Verbaan FJ, Schiffelers RM, Hennink WE, Storm G. Effect of cationic carriers on the pharmacokinetics and tumor localization of nucleic acids after intravenous administration. *Int J Pharm*. 2007 Mar 1;331(2):167-75.
58. Hwa Kim S, Hoon Jeong J, Chul Cho K, Wan Kim S, Gwan Park T. Target-specific gene silencing by siRNA plasmid DNA complexed with folate-modified poly(ethylenimine). *J Control Release*. 2005 May 5;104(1):223-32.
59. Kim SH, Mok H, Jeong JH, Kim SW, Park TG. Comparative evaluation of target-specific GFP gene silencing efficiencies for antisense ODN, synthetic siRNA, and siRNA plasmid complexed with PEI-PEG-FOL conjugate. *Bioconjug Chem*. 2006 Jan-Feb;17(1):241-4.
60. Biswal BK, Debata NB, Verma RS. Development of a targeted siRNA delivery system using FOL-PEG-PEI conjugate. *Mol Biol Rep*. 2009 Oct 9.
61. Davis ME, Zuckerman JE, Choi CH, Seligson D, Tolcher A, Alabi CA, et al. Evidence of RNAi in humans from systemically administered siRNA via targeted nanoparticles. *Nature*. 2010 Mar 21.
62. Kaufman HL, Disis ML. Immune system versus tumor: shifting the balance in favor of DCs and effective immunity. *J Clin Invest*. 2004 Mar;113(5):664-7.
63. Zou W. Immunosuppressive networks in the tumour environment and their therapeutic relevance. *Nat Rev Cancer*. 2005 Apr;5(4):263-74.

64. Hamdy S, Molavi O, Ma Z, Haddadi A, Alshamsan A, Gobti Z, et al. Co-delivery of cancer-associated antigen and Toll-like receptor 4 ligand in PLGA nanoparticles induces potent CD8⁺ T cell-mediated anti-tumor immunity. *Vaccine*. 2008 Sep 15;26(39):5046-57.